Activity Report
2006

Association
EURATOM / IPP.CR

INSTITUTE OF PLASMA PHYSICS, v.v.i.
ACADEMY OF SCIENCES OF THE CZECH REPUBLIC

TABLE OF CONTENTS

PREFACE

This report summarizes the main activities and achieved results of the Association EURATOM/IPP.CR in the year 2006. The Association participates in the joint European effort in mastering controlled fusion by carrying out relevant plasma physics and technology R&D, including participation in JET and other European devices and activities related to the international fusion experiment ITER.

The Association was founded on December 22, 1999 through a contract between the European Atomic Energy Community (EURATOM) represented by the European Commission and the Institute of Plasma Physics, Academy of Sciences of the Czech Republic (IPP). Several other institutions have been included in the Research Unit to contribute to the work programme in physics and technology research:

- Faculty of Mathematics and Physics, Charles University in Prague
- Institute of Physical Chemistry, v.v.i., Academy of Sciences of the Czech Republic
- Faculty of Nuclear Science and Physical Engineering, Czech Technical University
- Nuclear Physics Institute, v.v.i., Academy of Sciences of the Czech Republic
- Nuclear Research Institute, Rez, Plc
- Institute of Applied Mechanics, Brno, Ltd

The overall manpower involved in the Association's fusion research at the end of 2006 was 121, of which 91 (75%) were professionals (i.e. those with a University degree). The total effort expended is about 50 person years of which roughly 65% is devoted to physics tasks and the remaining 35% to underlying technology and technology tasks. The overall 2005 budget was about 1.35 M€.

Our activities in physics were based on the approved Work Programme 2006 both in experiment and theory. The fusion-relevant plasma physics was – for the last year – experimentally studied on the small tokamak CASTOR. The research was focused on the study of phenomena at the plasma edge, such as biasing and the measurement of the structure of edge turbulence. A part of our activities was devoted to studies of wave-plasma interaction. Some selected atomic processes relevant to fusion plasmas, such as the interaction of molecular ions with first wall elements, were studied in test-bed experiments. The research was performed in close collaboration with 15 other Associations (*CEA, CIEMAT, Conféderation Suisse, ENEA, Etat Belge, FZK, HAS, IPP, IPPLM, IST, MEdC, ŐAW, TEKES, UKAEA, VR) and JET EFDA.*

In the technology area, the R&D was substantially enhanced and focused on the fields Vessel/In Vessel, Tritium Breeding and Materials and Physics Integration. In total 16 Technology / Underlying Technology Tasks were worked upon, mostly exploiting the cyclotron, the fission reactor and computational capabilities of our Association.

After the definitive decision to re-install the COMPASS-D tokamak in the Institute of Plasma Physics, Prague, considerable part of our manpower concentrated on detailed preparation of this project, including proper definition of the subsystems that have to be included in the design of the new site for COMPASS-D. A brief 2006 progress report of the project – which obtained the EURATOM preferential support recently - makes an attachement to this 2006 Activity report of our Association.

Pavol Pavlo
Head of Research Unit
Association EURATOM/IPP.CR

Composition of the Research Unit

IPP **Institute of Plasma Physics, v.v.i., Academy of Sciences of the CR**
Address: Za Slovankou 3,
182 00 Praha 8, Czech Republic
Tel: +420 286 890 450
Fax: +420 286 586 389
Contact Person: Jan Stöckel
e-mail: stockel@ipp.cas.cz

JHIPC **J Heyrovský Institute of Physical Chemistry, v.v.i., Academy of Sciences of the CR**
Address: Dolejškova 3,
182 23 Praha 8, Czech Republic
Tel: +420 266 053 514
Fax: +420 286 582 307
Contact person: Zdeněk Herman
zdenek.herman@jh-inst.cas.cz

NPI **Institute of Nuclear Physics, v.v.i., Academy of Sciences of the CR**
Address: 250 68 Řež, Czech Republic
Tel: +420 266 172 105 (3506)
Fax: +420 220 941 130
Contact person: Pavel Bém
e-mail: bem@ujf.cas.cz

IAM **Institute of Applied Mechanics Brno, Ltd.**
Address: Veveří 85,
611 00 Brno, CR
Phone: +420 541 321 291
Fax: +420 541 211 189
Contact person: Lubomír Junek
e-mail: junekl@uam.cz

FMP **Faculty of Mathematics and Physics, Charles University**
Address: V Holešovičkách 2,
182 00 Praha 8, Czech Republic
Tel: +420 221 912 305
Fax: +420 221 912 332
Contact person: Milan Tichý
tichy@mbox.troja.mff.cuni.cz

FNSPE **Faculty of Nuclear Science and Physical Engineering, Czech Technical University**
Address: Břehová 7,
115 19 Praha 1, Czech Republic
Tel: +420 224 358 296
Fax: +420 222 320 862
Contact person: Vojtěch Svoboda
svoboda@br.fjfi.cvut.cz

NRI **Nuclear Research Institute Plc., Řež**
Address: 250 68 Řež, Czech Republic
Tel: +420 266 172 453
Fax: +420 266 172 045
Contact person: Karel Šplíchal
e-mail: spl@ujv.cz

Steering Committee

EURATOM

Johannes P.M. Spoor, Head Unit J7, DG RTD
David Campbell, Unit J6, DG RTD
Barry Green, Unit J6, DG RTD

IPP.CR

Ivan Wilhelm (Charles University)
Petr Křenek (Ministry of Education, Youth and Sports)
Pavel Chráska (Institute of Plasma Physics)

Head of Research Unit

Pavol Pavlo

Secretary of the SC

I RESEARCH UNIT

1 Association EURATOM/IPP.CR

International Board of Advisors of the Association EURATOM-IPP.CR

Prof. Hardo Bruhns	Chair
Dr. Carlos Hidalgo	CIEMAT, Madrid, Spain
Dr. Jochen Linke	Forschungszentrum Jülich GmbH, Jülich, Germany
Dr. Bernard Saoutic	CEA Cadarache, France
Prof. Fernando Serra	Centro de Fusao Nuclear, Lisboa, Portugal
Dr. Wolfgang Suttrop	Max-Planck-Institut für Plasmaphysik (IPP), Garching, Germany
Dr. Martin Valovič	UKAEA, Culham laboratory, United Kingdom
Prof. Guido Van Oost	Ghent University, Gent, Belgium
Dr. Henri Weisen	EPFL, Lausanne, Switzerland
Dr. Sandor Zoletnik	RMKI KFKI, Budapest, Hungary

The Board was established to help with the formulation of scientific program, and to assess the scientific achievements of the Association EURATOM-IPP.CR.

Representatives of the Association in European Committees

Consultative Committee for the EURATOM Specific Programme on Nuclear Energy Research - Fusion

Pavel Chráska	Institute of Plasma Physics, Academy of Sciences of the Czech Republic
Milan Tichý	Faculty of Mathematics and Physics, Charles University, Prague

Scientific and Technical Advisory Committee

Jan Stöckel	Institute of Plasma Physics, Academy of Sciences of the Czech Republic
Karel Šplíchal	Nuclear Research Institute pls., Řež

Administration and Finance Advisory Committee

Pavol Pavlo	Institute of Plasma Physics, Academy of Sciences of the Czech Republic

EFDA Steering Committee

Jan Dobeš	Institute of Nuclear Physics, Academy of Sciences of the Czech Republic
Jan Kysela	Nuclear Research Institute pls., Řež

Committee for Fusion Industry

Jan Musil	Škoda Power, Plzeň

2 Manpower and Budget

Manpower Analysis of the Association EURATOM/IPP.CR 2006

Institution	STAFF, PY			STAFF, Person					
	Physics	Technology	TOTAL	Female	Male	Prof.	Non-Prof.	TOTAL	Total, %
IPP	27.46	3.29	30.75	7	51	45	13	58	47.4
FMP	2.4	0	2.40	0	6	6	0	6	7.2
IAM	0	2.68	2.68	0	9	4	5	9	2.1
JHIPC	1.90	0	1.90	0	3	3	0	3	5.2
FNSPE	0.50	0.50	1.00	0	2	2	0	2	4.1
NRI	0	7.10	7.10	6	22	22	6	28	18.6
NPI	0	4.15	4.15	1	14	9	6	15	15.4
TOTAL	**32.26**	**17.72**	**49.98**	**14**	**107**	**91**	**30**	**121**	**100.0**
Total, %	**64.5**	**35.5**	**100.0**	**11.6**	**88.4**	**75.2**	**24.8**	**100.0**	

Expenditures 2006

	Euro
Physics	815 365
Underlying Technologies	283 682
Inertial Fusion Energy	15 000
EFDA Basic Support Technology	278
Sub-total	**1 114 325**
Technology tasks Art 5.1a	145 619
Technology tasks Art 5.1b	47 641
EFDA Article 6.3 Contracts	8 212
EFDA Article 9 - secondment to Garching	34 167
EFDA Article 9 - secondment to Culham	14 935
Sub-total	**250 574**
Mobility Actions	**73 012**
TOTAL	**1 437 911**

3 International Collaboration

Collaborative Projects in 2006

PROJECT NO.1**:** **Fluctuation measurements and edge plasma biasing**
Objective: Measurement of the edge fluctuations by Langmuir probe arrays in ohmic regime and in discharges with the edge plasma biasing on CASTOR and RFX.

Collaborating Associations:
- *CEA Cadarache*
- *Etat Belge (RMS + Ghent University)*
- *ENEA - Consorzio RFX, Padova*
- *CIEMAT*
- *IST*
- *HAS*
- *ÖAW – Innsbruck University*

PROJECT NO. 2: **Development of advanced probes**
Objective: Development of advanced probe for the edge plasma diagnostics, such as the tunnel probe for electron and ion temperature measurements, emissive probe, probe for measurement of the Reynolds stress, etc. Appropriate theory and modelling.

Collaborating Associations:
- *CEA Cadarache*
- *Etat Belge (RMS + Ghent University)*
- *ENEA - Consorzio RFX, Padova*
- *ÖAW – Innsbruck University*
- *CIEMAT*
- *MEdC*
- *HAS*

PROJECT NO. 3: **Edge plasma measurements on Tore Supra**
Objective: Measurements of the edge plasma parameters (electron temperature, density, ion temperature and ion flows) in large - scale devices (Tore Supra) and interpretation of experimental data.

Collaborating Associations:
- *CEA Cadarache*

PROJECT NO. 4: **Edge plasma modelling**
Objective: Modelling of the particle transport (bulk ions + impurities) at the plasma edge and comparison with experiment.

Collaborating Associations:
- *ÖAW - Innsbruck University*
- *VR – Alfven Laboratory*

PROJECT NO. 5: **Multilateral cooperation on impurity transport**
Objective: Optimization of the USX and VUV diagnostics for spectroscopy measurements and study the transport of impurities on TCV and CASTOR tokamak

Collaborating Associations:
- *Conféderation Suisse*
- *HAS*
- *ENEA – Consorzio RFX*

PROJECT NO. 6: **EBW on MAST and CASTOR**
Objective: Modelling of the conversion of Electron Bernstein Waves and comparison of the results with measurements of microwave radiation via radiometers.

Collaborating Associations:
- *UKAEA*

PROJECT NO. 7: **Generation of fast particles in front of LH grills and ICRH antennae**
Objective: Modeling of the generation of fast particles in front of Lower Hybrid (LH) grills and ICRH antennae and comparison of results with experiments.

Collaborating Associations:
- *CEA Cadarache*
- *TEKES*
- *ÖAW - Innsbruck University*
- *JET*
- *IPP Garching*

PROJECT No. 8: **Ion-surface Interactions**
Objective: Study of interaction of hydrocarbon ions with fusion-relevant surfaces

Collaborating Associations:
- *ÖAW - Innsbruck University*

PROJECT NO. 9: **Nuclear data for IFMIF**

Objective: Measurement of activation cross sections for Chromium (the EUROFER-97 steel constituent) at neutron energies below 35 MeV.

Collaborating Associations:
- *FZ Karlsruhe*

PROJECT NO. 10: **Cherenkov detectors**

Objective: Implementation of Cherenkov detectors for measurements of suprathermal electrons in the CASTOR plasma.

Collaborating Associations:
- *IPPLM*

PROJECT NO. 11: **Laser-induced tritium decontamination and characterization of decontaminated in-vessel components**

Objective: Analysis of materials exposed to laser radiation.

Collaborating Associations:
- *IPPLM*

PROJECT NO. 12: **SOL turbulence on TCV**

Objective: Turbulence in the Scrape-off layer of the tokamak TCV

Collaborating Associations:
- *Conféderation Suisse*

4 Main Facilities

The CASTOR Tokamak

The CASTOR tokamak is a small device built in the year 1958 in the Kurchatov Institute in Moscow (original name TM-1MH), which has been in operation in the IPP Prague since 1977. The vacuum vessel and plasma control systems were substantially reconstructed in the year 1985. The basic characteristics of the device are:

Major radius	40 cm
Minor radius	8,5 cm
Toroidal magnetic field	0,5-1,5 T
Plasma current	5-20 kA
Pulse length	<50 ms
Working gas	Hydrogen

The vacuum vessel (minor radius 100 mm) is made of stainless steel. The plasma cross section is defined by the poloidal limiter made of Molybdenum. Auxiliary microwave power (f=1.25GHz, P=40kW) can be injected into the ohmic plasma via a multijunction grill for non-inductive current drive. A graphite electrode is routinely used to polarize the edge plasma.

A great advantage of CASTOR is its flexibility. Good quality plasma discharges can be achieved within 1-2 days after opening the vessel to atmospheric pressure which makes it ideal for testing new diagnostics. Up to 70 reproducible discharges can be achieved during one experimental day. Typical plasma parameters are:

Central electron temperature	100-300 eV
Central ion temperature	50-100 eV
Line average density	$0.5\text{-}3.10^{19}$ m^{-3}
Energy confinement time	<1 ms

Diagnostics:

- Magnetic diagnostics
- Microwave interferometer at 70GHz
- Photomultipliers with interference filters for measurement of hydrogen and light impurities lines
- VUV spectrometer Seya-Namioka with a high spatial resolution
- XUV spectrometer with multi-layer mirror as disperse element
- Bolometer array for measurements of radiation losses
- Langmuir probe arrays for edge plasma monitoring both in radial and poloidal directions
- Advanced probes for measurements of ion and electron temperatures, plasma potential, and flows in the edge plasma
- Array of coils for measurement of magnetic fluctuations
- Radiometer of electromagnetic radiation at 17-27 GHz and 27-40 GHz
- Microwave reflectometer at 29, 33, and 35 GHz
- Charge exchange analyzer for measurement of ion temperature

Measured signals are digitalized by several A/D converters. Basic data (24 channels) are digitalized with the sampling frequency 40 kHz. For fluctuation data, the digitizers with a higher sampling frequency (80 channels, 1 MHz) are used. Data are stored in a database and processed *a posteriori* either by IDL or Matlab based software.

NRI Fission reactor LVR-15

LVR-15 is a light water moderated and cooled tank nuclear reactor with forced cooling, operated by the Nuclear Research Institute in Rez. The maximum power of the reactor is 10 MW. The reactor core is situated in the reactor vessel (outer diameter 2300 mm, total height of the vessel 6235 mm), which is made of stainless steel, the internal parts of the rector are made of an aluminium alloy. The reactor has a forced circulation of the coolant. The generated heat is transported via three cooling circuits to the nearby river.

The irradiation capacity

Main irradiation channels	**Thermal neutron flux density ($cm^{-2}.s^{-1}$)**
Irradiation channels 60 mm in fuel	1.10^{14}
Irradiation channels 60 mm, core periphery	7.10^{13}
Irradiation channels 60/40 mm in reflector	$3\text{-}5.10^{13}$
Horizontal channels 100/60 mm	1.10^{8}
Graphite thermal column	1.10^{11}
High pressure water loop	5.10^{13}
Doped silicon facility	1.10^{13}

The irradiation facilities are complemented with well-equipped hot cells, which allow for the irradiated specimens handling.

Experimental facilities: Light water loops

RVS-3: The loop is designed for material and radioactivity transport investigation under PWR/VVER conditions. It enables the performance of irradiation experiments over a wide range of operational parameters limited by the following maximum parameters:

Pressure	16,5 MPa
Temperature	345°C
Water flow rate	10 000 kg/hour
Neutron flux	10^{18} $n.m^{-2}s^{-1}$
Electrical capacity heat	100 kW

***BWR-1*:** The loop is designed for the investigation of structural materials behaviour and radioactivity transport under BWR conditions

Pressure	10 MPa
Temperature	300°C
Water flow rate	2 000 kg/hour
Neutron flux	10^{18} $n.m^{-2}s^{-1}$

***BWR-2*:** The loop is designed for material research simulating conditions of BWR

Pressure	12 MPa
Temperature	300°C
Water flow rate	1 000 kg/hour
Force applied to the specimen	152 kN
Duration of the specimen loading cycle	30 hours
Working fluid	ultra-pure water

The NPI cyclotron-based Fast Neutron Facility (NPI FNF)

The project of the International Fusion Material Irradiation Facility (IFMIF) aims to provide neutron irradiation tests of fusion materials at fusion-reactor relevant fluency. For testing the neutronic calculations of the IFMIF test cell, the NPI cyclotron-based Fast Neutron Facility (FNF) provides neutron beams with the IFMIF-like spectrum – the only source of its kind operated within the European Union.

Accelerator

The variable-energy cyclotron U-120M (K=40) of the Nuclear Physics Institute Rez is a versatile machine operating in both positive and negative regimes and accelerating light particles with the mass-to-charge ratio A/Z = 1-2.8. Accelerated beams and energy ranges are shown in the Table 1.

Table 1. *Beam parameters of the cyclotron U-120M*

Accelerated ions	H(+)	D(+)	^{3}He(++)	^{4}He(++)	H(-)	D(-)
Energy range (MeV)	**10 - 24**	**10 - 17**	**17 - 53**	**20 - 40**	**10 - 37**	**10 – 18**
Internal beam current (μA)	**100**	**80**	**40**	**40**	**40 -15**	**25 -10**
External beam current (μA)	**3**	**3**	**3**	**3**	**40 -15**	**25 -10**

The beam-line system with ion-optic equipment and target stations consists of three lines in the experimental hall (positive-ion mode, extraction by the deflection system) and one line in the cyclotron hall (negative-ion mode, extraction by the stripping-foil method). Two of these lines are dedicated to fast-neutronic experiments for the IFMIF project.

Neutron-spectrometry facility NG1

The cross-section data of neutron emitting reactions induced by charged-particle beams on investigated nuclides are experimentally studied at the NG1 target station. The angular distributions of the emitted fast neutrons (in the energy range from 0.7 to 35 MeV) are measured by the scintillator pulse-height unfolding technique based on the n-gamma discrimination hardware and many-parameter data-acquisition on a PC. A different target technique (including solid, liquid and gas samples) can be used on the NG1 target station. In order to conduct the benchmark tests of neutron-transport calculations provided for fusion relevant materials, the neutron source reactions $D_2O(^{3}He,xn)$ and $D_2O(p,xn)$ were investigated and used for a simulation of the IFMIF spectrum.

High-power neutron beam facility NG2

To reach a high-fluence neutron field for the activation-cross-section benchmark tests relevant to IFMIF neutronic calculations, a novel fast-neutron source was developed. The source takes advantage in high beam current of the negative-ion mode of the cyclotron operation. With this aim, the proton-induced reaction on a heavy-water flow target was investigated for the first time and used in the NG2 target station. Furthermore, the standard Be-targets for protons and deuterons are routinely operated as well in the NG2 beamline. The white-spectrum neutron fields with an energy range up to 35 MeV and flux density up to 3×10^{11} n.cm^{-2}.s^{-1} are available for the irradiation experiments.

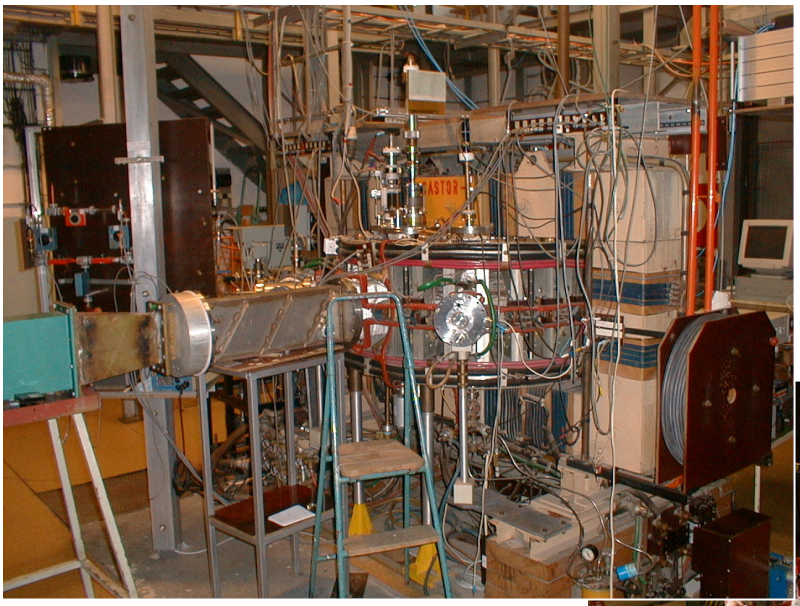

The CASTOR Tokamak

The NRI Fission reactor LVR-15

The NPI Fast Neutron Facility

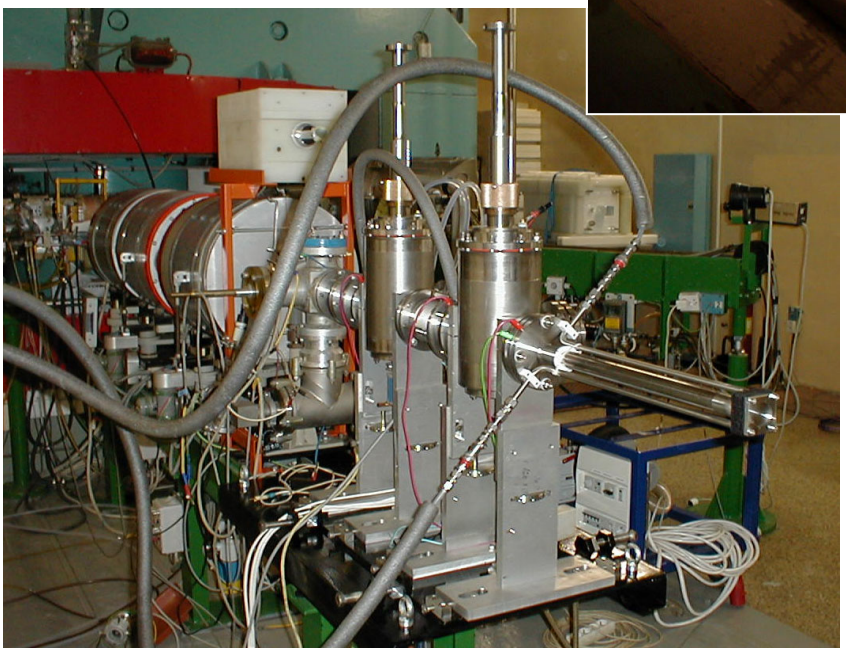

II PHYSICS

Overview of Activities - PHYSICS

The main areas of the research undertaken in the Association EURATOM/IPP.CR in 2006 were as follows:

1. Edge Plasma, Plasma-Wall Interaction and Magnetic Confinement Physics
2. Diagnostics Development
3. Wave Interactions in Plasmas
4. Atomic Physics and Data for Edge Plasma and Plasma Wall Interactions

Here, the most important results, activities and achievements are briefly summarized; details are given in sections II.1 – II.4 that follow the list of publications. Notice that the major part of the Association activities in Physics relies on broad collaboration with other EURATOM Associations.

1. Edge Plasma, Plasma-Wall Interaction and Magnetic Confinement Physics

Dynamics of the edge transport barrier at plasma biasing on the CASTOR tokamak A clear and reproducible transition to a regime with improved particle confinement has been studied in the CASTOR tokamak at edge plasma biasing. Fast relaxations of the edge profiles, with a frequency of about 10 kHz are observed, if the biasing electrode is inserted deep enough into the plasma (r/a ~ 0.5) of the CASTOR tokamak and biased above +250V [11,31,33,49,63]. Recently, more detail measurement of the dynamics of the relaxation events are studied by means of a new rake probe consisting of two rows of tips. This arrangement allows study the spatial temporal evolution of the radial and poloidal electric field in the transport barrier. It is demonstrated that the electric field resulting from plasma biasing is not strictly radial. A relatively strong poloidal electric field, which drives directly the edge plasma either inward or outwards is observed [66].

Asymmetries in SOL plasma measured by advanced oriented Langmuir probes on the CASTOR tokamak. Directional asymmetries in the radial profiles of ion saturation current, floating potential and electron temperature are investigated in the edge plasma of the CASTOR tokamak. Measurements by a radial array of conventional cylindrical Langmuir probes are compared with a novel diagnostic, the tunnel probe. The bidirectionality of the latter enables to distinguish the plasma behavior upstream and downstream along the magnetic field lines not only in case of flows but in electron temperature and floating potential as well. A hot tail of suprathermal electrons in the counter-current direction explains the observed asymmetries. Moreover, the collectors of the tunnel probe are concave, eliminating in theory any uncertainty of the effective collecting area that is needed to calibrate the probe for measurements of parallel ion current density. By direct comparison between the two types of probes, the effective collecting area of the conventional probe can be measured. It is found to be significantly larger than its geometrical cross section, clearly

demonstrating the effect of sheath expansion, which is also in concordance with the difference in floating potential measured by the two probes.

Edge plasma characterization in JET discharge scenarios with weak and strong internal transport barriers. Edge plasma characterization in discharge scenarios with weak and strong internal transport barriers was undertaken. We started to build up the database of around 80 relevant quantities measured during the S2 and S1 discharges in order to derive conclusions on compatibility of edge plasma during these "advanced scenarios" with wall and compare it with standard situation of ELMing H-mod edge. The database aim to characterize plasma geometry, basic plasma parameters including profiles of T_e, n_e, T_i, and all edge and SOL properties which are currently measured on JET. Each quantity is represented in this database by its average value in a user specified time window at any number of intervals in any given discharge. The main activities thus far include interaction with the responsible officers for each diagnostic in order to identify the best signals to be included into the database, pre-processing of some of the signals, preparing the configuration files for MDB, and tests of consistency of the initial versions of the database.

Characterization of the JET SOL and edge turbulence, comparison with edge turbulence model ESEL. The analysis of the turbulent density structures, represented by the ion saturation current signals in the JET SOL region and in the edge plasma was prepared. Ohmic discharges, which regime will be compared with the ESEL (Edge – SOL electrostatic) model later on, were of the main interest. Discharges in deuterium and helium are included in the database list. Statistical quantities – standard deviation, skewness, and kurtosis – and the probability distribution functions were determined with a sufficient radial resolution for individual signals from several shots.

Fluctuation studies on the CASTOR tokamak with the double rake probe. A newly designed probe head – the double rake probe has allowed determination of the position of the velocity shear layer on CASTOR with a precision ~ 1 mm. It is demonstrated that the position of the velocity shear layer is identical with the position of the last closed magnetic surface. The phase velocity deduced from correlation analysis roughly agrees with that deduced from the gradient of the floating potential [77, 3, 4].

Experimental measurements of the SOL parallel flows on the tokamak TCV. Ion flows parallel to the magnetic field in the tokamak scrape-off layer (SOL) are now widely suspected to be an important player in the process of material migration, itself known to influence fuel retention. Experiments on the TCV tokamak outside midplane have clearly identified (within a 10% error) the principal theoretical components of parallel flows: the dominant Pfirsch-Schlüter flow, much weaker ballooning-driven field-independent flow, and finally the divertor-sink flow was found to be negligible.

Evidence for a poloidally localized enhancement of radial transport in the scrape-off layer of the Tore Supra tokamak. Near-sonic parallel flows are systematically observed in the far scrape-off layer (SOL) of the limiter tokamak Tore Supra, as in many L-mode X-point divertor tokamak plasmas. The poloidal variation of the parallel flow has been measured by moving the contact point of a small circular plasma onto limiters at different poloidal angles [25,26]. The resulting variations of flow are consistent with the existence of a poloidally localized enhancement of radial transport concentrated in a 30° sector near the outboard midplane. If the plasma contact point is placed on the inboard limiters, then the SOL expands

to fill all the space between the plasma and the outboard limiters, with density decay lengths between 10 and 20 cm. On the other hand, if the contact point lies on the outboard limiters, the localized plasma outflux is scraped off and the SOL is very thin with decay lengths around 2 to 3 cm. The outboard radial transport would have to be about two orders of magnitude stronger than inboard to explain these results.

Edge tokamak plasma turbulence: comparison of experiments with a 2D interchange turbulence model ESEL. Boundary plasma interaction with the first wall determines strongly operation of future thermonuclear fusion reactors, such as ITER. Even though plasma turbulence had been considered responsible for the anomalously high radial particle transport observed in the tokamak boundaries for decades, and many related models have been developed, they were not capable to quantitatively describe the experimental observations until recently. Two-dimensional fluid model ESEL of interchange instability driven by classical plasma drifts are directly compared with experimental observations from the TCV tokamak (Switzerland). Excellent agreement with statistical character of most of the experimentally available data of a particular discharge demonstrates that the model is close to a valid description of the edge plasma turbulent transport. We further verify the model in various operational regimes including also the CASTOR tokamak, profiting from the installed unique Tunnel probe capable of fast temperature fluctuation measurement, filling thus the important missing gap in this model-experiment comparison.

SOL ionization by the lower hybrid wave during gas puffing. Gas puffing with a gas pipe situated near the JET Lower Hybrid (LH) antenna increases the scrape-off layer (SOL) electron density, ne,SOL, in the region magnetically connected to the gas pipe, which improves the LH wave coupling. This is important namely for ITER relevant shots with a large distance between separatrix and the LH grill mouth. The numerical modelling presented in this work shows the importance of taking into account an effect of the LH power on the SOL temperature, and hence on the ionisation, when modelling the SOL plasma. We studied the effects of variations of the gas puff and of the SOL heating rate, and we also considered effects of SOL heating by the fast particles. The gas puff without or with a low LH heating cools the SOL. On the contrary, large enough LH heating enhances the SOL plasma temperature and also the density. This SOL temperature enhancement is maximum without the gas puff. However, when the gas puff is accompanied by a large enough SOL heating, the SOL plasma density strongly rises, which can explain the observed improvement of the LH wave coupling. The modelled density growth is consistent with the modelled SOL ionisation source profiles, which for puff and heating are strongly enhanced and extend into the far SOL, contrary to the case without heating and/or without the gas puff. [50], [46], [70].

Anomalous diffusion of particles from tokamaks in presence of magnetic and electro-static perturbations. We have simulated ion diffusion in a system of magnetic islands using a fully Hamiltonian approach and compared the results to the traditional approach of field line tracing. The comparison revealed some surprising differences [12, 35]. We have also simulated ion diffusion in a periodic electrostatic potential, where the dynamics show interesting Levy-flight type behavior.

Self-consistent 2D simulations of plasma deposition in castellated tile gaps. In order to withstand thermomechanical stress in ITER's divertor, its armour will be castellated. Carbon layers and tritium will accumulate inside the gaps that separate the tiles. Experimental studies already show significant deposited layers in the gaps. We present here a two-dimensional

numerical study of plasma deposition inside the tile gaps using a standard particle-in-cell technique. The plasma deposition with respect to the depth and the width of the gap for different inclinations of the magnetic field lines are performed. Particle flow asymmetries occurring inside the gap are of particular interest, where strong electric fields govern the trajectories with the orientation of the magnetic field due to ExB drifts.

2. Diagnostics Development

A new probe-based method for measuring the diffusion coefficient in the tokamak edge region. A new method for measuring the diffusion coefficient in the edge plasma of fusion devices was developed. The method is based on studying the decay of the plasma fluctuation spectrum inside a small ceramic tube having its mouth flush with a magnetic surface and its axis aligned along the radial direction. The plasma fluctuations are detected by an electrode, radially movable inside the tube. The measurement was performed at different radial positions in the CASTOR edge region, so that a radial profile of the diffusion coefficient was obtained. Typical values of D are of 2-3 m^2/s, consistent with expectations from the global particle balance. The radial profile shows a tendency of the diffusion coefficient to increase going deeper into the plasma.

Development of advanced probe for edge tokamak plasmas. In accord with the work programme 2006 at the Faculty of Mathematics and Physics there continued the work on development of advanced probe for edge tokamak plasmas. The work progressed in collaboration with IPP in Prague, with association EURATOM-ÖAW, the group of Prof. R. Schrittwieser, and partly with Consorzio RFX, Padova, Italy, Prof. E. Martines. Several students from Innsbruck who participated in the research with emissive probe came to Prague in frame of CEEPUS project CII-AT-0063-02-0607 - “Applications and diagnostics of electric plasmas” coordinated by Prof. R. Schrittwieser. Proceeded also the development of particle codes for the simulation of processes in high-temperature plasma in the presence of magnetic fields in two and three dimensions. The publications concern mainly the investigations aimed at the understanding of the effect of the space charge around the emissive probe and of the variations of the electron saturation current of the emissive probe. The work, which arose from collaboration with RFX Padova deals with frequency analysis of fluctuations in low-temperature magnetized plasma of dc discharge in cylindrical magnetron. [6, 24, 36, 37, 52, 62].

Design of the Ball-pen probe for RFX and the first test. Four Ball-pen probes has been constructed for the direct measurements of the plasma potential on RFX in the edge plasma. The first successful test provided the information of optimal experimental arrangement and the radial profile of the plasma potential. Moreover, the radial profile of the electron temperature has been estimated from measured values of the plasma and floating potential.

Development and fabrication of RF probes for Tore Supra. A new system of RF miniaturized double probes for detecting and transmitting signals up to 10GHz has been designed and manufactured in the frame of long term collaboration between Associations IPP.CR, Prague and EURATOM-CEA, CEA/DSM/DRFC, CEA-Cadarache. The RF probes will be used for measurements of the wave as well as plasma parameters in the place connected by magnetic field lines directly with the LHW interaction region in front of the new LH C4 launcher on the tokamak Tore Supra.

Ion temperature measurements in the tokamak scrape-off layer The ion temperature is a particularly important but rarely measured plasma boundary quantity. We introduce a new electric probe, the segmented tunnel probe (STP), which measures ion temperature, electron temperature, and parallel ion current density simultaneously and with high temporal resolution. The probe was built and tested in the CASTOR tokamak. The STP was operated in a Mach-probe arrangement in a DC mode, providing bi-directional measurements with the temporal resolution of 1μs. Therefore, it has significant potential to be employed in the research of transient phenomena in tokamaks (e.g. turbulence, fluctuations and ELMs). We present radial profiles of the plasma parameters in the CASTOR tokamak measured by the STP [33], using calibrations from particle-in-cell simulations.

Fast bolometric measurements and a visualization of radiation fluctuations on the CASTOR tokamak. Fast AXUV-based bolometric arrays with unique temporal resolution of 1 μs and spatial resolution of about 1 cm and a very high signal to noise ratio allow a visualization of fine structures on the radiated power profile. A combination of the singular value decomposition (SVD), the cross-correlation analysis and the tomography is the best option to reach the desirable information. Typically, the dominating main plasma profile, a poloidally rotating asymmetric component and radially moving structures corresponding to symmetric component can be decomposed in the CASTOR shots [77]. The same method based on SVD applied on fast bolometric and SXR data was used for the analysis of snake-like structures after pellet injection in the T-10 tokamak [78]. The Cormack method of the tomographic reconstruction was implemented and was found it is suitable and very valuable for the analyses of the CASTOR plasma profiles, however, useless for the reconstruction of small-scale structures. Hence, more sophisticated tomographic methods are deliberated for such purposes in future.

Measurements of line radiation power in the CASTOR tokamak. The determination of absolute values of radiated power of selected spectral lines is required for comparison of VUV spectroscopic data with bolometric measurements to estimate the full radiated power and also the impurity content in plasma. In the paper the procedure of calibration of VUV spatial imaging spectrometer is described. The comparison of measured radiation power in different spectral regions is presented.

Implementation of Cherenkov detectors for measurements of suprathermal electrons in the CASTOR plasma. A prototype of the Cherenkov detector adapted to CASTOR experimental conditions was designed, constructed and placed on a movable manipulator enabling the measurements in different positions along the minor radius to be performed. The detection head contains a Cherenkov-radiator made of an aluminium-nitride (AlN) crystal protected from the visible light by the deposited Ti-layer. The radiator is fixed upon a light-pipe, which is made of a polished quartz rode placed inside the stainless-steel tube. The induced Cherenkov radiation is detected by means of a photomultiplier placed inside a shielding. The first experimental results demonstrate a generation of relatively intense Cherenkov signals depending on toroidal magnetic field and strongly different in the confined and non-confined plasma regions [32].

Carbon transport measurements at TCV. Knowledge of the impurity transport parameters and their relation with those of the main plasma particles is important for predicting the fusion performance of a tokamak reactor and provides an element for validating advanced transport models currently under development. The radial profiles of fully ionized carbon

C6+ (transition n=8-7, 529.1 nm) released from TCV (R = 0.88 m, a<0.25m, BT<1.5 T) wall tiles were measured using active Charge eXchange Recombination Spectroscopy (CXRS) [80]. A 1D impurity transport model was used to infer carbon transport parameters from the steady state profiles of fully ionized carbon. At high q95 a phenomenon of impurity accumulation of anomalous (rather than neoclassical) origin is observed.

JET neutron data analyses via inversion algorithms based on Minimum Fisher Regularisation. Analyses of neutron data form an integral part of the burning plasma diagnostics, where JET (under Task Force D) makes a key contribution to ITER [41]. The inversion methods based on Minimum Fisher Regularisation (MFR) have been successfully validated in collaboration with the Association Euratom-IPP.CR at JET, both in spatial analyses of plasma neutron emissivitiesmeasured by the JET profile monitor (MFR tomography, [9], [40]) and in spectral analyses of neutrons measured by the NE213 compact spectrometer (MFR unfolding, [39]).

Development and tests of Hall probe based magnetic diagnostics for fusion devices. Use of various configurations of flux loops for measurement of magnetic field in fusion devices is inherently limited by the pulsed operation of these machines. A principally new diagnostic method must be developed to complement the magnetic measurements in true steady state regime of operation of fusion reactor. One of the options is the use of diagnostics based on Hall sensors. Several experiments dedicated to testing of various types of Hall probes were done and are being prepared on CASTOR, JET, and TJ-II. In particular, the Hall probe based diagnostics were used to measure plasma position and safety factor profile on CASTOR, [34], [57], [58], [77]. Exploitation of Hall probes on TJ-II for turbulence studies is being prepared as well as ex-vessel measurements with the ITER candidate Hall sensors on JET [7].

Assessment of the techniques for in-situ calibration of impurity monitor for the ITER in connection with deterioration of the optical components. In the hard environmental conditions during long burn discharges in ITER, the deterioration of the optical components in the Diverter Impurity Monitor give rise to concern oneself with the correctness of measurements. The arrangement like a running in-situ recalibration of the monitor system performance and an axis optical alignment of elements guarantee a preservation of credibility of the spectroscopy data. Calibration issues regard preservation of the integrity of calibration, determination of the spectral efficiency over the 200 – 1000 nm range and alignment issues. The design of the Divertor Impurity Monitor is in its early stages, which allows considering some extra amendments, which may be beneficial for in-situ monitoring of system performance: (i) An integrated calibration beam line as a common line of sight for visible and VUV spectrometers that use black body thermal emission in the visible range and branching ratio cross calibration method in the VUV range, (ii) The installation of a diagnostic neutral beam injector in the divertor port for in-situ monitoring of the changes in transmission of lines of sight by means of Beam Emission Spectroscopy, and (iii) The injection of an exact amount of impurity in the form of preheated solid pellets or target illumination by a powerful laser.

3. Wave Interactions in Plasmas

Energy Distribution Measurements of Fast Particles Generated in Front of the LH Grill Mouth in Tore Supra. A retarding field analyzer (RFA) was used during lower hybrid (LH)

current drive experiments in the Tore Supra tokamak to characterize the supra-thermal particles emanating from the region in front of the LH grill. This work is the continuation of our previous efforts. In addition to fast electrons, we tried to observe fast ions accelerated due to a positive charge accumulated (and measured in the CASTOR tokamak) in front of the LH grill. The main results are: By varying the edge safety factor, we optimized the connection between RFA and the LH grill to obtain a maximum intensity of the fast electron beam. Clear indications of a fine poloidal structure were obtained for the first time. A strong variation of fast electron beam current with lower hybrid power was identified. For high power levels (greater than 1 MW), the electron energy is greater than 400 eV. Fast electrons exist even at low power levels (between 0.5 and 0.75 MW), and their energy is lower than 400 eV. These fast electron energy limits are consistent with a simple model of electron acceleration in the near-field of LH antennas. After separating those fast electrons from the RFA signal, we observe pure ion current. No clear evidence of suprathermal ions was found on the ion current profiles, but the decisive experiment that will separate thermals from suprathermals could not be performed due to technical problems. [51], [19], [23].

Electron Bernstein wave simulation for MAST and NSTX. Electron Bernstein wave emission simulation EBWE has been further developed [72,75]. MAST ELM-free H-mode simulation has been thoroughly analyzed and possibilities of magnetic field and density profile reconstructions are shown [72,60]. Recent NSTX EBE experiments and simulations analysis has been performed with good understanding of certain discharge types. Further experimental and modeling work is in progress [16,17,27,55,67,68,69,73,74,76].

Simulations of EBW heating in WEGA. 2.45 GHz electron Bersntein wave heating system for the WEGA stellarator has been simulated. Experiments show a resonant principle of the wave damping and the best performance with low magnetic fields. Simulations show possible mechanisms for this behaviour.

4. Atomic Physics and Data for Edge Plasma and Plasma Wall Interactions

Energy transfer and chemical reactions in collisions of ions with surfaces. Collisions of selected C_1 (CD_4^+, CD_5^+) and C_2 ($C_2D_4^+$) slow (15-50 eV) hydrocarbon ions with room-temperature and heated (600^0C) tungsten surfaces were studied by the scattering method and the results were compared with the previous results on scattering of these ions from carbon (HOPG) surfaces. The ion survival probability for ions incident on the surface under 30^0 were in general by up to 10-times lower than for the corresponding carbon surfaces. The collisions were in general strongly inelastic and – in case of room-temperature surfaces- product ion originated from both direct fragmentation of the projectile ion and from chemical reactions at surfaces (H-atom transfer, carbon chain build-up reactions), similarly as in the case of carbon surfaces. For heated surfaces, they originated only from fragmentation of the projectile ions (indication of surface removal by heating). Preliminary results on collisions of the hydrocarbon ions with beryllium surfaces indicate structures in both translational energy and angular distributions of the product ions, evidently connected with islands of oxides and carbides on the Be surface.

LIST OF PUBLICATIONS 2006 – PHYSICS

[1]	**Adámek J., Stöckel J., Panek R., Kocan M., Martines E., Schrittwieser R., Ionita C., Popa G., Costin C., Brotánková J., Van Oost G., van Peppel L.**: Simultaneous measurements of the parallel and perpendicular ion temperature by Katsumata and segmentwed tunnel probe. *9th Workshop "Electric Fields, Structures and Relaxation in Edge Plasmas",* Rome, Italy, 26-27 June, 2006, *Book of Abstracts*, p.13.
[2]	**Bencze A., Berta M., Zoletnik S., Stöckel J., Adamek J., Hron M.:** Observation of zonal flow-like structures using autocorrelation-width technique. *Plasma Phys. Control. Fusion* **48** (2006) S137-S153.
[3]	**Berta M., Bencze A., Tál B., Zoletnik S., Stöckel J., Hron M., Zajac J.**: The spatial structure of flows, Reynolds stress and turbulence in the CASTOR tokamak. *9th Workshop "Electric Fields, Structures and Relaxation in Edge Plasmas",* Rome, Italy, 26-27 June, 2006, *Book of Abstracts*, p.3
[4]	**Berta M., Tál B., Bencze A., Zoletnik S., Stöckel J., Hron M., Dejarnac R., Zajac J.**: The spatial structure of flows, Reynolds stress and turbulence in the CASTOR tokamak. *33rd EPS Conference on Plasma Phys. Contr. Fusion,* Rome, Italy, 19 – 23 June 2006, ECA Vol. **30I**, P-4.074.
[5]	**Bilykova O., Fuchs V., Pánek R., Urban J., Žáček F., Stöckel J., Voitsekhovitch I., Valovič M., Fitzgerald M.:** COMPASS-D magnetic equilibria with LH and NBI current drive. *Czech. J. Phys.* **56** [suppl.B] (2006) B24-B30.
[6]	**Bilykova O., Holík M., Kudrna P., Marek A., Tichý M.:** Observation of Wave-Like Structures in Magnetized DC Discharge in Cylindrical Symmetry in Argon, Contributions to Plasma Physics 46, 361-366, 2006.
[7]	**Bolshakova I., Coccorese V., Ďuran I., Gerasimov S., Holyaka R., Moreau P., Murari A., Saint-Laurent F., Stöckel J. and JET EFDA Contributors**: Present-day experience in the use of galvanomagnetic radiation hard transducers in fusion device. *Proceedings of 13th International Congress on Plasma Physics*, Kiev, Ukraine, 22 – 26 May 2006, B121p.
[8]	**Bonheure G., Popovichev S., Bertalot L., Murari A., Conroy S., Mlynář J., Voitsekhovitch I., JET EFDA:** Neutron Profiles and Fuel Ratio nT/nD Measurements in JET ELMy H-mode Plasmas with Tritium Puff. *Nuclear Fusion* **46** [7] (2006) 725-740.
[9]	**Brotánková J., Martines E., Adámek J., Popa G., Costin C., Schrittwieser R., Ionita C., Stöckel J., Van Oost G., van de Peppel L.:** A probe-based metod for measuring the transport coefficient in the tokamak edge region. *Czech. J. Phys.* **56** [12] (2006) 1321.
[10]	**Brotánková J., Martines E., Adámek J., Popa G., Costin C., Schrittwieser R., Ionita C., Stöckel J., Van Oost G., van de Peppel L.:** A new probe-based metod for measuring the diffusion coefficient in the tokamak edge region. *33rd EPS Conference on Plasma Phys. Contr. Fusion,* Rome, Italy, 19 – 23 June 2006, ECA Vol. **30I**, P-2.195.
[11]	**Brotánková J., Spolaore M., Stöckel J., Peleman P., Hron M., Stepan M.:** Deep analysis of relaxation events on the CASTOR tokamak. In: *Proceedings of Contributed Papers WDS'06*, Faculty of Mathematics and Physics, Charles University, Prague 2006, Part II, p. 227-232.
[12]	**Cahyna P., Krlín L.:** Full Hamiltonian description of the interaction of particles with magnetic islands in tokamak. *Czech. J. Phys.* **56** [4] (2006) 367-380.
[13]	**Dejarnac R., Gunn J.P.:** Kinetic calculation of plasma deposition in castellated tile gaps. *17th International Conference on Plasma Surface Interaction in Controlled Fusion Devices (PSI-17)*, 22 – 26 May 2006, Hefei, Anhui, China, p. P3-23.
[14]	**Dejarnac R., Gunn J.P.:** Self-consistent 2D simulations of plasma deposition in tile gaps. *33rd EPS Conference on Plasma Phys. Contr. Fusion,* Rome, Italy, 19 – 23 June 2006, ECA Vol. **30I**, D-5.018.

[15]	**Devynck P., Brotánková J., Peleman P., Spolaore M., Figueiredo H., Hron M., Kirnev G., Martines E., Stöckel J., Van Oost G., Weinzettl V.:** Dynamics of turbulent transport in the scrape-off layer of the CASTOR tokamak. *Physics and Plasmas*. **13**, 10 (2006), 102505-102513
[16]	**Diem S.J., Taylor G., Efthimion P., LeBlanc B.P., Philips C.K., Caughman J., Wilgen J.B., Harvey R.W., Preinhaelter J., Urban J.:** Thermal Electron Bernstein Wave Emission Measurements on NST. *Bulletin of the American Physical Society, 48th Annual Meeting of the Division of Plasma Physics*, Philadelphia, Pennsylvania, 30 October – 3 November 2006, paper NO1.00012, p. 134.
[17]	**Diem S.J., Taylor G., Efthimion P.C., LeBlanc P.C., Carter M., Caughman J., Wilgen J.B., Harvey R.W., Preinhaelter J., Urban J.:** Te(R, t) measurements using electron Bernstein wave thermal emission on NSTX. *Review of Scientific Instruments* **77** [10] (2006), 10E919, 1-10E919,4.
[18]	**Ďuran I., Vierebl L., Klupák V., Bolshakova I., Holyaka R.:** Investigation of stability of ITER candidate Hall sensors under neutron irradiation. *Czech. J. Phys.* **56** [suppl. B] (2006) B54-B60.
[19]	**Ekedahl A., Goniche M., Basiuk V., Bibet Ph., Chantant M., Colas L., Delpech L., Eriksson L-G., Joffrin E., Kazarian F., Moreau Ph., Petrzilka V., Portafaix C., Prou M., Roche H.:** Thermal and Non-Thermal Particle Interaction with the LHCD Launchers in Tore Supra. *Seventeenth International Conference on Plasma Surface Interaction in Controlled Fusion Devices* (PSI-17), 22 - 26 May 2006, Hefei Anhui, China, paper O-8 (oral).
[20]	**Fasoli A. for the TCV Team: Alberti S., ... , ... , Piffl V., ... , ... , Zucca C.:** Overview of TCV Results. In: *Proc. 21st IAEA Fusion Energy Conference*, October 16-21, 2006, Chengdu, China, paper OV/3-3.
[21]	**Fuchs V. and Gunn J.P.:** On the Integration of Equations of Motion for Particle-in-cell Codes. *J. Comput. Phys.*, 214 (2006) 299- 315.
[22]	**Fuchs V., Voitsekhovitch I., Bilyková O., Fitzgerald M., Pánek R., Urban J., Valovič M., Žáček F., Stöckel J.:** Modelling of plasma performance on COMPASS-D tokamak in the presence of NBI and LHCD, *33rd EPS Conference on Plasma Phys. Contr. Fusion,* Rome, Italy, 19 – 23 June 2006, ECA Vol. **30I**, P-1.103.
[23]	**Goniche M., Colas L., Ekedahl A., Chantant M., Petržílka V., Basiuk V., Bibet Ph., Delpech L., Eriksson L.-G., Gunn J., Heuraux S., Joffrin E., Kazarian F., Lombard G., Lowry C., Millon L., Mollard P., Moreau P., Portafaix C., Prou M., Roche H., Travère J.M.:** Interactions of RF Antennas with the Edge Plasma in Tore Supra Steady-State Discharges. *21st IAEA Fusion Energy Conference*, Chengdu, China, paper EX/P6-12.
[24]	**Gstrein R., Marek A., Ionita C., Kudrna P., Olenici S.B., Balan P.C., Schrittwieser R., Tichy M.:** Space Charge Effects Of Emissive Probes Investigated In A DP-Machine, *ICPP'06 Proceedings contributed papers CD,* paper A181, CD – A181p.pdf, 1-4, 2006.
[25]	**Gunn J. P., Boucher C., Dionne M., Ďuran I., Fuchs V., Loarer T., Nanobashvili I., Pánek R., Pascal J.Y., Saint-Laurent F., Stöckel J., Van Rompuy T., Zagórski R., Adámek J., Bucalossi J., Ciraolo G., Dejarnac R., Devynck P., Ghendrih P., Hertout P., Hron M., Moreau P., Pégourié B., Rimini F.G., Sarazin Y., Sarkissian A., Van Oost G.:** Links Between Wide Scrape-Off Layers, Large Parallel Flows, and Bursty Transport in Tokamaks. In: *Proceedings of 21st IAEA Fusion Energy Conference*, October 16-21, 2006, Chengdu, China, paper EX/P4-9.
[26]	**Gunn J., Boucher C., Dionne M., Ďuran I., Fuchs V., Loarer T., Nanobashvili I., Pánek R., Pascal J.-Y., Saint-Laurent F., Stöckel J., Van Rompuy T., Zagorski R., Adámek J., Bucalossi J., Dejarnac R., Devynck P., Hertout P., Hron M., Lebrun G., Moreau P., Rimini F., Sarkissian A., Van Oost G.:** Evidence for a poloidally localized enhancement of radial transport in the scrape-off layer of the Tore Supra tokamak. *17th International Conference on Plasma Surface Interaction in Controlled Fusion Devices (PSI-17)*, 22 – 26 May 2006, Hefei, Anhui, China.

[27]	**Harvey R.W., Cary J.R., Taylor G., Barnes D.C., Bigelow T.S., Coda S., Carlsson J., Caughman J.B., Carter M.D., Diem S., Efthimion P.C., Ellis R.A., Ershov N.M., Fonck R.J., Fredd E., Gartska G.D., Hosea J., Jaeger F., LeBlanck B., Lewicki B.T., Phillips C.K., Preinhaelter J., Ram A.K., Rasmussen D.A., Smirnov A.P., Urban J., Wilgen J.B., Wilson J.R., Xiang N.:** Electron Bernstein Wave Studies: Current Drive; Emission and Absorption with Nonthermal Distributions; Delta-F Particle in Cell Simulations. In: *Proceedings of 21st IAEA Fusion Energy Conference*, October 16-21, 2006, Chengdu, China, paper TH/P6-11.
[28]	**Hegazy H., Žáček F.:** Absolute measurements of the magnetic field generated by different coils in the center of EGYPTOR tokamak. *Journal of Fusion Energy* **25** (2006) 115-120.
[29]	**Hegazy H., Žáček F.:** Calibration of power systems and measurements of discharge currents generated for different coils in the EGYPTOR tokamak. *Journal of Fusion Energy* **25** (2006) 73-86.
[30]	**Horacek J., Garcia O.E., Pitts R.A., Nielsen A.H., Fundamenski W., Graves J.P., Naulin V., Rasmussen J.J.:** Understanding SOL plasma turbulence by interchange motions. *Oral at Workshop on Edge Transport in Fusion plasmas*, 11 – 13 September 2006, Kraków, Poland.
[31]	**Hron M., Peleman P., Spolaore M., Brotánková J., Dejarnac R., Bilykova O., Sentkerestiova J., Ďuran I., van de Peppel L., Gunn J., Stöckel J., Van Oost G., Horacek J., Adámek J., Stepan M.:** Detailed measurements of momentum balance during the periodic collapse of a transport barier. *33rd EPS Conference on Plasma Phys. Contr. Fusion,* Rome, Italy, 19 – 23 June 2006, ECA Vol. **30I**, P-4.076.
[32]	**Jakubowski L., Stanislawski J., Sadowski J. M., Zebrowski J., Weinzettl V., Stöckel J.:** Design and Tests of Cherenkov Detector for Measurements of Fast Electrons within Castor Tokamak. *Czech. J. Phys.* **56** [suppl. B] (2006) B98-B103.
[33]	**Kočan M., Pánek R., Stöckel J., Hron M., Gunn J.P., Dejarnac R.:** Ion temperature measurements in the tokamak scrape-off layer. *17th International Conference on Plasma Surface Interaction in Controlled Fusion Devices (PSI-17)*, 22 – 26 May 2006, Hefei, Anhui, China.
[34]	**Kovařík K., Ďuran I., Bolshakova I., Holyaka R., Erashok V.:** Measurement of Safety Factor Using Hall Probes on CASTOR Tokamak. *Czech. J. Phys.* **56** [suppl. B] (2006) B104-B110.
[35]	**Krlín L., Cahyna P.:** Particle diffusion in a system of magnetic islands in tokamaks in fully Hamiltonian approach. *Czech. J. Phys.* **56** [suppl. B] (2006) B111-B117.
[36]	**Marek A., Picková I., Kudrna P., Tichý M., Apetrei R.P., Olenici S.B., Gstrein R., Schrittwieser R., Ionita C.:** Experimental Investigation of the Change of the Electron Saturation Current of a dc-heated Emissive Probe, Czech. Jour. Phys, Suppl B, 56, B932-B937, 2006.
[37]	**Marek A., Apetrei R.P., Olenici S.B., Gstrein R., Pickova I., Kudrna P, Tichý M., Schrittwieser R**.: Emissive Probe Measurements in the DC Low Temperature Magnetized Plasma in Cylindrical Configuration, *ICPP'06 Proceedings contributed papers CD,* paper A168, CD – A168p.pdf, 1-4, 2006.
[38]	**Matějíček J., Weinzettl V., Dufková E., Piffl V., Peřina V.:** Plasma Sprayed Tungsten-based Coatings and their Usage in Edge Plasma Region of Tokamaks. *Acta Technica CSAV* **51** [2] (2006) 179-191.
[39]	**Mlynář J., Bertalot L., Tsalas M., Bonheure G., Conroy S. and JET-EFDA contributors:** Neutron Spectra Unfolding with Minimum Fisher Regularisation. In: *Proceedings of Science PoS(FNDA2006)063, International Workshop on Fast Neutron Detectors and Applications*, 3 – 6 April 2006, University of Cape Town, http://pos.sissa.it//archive/conferences/025/063/FNDA2006_063.pdf
[40]	**Mlynář J., Bonheure G., Murari A. and JET EFDA Contributors:** Prospects of the Minimum Fisher Regularisation in the Experimental Analyses of Plasma Particle Transport at JET. *48th Annual Meeting of the Division of Plasma Physics, Bull. Am. Phys. Soc.* p.196.

[41]	**Mlynář J., Bonheure G., Murari A., Bertalot L., Angelone M., Pillon M., Conroy S., Ericsson G., Kaellne J., Popovichev S., JET EFDA:** Progress in Neutron Diagnostics at JET. *Czech. J. Phys.* **56** [suppl. B] (2006) B118-B124.
[42]	**Neto A., Fernandes H., Duarte A., Carvalho B., Sousa J., Valcárcel D., Varandas C., Hron M.:** FireSignal – Data Acquisition and Control System Software. *24th Symposium on Fusion Technology*, 11 – 15 September 2006, Warsaw, Poland, P1-D-466.
[43]	**Neto A., Fernandes H., Valcárcel D., Varandas C., Vega J., Sánchez E., Pena A., Hron M.:** A standard data access layer for vision devices. *Ibid.,* P1-D-463.
[44]	**Notkin M.E., Livshits A.I., Hron M., Stöckel J.:** Absorption of suprathermal hydrogen particles at the CASTOR tokamak. *33rd EPS Conference on Plasma Phys. Contr. Fusion,* Rome, Italy, 19 – 23 June 2006, ECA Vol. **30I**, P-4.075.
[45]	**Notkin M.E., Livshits A.I., Hron M., Stöckel J.:** Measurements of the suprathermal hydrogen flux on the CASTOR tokamak, *Nuclear Instruments & Methods in Physics Research, Section B-Beam Interactions with Materials and Atoms* **251** [2] (2006) 512-516.
[46]	**Ongena J., Eriksson L.G., Graves J.P., Mayoral M.L., Mailloux J., Petržílka V., et al.:** Recent progress in JET on Heating and Current Drive studies in view of ITER. In: *Proceedings of 21st IAEA Fusion Energy Conference*, October 16-21, 2006, Chengdu, China, paper EX/P6-9.
[47]	**Pánek R. and CASTOR team**: Current ststus of the project for re-installation of the COMPASS-D tokamak at IPP Prague. In: *Sixth International Workshop and Summer School - Towards Fusion Energy - Plasma Physics, Diagnostics, Spin-offs* Kudowa Zdrój, Poland 18 - 22 September 2006 (Invited lecture)
[48]	**Pánek R., Bilyková O., Fuchs V., Hron M., Chráska P., Pavlo P., Stöckel J., Urban J., Weinzettl V., Zajac J., Žáček F.:** Reinstallation of the COMPASS-D tokamak in IPP ASCR. *Czech. J. Phys.* **56** [suppl. B] (2006) B125-B137.
[49]	**Peleman P., Xu Y., Spolaore M., Brotánkova J., Devynck P., Stöckel J., Van Oost G., Boucher C.:** Highly resolved measurements of periodic radial electric field and associated relaxations in edge biasing experiments. *17th International Conference on Plasma Surface Interaction in Controlled Fusion Devices (PSI-17)*, 22 – 26 May 2006, Hefei, Anhui, China, P3-23.
[50]	**Petržílka V., Corrigan G., Parail V., Erents K., Goniche M., Baranov Y., Belo P., Ekedahl A., Mailloux J., Ongena J., Silva C., Spence J., Žáček F. and JET EFDA contributors**: SOL ionization by the lower hybrid wave during gas puffing, *33rd EPS Conference on Plasma Phys. Contr. Fusion,* Rome, Italy, 19 – 23 June 2006, ECA Vol. **30I**, P-1.067.
[51]	**Petržílka V., Gunn J.P., Goniche M., L. Colas, Ekedahl A., Gauthier E., Mailloux J., Mazon D., Nanobashvili I., Pascal J.–Y., Žáček F.:** Energy Distribution Measurements of Fast Particles Generated in Front of the LH Grill Mouth in Tore Supra. *Ibid.*, P-5.108.
[52]	**Pickova I., Marek A., Tichý M., Kudrna P., Apetrei R.P.:** Measurements with the Emissive Probe in the Cylindrical Magnetron, Czech. Jour. Phys, Suppl. B, 56, B1002-B1008, 2006.
[53]	**Piffl V., Burdakov A., Korneva N., Polosatkin S., Weinzettl V.:** Measurements of line radiation power in the CASTOR tokamak. *Ibid.*, P-2.196.
[54]	**Plyusnin V.V., Riccardo V., Jaspers R., Alper B., Kiptily V.G., Mlynář J., Popovichev S., de La Luna E., Andersson F., JET EFDA:** Study of runaway electron generation during major disruptions in JET. *Nuclear Fusion*. **46**, 2 (2006), 277-284.
[55]	**Preinhaelter J., Urban J., Pavlo P., Diem S., Vahala L., Vahala G., Taylor G.:** Electron Bernstein wave simulations and comparison to preliminary NSTX emission data. *Review of Scientific Instruments*. **77** [10] (2006) 10F524, 1-10F524, 4.
[56]	**Rubel M.J., Coad J.P., Pitts R.A., Dejarnac R., Gunn J.P., Panek R.:** Co-deposition and fuel inventory in castellated plasma-facing components at JET. In: *Proceedings of 21st IAEA Fusion Energy Conference*, October 16-21, 2006, Chengdu, China, paper EX/P4-24.

[57]	**Sentkerestiová J., Ďuran I., Dufková E., Weinzettl V.:** Comparative measurements of plasma position using coils, Hall probes, and bolometers on CASTOR tokamak. *Czech. J. Phys.* **56** [suppl. B] (2006) B138-B144.
[58]	**Sentkerestiová J.:** Systematic plasma position measurements on CASTOR tokamak using systems of magnetic coils and Hall sensors. *Diploma Work*, Faculty of Nuclear Science and Physical Engineering, Czech Technical University, Praha 2006.
[59]	**Shevchenko V., Cunningham G., Gurchenko A., Gusakov E., Lloyd B., O´Brien M., Preinhaelter J., Saveliev A., Surkov A., Volpe F., Walsh M.:** Electron Bernstein Wave Heating Experiments on MAST. In: *Proc. 21st IAEA Fusion Energy Conference*, October 16-21, 2006, Chengdu, China, paper EX/P6-22.
[60]	**Schrittwieser R, Adámek J., Ionota C., Stöckel J., Brotánková J., Martines E., Popa G., Costin C., Van de Peppel L., Van Oost G.:** Direct measurements of the plasma potential by Katsumata – type probes. *Czech. J. Phys.* **56** [suppl. B] (2006) B145-B150.
[61]	**Schrittwieser R., Ionita C., Balan P.C., Stöckel J., Adámek J., Hron M., Tichy M., Martines E., Van Oost G., Figueiredo H.F.C., Cabral J.A., Varandas C., Silva C., Pedrosa M.A., Hidalgo C., Klinger T.:** Measurements of fluctuations with probes in the edge region of various toroidal plasmas. *Proceedings of 13th International Congress on Plasma Physics*, Kiev, Ukraine, 22 – 26 May 2006, B001o.
[62]	**Simek J., Hrach R., Hrachova V.:** Analysis of Multi-Dimensional Techniques for Particle Modelling in Tokamak Edge Plasma, Czech. J. Phys. 56 (2006), Suppl. B, B87-B92.
[63]	**Spolaore M., Brotánková J., Stöckel J., Ďuran I., Hron M., Peleman P., Dejarnac R., Bilykova O., Sentkeristiova J., Van de Peppel L., Gunn J.P., Van Oost G., Adámek J., Stepan M., Martines E.:** Periodic collapse of a transport barrier induced by biasing experiments in the CASTOR tokamak. *9th Workshop "Electric Fields, Structures and Relaxation in Edge Plasmas",* Rome, Italy, 26-27 June, 2006, *Book of Abstracts,* p.4.
[64]	**Stöckel J. and CASTOR team**: Edge plasma diagnostics in tokamaks. In: *Sixth International Workshop and Summer School Towards Fusion Energy - Plasma Physics, Diagnostics, Spin-offs* Kudowa Zdrój, Poland 18 - 22 September 2006 (Invited lecture)
[65]	**Stöckel J., Adámek J., Balan P.C., Bilyk O., Brotánková J., Dejarnac R., Devynck P., Ďuran I., Gunn J.P., Hron M., Horacek J., Ionita C., M. Kocan, Martines E., Panek R., Peleman P., Schrittwieser R., Van Oost G., Zacek F.:** Advanced probes for edge plasma diagnostics on the CASTOR tokamak. *2nd Int. Workshop and Summer School on Plasma Physics.* Kiten, Bulgary, July 3-9, 2006.
[66]	**Stöckel J., Spolaore M., Brotánková J., Horacek J., R Dejarnac, Devynck P., Ďuran I., Gunn J.P., Hron M., Kocan M., Martines E., Panek R., Peleman P., A. Sharma, Van Oost G.:** Dynamics of the edge transport barrier at plasma biasing on the CASTOR tokamak. *11th International Conference on Plasma Physics and Technology*. Alushta, Ukraine, September 11-16, 2006.
[67]	**Taylor G., Bigelow T.S., Caughman J.B., Carter M.D., Diem S.J., Efthimion P., Ellis R.A., Ershov N.M., Fredd E., Harvey R.W., Hosea J., Jaeger F., LeBlanc B.P., Philips C.K., Preinhaelter J., Ram A.K., Rasmussen D.A., Smirnov A.P., Urban J., Wilgen J.B., Wilson J.R.:** Electron Bernstein Wave Research on Overdense Plasmas in the National Spherical Torus Experiment. In: *Proceedings of EC-14, 14th Joint Workshop on Electron Cyclotron Emission and Electron Cyclotron Resonance Heating*, 9 – 12 May 2006, Santorini, Greece.
[68]	**Taylor G., Caughman J.B., Carter M.D., Diem S., Efthimion P.C., Harvey R.W., Preinhaelter J., Wilgen J.B., Bigelow T.S., Ellis R.A., Ershov N.M., Fonck R.J., Fredd E., Gartska G.D., Hosea J., Jaeger F., LeBlanck B., Lewicki B.T., Philips C.K., Ram A.K., Rasmussen D.A., Smirnov A.P., Urban J., Wilson J.R.:** Electron Bernstein Wave (EBW) Physics In NSTX and PEGASUS. *Innovative Confinement Concepts Workshop.* Austin, Texas, USA, February 13-16, 2006, pp. 1-24.

[69]	**Taylor G., Diem S.J., Caughman J., Efthimion P., Harvey R.W., LeBlanc B.P., Philips C.K., Preinhaelter J., Urban J.:** Electron Bernstein Wave Coupling and Emission Measurements on NSTX. *Bulletin of the American Physical Society, 48th Annual Meeting of the Division of Plasma Physics*, Philadelphia, Pennsylvania, 30 October – 3 November 2006, p. 177, paper QP1.00025.
[70]	**Tuccillo A., Bibet P., Ekedahl A., Goniche M., Granucci G., Ide S., Mailloux J., Mirizzi F., Panaccione L., Pericoli-Ridolfini V., Petrzilka V., Rantamaki K., Seki M., Wilson R.:** Progress in Lower Hybrid Toward ITER: A summary on coupling . *10th SSO – ITPA Meeting*, Chengdu, 23-26 October 2006, 21st IAEA Fusion Energy Conference, Chengdu, China.
[71]	**Urban J., Fuchs V., Pánek R., Preinhaelter J., Stöckel J., Žáček F., Davydenko V.I., Mishagin V.V.:** NBI system for reinstalled COMPASS-D tokamak. *Czech. J. Phys.* **56** [suppl. B] (2006) B176-B181.
[72]	**Urban J., Preinhaelter J., Pavlo P., Diem S.J., Taylor G., Shevchenko V., Valovic M., Vahala L., Vahala G.:** EBW Emission Simulations and Plasma Diagnostics. In: *Proceedings of EC-14, 14th Joint Workshop on Electron Cyclotron Emission and Electron Cyclotron Resonance Heating.* Santorini, Greece, May 9-12, 2006.
[73]	**Urban J., Preinhaelter J., Sabbagh S., Pavlo P., Vahala L., Vahala G.:** Effect of Various EFIT NSTX Equilibria on EBW Simulations. *Bull. of the American Phys. Society, 48th Annual Meeting of the Division of Plasma Physics*, Philadelphia, Pennsylvania, 30 October – 3 November 2006, paper QPI.00027.
[74]	**Urban J., Preinhaelter J., Sabbagh S.A., Pavlo P., Vahala L., Vahala G.:** Interpretation of EBW simulation and comparison with NSTX. *33rd EPS Conference on Plasma Phys. Contr. Fusion,* Rome, Italy, 19 – 23 June 2006, ECA Vol. **30I**, P-5.171.
[75]	**Urban J., Preinhaelter J.:** Adaptive finite elements for a set of second-order ODEs. *Journal of Plasma Physics*. **72** [6] (2006) 1-4.
[76]	**Vahala G., Preinhaelter J., Taylor G., Urban J., Diem S., Vahala L.:** Simulation of the time development of EBW emission from NSTX. *APS April Meeting 2006 held in conjunction with Sherwood Fusion Theory Conference*, April 22-25, 2006, Dallas, Texas.
[77]	**Van Oost G., Berta M., Brotánková J., Dejarnac R., Del Bosco E., Dufková E., Ďuran I., Gryaznevich M.P., Hron M., Malaquias A., Mank G., Peleman P., Sentkerestiová J., Stöckel J., Weinzettl V., Zoletnik S., Balász T., Ferreira J., Fonseca A., Hezagy H., Kuznetsov Y., Ossyannikov A., Sing A., Sokholov M., Talebitaher A.:** Joint Experiments on Small Tokamaks. In: *Proceedings of 21st IAEA Fusion Energy Conference*, October 16-21, 2006, Chengdu, China, paper EX/P4-34.
[78]	**Weinzettl, V., Dufková, E., Sarychev, D., Khimchenko L., Timchenko N., Kočan M.:** Snake-like structures after pellet injection in the T-10 tokamak. *33rd EPS Conference on Plasma Phys. Contr. Fusion,* Rome, Italy, 19 – 23 June 2006, ECA Vol. **30I**, P-4.080.
[79]	**Zabolotsky A., Bernard M., Bortolon A., Duval B.P., Fable E., Karpushov A., Maslov M., Sauter O., Piffl V., Schlatter Ch., Veres G., Weisen H.:** Particle and Impurity Transport in Electron-Heated Discharges in TCV. In: *Proceedings of 21st IAEA Fusion Energy Conference*, October 16-21, 2006, Chengdu, China, paper EX/P3-7.
[80]	**Zabolotsky A., Bernard M., Piffl V., Weisen H., Bortolon A., Duval B.P., Karpushov A.:** Carbon transport in TCV. *33rd EPS Conference on Plasma Phys. Contr. Fusion,* Rome, Italy, 19 – 23 June 2006, ECA Vol. **30I**, P2.145.
[81]	**Zajac J., Žáček F.:** Impulse Power Sources for Nuclear Fusion and Other Physical Experiments. *Programme & Abstract Book of the 22nd Symposium on Plasma Physics and Technology*. Praha, 2006, ISBN 80-01-03506-9, P-1.21.

1 Edge Plasma and Magnetic Confinement Physics

Dynamics of the edge transport barrier at plasma biasing on the CASTOR tokamak

J. Stöckel, J. Brotánkova, J. Adámek, I. Ďuran, J Horáček, R Dejarnac, M. Hron

In collaboration with:
M. Spolaore, E. Martines, Consorzio RFX, Associazione EURATOM-ENEA, Padova, Italy
P. Peleman, G. Van Oost, Department of Applied Physics, Ghent University, Ghent, Belgium
P. Devynck, J.P. Gunn, M. Kocan Association EURATOM-CEA, France

A clear and reproducible transition to a regime with improved particle confinement has been studied in the CASTOR tokamak at edge plasma biasing. Fast relaxations of the edge profiles, with a frequency of about 10 kHz are observed, if the biasing electrode is inserted deep enough into the plasma (r/a ~ 0.5) of the CASTOR tokamak and biased above +250V [1]. Recently, more detail measurement of the dynamics of the relaxation events are studied by means of a new rake probe consisting of two rows of tips. This arrangement allows study the spatial temporal evolution of the radial and poloidal electric field in the transport barrier. It is demonstrated that the electric field resulting from plasma biasing is not strictly radial. A relatively strong poloidal electric field, which drives directly the edge plasma either inward or outwards is observed.

The time evolutions of the electron and ion temperature, the ion saturation current and the floating potential simultaneously measured by a segmented tunnel probe [2] at biasing is shown in Fig. 1. It is seen that all plasma parameters start to oscillate periodically immediately after switching on the biasing voltage (+250 V) at 15 ms. The period of the oscillations is typically 100 μs. Let us focus on the evolution of the floating potential V_f (bottom panel), which oscillates between two values: the phase with the lower value is interpreted as the period when the transport barrier is formed. The maximum value of V_f corresponds to a collapse of the transport barrier.

The radial profiles at the plasma edge is measured by the double rake probe which consists of two radial arrays of Langmuir tips spaced poloidally by 2.5 mm. The distance between the tips in the radial direction is also 2.5 mm. The tips measure either the floating potential or the ion saturation current. The radial profiles of the ion saturation current were presented earlier in [1]. Here, we show the dynamics of the local electric field, which can be estimated as a difference of the floating potential of the neighboring tips. Thanks to the arrangement of the tips, the both components, the radial as well as the poloidal one can be calculated, neglecting variations of the electron temperature.

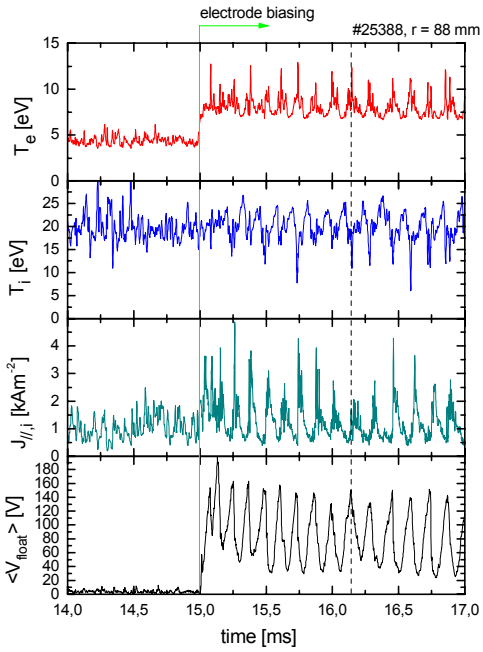

Fig. 1: Temporal evolution of the electron and ion temperature, the ion saturation current density and the floating potential measured by the segmented tunnel probe at r = 88 mm (in the limiter shadow). The biasing electrode is located at R = 50 mm.

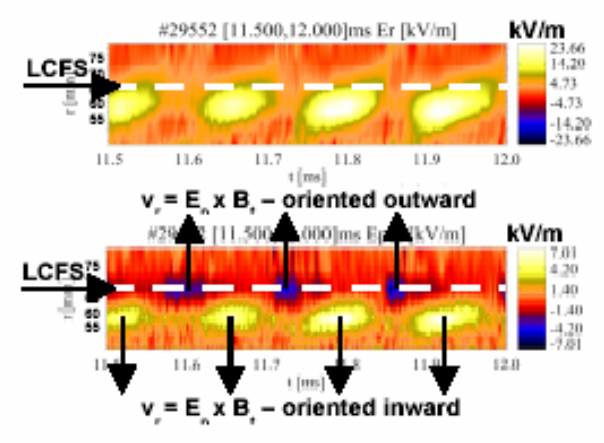

Fig. 2: Temporal evolution of the radial profiles of the radial component (the top panel) and the poloidal component (the bottom panel) of the electric field generated during the biasing phase. Position of the LCFS is 65 mm, the biasing electrode is at 50 mm.

The temporal evolutions of the radial and poloidal component of the electric field during the relaxation period are shown in Figure 2. The top panel displays evolution of the radial profile of the radial electric field. It is seen that a relatively narrow region of the amplified radial field (the transport barrier) is formed close to the biased electrode (located at r = 50 mm in this case). It propagates radially with the velocity ~200 m/s. When the barrier reaches the Last Closed Flux Surface (LCFS), it collapses. The bottom panel of Figure 2 clearly shows that a significant *poloidal* component of the electric field (marked by bright patterns) exists during the phase when the transport barrier is formed. The position of the region with the amplified poloidal field, E_p, corresponds to that of the radial component. It should be noted that the amplitude of E_p is of about 3 times less than the radial component, $E_r \sim 3E_p$. The resulting $E_p x B_t$ velocity is oriented inwards, i.e. the radial drift contributes to steepening of density profiles. On the other hand, the poloidal electric field of the *opposite* sign is formed during the collapse of the transport barrier, as marked by dark spots in Figure 2. This region of E_p is quite narrow and localized almost exactly at the LCFS. The corresponding $E_p x B_t$ velocity is oriented outwards. Consequently, the resulting radial particle flux is oriented towards the wall. This is confirmed by the temporal evolution of the ion saturation current which exhibits pronounced spikes as seen in Figure 1.

In conclusion, we demonstrate that the electric field resulting from plasma biasing is not strictly radial as usually expected. A relatively strong poloidal electric field is also formed and directly drives the edge plasma either inward or outward according its sign. Consequently, the radial transport can be either amplified or reduced. This mechanism is superimposed to the generally accepted biasing model, which assumes just the reduction of the transport at by sheared poloidal flows and consequent reduction of the edge turbulence.

References:

[1] Stockel J, Spolaore M, Brotankova J, Horacek J, Dejarnac R, Devynck P, Duran I, Gunn JP, Hron M, Kocan M, Martines E, Panek R, Peleman P, Sharma A, Van Oost G, Dynamics of the edge transport barrier at plasma biasing on the CASTOR tokamak, *Problems of Atomic Science and Technology: Plasma Physics*, 2006, No,6, 19-23.

[2] Hron M, Peleman P, Spolaore M, Brotankova J, Dejarnac R, Bilykova O, Sentkerestiova, J, Duran I, van de Peppel L, Gunn J, Stockel J, Van Oost G, Horacek J, Adamek J, Stepan M: Detailed measurements of momentum balance during the periodic collapse of a transport barrier. *33rd EPS Conference on Plasma Phys.,* Rome, Italy, 2006, ECA Vol. 30I., P-4.076.

[3] Kočan M, Pánek R, Stöckel J, Hron M, Gunn JP, Dejarnac R: Ion temperature measurements in the tokamak scrape-off layer. *17th International Conference on Plasma Surface Interaction in Controlled Fusion Devices*, 2006, Hefei Anhui, China, p. P3-59.

[4] Peleman P, Xu Y, Spolaore M, Brotankova J, Devynck P, Stockel J, Van Oost G, Boucher **C**: Highly resolved measurements of periodic radial electric field and associated relaxations in edge biasing experiments. *Ibid*., P3-23.

Asymmetries in SOL plasma measured by advanced oriented Langmuir probes on the CASTOR tokamak

R. Dejarnac, J. Stöckel, J. Adámek, J. Brotánková

In collaboration with:
J. P. Gunn, Association EURATOM-CEA, Centre de Cadarache, F-13108, France
C. Ioniță, Association EURATOM/ÖAW, University of Innsbruck, Austria

*The models that are used to interpret experimental data usually assume that the velocity distributions of charged particles are Maxwellian. This might not be true if collisionality is low and thus the probe measurements can lead to erroneous results. Here, we use two diagnostic tools to study the edge plasma in CASTOR [1] and search for evidence of deviations from the Maxwellian distribution. The first diagnostic, the tunnel probe (**TP**), is a new kind of Langmuir probe [2, 3], which was designed to measure the electron temperature (T_e) and the ion saturation current (I_{sat}) with high temporal resolution. In these experiments, two tunnel probes were mounted back-to-back in a Mach probe configuration in order to collect plasma either upstream or downstream along the magnetic field lines. The TP was also swept in order to record I-V characteristic to act as a directional Langmuir probe. The second diagnostic, the rake probe (**RP**), consists of an array of radially spaced cylindrical Langmuir tips, integrating both sides from the upstream and downstream directions. The edge profiles were measured by both probes at the top of the torus (poloidal angle 90° with respect to the outboard midplane) for B_t = 1.3 T and I_p = 10 kA in two series of reproducible discharges.*

Experimental results

Parallel ion current density profiles – collecting area of a cylindrical tip

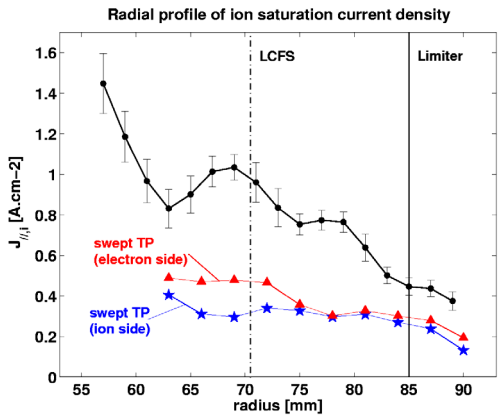

Fig. 1: Radial profile of the parallel ion current density as measured by the RP (black line-dots) and by the electron (red line-triangles) and ion (blue line-stars) side of TP.

The radial profiles of the parallel ion current density, $J_{//,i}$ are shown in Fig. 1. The poloidal limiter and the last closed flux surface are at different positions because of a downward shift of the plasma. To calculate the current density, the collecting area (A_c) of the probe must be known, since $J_{//,i} = I_{sat} / A_c$. It is usual to assume that A_c is equal to the geometrical projection A_{geo} of the probe along the field lines. This is true for the tunnel probe due to its concave geometry [4], but not necessary for the rake probe due to the sheath expansion around the tips. We estimate the A_c of the RP pins as the geometrical projection of the cylindrical tips along the magnetic field. It is evident from Fig. 1 that this choice of A_c leads to significantly higher values of $J_{//,i}$ as compared with the TP. This could imply that the actual collecting area of a cylindrical tip for these plasma conditions is more than twice as large as its geometrical projection along the field lines. The Larmor radius in the CASTOR SOL is around 0.5 mm which is comparable to the probe radius itself, so it is natural to expect that the probe can collect ions whose guiding centers would not normally intersect the surface. In addition, the strong perpendicular gradient of the electric field in the sheath can demagnetize the ion orbits and draw them away from their guiding center trajectories towards the probe. For the calculation of the ion current density we must consider that the collection area of Langmuir probe tips is modified with respect to the geometric area by a factor δ, which we expect to be a function of the plasma parameters ($A_i = \delta * A_{geo}$). By comparison with the TP, we are able to give a good estimate of this factor. Clearly the concave tunnel probe has a significant advantage over classical convex probes due

to the fact that its sheath electric field is entirely contained inside the probe and does not expand into the plasma to perturb the incoming ion orbits. The tunnel probe provides a much more accurate measurement of $J_{//,i}$ than cylindrical tips.

Electron temperature profiles – evidence for anisotropy of the electron distribution

Figure 2 shows the radial profiles of the electron temperature obtained from the experimental *I-V* characteristics. The T_e measured on the electron side T_e^{elec} is nearly a factor of 2 higher than that measured on the ion side, T_e^{ion}. The existence of an asymmetry could imply that the parallel electron distribution function is anisotropic. This would automatically mean that the electrons are not Maxwellian; if they were, once would expect to measure the same temperature on both sides of the TP. The fitting parameters T_e are not true temperatures in the thermodynamic sense, but can be interpreted as being qualitatively representative of the typical energies of the two counterstreaming tails of the parallel electron distribution function. Since the collisionality of fast electrons is low in CASTOR, it is reasonable to suppose that the ion/electron side asymmetry is caused by the electrons that carry the plasma current, driven by the induced toroidal electric field. In order to compare RP and TP, we summed the raw *I-V* characteristics of the TPs together and performed the same fitting routine. The resulting T_e, between those observed on the two sides of the TP, is similar to that measured by the RP. Clearly information is lost when classical tips are used. It is important to use bi-directional probes in order to detect deviations from the Maxwellian distribution.

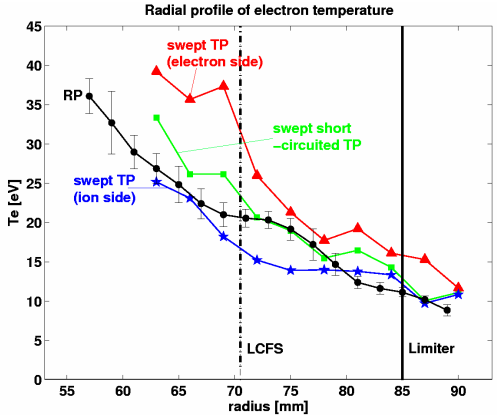

Fig. 2: Radial profile of the electron temperature as measured by RP (black line-dots) and by the electron (red line-triangles) and ion (blue line-stars) sides of TP. The measurement obtained by short circuiting both TPs together is shown too (green line-squares).

Floating potential profiles

A toroidal anisotropy is also present on the radial profiles of V_{fl} measured by the double TP. Using a simple model and assuming that each tail of the electron distribution can be described as Maxwellian, we show that the asymmetry in V_{fl} is in good agreement with the asymmetry of T_e measured by the TP. The probe measurements are dominated by the tail of the distribution function, rather than the thermal electrons that make up the bulk majority [5, 6]. Beside, a crude model also shows that enhanced ion collection by the RP tips could be responsible for the significant floating potential difference.

Summary: Two main themes were developed here. The first concerns the physics of charge collection by Langmuir probes in strongly magnetized, tokamak edge plasmas. Equating the effective collecting area of a cylindrical Langmuir probe tip with its geometrical projection along the field lines seems to lead to an overestimation of $J_{//,i}$ by a factor of 2 for the CASTOR plasma parameters, assuming that the effective collecting area of the tunnel probe is precisely known. The difference between the two probes is due to their respective geometries. The conventional cylindrical probe is subject to enhanced ion collection due to the strong electric field in the magnetized sheath that surrounds the convex pin. Three-dimensional kinetic simulations would be needed to model the problem, taking into account the electron temperature, density, applied probe voltage, and bulk flow velocity of the plasma. Such simulations are not within reach today, so one must simply accept that ion current density measurements by conventional probes are highly inaccurate. The concave geometry

of the tunnel probe ensures its immunity to sheath expansion effects, thus providing a precise calibration of the parallel ion current density. The second theme concerns directional asymmetries of the measured ion saturation current, electron temperature, and floating potential. In CASTOR, the electron side of the tunnel probe measures higher electron temperature and lower floating potential than the ion side. These two observations are consistent with a hot tail of suprathermal electrons streaming in the counter-current direction. The presence of anisotropic, non-Maxwellian electron distributions in the edge plasma can have important consequences, so it is useful to be able to obtain even qualitative information about them. It is therefore preferable to employ directional probes rather than conventional probes that average over both directions.

References:

[1] J. Stockel et al., Plasma Phys. Contr. Fusion, **47** (2005) 635-643

[2] J.P. Gunn et al., Rev. of Sc. Inst., vol.**75** number10 (2004) 4328

[3] J.P. Gunn et al., Czech. J. Phys. **55** number 3 (2005) 255

[4] J.P. Gunn, Physics of Plasmas, vol.**8**, number 3 (2001) 1040

[5] M. Shoucri et al., Contrib. Plasma Phys. **38**, 225 (1998).

[6] O. V. Batishchev et al., Phys. Plasmas **4**, 1672 (1997).

Fluctuation studies on the CASTOR tokamak with the double rake probe

J. Brotánkova, J. Stöckel, J. Adámek, I. Ďuran, J Horacek, R Dejarnac, M. Hron

In collaboration with:
M. Berta, A. Bencze, S. Zoletnik, KFKI, Association EURATOM-HAS, Budapest, Hungary
M. Spolaore, E. Martines, Consorzio RFX, Associazione EURATOM-ENEA, Padova, Italy
P. Peleman, G. Van Oost, Association EURATOM-Etat Belge, Ghent University, Belgium
P. Devynck, Association EURATOM-CEA, France

A newly designed probe head – the double rake probe has allowed determination of the position of the velocity shear layer on CASTOR with a precision ~ 1 mm. It is demonstrated that the position of the velocity shear layer is identical with the position of the last closed magnetic surface. The phase velocity deduced from correlation analysis roughly agrees with tat deduced from the gradient of the floating potential.

The edge plasma in the CASTOR tokamak and the electrostatic turbulence were characterized using a newly designed probe array, called the double rake probe. The probe head, shown in Figure 1a, consists of two arrays of 12 Langmuir tips spaced poloidally by 2.5 mm. The radial separation between two adjacent pins is also 2.5 mm. Pins are made of molybdenum wire of diameter 0.7 mm, their length is 2 mm. The probe head is inserted into the edge plasma from the top of the torus and oriented typically upstream with respect to the direction of the plasma current. Consequently, only the ion side of the velocity distribution function is studied.

A sweeping voltage is applied simultaneously to all tips, the I-V characteristics are recorded and the electron temperature is derived. An example of the radial profile of the electron temperature is shown in Fig. 1b.

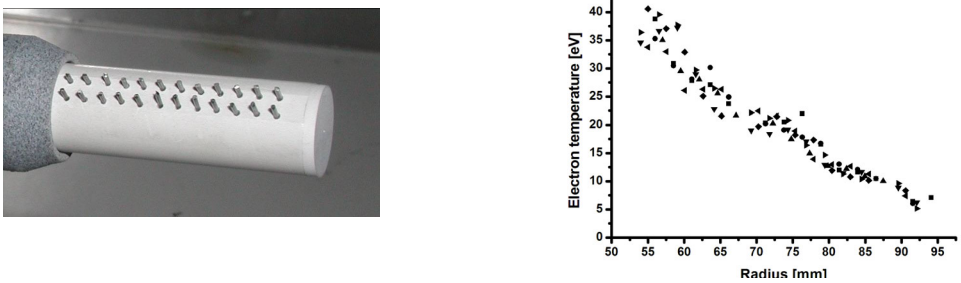

Fig. 1. a) Picture of the double rake probe. b) Radial profile of the electron temperature measured at several reproducible discharges.

Alternatively, the individual tips measure either the ion saturation current or the floating potential with the sampling rate 1 MHz. Such arrangement yields information about radial and poloidal structure of the edge electrostatic turbulence [1]. The result of such analysis is shown in Fig. 2. The left panel displays the radial profiles of the ion saturation current density and the floating potential measured at several reproducible discharges differing in the position of the double rake probe. The maximum, observed on the profile of the floating potential is attributed to the radial position of the Last Closed Flux Surface (LCFS) It has to be noted that the radial position of the LCFS at the top of the torus is noticeably less than the limiter radius, a = 85 mm. This is because of a downward shift of the plasma column on CASTOR.

Furthermore, from the time shift between the fluctuating signals of two poloidally separated tips it was possible to measure the poloidal velocity of fluctuating plasma density and floating potential structures. Since these time shifts were typically lower than the sampling rate (1μs), two statistical techniques were developed allowing the determination of the correlation length and phase velocity of fluctuations during a single shot: (i) polynomial curve fitting (fitting the cross-correlation by some polynomial function), and (ii) linear fitting of the phase function of

the cross-power spectral density. Both techniques provided similar results, as illustrated in the right panel of Fig.2. Both methods diverge in the proximity of the Last Closed Flux Surface (LCFS), which is associated with the maximum of the floating potential seen in the left graph of Fig.2. However, the position of the velocity shear layer (VSL) can be identified with a

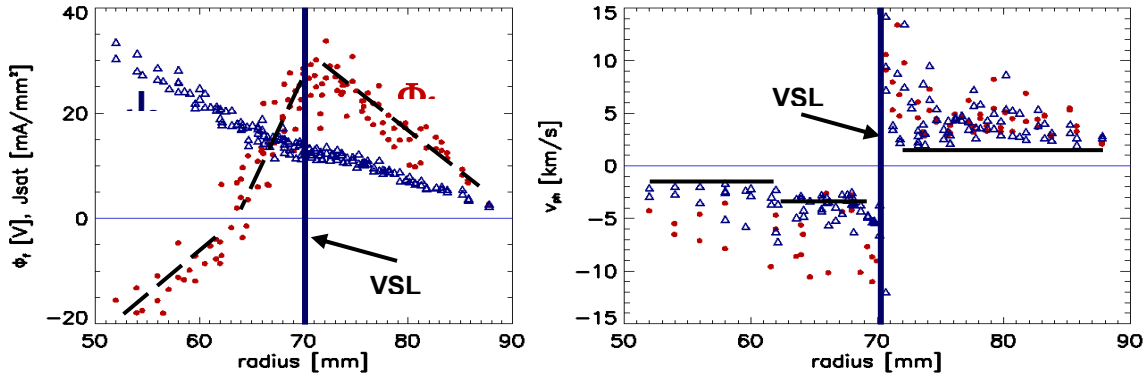

Fig. 1. Left graph: Radial profiles of floating potential Φ_f (red circles), and density of ion saturation current J_{sat} ($J_{sat}=I_{sat}/A$, A is 2π x radius x length of the probe). Right graph: Phase velocities of fluctuations obtained from Φ_f (red circles), and J_{sat} (blue triangles). Horizontal lines in the right panel show velocities calculated from the gradient of Φ_f. Both radial profiles are measured at the top of the torus.

precision of ~1 mm. From the gradient of floating potential (dashed line in the left graph of Fig. 2.), the phase velocities were roughly estimated as $v_{ph} = E_r/B$, where E_r is estimated as grad Φ_f, neglecting the gradient of the electron temperature. In the right graph of Fig.1, the velocities are depicted as three horizontal lines (in the region 50<r<60mm v_{ph}=-1.4km/s, for 60<r<70 mm v_{ph}=-3.3 km/s, and for 70<r<90 mm v_{ph}=1.3 km/s). It is evident that experimental points are above these lines, which implies that the electron temperature gradient cannot be fully neglected, if a precise comparison of the phase and ExB velocity is required. However, in spite of a huge shear, the levels of density and potential fluctuations do not change in the proximity of the velocity shear *layer*. Finally, it is interesting to note that the phase velocity of density fluctuations is systematically lower than that of potential fluctuations. The explanation of this observation requires more analysis.

Furthermore, from the spatio-temporal behaviour of cross-correlation functions of radially separated tips, a radial size of the fluctuating structures of about 1 cm was determined. The geometry of the probe head is also suitable for determination of the Reynolds stress. Such kind of analysis of the probe data was presented at [2, 3].

References:

[1] Van Oost G. et al..: Joint Experiments on Small Tokamaks. In: *Proceedings of 21st IAEA Fusion Energy Conference*, October 16-21, 2006, Chengdu, China, paper EX/P4-34

[2] Berta M., Bencze A., Tál B., Zoletnik S., Stöckel J., Hron M., Zajac J.: The spatial structure of flows, Reynolds stress and turbulence in the CASTOR tokamak. *9th Workshop "Electric Fields, Structures and Relaxation in Edge Plasmas",* Rome, Italy, 26-27 June, 2006, *Book of Abstracts*, p.3

[3] Berta M., Tál B., Bencze A., Zoletnik S., Stöckel J., Hron M., Dejarnac R., Zajac J.: The spatial structure of flows, Reynolds stress and turbulence in the CASTOR tokamak. *33rd EPS Conference on Plasma Phys. Contr. Fusion,* Rome, Italy, 19 – 23 June 2006, ECA Vol. 30I, P-4.074

Investigation of the SOL parallel flows on the tokamak TCV

J. Horáček

In collaboration with:
R.Pitts, Association EURATOM-CRPP, CRPP EPFL, Lausanne, Switzerland

Ion flows parallel to the magnetic field in the tokamak scrape-off layer (SOL) are now widely suspected to be an important player in the process of material migration, itself known to influence fuel retention. In addition to the neoclassical (field direction dependent), Pfirsch-Schlüter (P-S) component, a second contribution receiving increasing attention is a field direction independent flow, thought to be a consequence of the ballooning nature of cross-field transport into the SOL.

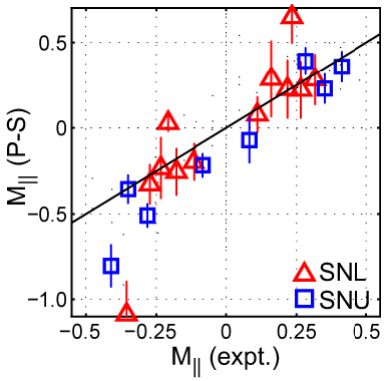

Experiments on TCV have measured the P-S component, demonstrating it to be of magnitude and direction expected by simple theory. This is demonstrated in the figure, for both single-null lower and single-null upper X-point configurations, the P-S flow Mach number estimated from radial gradients of plasma pressure and potential is compared with the value measured by the reciprocating Mach probe [1]. Clear identification of a possible "transport driven flow offset" has been performed, showing it to be of magnitude consistent with radial particle transport in the outboard SOL driven by convective interchange motions [2]. Nevertheless, given the chosen TCV magnetic equilibrium geometry and the measurement location *below* the outboard midplane of the discharge, it was not possible in this earlier study to exclude a particle sink effect of the outer divertor target driving a parallel flow extending into the main SOL and of similar magnitude to that expected as a consequence of perpendicular transport. In later experiments the shape flexibility of TCV has been used to eliminate this contribution and to demonstrate the poloidally localized nature of the ballooning component.

References:

[1] R.A. Pitts, J. Horacek, W. Fundamenski, O.E. Garcia, A.H. Nielsen, M. Wischmeier, V. Naulin and J. Juul Rasmussen. Parallel flow in TCV at the 17th International Conference on Plasma-Surface Interactions in Controlled Fusion Devices in Hefei Anhui, China, 22-26 May 2006. Published in Journal of Nuclear Materials 2007

[2] R. A. Pitts, J. Horacek. Neoclassical and transport driven parallel SOL flows on TCV. 34th EPS conference, June, Warsaw, Poland.

Evidence for a poloidally localized enhancement of radial transport in the scrape-off layer of the Tore Supra tokamak

R. Pánek, M. Hron, I. Ďuran

In collaboration with:
J. Gunn, T. Loarer, I. Nanobashvilli, J.-Y. Pascal, J. Bucalossi, P. Moreau, F. Rimini, Association EURATOM-CEA Cadarache, France
R. Zagorski, Association EURATOM-IPPLM Warsaw, Poland
T. Van Rompuy, Association EURATOM-Etat Belge, Ghent University, Belgium

Ion flow in the scrape-off layer (SOL) is both the cause and the symptom of many tokamak edge phenomena. Neutral recycling and impurity transport are intricately linked to edge flow patterns. SOL flows are believed to play a role in the asymmetric formation of carbon deposits in divertors [1], and they may influence the H-mode threshold [2]. It became evident a long time ago that radial cross field transport from the core into the SOL is anomalous and poloidally asymmetric, necessarily being strongest on the outboard side in order to explain certain experimental observations, such as large flows directed towards the inboard side [3]. Many calculations using 2D fluid codes can reproduce the general qualitative behaviour of the flow patterns by including "ballooning type" transport coefficient asymmetries (~1/R) or arbitrary unphysical forces, but most do not give high enough magnitudes of the flow.

Until now most SOL measurements were "passive" in the sense that flows and poloidal asymmetries might be observed, and anomalous ballooning type transport invoked to explain them, but little effort has been made to act upon the plasma in order to study the nature of the transport. Some of the most convincing recent results come from Alcator C-Mod where changing the X-point geometry from single to double null clearly demonstrates that a large fraction of the core-to-SOL particle flux is localized on the outboard side [4]. Here we present complementary measurements made in the Tore Supra tokamak that give new information both about the poloidal localization of the anomalous transport and its strength. By moving the contact point of a small plasma around the poloidal section, it is possible to modify the edge flows. Asymmetric flows are observed in cases that should be symmetric from simple geometrical considerations. The results indicate that the anomalous core-to-SOL outflux is poloidally localized in a 30° sector near the outboard midplane.

An experiment was performed on shot #35230 in order to estimate the poloidal extent of the region of enhanced radial transport. The plasma was displaced from the bottom to the top of the modular limiters in 10° steps of poloidal angle (Fig. 1). Despite nearly identical magnetic connections in all cases, the parallel flow exhibits spectacular reversal depending on whether the field lines sampled by the probe are connected to the outboard midplane via the positive or negative poloidal direction. The far-SOL flow was large and negative when the contact point was below the midplane due to the ions moving upwards from the outboard midplane towards the top of the torus; it was small for the 3rd and 4th intermediate positions, and reversed for the upper positions (Fig. 2).

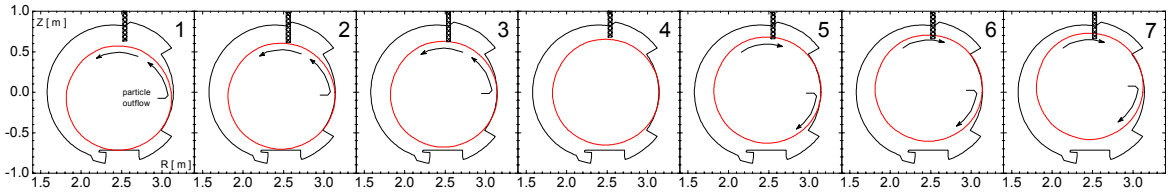

Fig. 1. Magnetic measurement of the LCFS as the plasma strike point is displaced upward along the outboard modular limiters. The arrows indicate the direction of flow past the Mach probe assuming that most of the SOL source is concentrated near the outboard midplane.

This experiment allows us to estimate that the region of enhanced radial transport is limited to a sector around 30° in poloidal extent roughly centered near the outboard midplane. If we make the crude assumption that the wide decay length with HFS contact is due to strong diffusive radial transport in a 30° poloidal sector, while that the short decay length with LFS contact is due to weaker transport over a full poloidal turn (implying that the effective parallel transport length is 12 times longer in the latter case), we find that the ratio of the two effective diffusion coefficients would be around 200, assuming the same rate of parallel transport in both cases.

Near sonic parallel flows are systematically observed in the SOL of the limiter tokamak Tore Supra, as in many L-mode X-point divertor tokamak plasmas. The poloidal variation of the Mach number of the parallel flow was studied by moving the contact point of a small circular plasma onto limiters at different poloidal angles. The resulting variations of flow, especially in the far SOL, are consistent with the existence of an enhanced core-to-SOL transport, strongly concentrated near the outboard midplane. If no object obstructs the parallel motion of the plasma that is transported onto open magnetic flux surfaces, which is the case when the contact point lies on the inboard midplane, the SOL expands to fill all the available volume between the LCFS and the wall. The mechanism that causes this spectacular expansion appears to be favoured by the existence of long field lines that pass unobstructed across the outboard midplane. This is demonstrated by moving the plasma from HFS to LFS contact: the SOL becomes very thin and a thick vacuum region separates the plasma from the wall.

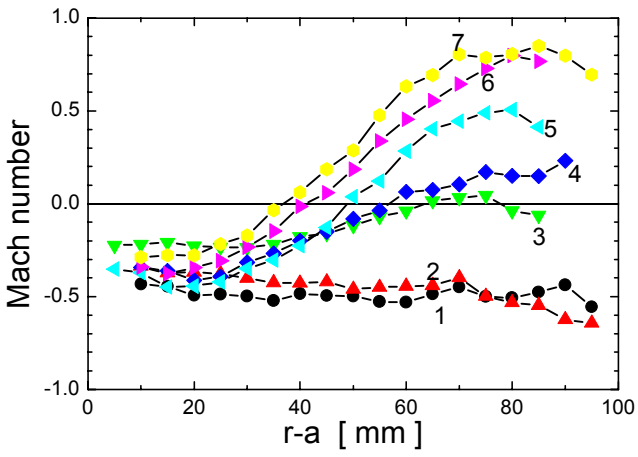

Fig. 2. Measured Mach number profiles on top of the torus for the seven magnetic configurations shown in Fig. 1.

These results, obtained in a limiter tokamak with a circular plasma cross section, seem to be similar to what is observed in L-mode X-point divertor tokamak plasmas, perhaps indicating the universality of the phenomenon. Our findings provide significant new information about the strong poloidal localization of the region where blobs are created.

References:

[1] G. F. Matthews, *J. Nuc. Mater.* **337-339**, 1 (2005).

[2] B. LaBombard, et al., Phys. Plasmas **12**, 056111 (2005).

[3] R. A. Pitts, G. Vayakis, G. F. Matthews, V. A. Vershkov, J. Nucl. Mater. **176-177**, 893 (1990).

[4] N. Smick, B. LaBombard, C. S. Pitcher, *J. Nucl. Mater.* **337-339**, 281 (2005).

Edge tokamak plasma turbulence: comparison of experiments with a 2D interchange turbulence model ESEL

J. Horáček, R. Dejarnac

In collaboration with:
O.E. Garcia, A.H. Nielsen, Association EURATOM-FOM, Riso, Roskilde, Denmark
R.A. Pitts, Association EURATOM-Confédération Suisse, CRPP EPFL, Switzerland

Boundary plasma interaction with the first wall determines strongly operation of future thermonuclear fusion reactors. Even though plasma turbulence had been considered responsible for the anomalously high radial particle transport observed in the tokamak boundaries for decades, and many related models have been developed, they were not capable to quantitatively describe the experimental observations until recently.

Two-dimensional fluid model ESEL of interchange instability driven by classical plasma drifts in curved magnetic field has been developed in the Risø National Laboratory (Denmark). Outputs of these numerical simulations have been directly compared with experimental observations from the TCV tokamak (Switzerland). Excellent agreement with statistical character of most of the experimentally available data of a particular discharge demonstrates that the model is close to a valid description of the edge plasma turbulent transport. This simulation comparison with experiment involved data from a reciprocating Langmuir probe in TCV. Density fluctuations probability distribution functions, its radial variations, characteristic time scales and frequency power spectra in experiment have all been found in agreement with the simulations. Especially, the absolute values of the radial particle flux derived from the simulations matched the experiment within 50% and thus higher by more than two orders of magnitude than the neoclassical estimate based on particle collisions in non-turbulent tokamak geometry [1,2,3,4,5].

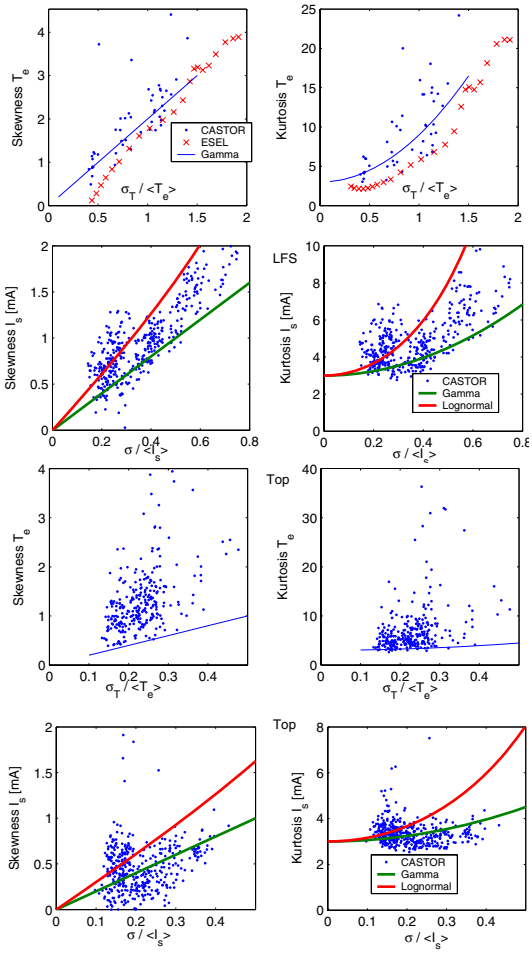

In 2006-7, further experimental verification and refinement of the model has been performed using both the TCV and CASTOR tokamak. On CASTOR, two unique diagnostics were planned to be used: a two-dimensional probe array and a tunnel probe. Unfortunately, the 2D array was found not to be possible because the probe is too much perturbing the plasma discharge. The tunnel probe yields fast temperature fluctuation, filling a missing gap in the model-experiment comparison. The results are shown in the figure: for both I_{sat} and T_e fluctuations, and at both top and LFS (i.e. the outer midplane) locations, the observed variations of the statistical moments are presented. This analysis follows previous works where the Gamma distribution has been found to describe well both the TCV and ESEL data of both I_{sat} and T_e, with the caveats that fast T_e measurement is not available on TCV, and all measurements in TCV are performed only at the LFS location. On CASTOR, for T_e at LFS even preliminary ESEL simulation results are shown. It should be noted, however, that the fast T_e measurements by the tunnel probe are questionable because the probe is not designed for plasma with so low

observed temperature T_e~1eV. Keeping in mind these limitations, this figure clearly confirms those previous results: *Gamma distribution is found for both T_e and I_{sat} at LFS, whilst it is not present at the top location*. This result is clearly consistent with the ESEL model of interchange instability with growth rate given by $\nabla B \times \nabla p$ which is positive at LFS (and thus unstable), negative at HFS (stabilizing) and zero at top and bottom (marginally stable). We think that finite fluctuations observed at the top location might be a projection along the field lines from the LFS.

As a sidetrack, using the reciprocating probe on TCV yielded collaboration on [6,7].

References:

[1] O.E. Garcia, J Horacek, V Naulin, A.H. Nielsen, R.A. Pitts and J.J. Rasmussen. Fluctuations, transport and flows in TCV scrape-off layer plasmas. *Nuclear Fusion* 2007.

[2] O.E. Garcia, J. Horacek, J.S. Larsen, J. Madsen, V. Naulin, A.H. Nielsen, R.A. Pitts, J.J Rasmussen. Convective transport by filamentary structures in scrape-off layer plasmas. 34th EPS conference, June, Warsaw, Poland.

[3] O.E. Garcia, R.A. Pitts, J. Horacek, A.H. Nielsen, W. Fundamenski, J.P. Graves, V. Naulin, J. Juul Rasmussen Turbulence simulations of interchange motions and intermittent transport in TCV scrape-off layer plasmas at the 17th International Conference on Plasma-Surface Interactions in Controlled Fusion Devices in Hefei Anhui, China, 22-26 May 2006. Published in Journal of Nuclear Materials (2007).

[4] W Fundamenski, O E Garcia, V Naulin, R A Pitts, A H Nielsen, J J Rasmussen, J Horacek, J P Graves and JET EFDA contributors. *Dissipative processes in interchange driven scrape-off layer turbulence*. journal Nuclear Fusion 47 (2007) 417-433

[5] J. Horacek, O.E. Garcia, R.A. Pitts: Further turbulence analysis. Talk at the CRPP Scientific meeting, Switzerland, 3/5/2007.

[6] A.V. Chankin, D.P.Coster, N.Asakura, G.D.Conway, Corrigan, S.K.Erents, W.Fundamenski, Günter, J.Horacek, A.Kallengach, M.Kaufmann, C.Konz, K.Lackner, H W Müller, J.Neuhauser, R.A.Pitts, M.Wischmeier. Discrepancy between modelled and measured radial electric fields in the scrape-off layer of divertor tokamaks: a challenge for 2D fluid codes? paper.pdf (on-line) journal *Nuclear Fusion 47 (2007) 479–489*

[7] B. Gulejová, R.A. Pitts, X. Bonnin, D. Coster, R. Behn, J. Horacek, J. Marki. Time-dependent modelling of ELMing H-mode at TCV with SOLPS5. 34th EPS conference, June, Warsaw, Poland.

SOL ionization by the lower hybrid wave during gas puffing

V. Petržílka, F. Žáček

In collaboration with:
G. Corrigan, V. Parail, K. Erents, J. Spence, Y. Baranov, J. Mailloux, Association EURATOM-UKAEA, Culham Science Centre, Abingdon, OXON OX14 3DB, UK
M. Goniche, A. Ekedahl, Association EURATOM-CEA Cadarache, DRFC, France
C. Silva, P. Belo, Association Euratom-IST, Centro de Fusao Nuclear, Lisboa, Portugal
J. Ongena, Association EURATOM – Belgian State, ERM, Brussels, Belgium

Gas puffing with a gas pipe situated near the JET Lower Hybrid (LH) antenna increases the scrape-off layer (SOL) electron density, $n_{e,SOL}$, in the region magnetically connected to the gas pipe, which improves the LH wave coupling [1], [2]. This is important namely for ITER relevant shots with a large distance between separatrix and the LH grill mouth. Numerical modelling with the fluid code EDGE-2D [3] suggested that enhanced edge radial plasma transport [4] can play a role in the $n_{e,SOL}$ increase, but the agreement with the measured profiles was reached by using ad hoc modifications of the transport. The modelling also did not take into account direct ionisation by the LH wave, which is thought to contribute [1], either because of the oscillatory motion in the LH wave, or due to the fast electrons created parasitically in front of the grill mouth [5], or both.

In the work presented here, EDGE-2D was used to include a simple representation of the LH wave and used to explore its effect on $n_{e,SOL}$. Since EDGE-2D includes only 2 dimensions, it was assumed that the ionisation by the LH wave is produced due to the local SOL electron heating by the wave in a radially narrow belt in SOL near the separatrix, with poloidal width corresponding to the LH grill height, in which heating the above mentioned locally generated fast particles can participate, too. We supposed that the overall SOL heating (the input in the code) is about 20 times higher. This coefficient of 20 was obtained as the ratio of the toroidal tokamak circumference 2.*pi*R (R taken as 3 m) to the grill toroidal width L (L taken as 1 m). As we assume, this option might give a better estimate of the sources due to ionisation. The ionisation is computed in the code under the assumption that the electron velocity distribution is Maxwellian. Modifications to EDGE-2D were required to accommodate the large SOL widths in the discharges which are of interest for LH wave coupling in ITER, where the distance between the separatrix and the LH launcher $d_{PL} \geq 8$cm. The effects of varying the LH heating and the gas puffing rate on $n_{e,SOL}$ are shown, and compared to experiments. For example, the slope and magnitude of the measured n_e profile for two shots with d_{PL}=8 and 9 cm, are reproduced by the modelling, with the SOL temperature locally elevated by the LH power. Let us note that the maximum ionisation cross section for hydrogen is about 30 eV, and slowly decreases to higher temperatures. Also, the ionisation sources were calculated for various LH heating and puffing rates. Two values of the plasma density at the separatrix were chosen: 5.e18 and 1.e19 m^-3 in the modelling. They correspond to typical values measured in JET in scenarios similar to those modelled.

Computational results and comparison with experiments

We will illustrate the EDGE2D modelling results on two shots with a long distance between separatrix and the LH grill mouth. First, it is the shot 58667 from series of shots with long distance coupling [2]. We note that this shot exhibited also hot spots on the divertor apron, caused by the fast particles locally accelerated in front of the grill mouth [5]. Second, it is the shot 59187, from the series of shots, in which effects of gas puffing on the LH wave coupling were studied [6]. The comparison of the SOL density profiles from modelling and measurements was done for these two shots, #58667 and #59187, as there are available good SOL density measurements by the reciprocating probe. The probe was in the time of the density measurements magnetically connected to the LH grill mouth, and to the gas pipe GIM6. Some magnetic surfaces from the locations in front of the grill mouth hit the inner

wall. EDGE2D can only cope with intersections of magnetic flux surfaces in the divertor region, and consequently the intersections with the inner wall were approximated by introducing particle and energy sinks [7]. The actual computational grid extends outside the vessel, but in regions where the vessel intersects the grid, recombination was greatly enhanced. The resulting neutralisation of the plasma creates sharp ion and electron pressure gradients at the plasma-vessel interface, which drives a plasma flow to the vessel where it is recycled as neutrals via recombination.The exact radial profile and the rate of the LH wave dissipation in the boundary plasma is not known.

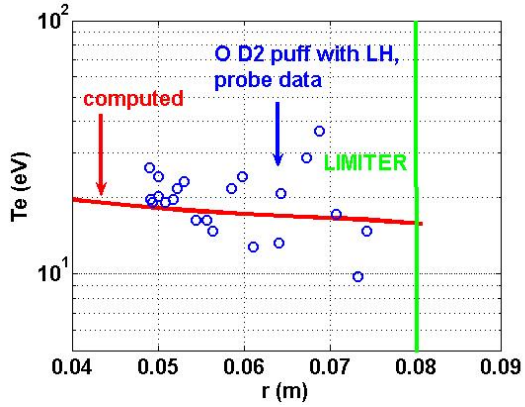

Fig. 1. Blue circles: SOL temperature measurements by the reciprocating probe, shot #58667, LH heating 2.5 MW, B=3T, Ip ramp from 1.5 to 2.7 MA. The red curve is the computed curve, puff 1.e22 el/s, heating 300 kW in the slab between 2-4 cm from the separatrix.

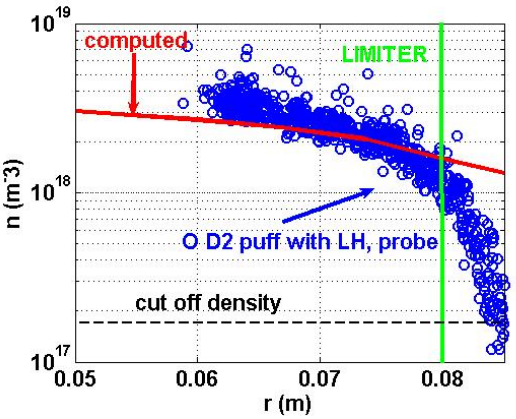

Fig. 2. Electron density profile (blue circles) measured by the reciprocating probe, shot #58667, D2 puff 8.e21 el/ s. The red curve is the computed curve, puff 1.e22 el/s, heating 300 kW in the slab between 2-4 cm from the separatrix. Edge2D can not model the density decrease near and behind the limiter, which is seen in the experiment.

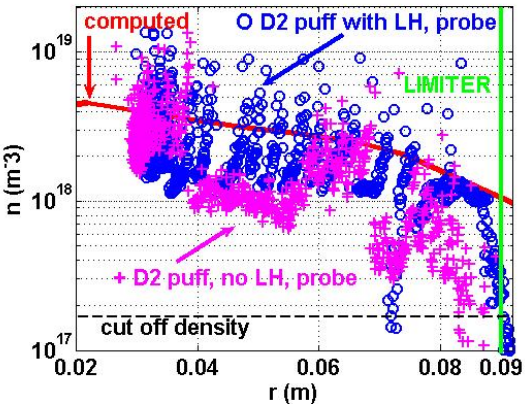

Fig. 3. Electron density profiles measured by the reciprocating probe, shot #59187, LH heating 2.5 MW, B=3T, Ip 1.5 MA: blue circles - D2 puff 5.e21 el/s with LH; magenta crosses – D2 puff without LH. The red curve is the computed curve, puff 1.e22 el/s, heating 300 kW in the slab between 2-4 cm from the separatrix.

Therefore, in the computations, two values of the width (2 and 7 cm) of the SOL layer with LH wave heating were considered, between 2-4 cm, between 6-8 cm, and between 2-9 cm from the separatrix (the wall is 9.5 cm from the separatrix in the midplane in the modelling). LH heating rates beteween 100 kW and 1 MW in the JET SOL plasma were considered in the computations. The case of 300 kW heating in the SOL appears to give the best comparison

with experiments, cf. Figs. 1- 3, for the plasma density at the separatrix 1.e19 m^-3. Let us note that 300 kW does not simply mean 300 / 20 = 15 kW in front of the grill mouth (the factor of 20 is explained in the Introduction). Because of the large parallel transport, in a 3d model the 300 kW dissipated would also be distributed along a much larger length than is the toroidal grill width. The D_2 gas puffing was varied between 1.e21 el/s and 1.e22 el/s.

Discussion and Conclusion

The numerical modelling presented in this work shows the importance of taking into account an effect of the LH power on the SOL temperature, and hence on the ionisation, when modelling the SOL plasma. In addition to the modelling presented in the figures, we studied the results of variations of the gas puff and of the SOL heating rate. The gas puff without or with a low LH heating cools the SOL, and therefore, can even result in the plasma density decrease. On the contrary, large enough LH heating enhances the SOL plasma temperature and also the density. This SOL temperature enhancement is maximum without the gas puff. However, when the gas puff is accompanied by a large enough SOL heating, the SOL plasma density strongly rises, which can explain the observed improvement of the LH wave coupling. The modelled density growth is consistent with the modelled SOL ionisation source profiles, which for puff and heating are strongly enhanced and extend into the far SOL, contrary to the case without heating and/or without the gas puff. We note that EDGE2D can not model the density decrease behind the limiter, which is important for the LH coupling predictions. Therefore, we plan to introduce into EDGE2D features enabling estimates of the density profile also behind the limiter. *Supported partly by the project GACR 202/04/0360.*

References :

[1] V. Pericoli-Ridolfini et al, Plasma Phys. Contr. Fusion 46 (2004) 349-368.

[2] A. Ekedahl et al., Nucl. Fusion 45 (2005) 351-359.

[3] R. Simonini et al., Contrib. Plasma Phys. 34 (1994) 2/3 368-373.

[4] G.F. Matthews et al.,.Plasma Phys. Contr. Fusion 44 (2002) 689.

[5] K.M. Rantamaki et al., Plasma Phys. Contr. Fusion 47 (2005) 1101-8.

[6] G. Granucci et al., 30th EPS Conf., St. Petersburg, Russia, ECA **27A** (2003), P-1.191.

[7] R. Zagorski and H. Gerhauser, Physica Scripta Vol. 70 (2004) 170-186.

Anomalous diffusion of particles from tokamaks in presence of magnetic and electrostatic perturbations

L. Krlín, P. Cahyna, R. Papřok, V. Svoboda

In collaboration with:
S. Kuhn, D. Tskhakaya, Association EURATOM-ÖAW, Innsbruck University, Austria
M. Tendler Association EURATOM-VR, Alfven Laboratory, Sweden

In this work we investigated anomalous diffusion of ions caused by two effects: magnetic islands and electrostatic perturbations appearing in the edge plasma due to low-frequency turbulence. Magnetic islands in tokamak plasmas are structures resulting from perturbation of the magnetic field, either artificially applied or resulting from MHD instabilities. It is expected that their presence increases transport of particles due to appearance of an ergodic layer. Currently, this effect is used as a method of ELM mitigation by resonant magnetic perturbations, in the ergodic divertor, and may play a role in the origin of internal transport barriers. In our work, we made a step forward from the traditional approach, which follows only diffusion of the magnetic field lines, and we described diffusion of particles by the corresponding Hamiltonian. We were interested in possible differences between those two approaches.

To estimate diffusion of particles, the corresponding Hamiltonian formalism was developed and used for a case of a simple system of magnetic islands on one or two rational surfaces. Intersections of particle trajectories and trajectories with a poloidal surface were plotted, resulting in a Poincaré section. We have found that there are important differences, caused by the vertical drift of particles due to field line toroidal curvature, which is necessarily neglected in field line tracing. Namely, we have found that in the case of an island chain on only one rational surface the field lines do not exhibit any ergodic behaviour at all, but a marked diffusion of particles appears (Fig. 1). In the case of magnetic island chains on two rational surfaces, there is a regime where the field lines are chaotic, but the particle motion in this field is rather regular (Fig. 2). We also expected that there might be differences due to the fast Larmor motion. To confirm that, we have constructed an artificial cylindrical model with neglected curvature where the drift does not appear. Our results so far do not indicate such effect, particle behaviour in this case is comparable to that of field lines. Those results were published in papers [1], [2].

Electrostatic turbulence originates in edge plasma by drift waves. It is a low-frequency perturbation of electron density and a resulting perturbation of electrostastic potential. In literature, this problem is usually solved by simulating the generation of such perturbation by Hasegawa-Wakatani equations. Electrostatic potential obtained in this way has similar traits as a potential we have already used before for simulations of particle diffusion. In this approach we used a spatially periodical and time-independent potential, where the wave number was taken according to experiments. In the literature, besides the Gaussian diffusion, the anomalous Lévy-walk diffusion was detected, therefore we discuss this problem in our periodical potential. We have found that for usual parameters of the electrostatic turbulence, the anomalous diffusion, which is characterized by a nonlinear dependence of variance of particle trajectories on time, appears. Moreover, the diffusion is strongly inhomogeneous due to the existence of the system of "islands around islands", corresponding to the last results of analytical studies of Zaslavsky [3].

In future work in the area of magnetic islands, we intend to calculate diffusion coefficients for the cases of chaotic particle motion that we have found and more systematically explore dependence of those effect on parameters. Concerning the results of anomalous diffusion in electrostatic turbulence, we intend to study these effects in experimentally found potential

from tokamak CASTOR. Further, we shall compare our results with effects found in electrostatic turbulence with a potential obtained from H.-W. equations.

So far, we have carried independent research of magnetic islands and electrostatic turbulence. Our next aim is to investigate the combined effect of those two types of perturbations.

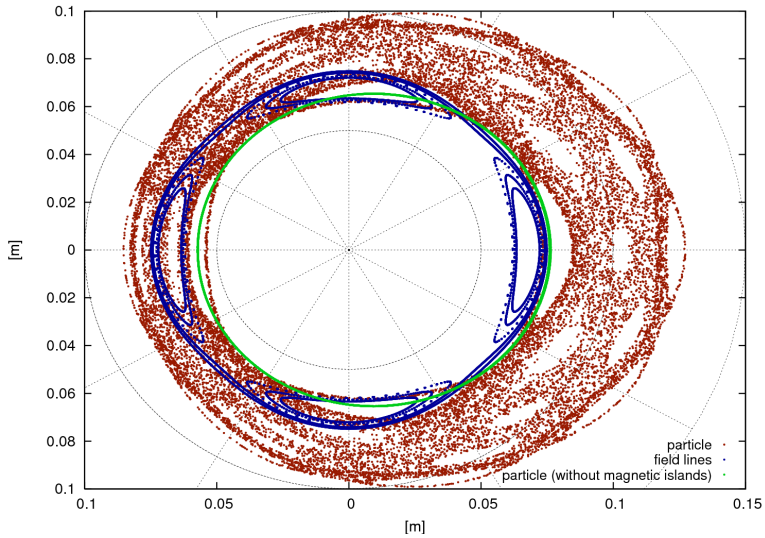

Fig. 1: Magnetic field lines (blue) and stochasticity of particle trajectory (red) in one magnetic island chain, and nonstochatic motion of a particle without magnetic islands (green).

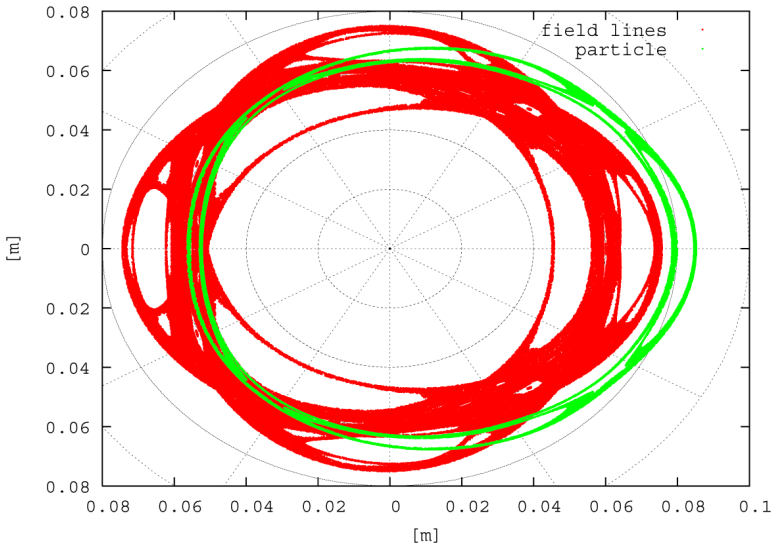

Fig. 2: Stochasticity of field lines (red) and fairly regular motion of particles (green) in the case of two magnetic island chains.

References:

[1] P. Cahyna, L. Krlín: Full Hamiltonian description of the interaction of particles with magnetic islands in tokamak, Czech. J. Phys. **56** (2006) 367-380.

[2] L. Krlín, P. Cahyna: Particle diffusion in a system of magnetic islands in tokamaks in fully Hamiltonian approach. 22nd Symposium on Plasma Physics and Technology, Praha, Czech Republic, Czech. J. Phys. **56** [suppl. B] (2006) B111-B117.

[3] Zaslavsky G. M.: „Hamiltonian chaos and fractional dynamics“, Oxford University Press 2005.

Self-consistent 2D simulations of plasma deposition in castellated tile gaps

R. Dejarnac and J. P. Gunn

In collaboration with:
J.P. Gunn, M. Kocan Association EURATOM-CEA Cadarache, France

The numerical tool we have developed for this study is a three velocity – two-dimensional kinetic code based on PIC technique [1]. The novelty of the code is its ability to inject arbitrary velocity distribution functions. For the ions, we use a non-Maxwellian distribution given by a one-dimensional quasineutral kinetic calculation of the scrape-off layer [2, 3] that satisfies the kinetic Bohm criterion at the sheath entrance.

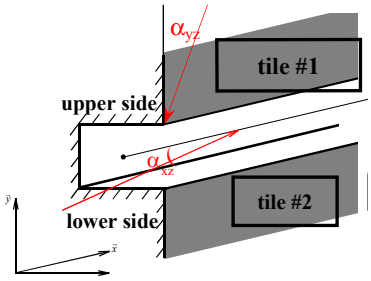

Figure 1: Scheme of the simulation domain in Cartesian coordinates.

Two types of gaps are simulated, with typical widths $l_{gap} = 0.5\text{-}1$ *mm*, according to their orientations with the magnetic field lines: gaps perpendicular to ***B*** (poloidal gaps) and gaps parallel to ***B*** (toroidal gaps). Two cases are investigated: $l_{gap} = 1mm$, $\alpha = 20^o$ [REF] and $l_{gap} = 0.5mm$, $\alpha = 5^o$ [ITER], where α is the angle between the magnetic field line and the surface (Fig.1). For better understanding, we use the terms *vertical* and *horizontal* relatively to the *y*- and *z*- directions, respectively and the two sides of the gap are named *upper side* and *lower side*.

The electric potential distribution in the simulation region shows a strong positive peak inside the gap (Fig.2a). This structure is due to the different degree of magnetization of ions and electrons. Electrons remained tied to the ***B*** lines, but ions can move freely in the horizontal direction due to their Larmor gyration and the polarization drift [4]. This leads to strong positive charge separation. Fig.3a shows the vertical ion flux falling onto the two sides of the gap along the horizontal axis. This flux is normalized to the theoretical unperturbed flux that impinges on the tile far from the gap. Around 70% of the incident ion flux flows downward on the wetted side of the gap. Some flux (only <1%) is collected on the magnetically shadowed upper side due to parallel flow reversal of the ions that just graze the edge of the upper tile and get reflected by the positive potential inside the gap. The missing incident flux is expelled from the gap by the charge separation field; they continue along field lines to be collected on the leading edge of the lower tile (Fig. 2a). Fig.4a shows the ion flux perpendicular to the tiles normalized by the theoretical 1D influx. We observe in the gap interval a decrease of the horizontal flux that is compensated by an increase of the

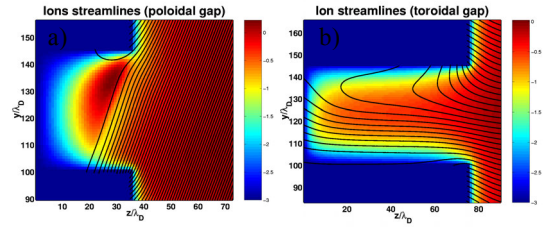

Fig. 2: Ion streamlines in the case of poloidal (a) and toroidal (b) gaps plotted over the electric potential normalized to kT_e/e for the reference case, i.e, an angle of 20° and a gap width of 1mm.

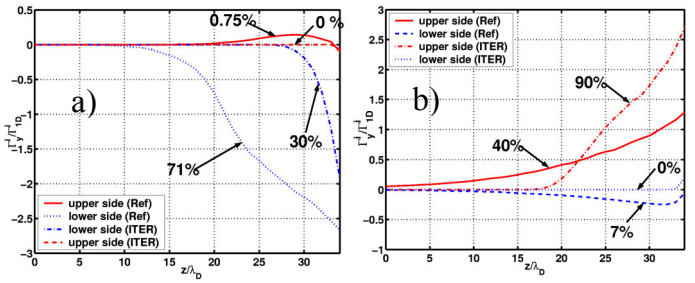

Fig. 3: Vertical ion flux falling on the sides of the gap for poloidal (a) and toroidal (b) cases normalized to the non-perturbed influx flowing onto tile surface for the cases (20°, 1mm) and (5°, 0.5mm). The percentages correspond to the total incident current normalized by the sheath edge current density integrated across the gap entrance.

vertical flux in this area. Indeed, we observe a significant increase of the horizontal particle flux deposited on the leading edge of tile#2. This confirms that a non-negligible fraction of the ions flowing into the gap in the parallel direction is expelled by the charge separation potential to be deposited on the top of tile#2 within *1mm*. In the ITER case, due to such a small incident angle, only few particles enter the gap, therefore the particle flux deposited on the two sides on the gap is strongly reduced (Fig.3a). Decreasing the angle of incidence thus leads to an increase of the flux expulsion onto the lower tile (Fig.4b).

In the case of toroidal gaps (Fig.2b), there is a strong asymmetry in particle trajectories caused by the ***ExB*** drift in the magnetized sheath; at the tile surfaces this drift is directed upwards along the y- axis. Inside the gap, the ***ExB*** drift tends to sweep ions preferentially onto the upper surface. There, the drift can even cancel the incoming parallel flow, leading to a purely vertical flow onto the upper side of the gap. Fig.3b shows that 40% of the influx is collected on the upper side of the gap and 7% on the lower side. The gap was not deep enough for the reference case of 20°, so a significant amount was also collected on the bottom of the gap (45%). Presumably this flux would go to the upper side if we had simulated a deeper gap. The missing flux (8%) is not expelled as in the case of poloidal gaps, but is lost before entry due to strong focusing of the electric field on the corner of tile#2. In the ITER case, we observe the same strong asymmetric deposition with no particles collected on the lower side (Fig.3b). This is due to the fact that the ***ExB*** drift dominates the horizontal projection of the parallel inflow for nearly grazing ***B*** angles.

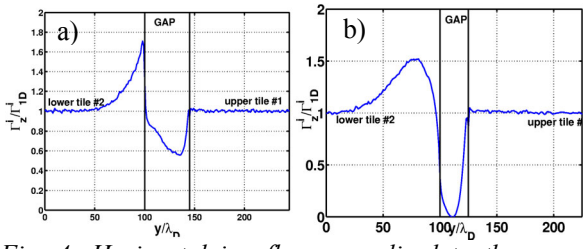

Fig. 4: Horizontal ion flux normalized to the non-perturbed influx flowing onto tile surface along the vertical coordinate at gap entrance for a poloidal gap for a) reference case (20°, 1mm) and b) ITER (5°. 0.5mm).

To summarise, the plasma deposition is asymmetric in both poloidal and toroidal tile gaps. Particle collection is a function of the gap dimension and the incidence of magnetic field lines. Strong electric fields developed along the sides of the gap govern the trajectories with the orientation of the magnetic field due to ***ExB*** drifts. In case of small poloidal gaps with grazing magnetic field lines, most of the incident ion flux is diverted over the entrance of the gap by the charge separation field and collected over *1mm* of the leading edge of the downstream tile. This will lead to significantly enhanced local power loading, so these findings should be taken into account in thermomechanical modeling of the tiles. In the case of toroidal gaps, practically all the flux that enters will impinge on the side favored by the ***ExB*** drift. This finding is consistent with the observation that carbon layers form preferentially on the high field side of toroidal gaps on the toroidal limiter in Tore Supra [5].

This work has been done under the Euratom fellowship Contract No 012801 (FU6).

References:

[1] C.K. Birdsall and A.B. Langdon, *Plasma Physics via Computer Simulation* (1985).

[2] V. Fuchs et al., 32nd EPS Plasma Physics Conference, Tarragona 2005.

[3] J. P. Gunn, J. Nucl. Mater. **337-339**, 310 (2005).

[4] J. P. Gunn, Phys. Plasmas **4,** 4435(1997).

[5] C. Brosset, private communication (2006).

2 Diagnostics Development

A new probe-based method for measuring the diffusion coefficient in the tokamak edge region

J. Brotánková, J. Adámek, , J. Stöckel

In collaboration with:
E. Martines, Consorzio RFX, Associazione Euratom/ENEA sulla Fusione, Padova, Italy
G. Popa, C. Costin, Association EURATOM-MEdC, F. of Ph., Al. I. Cuza Un. Iasi, Romania
R. Schrittwieser, C. Ionita, Association EURATOM-ÖAW, LFU Innsbruck, Austria
G. Van Oost, Department of Applied Physics, Ghent University, Belgium
L. van de Peppel, Hogeschool Rotterdam, Rotterdam, Netherlands

A new method for measuring the diffusion coefficient in the edge plasma of fusion devices was developed. The method is based on studying the decay of the plasma fluctuation spectrum inside a small ceramic tube having its mouth flush with a magnetic surface and its axis aligned along the radial direction. The plasma fluctuations are detected by an electrode, radially movable inside the tube. The measurement was performed at different radial positions in the CASTOR edge region, so that a radial profile of the diffusion coefficient was obtained. Typical values of D are of 2-3 m^2/s, consistent with expectations from the global particle balance. The radial profile shows a tendency of the diffusion coefficient to increase going deeper into the plasma.

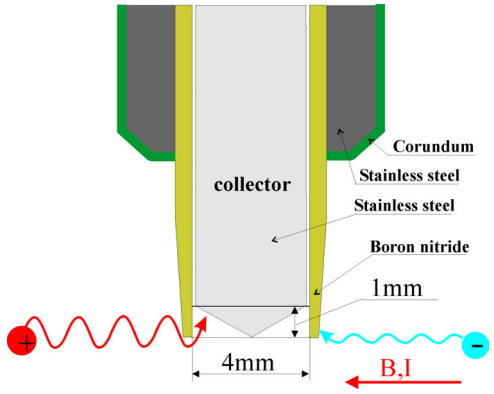

Fig.1 Schematic representation of the ball-pen probe.

Our method is based on the use of a novel type of probe, called "ball-pen probe" which was developed to obtain a direct measurement of the plasma potential [1,2]. The probe, which is based on the Katsumata probe concept, consists of a movable collector with a conical tip housed inside an insulating boron nitride shielding, as shown in Fig. 1. The collector can be moved radially, and adjusted so as to collect equal fluxes of ions and electrons, thanks to the shadowing effect of the shielding. When such condition is reached, and the collector is floating, the collector potential will be equal to the plasma potential.

We used the same probe in a different way, namely measuring the collector potential fluctuations for different values of the collector radial position h and studying the spatial decay of the fluctuation power spectrum. The measurements were performed in the edge region of the CASTOR tokamak (R = 0.4 m, a = 0.085 m), in discharges having a toroidal magnetic field, B =1.2 T, and a plasma current I_p = 10 kA.

An example of power spectra, measured with the probe at r = 65 mm, for several values of the collector position h ($h > 0$ means that the collector tip is protruding from the shielding, while $h < 0$ means that it is hidden inside it) is shown in Fig. 2. It can be clearly observed that the spectrum decays as the collector is pulled inside the shielding, and that this decay is faster for higher frequencies than for lower ones.

In order to interpret the observed spectral decay, we have developed a simple model based on the assumption that the penetration of the plasma inside the boron nitride shielding is purely diffusive [3].

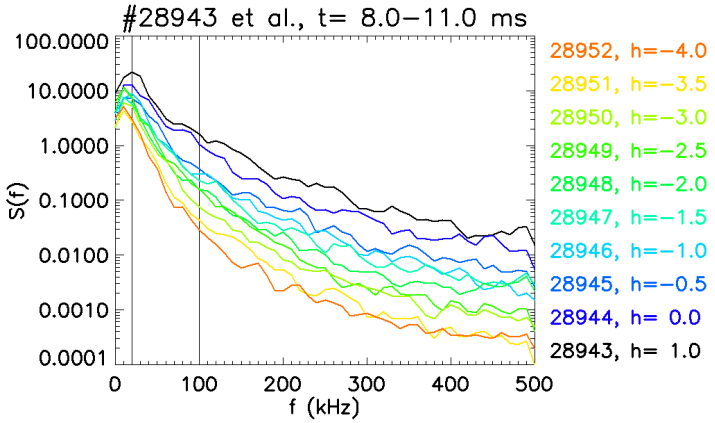

Fig. 2 Fluctuation power spectra for different collector position *h [mm]*.

A radial profile of the diffusion coefficient in the CASTOR edge plasma is shown in Fig. 3 (red line). Each point is the result of the analysis procedure described above, and is obtained from a set of discharges where the probe was held fixed, and the collector position was changed on a shot-to-shot basis.

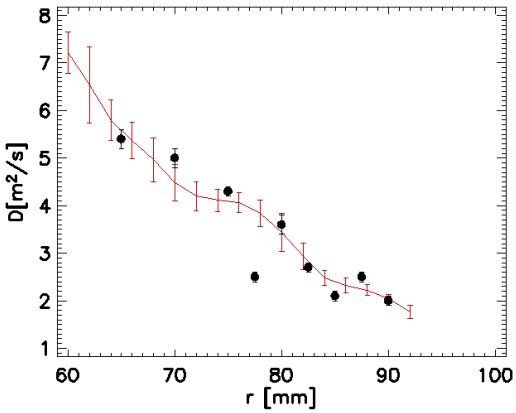

Fig.3: Radial profile of the measured diffusion coefficient (black points) compared with the Bohm one (red line).

The values of the Bohm diffusion coefficient, obtained using the toroidal magnetic field values and the electron temperature measured with a Langmuir probe, are plotted in the same graph. This latter quantity was multiplied by an arbitrary constant equal to 4. We observe that the measured diffusion coefficient increases moving from the edge towards the core, and that it tracks very well the Bohm diffusion coefficient profile. This gives a further motivation to assume that the measured values are indeed representative of the properties of the main plasma, although further analysis will be required to assess the possible influence of processes taking place inside the shielding, in particular due to the boundary conditions.

This work was carried out within the Associations EURATOM-IPP.CR, -ENEA, -MedC, and –ÖAW and was supported by project GA AV B100430601 of the Grant Agency of AS CR, and by INTAS Grant 2001-2056.

References:

[1] J. Adámek, J. Stöckel, M. Hron, J. Ryszawy, M. Tichý, R. Schrittwieser, C. Ioniță, P. Balan, E. Martines, G. Van Oost, *Czechoslovak J. Phys.* **54** (2004), C95-C99.

[2] J. Adámek, J. Stöckel, I. Ďuran, M. Hron, R. Pánek, M. Tichý, R. Schrittwieser, C. Ioniță, P. Balan, E. Martines, G. Van Oost, *Czechoslovak J. Phys.* **55** (2005), 235-242.

[3] J Brotánková, E Martines, J Adámek, J Stöckel, G Popa, C Costin, R Schrittwieser, C Ionita, G. Van Oost, *Czechoslovak. Journal of Physics,* Vol. **56**, No.12 (2006).

Development of advanced probe for edge tokamak plasmas: Emissive and tunnel probes

M. Tichý, P. Kudrna, A. Marek, R. Hrach, O. Bařina, J. Šimek

In collaboration with:
R. Schrittwieser, Petru Balan, Association EURATOM-ÖAW, Innsbruck University, Austria
J.P. Gunn, Association EURATOM-CEA Cadarache
E. Martines, Consorzio RFX, Padova

The milestones for the year 2006 were formulated as: (i) develop more precise models of diagnostic systems in CASTOR tokamak in collaboration with IPP in Prague, (ii) test final versions of particle codes for the simulation of processes in high-temperature plasma in the presence of magnetic fields in two and three dimensions, and (iii) test functional emissive probe diagnostic for laboratory system in FMP Prague.

Performance of the Katsumata Tunnel probe (KTP) was modeled by the PIC code. The KTP consists of tunnel electrode(s) shielded by diaphragm (see figure 1a) and exploited for measurements of the ion temperature at the edge of the CASTOR tokamak. Results of simulation are compared with experimental data in Fig. 1b; where the IV characteristics of the tunnel are plotted.

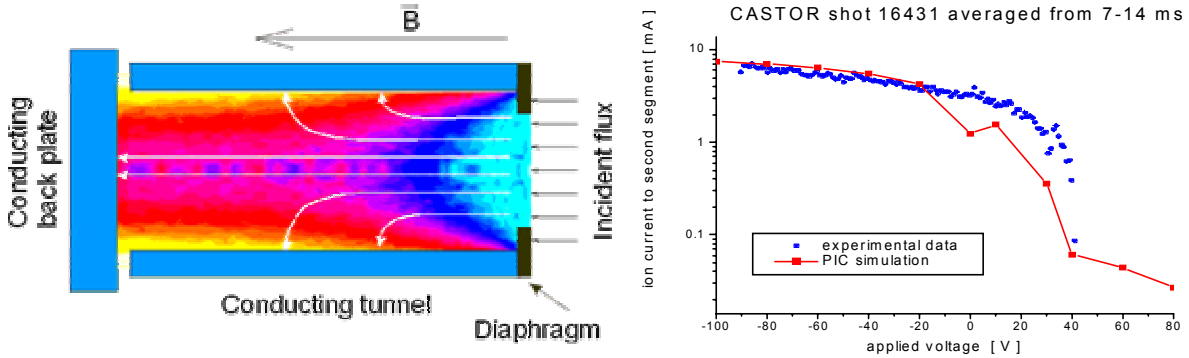

(a) (b)

Fig. 1. (a) The Katsumata tunnel probe, (b) IV characteristic of the tunnel.

Agreement is reasonably good at large negative voltages, while the model does not follow experiment at positive part of the IV characteristic. It was concluded that 3D modeling is required to get better agreement. The necessary software is in preparation.

The work on the second milestone was devoted to the analysis of time demands of particle simulation codes and to the discussion of ways how to increase their performance both in low- and high-temperature plasmas. The basic motivation of our work is the interpretation of experimental data obtained by probes of complicated forms from edge plasma in the CASTOR tokamak. In order to analyze the performance of models of plasma-solid interactions in several dimensions, we prepared our own two- and three-dimensional particle codes, based on the combination of deterministic movement of charged particles in electric and magnetic fields and on stochastic treatment of scattering events. In the work [1] the efficiency of different computer codes was tested. From the results published in [1] it follows that for the preparation of operational three-dimensional particle codes it is necessary to introduce much more efficient Poissson solvers or to apply quite different computational approaches, which is not based on the PIC technique.

As for the third milestone, the work progressed in collaboration with IPP in Prague [2], with Association EURATOM-ÖAW, the group of R. Schrittwieser [3], [4], [5], [6], and partly with Consorzio RFX, Padova, Italy [7]. The facilities in which the emissive probe was tested are depicted in Figure 2. Several students from Innsbruck University who participated in the research with emissive probe came to Prague in frame of CEEPUS project CII-AT-0063-02-0607 - "Applications and diagnostics of electric plasmas" coordinated by R. Schrittwieser. The publications concern mainly the investigations aimed at the understanding of the effect of the space charge around the emissive probe [4], [5], [6] and of the variations of the electron saturation current of the emissive probe [3]. The paper [7] deals with frequency analysis of fluctuations in low-temperature magnetized plasma. The second and the third milestones were completed in 2006.

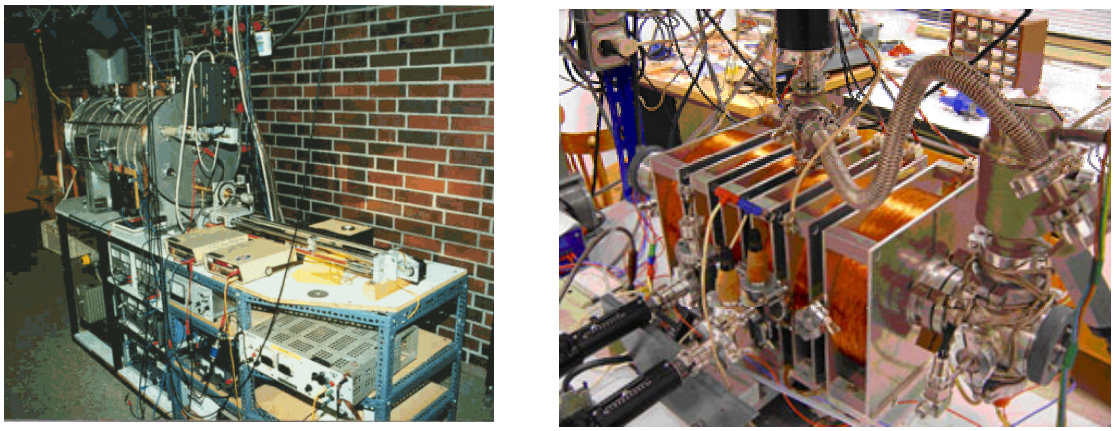

(a) (b)

Fig. 2. Double-Plasma Machine, University of Innsbruck, Austria (left) Cylindrical magnetron at the Department of Surface and Plasma Science, Charles University in Prague (right).

References:

[1] J. Šimek, R. Hrach, V. Hrachová, Analysis of Multi-Dimensional Techniques for Particle Modelling in Tokamak Edge Plasma, Czech. J. Phys. 56 (2006), Suppl. B, B87-B92.

[2] R. Schrittwieser, C. Ioniță, P.C. Balan, J. Stöckel, J. Adámek, M. Hron, M. Tichý, E. Martines, G. Van Oost, H.F.C. Figueiredo, J.A. Cabral, C. Varandas, C. Silva, M.A. Pedrosa, C. Hidalgo, T. Klinger, Measurements Of Fluctuations With Probes In The Edge Region Of Various Toroidal Plasmas, *ICPP'06 Proc. contributed papers CD,* paper D120, CD – B001o.pdf, 1-4, 2006.

[3] A. Marek, I. Picková, P. Kudrna, M. Tichý, R.P. Apetrei, S.B. Olenici, R. Gstrein, R. Schrittwieser, C. Ionita, Experimental Investigation of the Change of the Electron Saturation Current of a dc-heated Emissive Probe, Czech. Jour. Phys, Suppl B, 56, B932-B937, 2006.

[4] I. Picková, A. Marek, M. Tichý, P. Kudrna, R.P. Apetrei, Measurements with the Emissive Probe in the Cylindrical Magnetron, Czech. Jour. Phys, Suppl. B, 56, B1002-B1008, 2006.

[5] A. Marek, R.P. Apetrei, S.B. Olenici, R. Gstrein, I. Picková, P. Kudrna, M. Tichý, R. Schrittwieser, Emissive Probe Measurements in the DC Low Temperature Magnetized Plasma in Cylindrical Configuration, *ICPP'06 Proceedings contributed papers CD,* paper A168, CD – A168p.pdf, 1-4, 2006.

[6] R. Gstrein, A. Marek, C. Ionita, P. Kudrna, S.B. Olenici, P.C. Balan, R. Schrittwieser, M. Tichý, Space Charge Effects Of Emissive Probes Investigated In A DP-Machine, *ICPP'06 Proceedings contributed papers CD,* paper A181, CD – A181p.pdf, 1-4, 2006.

[7] O. Bilyk, M. Holík, P. Kudrna, A. Marek, M. Tichý, Observation of Wave-Like Structures in Magnetized DC Discharge in Cylindrical Symmetry in Argon, Contributions to Plasma Physics 46, 361-366, 2006.

Design of the Ball-pen probe for RFX and the first test

J. Adámek, J. Stöckel

In collaboration with:
E. Martines, V. Antoni, M. Spolaore, G. Serianni, R. Cavazzana, N. Vianello, M. Zuin,
Association EURATOM–ENEA, Consorzio RFX, Padova, Italy

The Ball-pen probe (BPP) [1] has been designed for the direct measurements of the plasma potential and the method is based on the Langmuir probe theory described by Eq.(1)

$$V_{fl} = \Phi - \left(\frac{kT_e}{e}\right)\ln(R)\,, \qquad (1)$$

where V_{fl} is the floating potential and T_e the electron temperature, k and e denote the Boltzmann constant and elementary charge, respectively. The quantity $R = I^-_{sat}/I^+_{sat}$ represents the ratio of the electron to the ion saturation current. The BPP can modify the value of the ratio R. If the value is adjusted to be equal to one than the floating potential of the probe is equal to the plasma potential, as evident from Eq. (1).

The BPP head for RFX and the first test

The probe head in Fig.1 consists of four BPPs and collectors are fixed at different position (h = 0 mm, 3 mm, 6 mm, 9 mm) within the shielding tubes. The tubes are made of one piece of boron nitride. The axis of each probe is perpendicular to the magnetic field lines. The massive side of the probe head is exposed to the intensive electron flux.

Fig.1: Four Ball-pen probes (collector diameter ∅ 4 mm - carbon and copper, shielding tube with inner diameter ∅ 6 mm) for the experiment on RFX. Boron nitride has a diameter ∅ 50 mm and length 90 mm.

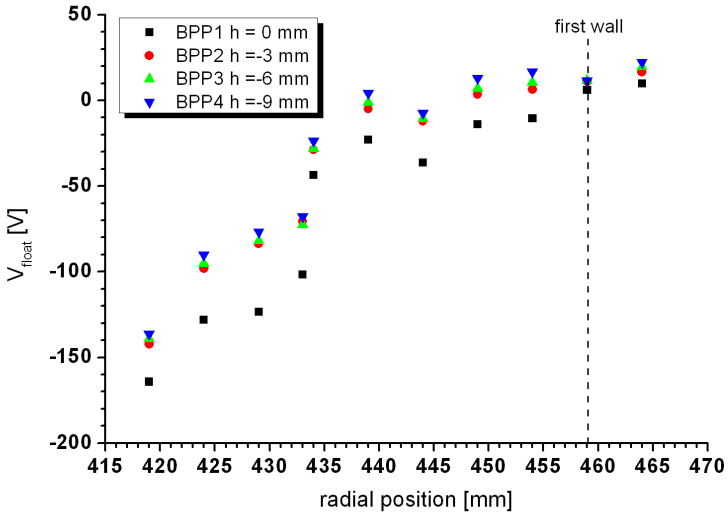

Fig.2: Radial profiles of the BPPs floating potential. Collectors are retracted at different positions h = 0 mm, -3 mm, -6 mm, -9 mm .

The first test of the BPP on toroidal device RFX (Reversed Field Pinch) in Padova (Consorzio RFX, Padova, Italy) has been performed in November 2006. The probe head was inserted in the edge plasma ($B \cong 0.1$ T, $n \cong 1{\cdot}10^{19}$ m^{-3}, $T_e \cong 20$ eV) and fixed on the radial position during the discharge. The main result of the first measurements is plotted in Fig.2. The first wall is located at the radial position r = 459 mm. The graph shows that the values of the floating

potential of the BPPs are almost identical when the collector is retracted more than 3 mm. The saturation of the potential inside the boron nitride shielding tube was also observed in the measurements on CASTOR tokamak [1], where the applied magnetic field was approximately $B \cong 1$ T. The value of the saturated potential is determined as the plasma potential Φ. It is also seen from the figure 2 that the potential of the BPP1 with the collector at $h = 0$ mm is systematically lower that the others. That probe in low magnetized plasma operates as a conventional Langmuir probe and therefore its potential is close to the floating potential of a Langmuir probe V_{fl} . The difference of the plasma and floating potential give us the value of the electron temperature T_e as

$$T_e = \frac{\Phi - V_{fl}}{\alpha}, \tag{2}$$

where the coefficient α is 2.89 for hydrogen plasmas [2]. The radial profile of the electron temperature is plotted in Fig. 3. The next systematic measurement is planned in autumn 2007.

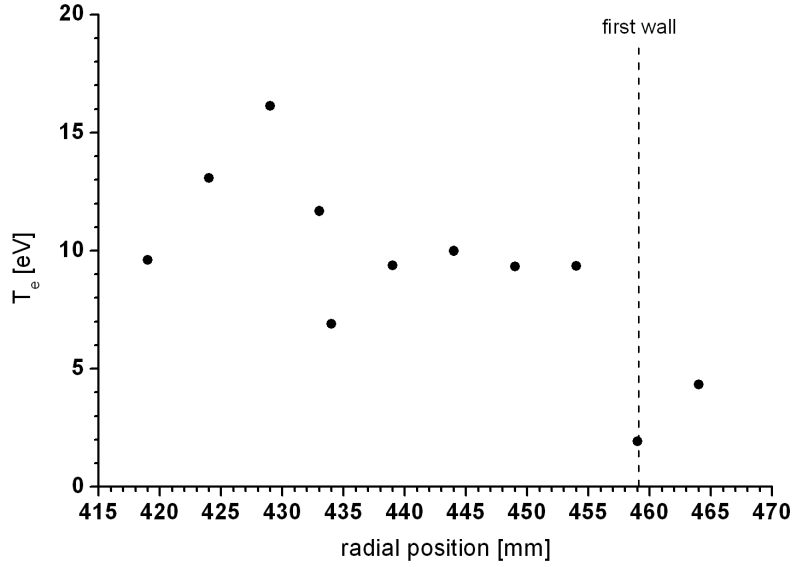

Fig.3: Radial profile of the electron temperature calculated from the difference of the plasma and floating potential using the equation (2).

References:

[1] J. Adámek, P. Balan, M. Hron, C. Ionita, E. Martines, J. Ryszawy, R. Schrittwieser, J. Stöckel, M. Tichý, G Van Oost: Czech. J. Phys., Vol. 54/C95 (2004).

[2] Adamek J., Stockel J., Schrittwieser R, Ionota C., Tichy M., Van Oost G., 32nd EPS, Tarragona June 27 - July 1, 2005, ECA Vol. 29C, P5.081

Development and fabrication of RF probes for Tore Supra

F.Žáček

In collaboration with:
M. Goniche, Association EURATOM-CEA, Cadarache, Saint Paul-lez-Durance, France

A new system of RF miniaturized double probes for detecting and transmitting signals up to 10GHz has been designed and developed in the frame of long term collaboration between Associations IPP.CR, Prague and EURATOM-CEA, CEA/DSM/DRFC, CEA-Cadarache, see construction design in Fig.1. The probe are ±3.5mm radially movable and their construction must endure the first wall conditions in the tokamak Tore Supra.

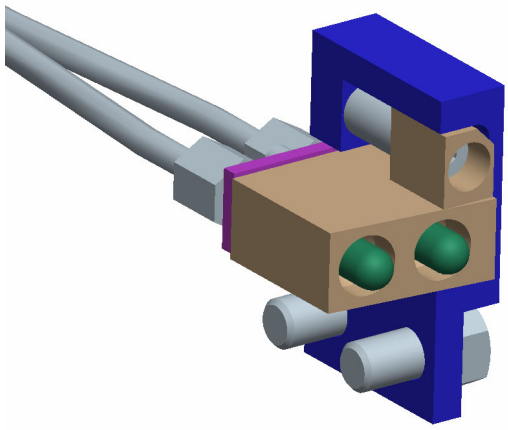

Fig. 1. Double RF probe for new Tore Supra launcher C4

Two identical probes shown in the Fig. 1, every having two receiving antennas spaced 10mm toroidally (the green tips in the figure), will be located symmetrically in equatorial plane on the both sides of the new LH grill launcher C4 of the tokamak Tore Supra, see Fig.2. Distance of the grill side edges from the grill centre is ±288mm.

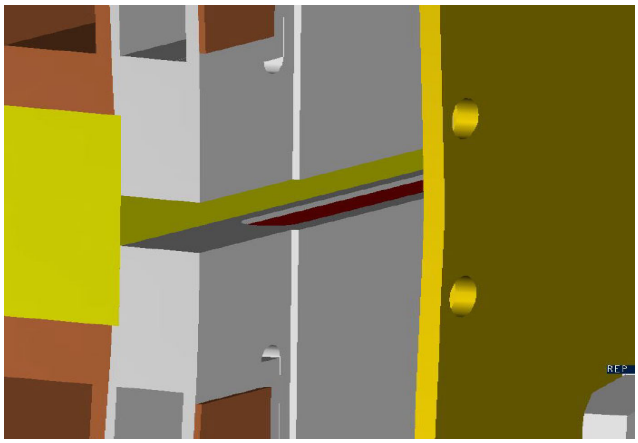

Fig.2. The groove in the C4 grill side-wall, where RF probe will be fixed.

In the course of the year 2006 the probes have been manufactured in IPP Prague. A special low cobalt stainless steel 316L has been used for this purpose. The plasma facing probe receiving antennas visible in the figure 1 (green color), will be made of CFC (Carbon Fiber Composite) and will be brazed to the ongoing inner conductor of the transmitting line (made

of stainless steel) in CEA Cadarache by a special technology (no such technology is accessible in IPP Prague). The transmitting line ends with SMA connector. The impedance of the line is smoothly changing from the 24Ω in the cross-section of the receiving antenna to the 50Ω in the output SMA connector. The photograph of the probe manufactured, but still without CFC antennas, is given in Fig.3 from the both sides. Manufacturing and completing of these antennas and RF test the whole probes must be still performed.

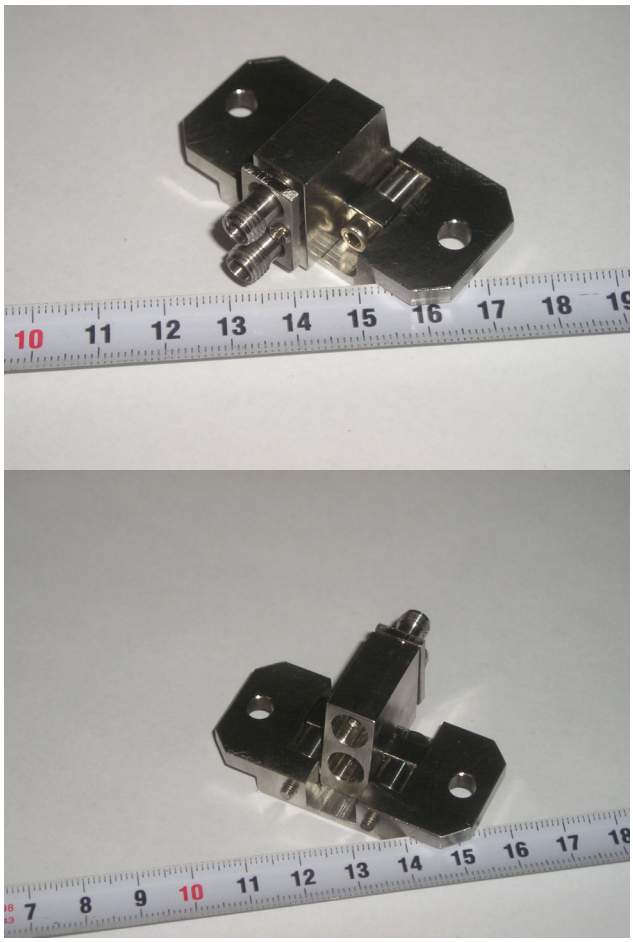

Fig.3. Photographs of one double RF probe from the both sides (still without CFC receiving "noses" in the lower picture), together with the probe holder and system of the probe radial position shift (end of antennas ±3.5mm with respect to the launcher mouth).

The RF probes will be used for measurements of the wave as well as plasma parameters in the place connected by magnetic field lines directly with the LHW interaction region in front of the launcher. In this way, changes arising under LHW effect, e.g. parasitic acceleration of the peripheral electrons (and maybe even ions) will be observable directly (resulting in formation of "hot spots", dangerous for the first wall elements). Moreover, direct measurement of the toroidal electric field and its correlations characteristics will be also possible using such double probe, similarly those performed on tokamak CASTOR. Note, that such measurements have not been possible up to now on the Tore Supra.

Ion temperature measurements in the tokamak scrape-off layer

R. Pánek, J. Stockel, M. Hron, R. Dejarnac

In collaboration with:
J. Gunn, Association EURATOM-CEA Cadarache, France
M. Kočan, Association EURATOM-CU, Comenius University, Bratislava, Slovakia

The ion temperature, T_i, in the tokamak scrape-off layer (SOL) is notoriously difficult to measure and thus rarely available (see e.g. [1]]. This work describes a new Langmuir probe, the segmented tunnel probe (STP), that measures ion and electron temperatures, and parallel ion current density simultaneously with high temporal and spatial resolution. Here we focus primarily on the measurements of ion temperature.

The STP consists of a hollow conducting tunnel a few millimeters in diameter and typically 5 mm deep, closed at one end by an electrically isolated conducting back plate. The tunnel axis is parallel to the total magnetic field. To repel electrons, the conductors are negatively biased. The ions flowing into the tunnel orifice get unmagnetized by an intense radial electric field in the magnetic pre-sheath, and redistributed between the back plate and the tunnel, Fig. 1 (left). The tunnel-to-back-plate ion current ratio is therefore a function of electron temperature. The sum of the tunnel and the back plate currents divided the cross section of the tunnel orifice gives the incident parallel ion current density, $J_{//,i}$.

The axial distribution of ion flux onto the tunnel decays with a characteristic length scale that is determined by the relative strength of the radial acceleration with respect to the incident parallel ion velocity. The latter is a function of the ion sound speed. Therefore, in addition to the electron temperature and ion current density measurements, if we divide the tunnel into two segments, the ion temperature can also be obtained from the ratio of ion current to the first and the second segment, $R_c = I_{seg1}/I_{seg2}$.

To account for the influence of the plasma flows in the SOL, two tunnels are mounted back-to-back in a Mach probe arrangement, Fig. 1 (right),

The advantage is that the probe operates in DC mode and thus provides fast measurements of the above mentioned quantities. Moreover, due to clearly defined tunnel orifice, the STP is not subject to the uncertainties of collecting area from which classical convex probes suffer.

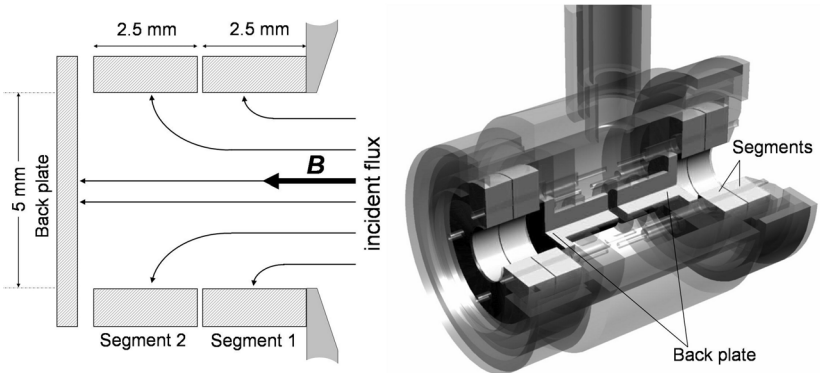

Fig. 1: Left: Scheme of the STP tunnel. The ion trajectories are shown by black arrows. Right: Schematic drawing of the probe head in a Mach probe arrangement.

Particle-in-cell simulations of the STP

Particle-in-cell (PIC) simulations were used for the calibration of the probe for ion and electron temperature measurements. We used two-dimensional PIC code XOOPIC [2]. In the simulations, Maxwellian electrons and ions with different combinations of temperatures ($T_{i,e}$) and current densities ($J_{//,i,e}$) are injected into the simulation domain from the right hand boundary, Fig. 1 (left). The code calculates the ion current collected by each segment which

enables to evaluate the ratio R_c. It must be noted that the value of R_c does not depend only on T_i, but to some extent also on electron temperature T_e and parallel ion current density $J_{//,i}$. However, T_e is measured simultaneously from the tunnel-to-back-plate ion current ratio. The sum of the tunnel segments and the back plate divided the cross section of the orifice gives $J_{//,i}$. Therefore, the ion temperature $T_i = T_i(R_c, T_e, J_{//,i})$ is unambiguously determined by the variables measured by the same probe.

From the simulation database we derived the analytical fitting formulae for T_i

$$T_i = 1.488 \cdot 10^2 + 2.539 \cdot 10^{-4} T_e^2 + 72.452 J_{//,i}^{-1} - 37.51 R_c \quad (1)$$

for $J_{//,i} = 1 \div 3$ kAm^{-2} and $V_{bias} = -200$ V, and

$$T_i = 3.081 \cdot 10^2 + 0.347 T_e + 2.107 \cdot 10^2 J_{//,i}^{-1} - 91.488 R_c \quad (2)$$

for $J_{//,i} = 3 \div 6$ kAm^{-2} and $V_{bias} = -200$ V.

Generally, the probe is able to measure the ion temperature approximately in the range $T_i \sim 5 - 100$ eV, and plasma density n_e up to 10^{19} m^{-3}. However, detail study and optimization is under way now.

Experimental results

A prototype of the STP has been built and tested in the CASTOR tokamak [3]. The ion currents collected by each segment and the back plate were measured separately with 1 μs time resolution. A radial scan of the plasma parameters was performed on a shot-to-shot basis in successive reproducible discharges.

Using Eqs. (1) and (2), the radial profile of the ion temperature was constructed. Fig. 2 (top) shows a typical radial profile of ion and electron temperatures in CASTOR obtained from the STP, plotted against the distance from the vessel centre, r. In addition, T_e from the STP is compared with similar measurements obtained from the radial array of Langmuir probes (so called "rake probe").

For $r < 65$ mm the ion temperature increases towards the plasma centre, but, as a consequence of the Ohmic-heating, T_e is higher than T_i. At $r_{LCFS} = 65$ mm T_i and T_e become comparable. In the region of 65 mm $< r <$ 85 mm (i.e. between the LCFS and the poloidal limiter) the T_i profile flattens. Here the effect of the plasma pre-sheath starts to play role.

At $r = 85$ mm the ratio of T_i/T_e approaches the value of ~3. This is probably caused by volumetric power losses, impurity radiation, hydrogenic recycling, etc. However, it might be also caused by the fact that the calibration breaks down at very low $J_{//}$ due to physical phenomena that XOOPIC simulations do not take into account (recycling etc.).

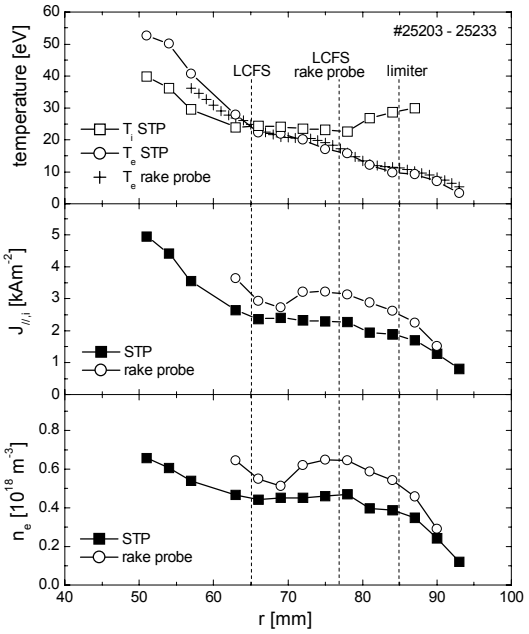

Fig. 2: Radial profiles of the ion and electron temperatures, parallel ion current density, and electron density (from top to bottom) in CASTOR measured by means of the STP and the rake probe.

To conclude, the segmented tunnel probe has already reached the level of technical performance at which it starts to provide a wide range of useful scientific results and can be experimentally tested in larger fusion devices.

References:

[1] R. A. Pitts et al., Review of Scientific Instruments 74 (2003) 4644.

[2] J. P. Verboncoeur, A. B. Langdon, N. T. Gladd, Comp. Phys. Comm. 87 (1995) 199.

[3] M. Kočan, R. Pánek, J. Stöckel, M. Hron, J.P. Gunn and R. Dejarnac; Journal of Nucl. Matterials 363-365 (2007) 1436-1440

Fast bolometric measurements and visualization of radiation fluctuations on the CASTOR tokamak

V. Weinzettl, E. Dufková

In collaboration with:
M. Kočan, Association EURATOM-CU, Comenius University, Bratislava, Slovakia
D. Sarychev, L.Khimchenko, N.Timchenko, RRC "Kurchatov Institute", Moscow, Russia

Fast measurements with AXUV bolometric arrays indicate a possibility to identify radiation fluctuations, which is the next step for understanding of anomal transport of particles and energy in tokamaks. The temporal resolution of AXUV-based bolometers of 1 μs together with the sufficient spatial resolution of 1 cm and a good signal to noise ratio are suitable for using of a tomographic techniques. The tomographic reconstructions finally give information on real fluctuations evolution in time and space.

Fast AXUV-based bolometric arrays with unique temporal resolution of 1 μs and spatial resolution of about 1 cm and a very high signal to noise ratio allow a visualization of fine structures on the radiated power profile [1]. A combination of the singular value decomposition (SVD), the cross-correlation analysis and the tomography is the best option to reach the desirable information. Typically, the dominating main plasma profile, a poloidally rotating asymmetric component and radially moving structures corresponding to symmetric component can be decomposed in the CASTOR shots [2,3]. The same method based on SVD applied on fast bolometric and SXR data was used for the analysis of snake-like structures after pellet injection in the T-10 tokamak [4]. The Cormack method of the tomographic reconstruction was implemented and was found it is suitable and very valuable for the analyses of the CASTOR plasma profiles, however, useless for the reconstruction of small-scale structures. Hence, more sophisticated tomographic methods are deliberated for such purposes in future.

Two arrays of fast AXUV-based bolometers with 16 and 19 channels were installed in the same poloidal cross-section in mutually perpendicular directions (from the bottom and LFS) to monitor the radiated power profile on the CASTOR tokamak. Typically, the measured AXUV data are used to find the evolution of the total radiation, radiation peak position (shift), radiation FWHM and the brightness profile. However, this arrangement with unique temporal resolution of 1μs and spatial resolution of about 1 cm and a very high signal to noise ratio allows a visualization of fine structures on the radiated power profile [1]. In usual case, either the quality of the data or a limited number of detectors does not allow to make a clear tomographic reconstruction directly. The data are smoothed in time or space, noisy, there is an overlapping of more plasma features or the number of projections is insufficient to see a complex structure of the physical image. Then, a combination of the singular value decomposition (SVD), the cross-correlation analysis and the tomography is the best option to reach the desirable information.The most promising way how to prepare suitable input for the next analysis is a data separation into spatio-temporal components by the Singular Value Decomposition method (SVD) [2]. In such way, components with a different spatial or temporal behaviour can be distinguished from each other and interpreted typically as the dominating main plasma profile, a poloidally rotating asymmetric component and radial structures corresponding to symmetric component, see Fig.1. A high contrast between the k=1 component and higher ones, usually of the order of the weight ratios 99.6:0.3:0.05, is observed for a typical ohmically heated CASTOR plasma. With biasing, higher components are amplified up to 98.5:1.1:0.2, as shown at the end of the biasing phase in Fig.1. Topos, spatial eigenvectors, show a type of the evolution (amplitude change, poloidal or radial

movement) and a localization of each structure, meanwhile chronos, temporal parts, indicate their presence, amplitude and periodicity. In Fig.1, a vanishing of the 6 kHz radial and poloidal structures after the end of the biasing phase is observed [3].

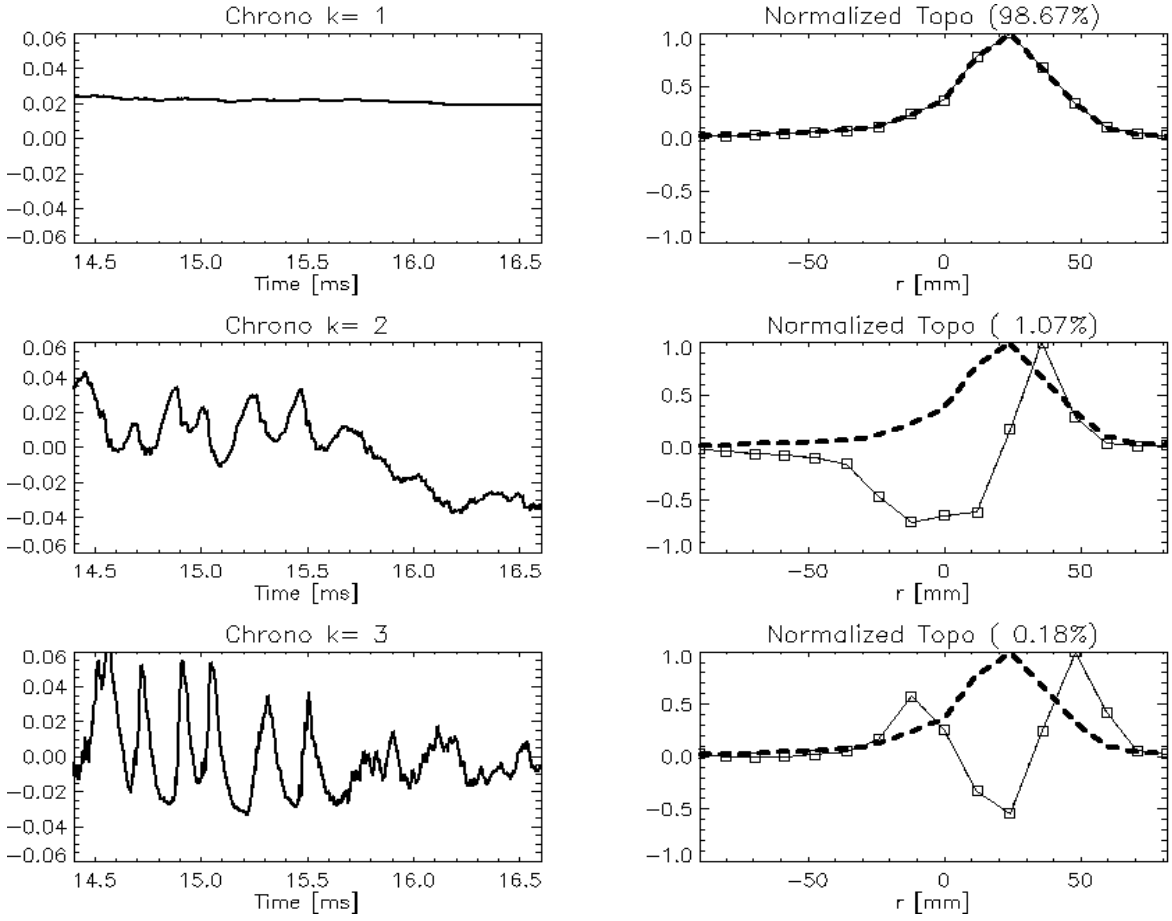

Fig. 1. Example of fluctuations analysis of fast bolometric signals from the bottom AXUV array with 1μs temporal and 1 cm spatial resolution in a shot with edge plasma biasing (#26995, r_E=60mm, U_B=+250V). Temporal and spatial eigenvectors of the first three significant components of the Singular Value Decomposition (SVD) are drawn and compared with an averaged emission profile (dashed line). Chronos (on the left) show temporal behaviour of the radiation losses which can be divided into a dominating quasi-stationary spatial part (k=1), a rotating asymmetric component (k=2) and radial structures (k=3). The normalized energy (weight) of each component is given in brackets. Open squares on topos represent chord radii of the individual bolometric channels.

The same method based on SVD applied on fast bolometric and SXR data was also used for the analysis of snake-like structures after pellet injection in the T-10 tokamak [4]. The experimental data were separated into spatio-temporal components by SVD to distinguish the main plasma profile (k=1), sawtooth (k=2 for long period t>>5ms of SXR data) and finally island radiation (k=2 for short period of AXUV and SXR data). From the k=2 components, the sawtooth inversion radius (used for estimation of the q=1 surface position), island evolution, position, its radiating width and poloidal rotation frequency were computed.

A next possibility how to process fast bolometric data is the analysis of the fluctuating part of raw data obtained by subtracting the mean value or the analysis of the data decomposed by SVD [2]. The data are chord integrated, thus the result does not correspond with the evolution of single local turbulent event but with their sum along the whole chord. By the auto-correlation analysis, the event frequency can be obtained from the periodicity of the auto-correlation function. The cross-correlation of one channel with neighboring ones in principle

gives the velocity and the movement direction, while the cross-correlation with a perpendicular bolometric chord gives the localization of the event. As an illustration, the cross-correlation analysis (horizontal chord at 40 mm against bottom chords) of shot #26991 with a biasing period at 10-15 ms is shown in Fig.2. Prior to biasing, clear structures with repetition frequency about 30 kHz are present. During biasing, the periodicity is destroyed, but the surface near radius 50 mm shows a high level of correlation indicating the presence of a well-localized structure. A few milliseconds after the end of biasing, the periodicity is still not restored, however a well-correlated, radially moving event is registered.

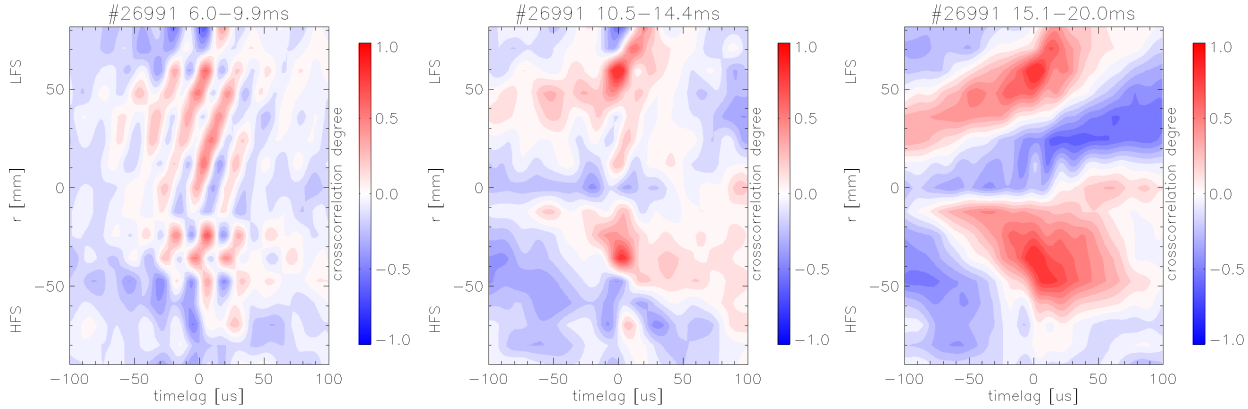

Fig. 2. Cross-correlation between one horizontal chord at 40 mm against all bottom chords shows moving structures in shot #26991. Prior to biasing (left figure), the presence of the periodic events with frequency 30 kHz and velocity 2.3 km.s^{-1} are demonstrated. During biasing with biasing voltage +150V (middle figure), the surface near radius 50 mm shows a high level of correlation indicating the presence of well-localized structure. After biasing (right figure), a well-correlated, radially moving event is registered.

The tomographic reconstruction based on the Cormack method was chosen for CASTOR because of its circular plasma cross-section and was implemented with very good results in standard ohmically heated shots, see Fig.3. The accuracy of reconstruction was verified by several kinds of test functions. For cylindrically shaped radiation profiles, the tomographic reconstruction perfectly matches the origin. For non-symmetric profiles or profiles with, for example, banana shape, the reconstruction is not perfect, but still agreement with the test function is reasonable. Many profiles resemble to real measurements were tested, including noisy data, successfully. However, a reconstruction of small events like radiation of local material erosion or fluctuations was not successful. In such cases, a small event is smoothed in the reconstruction and cannot be distinguish from the background radiation. The mean profile can also be subtracted from input data before the reconstruction. Nevertheless, the reconstruction is still wrong and/or a lot of false signal are generated. Concluding, the Cormack method of the tomographic reconstruction is suitable and very valuable for the analyses of the CASTOR plasma profiles but it is not usable for the reconstruction of small-scale structures. Hence, more sophisticated tomographic methods are deliberated for such purposes in future.

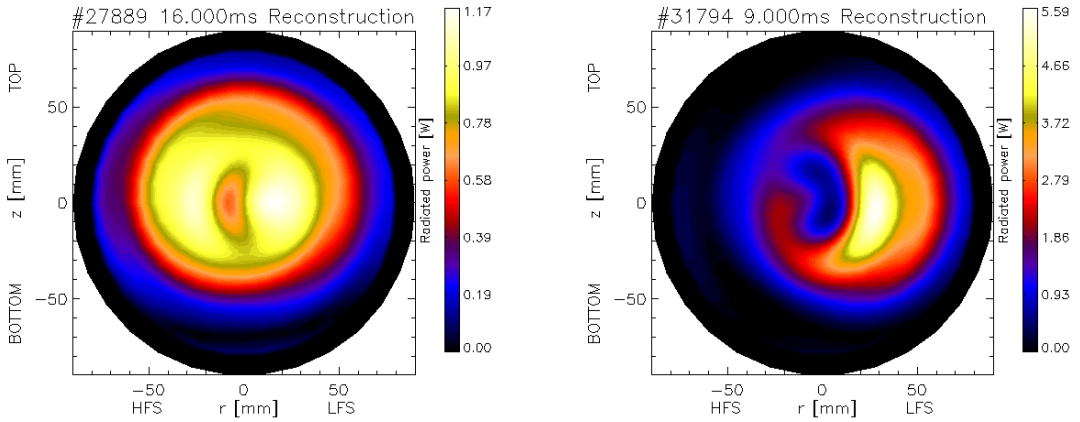

Fig. 3. Real data tomographic reconstruction by the Cormack method.

References:

[1] E.Dufková, V.Weinzettl, D.Sarychev, M.Kočan: Fast bolometry on the CASTOR tokamak, 32nd EPS Conference on Plasma Phys. Tarragona, 27 June - 1 July 2005, ECA Vol.29C, P-2.074 (2005)

[2] G. Van Oost et al: "Joint Experiments on Small Tokamaks", presentation No. EX/P4-34 on 21st IAEA Fusion Energy Conference, 16-21 October, Chengdu, China

[3] G. Van Oost et al: "Joint Experiments on Small Tokamaks: Edge plasma studies on CASTOR", Nucl. Fusion 47 (2007) 378–386

[4] V.Weinzettl, E.Dufková, D.Sarychev, L.Khimchenko, N.Timchenko, M.Kočan: "Snake-like structures after pellet injection in the T-10 tokamak", 33nd EPS Conference on Plasma Physics, Roma, 19/6-23/6/2006, P-4.080

Measurements of line radiation power in the CASTOR tokamak

V.Piffl, Vl.Weinzettl

In collaboration with:
A.Burdakov, S.Polosatkin, Budker Institute of Nuclear Physics, Novosibirsk, Russia
N.Korneva, Novosibirsk State Technical University, Novosibirsk, Russia

The determination of absolute values of radiated power of selected spectral lines is required for comparison of VUV spectroscopic data with bolometric measurements to estimate the full radiated power and also the impurity content in plasma. In the paper the procedure of calibration of VUV spatial imaging spectrometer is described. The comparison of measured radiation power in different spectral regions is presented.

Calibration of VUV spectrometer

The technique of calibration of spatial imaging VUV spectrometer was developed on the GOL-3 facility in the Budker Institute [2]. The line branching ratio method is used for calibration [3]. The main idea of the method is followed: two spectral lines with common upper level, lying in the VUV and visible spectral ranges, are simultaneously observed. The ratio of intensities of selected lines is a constant, depending only on internal atomic structure of radiating ion. In the visible branch, the calibration can be carried out by conventional technique using black-body radiation source.

Spatial resolved spectrometer allows to simplify the calibration procedure. In such a case the distance from the radiation source as well the area of collection of radiation does not influence the results of measurements, if the VUV and visible spectra are recorded along a common chord of view.

The wide list of spectral line pairs suitable for calibration is given in [3]. In presented experimental measurements the pair of hydrogen lines Lβ (102.6 nm) / Hα (656.3 nm) with intensity ratio equal to 12 is used. (PMT)-based detector with interference filter calibrated by

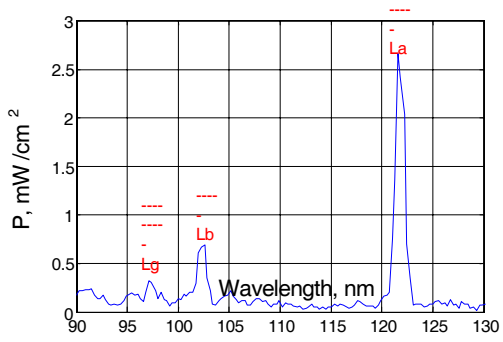

Fig.1 Spectrum of plasma radiation during the first millisecond of discharge

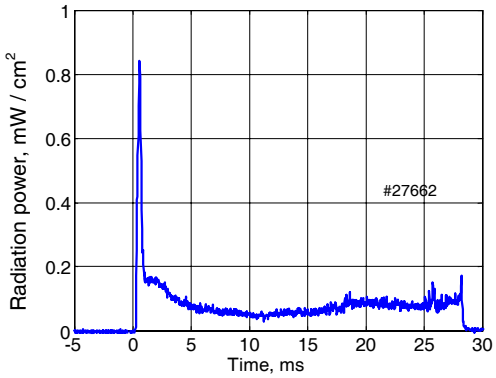

Fig.2 The time history of the Hα (656.3 nm) spectral line. The peak observed in the first millisecond corresponds to bulk ionization of hydrogen.

black-body source (tungsten filament lamp) is used for light registration in visible branch. The main problem of calibration using these lines is that Lβ line lies near to bright oxygen doublet OVI (103.2, 103.7 nm) and can not be sufficiently resolved by spectrometer. Thus, first millisecond of discharge, when hydrogen lines dominate in spectrum, is used for calibration, Fig.1.

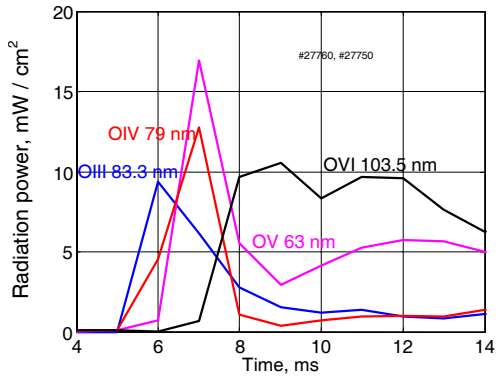

Fig.3. The time history of line radiation power of different Oxygen ionisation stages detected during the CASTOR plasma discharge.

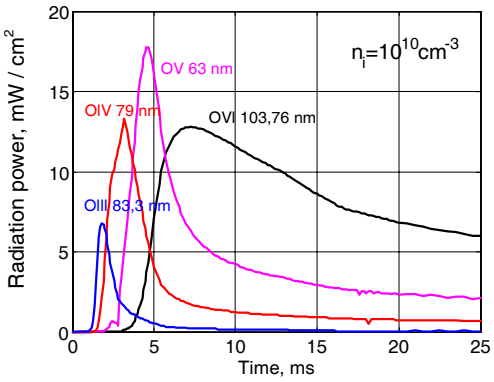

Fig.4. The modeling results of line radiation power dynamic of different Oxygen ionisation stages carried out by STRAHL code. (calculation done in $n_i=10^{16}$ m^{-3}).

Hydrogen lines radiation.

During the first millisecond after start of discharge, the hydrogen lines dominate in the spectrum and are suitable for the calibration procedure. The time history of the Hα spectral line is shown in Fig.2. The peak observed in the first millisecond corresponds to bulk ionization of hydrogen. It is well-known that the rate of ionization and excitation of atom fulfill a similar dependence on temperature and density. The ratio of ionization rate to radiation probability of selected line, S/(XB) (ioniSation/(eXcitation·Branching_ratio)) is practically constant for wide range of plasma parameters. For Hα spectral line the S/(XB)=15 in the plasma temperature range from 10 to 1000eV. It means, that fifteen ionization events are accompanied by emission of one Hα photon [4]. Thus the increase of ionized hydrogen atoms can be derived from detected Hα radiation power during the ionization peak. In the presented shot in fig.2 the value of estimated ionized hydrogen atoms density, $0.6\cdot10^{19}$ m^{-3}, is compared with measured plasma density by interfeter, $0.8\cdot10^{19}$ m^{-3}. The electron temperature measured by electric probes exceeds some eV even in the shadow of limiter. Recombination of hydrogen is negligible in the plasma edge. So the neutral hydrogen flux can be calculated from Hα power measurement via S/(XB) value. Such an estimation gives the value equal to $(3\text{-}5)\cdot10^{19}$ atoms/m^2·s of the neutral hydrogen influx.

Dynamics of ionisation of impurities.

The time history of line radiation power of different Oxygen ionisation stages detected during the CASTOR plasma discharge is seen in fig.3. The plasma temperature linearly growths during the first 5 ms, as can be found from plasma conductivity. The different Oxygen ionisation stages gradually appears The intensity of OVI spectral lines achieves the maximum at 4 ms after the discharge begining.

The experimental measured time evolution of spectral line intensities are compared with calculation of impurity radiation dynamic carried out by STRAHL code [5]. In the modeling the n_{imp} is constant, electron density is taken from interferometric measurements, electron temperature was calculated from plasma conductivity supposing $Z_{eff}=1$. The modeling results are shown in fig.4. Comparison of measured and calculated provides the oxygen ion density of 10^{16} m^{-3}. According to the like same modeling, the carbon ions density is of $(0.2\text{-}0.3)\cdot10^{16}$ m^{-3} in the same plasma discharge.

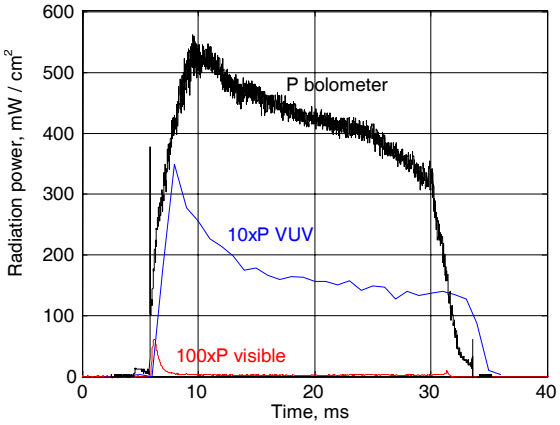

Fig.5. Plasma radiation power in different spectral regions. The radiation power in visible and VUV ranges is low in comparison with full radiated power

Comparison of radiation power in different spectral ranges

The time behaviour of plasma radiation power in different spectral ranges is shown in Fig.5. Radiation in visible range was measured by photo multiplayer tube without filters in the wavelength range from 400 to 700 nm. The VUV radiation power is measured by VUV spectrometer in zero order (without spectral selection) in 50-200 nm range, which is limited by grating reflectivity in short and by detector sensitivity in long wavelength ranges. The full plasma radiation power is detected by AXUV bolometers characterized by constant sensitivity from IR up to soft x-ray region.

As it seen in Fig.5, the radiation power in visible and VUV ranges is low in comparison with full radiated power. We have found, that the bolometric signal is determined by short wavelength radiation (XUV and SX) from high temperature plasma core. So the installed imaging system based on AXUV detectors can be applied for hot core plasma shape determination and a control of magnetic surfaces time evolution.

Conclusions

The variation of branching ratio method of absolute calibration of spatially resolved VUV spectrometer was successfully applied on tokamak CASTOR. Neutral hydrogen flux and concentration of light impurities in plasma were estimated by measurement of spectral lines radiation power. It was shown, that main radiation loses are due to the short wavelength radiation emitted by plasma core.

This work is supported by the Academy of Science of the Czech Republic, AVOZ 20430508 and by the Russian Ministry of Education and Science (project no. RI-111/002/129)

References:

[1] V.Piffl , V.Weinzettl, A.Burdakov, S.Polosatkin, *Czechoslovak Journal of Physics,* 2002, Vol.52, Suppl.D, p.D70-D76

[2] R.Yu. Akentiev, et. al., *Instruments and Experimental Techniques,* Vol. 47, No. 2, 2004, pp. 224–229.

[3] P.Bogen, et.al.., *J. Nucl. Mat.,*1984, N.128 & 129,P.157.

[4] J. Z. Klose and W. L. Wiese // *J. Quant. Spectrosc. Radiat. Transfer,* Vol. 42, No. 5, pp. 337-353, 1989

[5] K.Berhringer, *JET-R(87)08, JET Joint Undertaking,* Culham (1987).

Implementation of Cherenkov detectors for measurements of suprathermal electrons in the CASTOR plasma

V. Weinzettl, J. Stöckel

In collaboration with:
L.Jakubowski, M.J.Sadowski, J.Stanislawski, K.Malinowski, J.Zebrowski, Association EURATOM-IPPLM, The Andrzej Soltan Institute for Nuclear Studies (IPJ), Poland

A prototype of the Cherenkov detector adapted to CASTOR experimental conditions was designed, constructed and placed on a movable manipulator enabling the measurements in different positions along the minor radius to be performed. The detection head contains a Cherenkov-radiator made of an aluminium-nitride (AlN) crystal protected from the visible light by the deposited Ti-layer. The radiator is fixed upon a light-pipe, which is made of a polished quartz rode placed inside the stainless-steel tube. The induced Cherenkov radiation is detected by means of a photomultiplier placed inside a shielding. The first experimental results demonstrate a generation of relatively intense Cherenkov signals depending on toroidal magnetic field and strongly different in the confined and non-confined plasma regions [1].

Measurements of fast electrons produced and escaping from tokamak-type facilities appeared to be of particular interest due to the fact that such electrons inform about non-linear processes occurring inside plasma, and in some cases they can cause a strong erosion of the chamber walls. Probes based on the detection of the Cherenkov radiation, which is emitted immediately (with a delay less than 0.1 ns) and with a very high intensity, can reach high spatial- and temporal resolutions. Appropriate Cherenkov radiators enable to record electrons

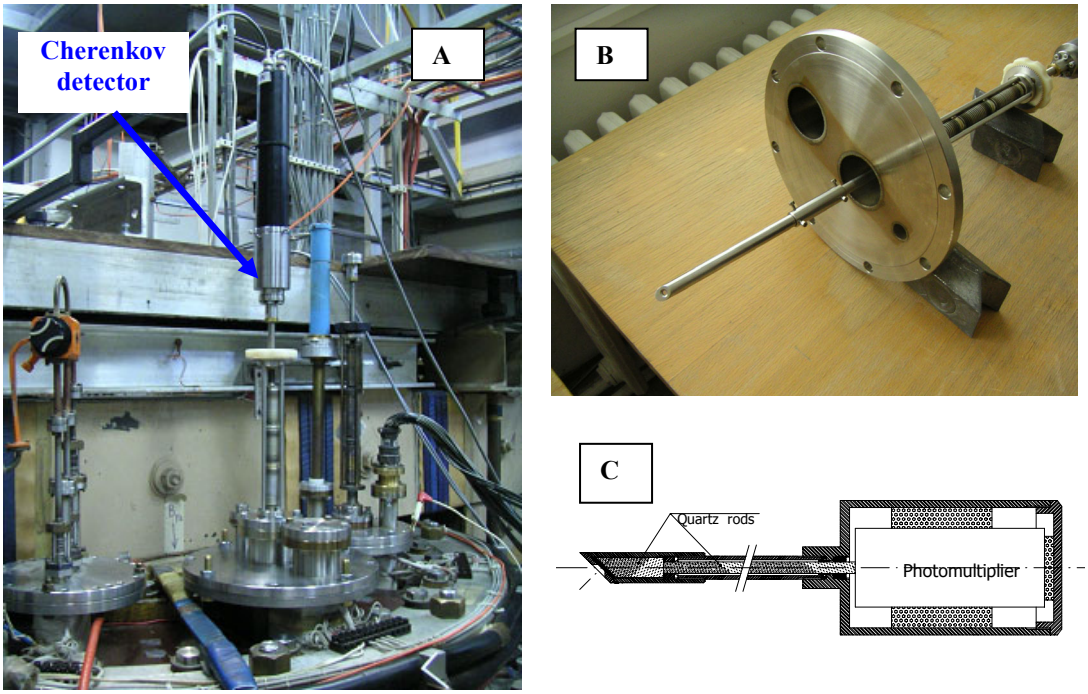

Fig.1: Overview of the Cherenkov-radiation detection system. The measuring head (indicated by an arrow), which was mounted upon the top diagnostic port of the CASTOR tokamak (A); its view (B) and scheme (C). The Cherenkov-radiator is hidden inside the diagnostic port and connected to the photomultiplier through a quartz light-pipe; both parts are shielded against X-rays by the stainless-steel tube.

of energy higher than 50 keV. A prototype of the Cherenkov measuring head adapted to CASTOR experimental conditions was designed, constructed and placed on a movable manipulator enabling the measurements in different positions along the minor radius to be performed, see Fig.1.

The detection head contains a Cherenkov-radiator made of a small aluminium-nitride (AlN) crystal protected from the visible light emitted from surrounding plasma by the deposited Ti-layer. The AlN crystal radiator was chosen due to its relatively low energy threshold, good thermal conductivity and a relatively low price. The radiator is fixed upon a light-pipe, which is made of a polished quartz rode placed inside the stainless-steel tube. The induced Cherenkov radiation is detected by means of a photomultiplier placed inside an appropriate shielding located above the tokamak chamber.

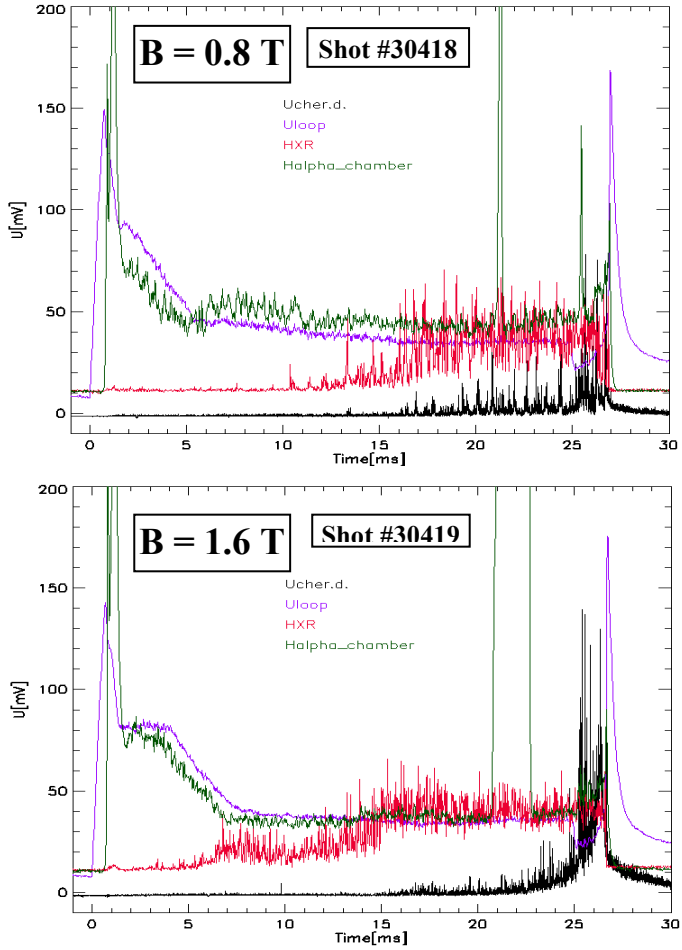

*Fig. 2: Typical traces recorded during tests of the Cherenkov detector in the CASTOR tokamak at different toroidal magnetic field **B**. The red waveforms show signals from the hard X-ray detector (HXR), while the black curve presents signals obtained from the tested Cherenkov-detector head, which was placed at R = 75 mm. The other traces show U-loop and H_α signals.*

The first experimental results, see Fig.2 and [1], demonstrate that relatively intense Cherenkov signals appear particularly during the final phase of the CASTOR discharge. The averaged values of the recorded signals depend on the radial position of the Cherenkov detection head in the edge plasma, and they increase strongly at the radial positions corresponding to the plasma confinement region. This observation confirms that the recorded signals originate from the appearance of the fast electrons in the investigated plasma. Moreover, the anticipated dependence of such signals on the magnetic field value constitutes another experimental evidence of the fast particle generation within the CASTOR tokamak.

Experimental data from CASTOR, together with additional laboratory tests, showed a relatively strong influence of hard X-rays on the Cherenkov detection system. It might be induced by the generation of bremsstrahlung in the detector shielding and the interaction of that with the AlN-crystal and quartz light-pipe. One should take into account also some immediate influence of hard X-rays on the photocathode and dynodes of the applied photomultiplier. Such effects will require further investigation.

Reference:

[1] L.Jakubowski, J.Stanislawski, M.J.Sadowski, J.Zebrowski, V.Weinzettl, J.Stöckel: " Design and tests of Cherenkov detector for measurements of fast electrons within castor tokamak", Czech.J.Phys., Vol.56 (2006), Suppl. B, pp. 98-103

JET neutron data analyses via inversion algorithms based on Minimum Fisher Regularisation

J. Mlynář

In collaboration with:
*G. Bonheure,*Association EURATOM-Etat Belge, ERM/KMS, Brussels, Belgium
A. Murari, Association EURATOM-ENEA, Consorizio RFX, Padova, Italy
M.Tsalas, Association EURATOM-Hellenic Republic, N.C.S.R. "Demokritos",Greece
S. Popovichev, Association EURATOM-UKAEA, Culham Science Centre, Abingdon, UK
S. Conroy, Association EURATOM-VR, Uppsala University, SE-751 05 Uppsala, Sweden
and JET EFDA contributors

Minimum Fisher Information principle proved to provide robust analyses of sparse data in plasma diagnostics. At JET, in collaboration with the Association Euratom-IPP.CR, the inversion methods based on Minimum Fisher Regularisation (MFR) [1] have been successfully validated both in spatial analyses of plasma neutron emissivities measured by the JET profile monitor (MFR tomography) and in spectral analyses of neutrons detected by the NE213 compact spectrometer (MFR unfolding).

MFR tomography of the JET neutron emissivity

The spatial plasma coverage provided by the JET neutron profile monitor is adequate for 2D tomography – i.e. for the inverse reconstruction of the neutron emissivity cross-section – albeit with a rather sparse spatial resolution. In order to validate the potential of neutron tomography at JET, the MFR inversion algorithm was adapted to analyse data from the profile monitor [2].

The MFR tomography has been used for spatial analyses of both 2.5 MeV (D-D fusion) and 14 MeV (D-T fusion, from the TTE campaign) neutron emissivities. It has been demonstrated that spatially resolved measurements of the neutron emissivity dynamics after tritium puff could significantly contribute to studies of tritium transport [3]. In the procedure, Fuel Ratio method [4] and Singular Value Decomposition analysis (see Fig. 1, from [3]) provide powerful tools.

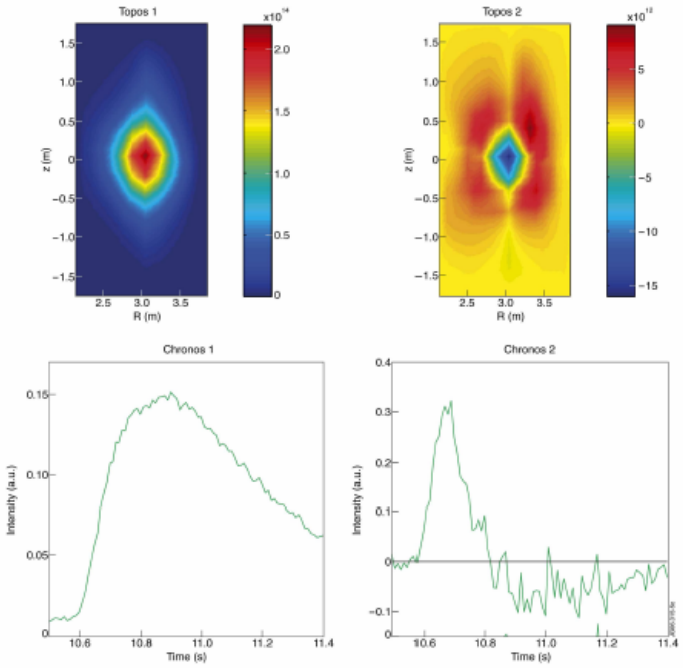

Figure 1: Two main orders of the Singular Value Decomposition of the MFR tomography showing the D-T neutrons emissivity evolution after Tritium puff.

In both 2.5 MeV and 14 MeV neutron energies a clear assymetry of the emissivity in the case of neutral beam heating is observed, with a maximum shifted towards the low field side. The assymetry increases with plasma density. Due to the low spatial resolution of the profile monitor, further smoothing constraints must be implemented into the MFR algorithm before the assymetric emissivities can be studied in detail [3].

Due to these encouraging results, the technique is currently under further developement to include profile inversion (abelisation) as well as a new constraint – unisotropic smoothing along magnetic flux surfaces.

MFR unfolding of the JET neutron spectra

The organic liquid scintillators known as NE213 combine high efficiency, high light output and good pulse shape discrimination properties in neutron detection. However, the pulse height spectrum correspond to recoil protons that originate in the scintillator's volume, while there is no information on the recoil angle. The MFR algorithm was successfully adapted to run the unfolding process for the NE213 data [5]. In a recent upgrade of MFR unfolding the L-curve principle was successfully implemented [6] and the algorithm was provided for a general semi-automated use at JET. Unfolded spectra in both D-D (2.5 MeV) and D-T (14 MeV) energy regions often show interesting and complex peak deformations dependent on plasma density and heating method and power, providing an incentive for corresponding efforts in plasma modelling.

The MFR results are in good agreement with the standard MAXED unfolding code [7], see for example Fig. 2 from [6]. This conclusion clarified that minor artifacts in the unfolded spectra are due to uncertainties in the available response function. Therefore, a detailed callibration of NE213 is foreseen as an significant part of the future upgrades of the JET diagnostics.

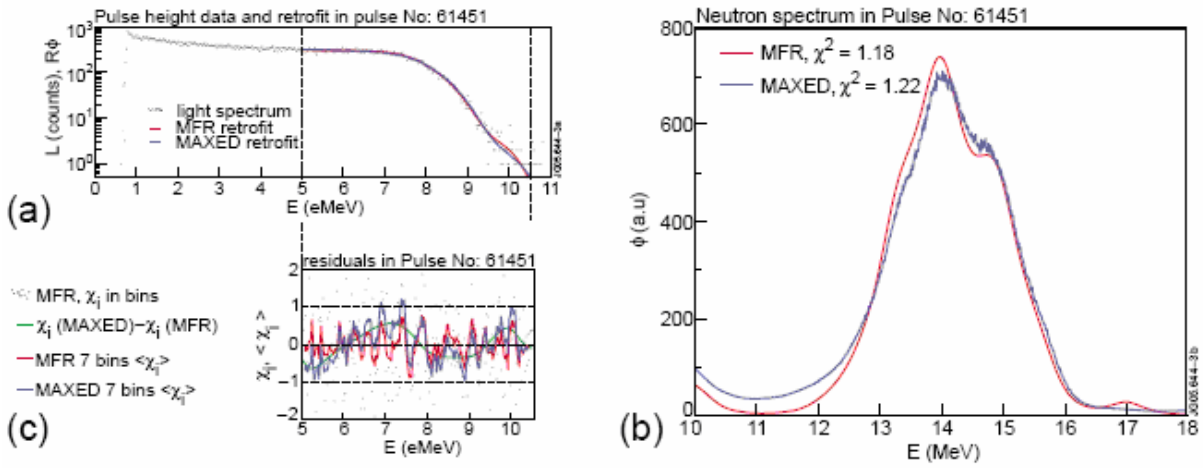

Fig. 2: NE213 spectrum of D-T neutrons in a JET plasma with Ion Cyclotron Resonant Heating: (a) data in light energy bins showing the retrofit, (b) unfolded spectrum of neutrons, (c) residuals ε_i/σ_i

Due to the promising results of the MFR algorithms, a new IPP collaborative activity „Application of the Minimum Fisher Infromation inverse methods in the JET neutron cameras and compact spectrometers data analyses" was launched. Within this activity, extension of the unfolding method to the JET Stilbene neutron spectrometer is foreseen.

References:

[1] M. Anton et al., X-ray tomography on the TCV tokamak, Plasma Phys. Control. Fusion **38** (1996) 1849-1878

[2] G. Bonheure et al.: 2-D spatial distribution of D-D and D-T neutron emission in JET ELMy H-mode plasmas with Tritium puff. 32nd EPS Conference on Controlled Fusion and Plasma Physics, Tarragona, Spain, Europhysics Conference Abstracts **29C** (2005) P-1.083

[3] J. Mlynar, G. Bonheure, A. Murari and JET EFDA Contributors: Prospects of the Minimum Fisher Regularisation in the Experimental Analyses of Plasma Particle Transport at JET. 48th Annual Meeting of the Division of Plasma Physics, Bull. Am. Phys. Soc. p.196.

[4] G. Bonheure et al., Neutron profiles and fuel ratio *n*T/*n*D measurements in JET ELMy H-mode plasmas with tritium puff, Nucl. Fusion **46** (2006) 725

[5] J. Mlynar, J.M. Adams, L. Bertalot, S. Conroy, First results of Minimum Fisher Regularisation as unfolding method for JET NE213 liquid scintillator neutron spectrometry, Fusion Engineering and Design **74** (2005) 781-786

[6] J. Mlynar et al, Neutron Spectra Unfolding with Minimum Fisher Reguarisation, International Workshop on Fast Neutron Detectors and Applications FNDA 2006, Cape Town, Proceedings of Science PoS(FNDA2006)063

[7] M. Reginatto, P. Goldhagen, S. Neumann, Spectrum unfolding, sensitivity analysis and propagation of uncertainties with the maximum entropy deconvolution code MAXED, Nucl. Instrum. Methods **A476** (2002) 242-786

Development and tests of Hall probe based magnetic diagnostics for fusion devices

I. Ďuran, J. Sentkerestiová, M. Hron, K. Kovařík, O. Bilyková, J. Stöckel

In collaboration with:
I. Bolshakova, R. Holyaka, V. Erashok, MSL, Lviv Polytechnic National University, Ukraine
M. Spolaore, Association EURATOM-ENEA, Consorzio RFX, Padova, Italy
V. Coccorese, Association EURATOM-ENEA/CREATE, Italy
C. Hidalgo, M.A. Pedrosa, Association CIEMAT, Spain

Use of various configurations of flux loops for measurement of magnetic field in fusion devices is inherently limited by the pulsed operation of these machines. A principally new diagnostic method must be developed to complement the magnetic measurements in true steady state regime of operation of fusion reactor. One of the options is the use of diagnostics based on Hall sensors. This technique is well established for many applications in experimental physics as well as industry, although it is rarely implemented in the fusion plasma physics. Therefore, besides the tests of radiation hardness of the ITER candidate Hall sensors, the experience with their use in tokamak environment must be gathered. Although, principally aimed for steady state applications, Hall sensors offer some advantages over magnetic coils also for present pulsed fusion devices. It is mainly their smaller size and direct relation of the measured signal to the magnetic field. The frequency response is typically limited to few tens of kilohertz. Several experiments dedicated to testing of various types of Hall probes were done and are being prepared on CASTOR, JET, and TJ-II.

Ring of 16 integrated Hall sensors on CASTOR

The full poloidal ring of 16 magnetic coils, 16 Hall sensors and 96 Langmuir probes uniformly distributed around the whole poloidal circumference of CASTOR was routinely exploited through the 2006 experimental campaigns. All magnetic sensors are aligned to measure the poloidal component of magnetic field. Low cost commercially produced Hall sensors of Allegro A1322LUA type, installed in-vessel at radius of 95 mm were used. These sensors are linear output sensors, with dynamic range ±80 mT. Their operating temperature is -40ºC to 150ºC, frequency range is 0-10 kHz, nominal sensitivity is 31.25±1.56 mV/mT and supply voltage is 5 V.

The arrays of magnetic coils and Langmuir probes were used mainly to investigate relaxation phenomena occurring during polarization of edge plasmas via electrode biasing [1]. The array of Hall sensors was used as an additional magnetic system measuring plasma position on CASTOR. The systematic comparative measurements with Hall probes and all other systems providing information on plasma position (standard set of magnetic coils, arrays of bolometers, rakes of Langmuir probes) were performed. Qualitative agreement between all types of diagnostics was achieved. However, significant systematic quantitative discrepancies were found particularly between vertical plasma position deduced from Hall sensors and separatrix position as deduced from the rakes of Langmuir probes [2]. Explanation of this discrepancy was proposed, suggesting that the magnetic measurements have to be corrected for pick-up of stray magnetic fields induced by external tokamak windings. Redistribution of Hall sensors on the poloidal ring was proposed to validate this hypothesis experimentally. The new arrangement allows 2D magnetic field (vertical and horizontal) measurements at four locations (top, bottom, low field side, high field side). Experiments using this set-up were done late in 2006 and will be validated in 2007.

CASTOR 3D Hall

A new magnetic probe diagnostic based on Hall sensors (developed by MSL, Lviv Polytechnic National University, Ukraine) was used on CASTOR to measure the magnetic field vector well within the plasma confinement region. The probe head contains 3 Hall sensors and 3 coils arranged to measure all three components of magnetic field approximately in a single point of space. The probe is compatible with in-vessel use well in confinement region of CASTOR. It is fully controlled by multi-functional electronic system that drives the Hall probes, amplifies their output signals, performs the A/D conversion and stores the measured data on PC. The bandwidth of the system is up to 200kHz with the Hall sensors providing a good frequency response up to 10 kHz. Radial profile of the magnetic field vector was measured on a shot to shot basis up to r=60 mm and it was used for evaluation of profile of safety factor [3]. Design of the system is similar to that previously used on Tore Supra for measurement of ex-vessel magnetic field. Rather similar system is also being prepared for JET ex-vessel measurements within EP2 project Radiation-hard Hall probe.

JET EP2 project – Radiation-hard Hall probe

The project aims for enhancement of the existing JET ex-vessel magnetic diagnostics system, by installing new sensors, capable of measuring the magnetic field both directly via sets of 3D Hall sensors and also by integrating voltages of coils which are attached to all the Hall sensors. The main rationale behind this project from the JET point of view is to provide additional data to enhance the database for iron core modelling and to improve equilibrium reconstruction. From ITER point of view, it is extremely important to test performance of these ITER candidate sensors under fusion neutron spectrum and also to gather experience from operating them at the large tokamak facility like JET. The project is led by Ass. ENEA, the probes and electronics will be provided by MSL, Lviv Polytechnic National University, Ukraine. The main responsibility of Ass. IPP.CR will be the high level commissioning of the system on JET including analysis and assessment of the measured signals. In 2006, the project was lunched and basic design of the system was agreed. The main part of activities with significant IPP.CR involvement is expected in 2007 and beginning of 2008.

Combined probe for investigation of electromagnetic features of turbulence on TJ-II

The first tests of a combined probe containing one set of Hall sensors in 2D arrangement and two sets of coils in 3D arrangement together with the set of Langmuir probes on TJ-II stellarator were envisaged in 2006. The probe is aiming for investigation of relation between electrostatic and magnetic properties of turbulence and flows in TJ-II edge plasmas. Due to the significant delay in commissioning of the new reciprocating probe drive on TJ-II, the first tests of this diagnostic were postponed to 2007.

References:

[1] M. Hron, P. Peleman, M. Spolaore, J. Brotankova, R. Dejarnac, O. Bilykova, J. Sentkerestiova, I. Duran, L. van de Peppel, J. Gunn, J. Stockel, G. Van Oost, J. Horacek, J. Adamek, M. Stepan: Detailed measurements of momentum balance during the periodic collapse of a transport barier. 33rd EPS Conference on Plasma Phys., Rome, Italy, 19 – 23 June 2006, ECA Vol. **30I**, P-4.076

[2] J. Sentkerestiová, I. Ďuran, E. Dufková, V. Weinzettl: Comparative measurements of plasma position using coils, Hall probes, and bolometers on CASTOR tokamak. Czech. J. Phys. **56**, Suppl.B (2006), B138-B144.

[3] K. Kovařík, I. Ďuran, I. Bolshakova, R. Holyaka, V. Erashok: Measurement of Safety Factor Using Hall Probes on CASTOR Tokamak. Czech. J. Phys. **56**, Suppl.B (2006), B104-B110.

Assessment of the techniques for in-situ calibration of impurity monitor for the ITER in connection with deterioration of the optical components

V. Piffl

In collaboration with:
M. Valisa, F. Sattin, Association EURATOM-ENEA, Consorzio RFX, Padova, Italy
M. Stamp, M. O'Mullane, Association EURATOM-UKAEA Culham, UK
W. Biel, Association EURATOM-FZJ, IPP Jülich, Germany
Part of Final Report of Deliverable 2/8.3 of Contract EFDA/03-1114, April 2006

The main functions of the ITER Divertor Impurity Monitor [1] are to identify impurity species and isotopes of hydrogen and to measure the time evolution of two-dimensional distributions of the particle influxes in the divertor plasmas [2], as well as to diagnose divertor target, wall conditions and to control the radiation loss in the divertor region.

The proposed ITER Divertor Impurity Monitor is based on spectroscopic techniques operating in visible (200 – 1000 nm) [3] and VUV (1 – 200 nm) [4] wavelength ranges. A calibration of the monitor spectroscopy system in ITER divertor involves the following main problems:

- Preservation of the integrity of calibration of the divertor monitor system to obtain reliable spectroscopic data.
- Careful determination of the spectral efficiency of the installed instruments over the whole wavelength range.
- Permanent (running in-situ) recalibration of the optical performance of the monitor system in connection with the deterioration of optical elements in a harsh environment characterised high neutron fluences and mass transfer from areas of net erosion to areas of net deposition.
- Optical alignment of the monitor system when various supporting structures may mechanically move during the plasma discharge.

In the hard environmental conditions during long burn discharges in ITER, the deterioration of the optical components in the Diverter Impurity Monitor give rise to concern oneself with the correctness of measurements. The arrangement like a running in-situ recalibration of the monitor system performance and an axis optical alignment of elements guarantee a preservation of credibility of the spectroscopy data.

Calibration issues regard preservation of the integrity of calibration, determination of the spectral efficiency over the 200 – 1000 nm range and alignment issues. The design of the Divertor Impurity Monitor is in its early stages, which allows considering some extra amendments, which may be beneficial for in-situ monitoring of system performance.

The various solutions are proposed:

- An arrangement of the integrated calibration beam line as a common (or at least equivalent) line of sight for visible and VUV spectrometers in the Diverter Impurity Monitor permits an implantation of the proven calibration methods using thermal emission of black body in the visible range and branching ratio cross calibration method in the VUV range.
- The injection of an exact amount of impurity in the form of preheated solid pellets or target illumination by a powerful laser in divertor area.
- The installation of Diagnostic Neutral Beam as a integrated design including the CXRS and BES in ITER divertor port.

We propose to consider the installation of 1 MW Diagnostic Neutral Beam based on positive ion technology in ITER divertor port as a integrated design including the CXRS and BES.

The CXRS and BES joint system is highly promising to involve effective in-situ calibration technique. An observation system for collecting the beam emission radiation, mostly in the visible, allows an in-situ monitoring of the changes in optical transmission of the sight line due to the energy and particle load (dominantly on the first mirror) from the plasma.

The technology of the positive ion based DNB is well developed and allows He doping of beam. A specific divertor diagnostic neutral beam could operates with any mixture of He and deuterium The required beam intensity is determined more by CXRS needs, to select some of the transitions of interest at high background intensity, than necessarily for calibration by BES. Because the required beam penetration is modest, a relatively low energy beam, 60 – 80kV, would be sufficient.

Some limitation for the DNB performance in the ITER divertor may be the high neutral density, which would penetrate into the beam duct, causing an unknown and probably important amount of attenuation. This may spoil the calibration, because the exact beam intensity would not be known. However it may be possible to check the beam attenuation by the heat deposition in the divertor tiles opposite by infrared thermography installed in appropriate diverter port.

As far as we know, the DNB in combination with CXRS and BES was not involved in ITER divertor diagnostic system yet. The feasibility of such a proposal, the reallocations of ports and other technical issues should not be an obstacle to consider the proposed project, namely from more general point of view: an installation of complete high desired diagnostic system to investigate the important physical processes in the ITER divertor. There is a first plan task: to monitor the impurities behaviour in divertor. It seems, that the CXRS technique is well tested diagnostic approach to investigate the impurity transport phenomena. Recently we have shown, that the line integrated spatial emission profiles created by conventional multi-channel monochromator provide a significant constraint for determining the transport coefficient in edge plasma [5]. The indication of charge exchange radiation makes possible the local measurements of ion quantities. Combination of CXRS and BES enables deduction of ion densities even without absolute calibration and optical transmission measurement. [see Manfred von Hellermann, EU Activities Core CXRS diagnostic on ITER, EU/RF workshop on ITER CXRS, TRINTI Troitsk, September 14 -16, 2005]

The technical solution of the spectroscopy instruments lay out with the respect to the proposed technique of in-situ calibration is not discussed in this assessment. The detailed feasibility studies are necessary to reflect the knowledge of diagnostic availability and the constraint for diagnostic exploitation. Consequently, the emphasis is done on involvement of appropriate construction principles reflecting the in-situ calibration requirements already during the design of Impurity Monitor for ITER Divertor Plasma.

References:

[1] K. Ebisawa, T. Ando, A. E. Costley, G. Janeschitz, E. Martin and T. Sugie: Vacuum ultraviolet divertor impurity monitor for the ITER Rev. Sci. Instr. 70 1 (1999) 328

[2] T.Sugie, H.Ogawa, T.Nishitani, s.Kasai, J.Katsunuma, M.Maruo,K. Ebisawa, T. Ando, Y.Kita, Divertor impurity monitor for the ITER Rev. Sci. Instr. 70 1 (1999) 351

[3] T.Sugie, A.E.Costley, A.Malaquias, A.Medvedev and C.I. Walker, Spectroscopic Measurement System for ITER Divertor Plasma: Divertor Impurity Monitor, 30th EPS Conference on Contr. Fusion and Plasma Phys., St. Petersburg, 7-11 July 2003, ECA Vol. **27**A, P-4.63

[4] W. Biel, R. Barnsley and G. Bertschinger Design of VUV impurity monitors and VUV imaging spectrometers for ITER 31st EPS Conference on Plasma Phys. London, 28 June - 2 July 2004 ECA Vol.28G, P-1.13

[5] V.Piffl, H.Weisen, A.Zabolotsky, Ultra-soft X-ray spectroscopy using multilayer mirrors on TCV, Plasma Phys.Control.Fusion 46, 11 (2004) 1659

3 Wave interactions in Plasmas

Energy Distribution Measurements of Fast Particles Generated in Front of the LH Grill Mouth in Tore Supra

V. Petržílka, F. Žáček

In collaboration with:
J. Gunn, M. Goniche, L. Colas, A. Ekedahl, E. Gauthier, D. Mazon, I. Nanobashvili, J.–Y. Pascal, Association EURATOM-CEA, CEA/DSM/DRFC Cadarache, France
J. Mailloux, Association EURATOM-UKAEA, Culham Science Centre, Abingdon,UK

A retarding field analyzer (RFA) was used during lower hybrid (LH) current drive experiments in the Tore Supra tokamak to characterize the supra-thermal particles emanating from the region in front of the LH grill. This work is the continuation of our previous efforts [1,2]. In addition to fast electrons, we tried to observe fast ions accelerated due to a positive charge accumulated (and measured in the CASTOR tokamak [3]) in front of the LH grill.

In the RFA, the plasma particles pass through a slit and two grids to a grounded collector. The slit (30 μm by 5 mm section, cut in a 150 μm nickel plate) is biased negatively (-50 to -100 V) to repel thermal electrons. All ions, as well as electrons with energy greater than the slit voltage, pass through the slit. Both grids are biasable to ±1000V, allowing us to scan the particles according to their energy, and separate the ions from the electrons (if their energies are less than 1000 eV).

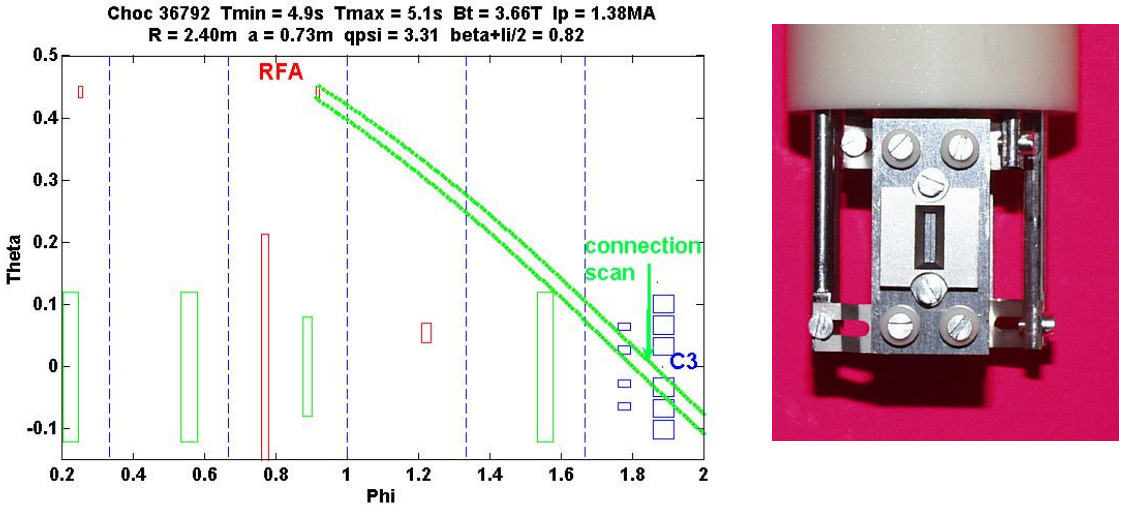

Fig.1. Left: Scheme of the connection scan between C3 LH launcher and the RFA Right: Photograph of the RFA entrance slit.

The RFA collects particles that flow along field lines from the outboard side of the tokamak. The measurements were performed when one of the wave-guide rows of the C3 launcher was magnetically connected to the RFA. First, in shot #35613, the top C3 waveguide row was connected to the RFA. We found that -400V applied potential was not large enough to repel all the fast electrons for the launched C3 power of P_{LH}=2 MW. The upper energy boundary of

the fast electron beam is therefore higher than 400 eV for the 2 MW launched, which is consistent with modeling [4]. For the same magnetic connection, we found in shot #35616 that even +300V is not enough to repel all ions. However, the analysis of the ion current shows no traces of fast ion beams in this shot, and the observed ion current might be produced by the thermal ion acceleration in the near slit sheath voltage.

We decided to try operating at lower power levels in order to be able to fully repel even the suprathermal electrons and try to identify any suprathermal ions. In the shot #36791, we optimized the magnetic field connection by a coarse scan of the plasma current, for P_{LH}=0.75 MW, ion grid 0V, electron grid –100 V. The scan was performed from the top C3 waveguide row downwards, cf. Fig. 1.

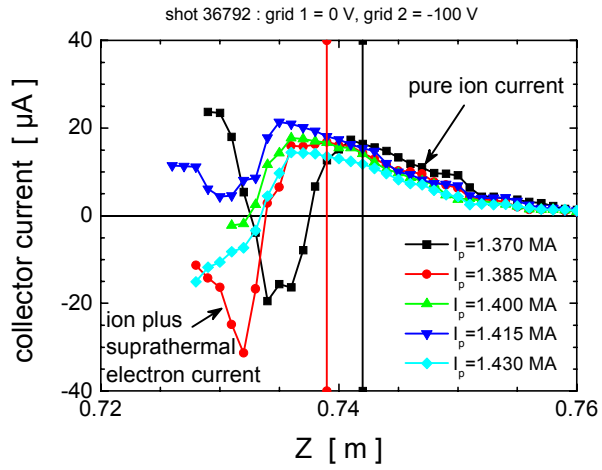

Fig.2. Collector current measured during the fine connection scan between C3 LH launcher and RFA. The negative dips are caused by electrons with energy greater than 100 eV. The black and red vertical lines indicate the magnetic connection to the leading edge of the LH launcher for the first and second reciprocations respectively. The 3mm shift is due to slight outward drift of the plasma at the beginning of the discharge. The magnetic connections for the later reciprocations (I_p≥1.4 MA) are identical to the second one (red).

The fast electron RFA signal from the 3rd row from the C3 bottom was then optimized by a fine scan in shot #36792, Fig.2, ion grid 0V, and electron grid –100V, P_{LH}=1.5 MW. The collector current is composed of electrons with energy greater than 100 eV, and ions. It should be noted that we plot here the time-averaged current at each position. Both inward and outward phases of the probe reciprocation are included in the average. The time window for averaging is 2 ms. In reality the electron current signal is extremely bursty, with nearly 100% variance, but we will not discuss this aspect in this paper. Within experimental uncertainties (<5 mm), the fast electron beam does indeed seem to be created immediately in front of the LH launcher. The peak current lies between 5 and 10 mm in front. The beam, as seen in the past, is about 10 mm wide. Even though the RFA did not fully penetrate the beam in each case, we see a clear variation of the beam strength caused by the poloidal scan of the magnetic field line in front of the wave guide row.

In the future we will try to make a more detailed poloidal scan and produce a 2D poloidal-radial map of the electron current. In shot 36793, we observed that +400V on the ion grid is not enough to repel all ions at the LH power of 1.5 MW. The variations of the fast electron and ion signal as a function of the LH power were studied in shots #36794 and 36795, cf. Fig. 3. Fig. 3a shows growth the fast electron signal with LH power, the ion grid was at +200V, so that all thermal ions should be stripped from the signal; the electron grid was at 0V due to a technical problem, so only the entrance slit at -80 V repelled thermal electrons. The electron signal is mostly due to suprathermals, but it cannot be excluded that a small fraction of thermals is present. It is clear that the electron current increases roughly as the square of the LH power. When the electron grid is at –400V (shot #36795), the fast electron signal disappears, Fig. 3b.

This means that, as we hoped, it is possible to repel all suprathermals at low values of LH power. Here, the ion grid was at 0V, allowing all ions to flow to the collector (that is, thermals as well as any suprathermals that might exist). There do not appear to be any singular features that would indicate the presence of suprathermal ions. It would be necessary to scan the ion repelling voltage to increasingly positive values in order to gradually strip away the thermals and see if any radial structure exists at large energies. Unfortunately the experiment session was terminated by a technical problem and we were unable to continue. It is planned to try again in the near future.

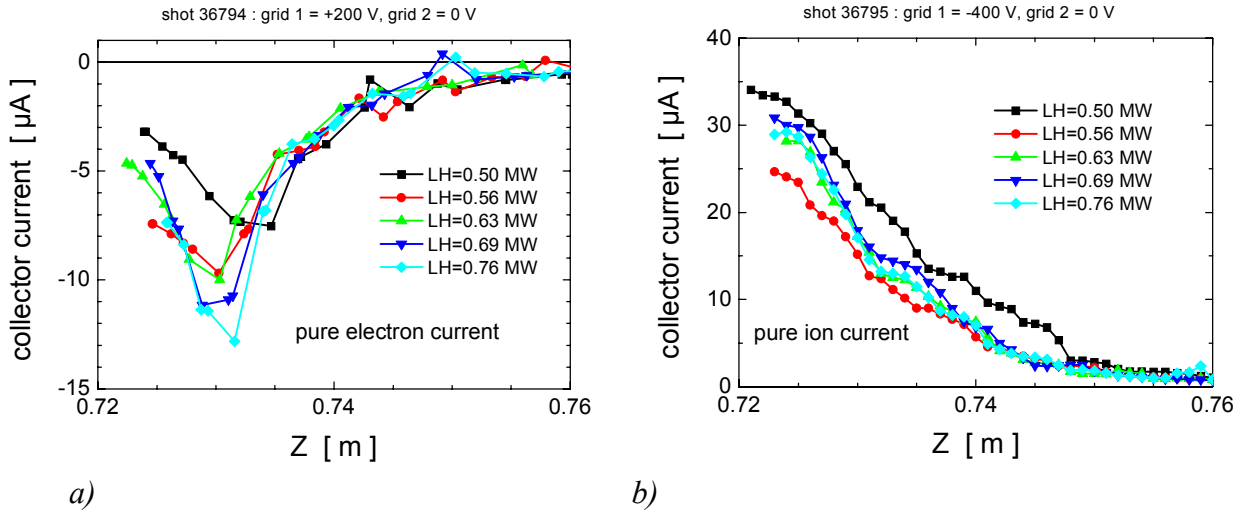

Fig.3: Dependence of the fast electron and ion signal on LH power: a) ion grid +200V, electron grid at 0V; b) ion grid at 0V, electron grid at –400V. The first profile (black) is slightly shifted outward due to a slow movement of the plasma at the beginning of the discharge, as in Fig. 2.

The main results are as follows: By varying the edge safety factor, we optimized the connection between RFA and the LH grill to obtain a maximum intensity of the fast electron beam. Clear indications of a fine poloidal structure were obtained for the first time. A strong variation of fast electron beam current with lower hybrid power was identified. For high power levels (greater than 1 MW), the electron energy is greater than 400 eV. Fast electrons exist even at low power levels (between 0.5 and 0.75 MW), and their energy is lower than 400 eV. These fast electron energy limits are consistent with a simple model of electron acceleration in the near-field of LH antennas [4]. After separating those fast electrons from the RFA signal, we observe pure ion current. No clear evidence of suprathermal ions was found on the ion current profiles, but the decisive experiment that will separate thermals from suprathermals could not be performed due to technical problems. These original results are quite encouraging, and will be further explored in the near future.

Supported partly by the project GACR 202/04/0360.

References:

[1] M.Goniche, et al., 31th EPS Conference, London, June 2004, P-4.110.

[2] V. Petrzilka , EPS 2005 Conference, Tarragona, Spain, P-2.096.

[3] F. Zacek, V. Petrzilka, M. Goniche: Plasma Phys. Contr. Fusion 47 (2005) No.7, L17.

[4] M. Goniche, et al., Nuclear Fusion 28 (1998) 919.

Electron Bernstein wave simulations for MAST and NSTX

J. Preinhaelter, J. Urban

In collaboration with:
V. Shevchenko, M. Valovic, Association EURATOM-UKAEA, Culham Science Centre, UK
S.J. Diem, G. Taylor, Princeton Plasma Physics Laboratory, Princeton, New Jersey, USA
L. Vahala, Old Dominion University, Norfolk, Virginia, USA
G. Vahala, College of William & Mary, Williamsburg, Virginia, USA

Simulations for MAST. *For the MAST ELM-free H-mode discharge 8694, the measured electron Bernstein wave emission does not correspond to the simulations results, which use EFIT magnetic equilibrium and high resolution (ruby laser) Thomson scattering (TS) density and electron temperature profiles. The first discrepancy is that the minima in the measured spectrum occur at higher frequencies than in the simulated spectrum. The second discrepancy is in the amplitude of the maxima in the spectrum, particularly the 1st harmonic emission, which is different in the simulation and in the experiment.*

A possible reason for the discrepancy in the minima is an inaccuracy in the edge magnetic field. Minima in an EBE spectrum must occur at frequencies at which the UHR coincides with an EC harmonic, i.e.

$$f_{UHR} = kf_{ce}, \quad k = 1, 2, \ldots \tag{1}$$

Under such condition, no EBW is emitted because the space where EBW can exist shrinks to zero and $T_{rad} = 0$. From (1) we can approximately determine the magnetic field assuming that the emission comes from the equatorial plane. The results are depicted in Fig. 1. The experimental and simulated spectra are shown (left) as well as the resulting magnetic field, which shows a magnetic well behaviour (right). Qualitatively similar magnetic configuration can be obtained by imposing additional pressure constraints in the EFIT code [1].

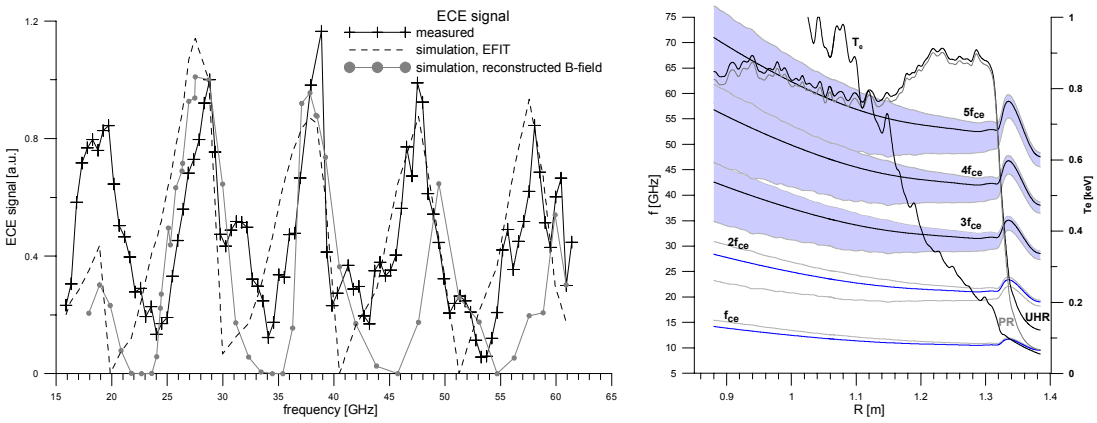

Fig. 1: EBE for MAST shot 8694, t=280 ms, comparison between experiment and simulations using EFIT and reconstructed magnetic fields (left). Characteristic frequencies for the reconstructed magnetic field with Doppler broadening of EC harmonics (right).

As already noted, there are also discrepancies in the amplitudes of the maximums in the EBE spectrum. The largest difference is between the 1st and the 2nd harmonic emission, where the simulated intensity is a factor of two lower than in the experiment. The discrepancy can be caused by inaccurate density profile in the conversion region, i.e. in the edge plasma [1].

Simulations for NSTX. There is a qualitative agreement between experimental and simulation results on antenna aiming for L-mode plasmas. This has been tested for several shots, including some H-mode plasmas. During flattop current discharges it seems that the optimal angles are quite rugged and are independent of time. There is a good agreement in the time development of the emission for the low frequency antenna between simulation and experiment [2,3]. The simulated frequency dependence of the emission shows some deviations from experiment for the low frequency antenna, but this should be corrected by inclusion of collisional damping corresponding to high Z_{eff} in helium discharges. For the high frequency antenna (simulation results in Fig. 2), the final experimental results are being recalibrated and so are not yet available for comparison with simulated ECE [4].

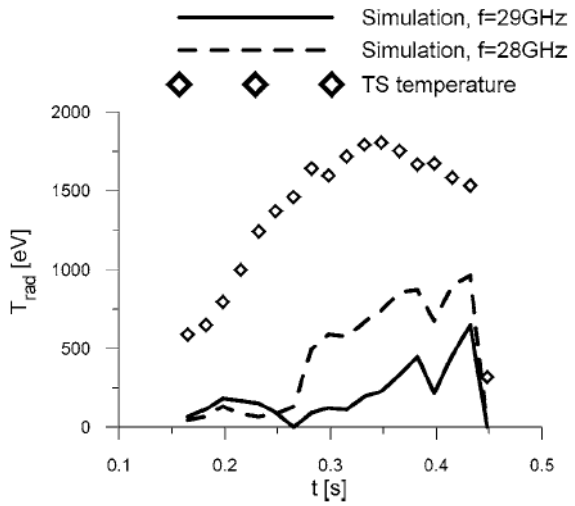

Fig. 2: A time development of EBWE at both 28 and 29 GHz for shot 120278. TS represent Thomson scattering data. Experiment antenna orientation is ϕ_{dev}= +22.4°, ϕ_{long}= +18°.

References:

[1] Urban, J., Preinhaelter, J., Pavlo, P., Diem, S.J., Taylor, G., Shevchenko, V., Valovic, M., Vahala, L., Vahala, G.: *EBW Emission Simulations and Plasma Diagnostics*. 14th Joint Workshop on Electron Cyclotron Emission and Electron Cyclotron Resonance Heating, Santorini, Greece (2006)

[2] Preinhaelter, J., Urban, J., Pavlo, P., Taylor, G., Diem, S., Vahala, L., Vahala, G.: Electron Bernstein wave simulations and comparison to preliminary NSTX emission data. *Review of Scientific Instruments* 77 (2006) p. 10F524

[3] Harvey, R.W., Cary, J.R., Taylor, G., Barnes, D.C., Bigelow, T.S., Coda, S., Carlsson, J., Caughman, J.B., Carter, M.D., Diem, S., Efthimion, P.C., Ellis, R.A., Ershov, N.M., Fonck, R.J., Fredd, E., Garstka, G.D., Hosea, J., Jaeger, F., LeBlanc, B., Lewicki, B.T., Phillips, C.K., Preinhaelter, J., Ram, A.K., Rasmussen, D.A., Smirnov, A.P., Urban, J., Wilgen, J.B., Wilson, J.R., Xiang, N.: Electron Bernstein Wave Studies: Current Drive; Emission and Absorption with Nonthermal Distributions; Delta-F Particle in Cell Simulations. *21st IAEA Fusion Energy Conference*, Chengdu, China (2006)

[4] Diem, S.J., Taylor, G., Efthimion, P.C., LeBlanc, B.P., Carter, M., Caughman, J., Wilgen, J.B., Harvey, R.W., Preinhaelter, J., Urban, J.: T-e(R, t) measurements using electron Bernstein wave thermal emission on NSTX. Review of Scientific Instruments **77** (2006) p. 10E919

Simulations of EBW heating in WEGA

J. Preinhaelter, J. Urban

In collaboration with:
H.P. Laqua, Y. Podoba, Association EURATOM-IPP, Greifswald, Germany

Discharges in the WEGA stellarator are sustained exclusively by 2.45 GHz RF heating. Plasma density is typically far above the critical density so only electron Bernstein waves (EBWs) can propagate inside the plasma. Experiments show dependence on the magnetic field magnitude testifying a resonant principle of the wave damping. The best performance (the most central power deposition) is usually achieved with 0.65 times the resonant magnetic field B_{ce} = 0.0875 T. Typical electron temperatures in WEGA are ~10 eV.

EBWs behaviour has been simulated with O-X-B conversion efficiency and ray-tracing calculations. Detailed analysis is made difficult because the upper hybrid resonance is far outside the last closed flux surface, where the plasma profiles are fluctuating and the magnetic field is ergodic; therefore, an averaged and extrapolated configuration is used in the calculations. However, possible mechanisms are clearly seen from the simulations results (see Fig. 1 and 2). Growth of the parallel wave number up to ~30 along with the characteristic admixture of energetic electrons produced by the RF heating allow strong resonant absorption at the Doppler shifted electron cyclotron resonance so that the deposition region moves towards the plasma centre when the magnetic field is decreasing from 0.85 Bce to 0.65 Bce, see [1].

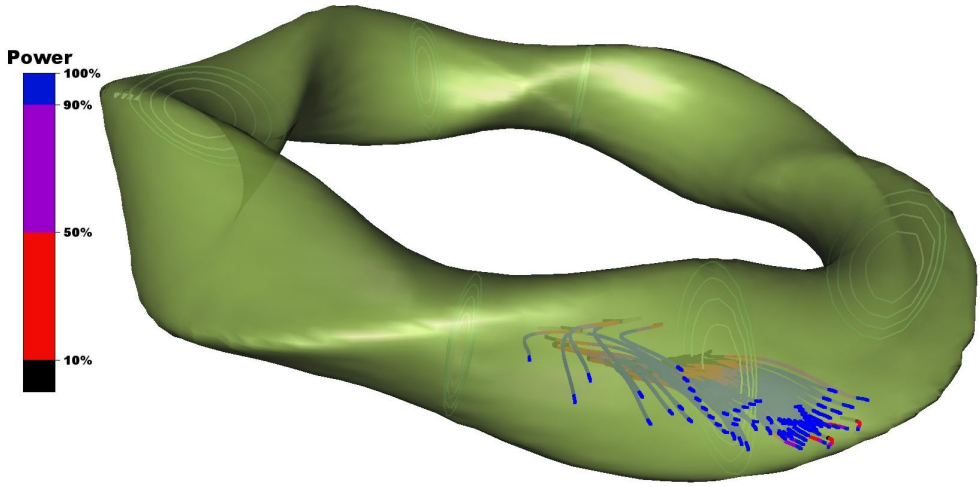

Figure 1: EBW rays in WEGA. The power is indicated by the colour, i.e. 80% of the power is absorbed in the violet – red region.

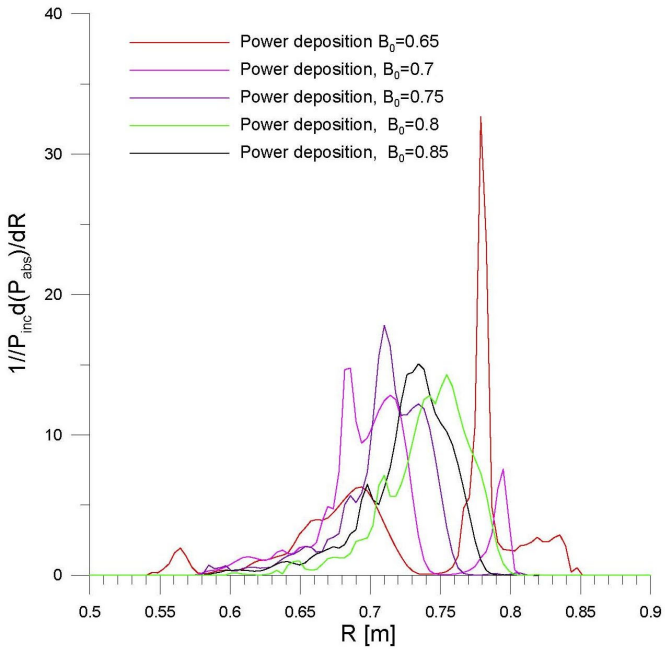

Fig. 2: EBW power deposition in WEGA including hot electrons effects.

References:

[1] Preinhaelter, J., Urban, J., Laqua, H.P., Podoba, Y., Vahala, L., Vahala, G.: *Simulation of EBW Heating in WEGA*. 17th Topical Conference on Radio Frequency Power in Plasmas, Clearwater, Florida, USA (2007)

4 Atomic Physics and Data for Edge Plasma and Plasma–Wall Interactions

Energy transfer and chemical reactions in collisions of ions with surfaces

Z. Herman, J. Žabka, A. Pysanenko
J. Heyrovsky Institute of Physical Chemistry, Academy of Sciences of the CR

In collaboration with:
Research Group of Prof. T. D. Märk, Association EURATOM-ÖAW, Institute for Ion and Applied Physics, University of Innsbruck, Austria

In 2006, systematic studies of interactions of slow (15-50 eV) hydrocarbon ions with surfaces, relevant to plasma and fusion systems, were extended to different surfaces. Earlier, we described results on collisions of C_1 , C_2 , and C_3 hydrocarbon ions with room-temperature and heated (600^0 C) carbon surfaces, and a comparison of dication and cation collisions, using model C_7 hydrocarbon ions. In 2006, we concentrated on studies of interaction of small hydrocarbon ions with tungsten and beryllium surfaces. These studies originated from direct demands to obtain analogous data, gathered earlier for carbon surfaces, for other surface materials, of importance in fusion research.

The experimental method consisted, similarly as earlier, in directing the projectile ion reactant beam of a well-specified incident energy under a pre-selected angle (in our case 30^0 with respect to the surface) towards a carbon surface, and in measuring mass spectra of product ions as well as their translational and angular distributions. The data provide information on ion survival probability of the projectile ions in ion-surface collisions, on surface-induced dissociation processes and on chemical reactions with the surface material. The data can also serve in determining the mechanism of reactions at surfaces, to elucidate energy transfer in collisions with surfaces, the extent of inelasticity of the collisions and the degree of incident-to-internal energy transfer for ions of increasing complexity. The surfaces used in these experiments were samples of polycrystalline tungsten and beryllium. These surfaces could be studied either at room temperature, when they were covered -as shown earlier for carbon surfaces- by a layer of hydrocarbons, or at a temperature of about 600^0 C, when this hydrocarbon layer was effectively removed. An off-line analysis of the samples by the ESCA method was available to determine the sample composition.

Collisions of low-energy C_1 and C_2 hydrocarbon ions with room-temperature and heated tungsten surfaces

The polycrystalline W-surface was chemically cleaned to remove impurities. The sample used in the scattering experiments was at room-temperature covered by a layer of hydrocarbons (as indicated by the occurrence of a strong H-atom transfer reaction between radical ion projectiles a terminal CH_3- groups of the surface hydrocarbons). ESCA analysis of this surface showed, besides hydrocarbons (CH-groups in the spectra) small amounts of oxides and carbide on the surface. Experiments with the surface at room temperature, showed that a certain fraction (few percent) of the incident projectile ions recoiled was deflected from the surface with full energy. It appears that these ions never collided with the surface, but they were deflected by surface charges. Heating of the surface to 600^0C led to a decrease of this fraction of full-energy projectile ions to less than 0.1 % of the scattered ions. ESCA analysis of the surface after heating showed a strong increase of the W-carbides on the

surface. We assume that this is due to transformation of insulating oxides on the surface to carbides formed by cracking of the surface hydrocarbons. Results are the following:

- The ion survival probability in collisions with room-temeprature and heated tungsten surfaces was usually several times smaller than the survival probability on the respective carbon (HOPG) surfaces. Typically, it was for CD_4^+ 0.05% (HOPG 0.35%), for CD_5^+ about 1% (HOPG 12%), and for $C_2D_4^+$ 0.2% (HOPG 1-2%).
- The W-surface at room temperature was covered by hydrocarbons, similarly as in the studies of carbon surfaces. Mass spectra of the ion products showed both ions formed by direct dissociation of the projectile hydrocarbon ion and (in case of radical ion projectiles) ions formed in chemical reactions with hydrocarbbons on the surface; these were H-atom transfer reactions (protonated projectiles and their fragmentation products) and carbon chain build-up reactions (C_3 hydrocarbon ions from C_2 projectiles). In general, the extent of fragmentation incresed with increasing incident energy and it was similar to that from collisions with carbon sufaces. Collisions with the W-surface heated to or above 600^0C showed only fragmentations of the projectile ions, no chemical reactions, indicating effective removal of the hydrocarbon layer on the surface. Fig. 1 shows examples of mass spectra of product ions of a radical cation $C_2D_4^+$ and closed-shell ion CD_5^+ interaction with a room-temperature (upper part) and heated W-surface (lower part); $C_2D_4^+$ interacting with the room-temperature W-surface shows chemical reactions of H-atom transfer (blue) and carbon chain bulid-up reactions (green). The closed-shell non-reactive CD_5^+ shows only fragmentation.

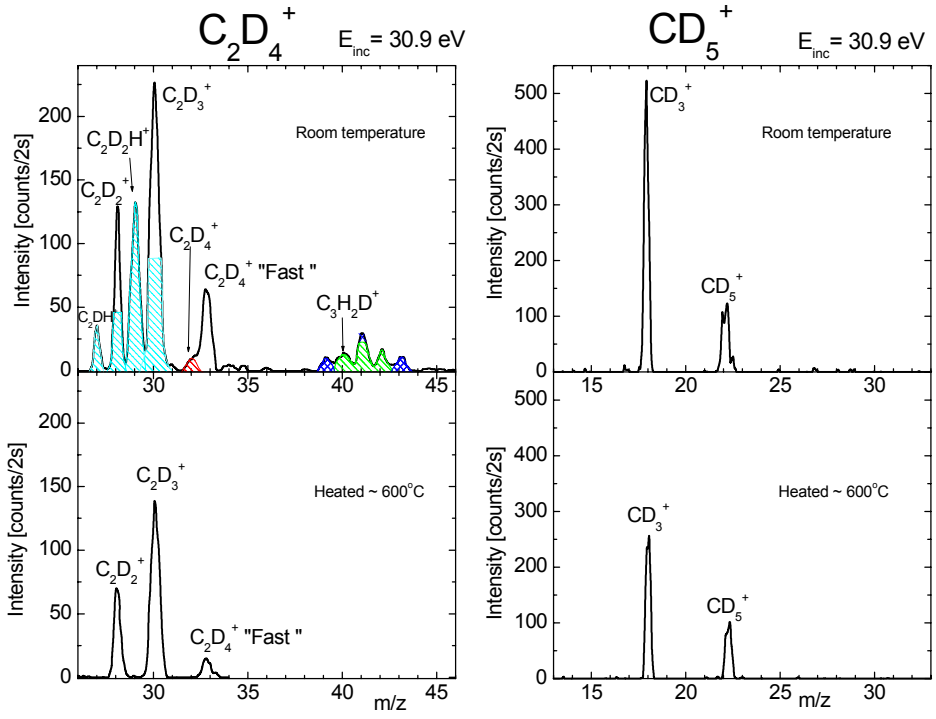

Fig. 1. Mass spectra of product ions from collisions of the projectiles $C_2D_4^+$ and CD_5^+ with tungsten surfaces at the incident energy of 30.9 eV

- The collisions of the hydrocarbon ions with both room-temperature and heated surfaces were inelastic, the translational energy of the product ions was 20-50 % of the of the incident energy on room-temperature surfaces, and 30-70 % of the incident energy on heated surfaces, slightly increasing with collision energy, especially for the C_1 ions. Examples are shown in Fig. 2.

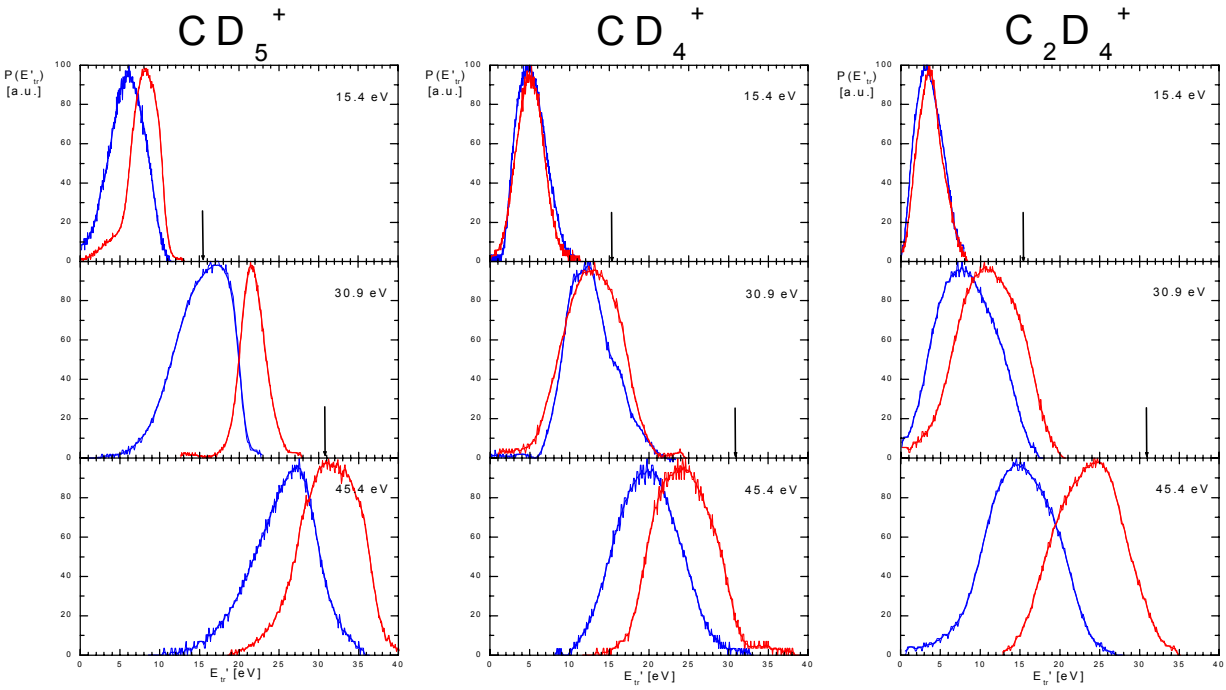

Fig. 2. Translational energy distributions of inelastically scattered non-dissociated product from collisions of CD_5^+, CD_4^+, and $C_2D_4^+$ with room-temperature (blue) and heated (red) tungsten surfaces.

Collisions of low-energy C_1 and C_2 hydrocarbon ions with room-temperature and heated beryllium surfaces

Preliminary data were obtained on scattering of CD_4^+, CD_5^+, and $C_2D_4^+$ from room-temperature and heated surfaces of Be. At room temperature, the surface was covered by hydrocarbons, as in all previous cases. The scattering of the above mentioned ions showed structure in both angular and translational energy distributions of the ion products: up to 3 peaks in the angular distributions were connected with different inelastic energy losses. In this sense, the Be surface appears to be the most complicated of all surfaces studied earlier (carbon, tungsten). Be surface analysis by the ESCA method showed that under the layer of hydrocarbon, on the Be surface there were both Be oxides and Be carbides, forming presumably micro-islands. The structures in the scattering results are evidently connected with scattering of ions from these micro-islands of different chemical nature.

The experiments in the next period will concern chemical modification of the Be surface (sputtering, oxidative ion bombardment etc.) with the aim of assigning features in the scattering to the particular chemical material of the surface.

Papers summarizing the above data are under preparation.

III TECHNOLOGY

OVERVIEW OF TECHNOLOGY TASKS

Most of the technology tasks within Association EURATOM-IPP.CR deal with the properties of various diagnostic and structural elements and materials of future thermonuclear reactors, before and under neutron irradiation. For the latter purpose, two irradiation sites are utilized: light water experimental fission reactor LVR-15 (operated by NRI plc), and the isochronous cyclotron U-120M with the maximum proton energy of 37 MeV (operated by NPI ASCR). Both devices are located in Řež about 20 km from Prague and they are integrated within the Association EURATOM-IPP.CR.

In 2006, technology research of the Association EURATOM/IPP.CR covered the following areas:

- **Tritium Breeding and Materials**
  - **Breeding Blanket**
  - **Materials Development**
- **Physics Integration**
  - **TPDC Diagnostics - Ceramics**
- **Vessel/In Vessel**
  - **Blanket**

In total, researchinstitutes of our Association investigated eight different EFDA Technology tasks and seven Underlying technology taska. The tasks are listed below; further on, the progress in individual deliverables is described in detail.

1. Technology Tasks

TW2-TTMS-001b
RAFM Steels: Irradiation Performance
Field/Area: Tritium Breeding and Materials/ Materials development
Deliverable: Static and dynamic toughness testing at the transition temperature: Neutron irradiation of plates and weldments up to 2.5 dpa at 200-250°C and post irradiation examination.
Principal Investigator: *Petr Novosad,* NRI Řež
Collaborative Staff: *K. Šplíchal, W. Soukupová, M. Andrejsek, V. Krhounek*

TW3-TTMS-003
RAFM Steels: Compatibility with Hydrogen and Liquids
Field/Area: Tritium Breeding and Materials/ Materials development
Deliverable: Crack growth kinetic and fracture toughness on EUROFER in presence of hydrogen (up to 10 wppm) at RT, 250°C

Principal Investigator: *Karel Šplíchal,* NRI Řež
Collaborative Staff: *J. Berka, J. Burda, M. Žamboch*
Deliverable: In-pile PbLi corrosion testing of TBM´s weldments (stiffeners and bottom plate relevant)
Principal Investigator: *Vladimír Masařík* (replaced Milan Zmitko), NRI Řež
Collaborative Staff: *J. Berka, J. Dušek, E. Vlasák*

TW5-TTBC-005
Helium Cooled Lithium Lead: Process and Auxiliary Components
Field/Area: Tritium Breeding and Materials / Breeding Blanket
Deliverable: Development and testing of components for the liquid metal loop (cold traps, high temperature flanges and circulation pump)
Principal Investigator: *Vladimir Masarik,* NRI Řež
Collaborative Staff*: K. Šplíchal, J. Berka, J. Dušek, P. Hájek*

TW3-TVB-INPILE
In-pile experiment on PFW Mock-ups
Field/Area: TV – Vessel/In Vessel, TVB/ Blanket
Deliverable: Perform in-pile testing of Be protected PFW mock-ups under heat flux.
Principal Investigator: *Tomáš Klabík* (replaced M. Zmítko), NRI Řež
Collaborative Staff: *P. Hájek, V. Masařík, J. Dušek*

TW4-TVB-TFTEST2
Thermal fatigue tests of Be coated Primary First Wall Mock-ups
Field/Area: TV – Vessel/In Vessel, TVB/ Blanket
Deliverable: Construction of the facility for thermal fatigue tests of Be coated primary first wall mock-ups
Principal Investigator: *Tomáš Klabík* (replaced J. Bohata), NRI Řež
Collaborative Staff: *P. Hájek, V. Masařík, J. Dušek*

TW6-TTMI-003, D4
Development of activation foils dosimeters for determination of IFMIF-relevant flux spectra: validation experiments
Field/Area: Tritium Breeding and Materials / IFMIF
Principal Investigator: *P. Bém,* Nuclear Physics Institute Řež
Coauthors: *V. Burjan, M. Götz, M. Honusek, V. Kroha, J. Novák and E. Šimečková*
In collaboration with: *U. Fischer and S.P. Simakov*, Association FZK-Euratom, Forschungszentrum Karlsruhe, Germany

TW6-TTMN-002, D5
Experiments for validation of cross-sections up to 55 MeV in an IFMIF-like neutron spectrum: activation experiment on Cr
Field/Area: Tritium Breeding and Materials / Materials Development
Principal Investigator: *P. Bém*, Nuclear Physics Institute Řež
Co-authors: *V. Burjan, M. Götz, M. Honusek, V. Kroha, J. Novák and E. Šimečková*
In collaboration with: *U. Fischer and S.P. Simakov,* Association FZK-Euratom, Forschungszentrum Karlsruhe, Germany

TW6-TVV-SYSEG
Assessment of PSM welding distortions and field welding
Principal Investigator: *Lubomír Junek,* IAM Brno
Co-authors: *Slováček Marek, Diviš Vladimír, Ochodek Vladislav*, Institute of Applied Mechanics Brno Ltd.

2. Underlying Technology

IPP-CR_UT06_TVM_Spray
Plasma sprayed tungsten-based components
Objective: The development of plasma facing components for potential application in ITER, produced by plasma spraying of tungsten-based materials.
Principal investigator: *Jiri Matejicek,* IPP AS CR Prague

IPP-CR_UT06_TVM_PFW
Thermal Fatigue tests of Beryllium coated Primary First wall mock-ups
Objective: Workplace building-up for handling and manipulations with Beryllium coated Primary First Wall mock-ups.
Principal investigator: *Vladimír Masařík,* NRI Řež plc

IPP-CR_UT06_TVV_Weld
Heat source models development for individual ITER welding technologies and its influence on the final ITER distortion.
Objective: Determination of heat source models for individual ITER welding technologies.
Principal Investigator: *L. Junek,* IAM Brno Ltd.

IPP-CR_UT06_TPP_LASRAD
Characterization of the in-vessel Components treated by Laser Radiation
Objective: Surface examination of the laser treated components.
Principal Investigator: *B. Kolman,* IPP AS CR Prague

IPP-CR_UT06_TTM_PbLi
Development of methods for post-irradiation examination of PbLi alloys
Objective: to develop and test suitable methods for post-irradiation examination of Pb-17%Li alloy irradiated in the framework of the EFDA task TW2-TTMS-003b-D4.
Principal investigator: *Karel Šplíchal,* NRI Rez

IPP-CR_UT06_TTM_IFMIF
Measurement of activation cross sections at neutron energies below 35 MeV.
Objective: Determine cross sections for Chromium (the constituent of Eu-97 steel)
Principal Investigator: *P. Bém,* NPI AS CR, Řež

IPP-CR_UT06_TPD_Hall
Evaluation of candidate Hall sensors performance in in-vessel tokamak environment
Objective: Evaluate in-vessel performance of two types of Hall probes-based systems on a small and flexible tokamak device CASTOR.
Principal Investigator: *I. Ďuran,* IPP AS CR Prague

1 Technology Tasks

Static and dynamic toughness testing at the transition temperature: Neutron irradiation of plates and weldments up to 2.5 dpa at 200-250°C and post irradiation examination

Principal investigator: Petr Novosad, NRI Rez
nov@ujv.cz, tel: +420-26617-3661

Task: TW2-TTMS-001b - RAFM Steels: Irradiation Performance
Field: Tritium Breeding and Materials, Area: Materials development
Collaborative Staff*: K. Šplíchal, W. Soukupová, M. Andrejsek, V. Krhounek*
Due date: revised due date 31.12.07, in progress

The main objectives of this task is to perform static and dynamic toughness testing of irradiated EUROFER specimens prepared from the base metal and weldments. The target neutron flux representing material damage up to 2.5 dpa (displacement per atom) should be achieved by neutron irradiation.

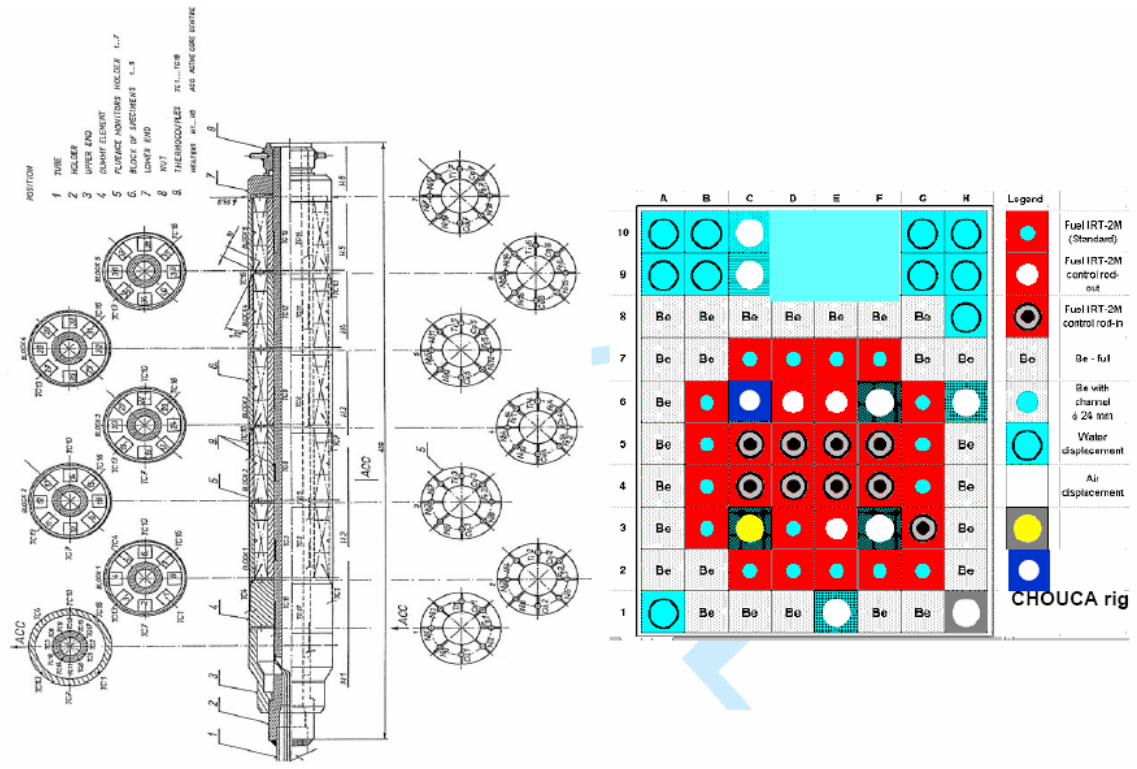

Fig. 1: CHOUCA irradiation rig and its position in the core of LVR-15 research reactor

Neutron irradiation was performed in research reactor LVR-15, operated in Nuclear Research Institute (NRI) Rez, using a dedicated CHOUCA rig. The irradiation campaign, which started in September 2003, has been completed in February 2006 achieving irradiation dose of 2.51 dpa. This irradiation dose represents irradiation time of 11 246 hours and total reactor work about 96 924 MWh. Irradiation parameters were as follows: irradiation temperature 235°C,

fast neutron flux 4.4x1013 cm-2 s-1. Irradiation was performed in a CHOUCA rig in He atmosphere at pressure of 100 kPa. Temperature and He pressure were online monitored during the irradiation campaign.

After the irradiation campaign the CHOUCA rig was transported into the hot cells for dismounting. The dismounting procedure of the CHOUCA irradiation rig has been started in hot cell and is currently in progress.

Foreview of the next activities:

- Introduction of measurements of static and dynamic fracture toughness on irradiated specimens.
- Tests of the static and dynamic fracture toughness of irradiated EUROFER specimens.
- Evaluation of the measured data, preparation of the final report

Reference:

[1] Andrejsek M., Krhounek Vl., Lahodová Zd., Soukupová W., Svoboda J., Vierbl: Report on EFDA samples irradiation, NRI – DITE 306/25, 2006

In-pile PbLi corrosion testing of TBM´s weldments (stiffeners and bottom plate relevant)

Principal investigator: Vladimir Masarik, NRI Rez
mas@ujv.cz, tel: +420-26617-2460

Task: TW2-TTMS-003b - RAFM Steels: Compatibility with Hydrogen and Liquids
Field: Tritium Breeding and Materials, Area: Materials development
Collaborative Staff: *J. Berka, J. Dušek, E. Vlasák*
Due date: revised due date 31.12.06, in progress

The main objective of this task is to study corrosion behaviour of EUROFER material including weldments in liquid metal Pb-Li under neutron irradiation. The eutectic liquid metal alloy Pb-15.7Li will be used in the European Helium Cooled Lithium Lead (HCLL) Test Blanket Module (TBM) concept and its compatibility with EUROFER structure material is an issue. The target neutron flux representing material damage up to 1-1.5 dpa should be achieved by neutron irradiation.

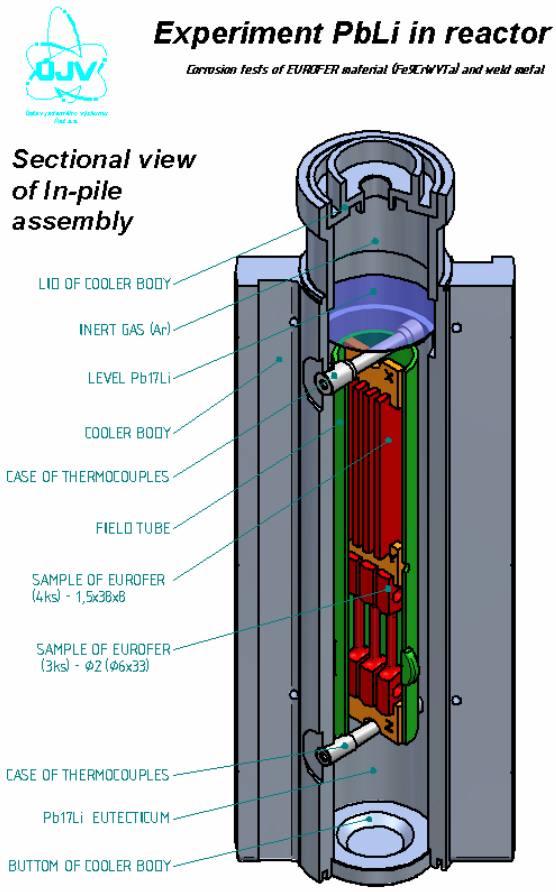

Fig. 1: Principle design of Pb-Li in-pile rig extracted from Pb-Li and cleaned in molten sodium

Neutron irradiation was performed in research reactor LVR-15, operated in NRI Rez, using a dedicated in-pile rig. Irradiation campaign, which started on February 2005, has been completed in May 2006 achieving total irradiation time 247 EFPD, i.e. 1.45 dpa. The in pile rig contained four corrosion plain specimens (38 x 8 x 1.5 mm) and three tensile test specimens (Ø 2mm) of weld metal of EUROFER joint. Temperature of rig hot leg was held

at 500°C ± 10°C and cold leg at 320-340°C. He pressure of inert part is kept at 120 kPa, outer part at 240 kPa.

Dismounting of in-pile ring was performed in hot cell. The procedures of EUROFER specimen separation were carried out under inert atmosphere. The holders with corrosion and tensile specimens were heated in furnace under Ar and Pb-Li melt was removed at 400° C. After that the holders with specimens were exposed to sodium melts at 300°C and a rest of liquid metals was dissolved. Sodium surface layers from the holders and specimens were removed by washing in alcohol.

Pb-Li specimens were prepared during heating and removing of melt form the holder and sampling of lens-type Pb-Li specimens directly from molten eutectic. The investigation of Pb-Li melt was performed by LM, SEM and by energy dispersive X-ray analyses and ISP-MS (Inductively couple plasma-mass spectroscopy). The presence of radioisotopes after irradiation was measured by gamma and alpha spectrometry and beta scintillation method. The contents of impurities in the melt after irradiation were found to be rather low. Lower contents of Fe, Cr, Mn, Ta and V proved that the corrosion attack of EUROFER specimens during irradiation was low and did not lead to increase impurities contents in eutectic melt. Evaluations of contents of radioisotope in melts have shown that transmutation reactions produced tritium and polonium and other ones bismuth. The comparison of measured and calculated values show that measured value does not differ for Po but is about two orders lower for H3 isotope.

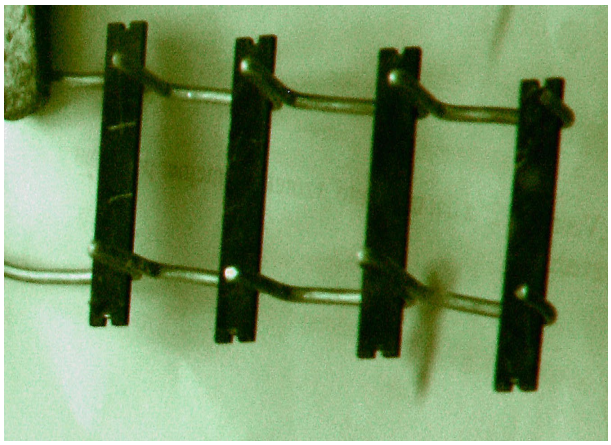

Fig. 2: Corrosion specimens

The evaluations of EUROFER specimens continue and will be finished ion this year. Corrosion behaviour of the irradiated specimens will be performed with special emphasis on type of corrosion attack, corrosion rate, surface morphology and liquid metal embrittlement.

References:

[1] K. Šplíchal, J. Berka, J. Burda, Z Lahodová, Vl. Masařik, L. Vierebl: Evaluation of corrosion and radiation behaviour TBM materials in Pb-Li melts (in Czech), NRI –DRS 1326, 2007

[2] K. Šplíchal, J. Berka, M. Zmítko: Compatibilita of EUROFER martensitic steel with Pb-17Li at 550°C, Proceeding of Conf.: Corrosion and its influence on strength and lifetime of steel structure, Brno, 2005

[3] J. Zmítková: Simulating and evaluation of thermodynamics condition and operational parameters of Pb-Li irradiation rig, NRI Report 12 161, Rez, 2005

[4] K. Šplíchal, V. Masařík, L. Zmítková: In pile Pb-Li testing of TBM weldments under LVR-15 reactor condition, EFDA meeting, Garching, 2005

Crack growth kinetic and fracture toughness on EUROFER in presence of hydrogen (up to 10 wppm) at RT, 250°C

Principal investigator: Karel Šplíchal, NRI Rez
spl@ujv.cz, tel: +420-26617-2456

Task: TW3-TTMS-003 - RAFM Steels: Compatibility with Hydrogen and Liquids
Field: Tritium Breeding and Materials, Area: Materials development
Collaborative Staff: *J. Berka, J. Burda, M. Žamboch*
Due date: 30.09.06, completed

The main objective of this task is to investigate more deeply the effect of hydrogen on the fatigue crack propagation and fracture toughness of Eurofer in the as-received and welded state.In the reported period investigation experimental work was completed and final report has been prepared and sent to EFDA.

The testing of hydrogen effect on basic metal as well as weld metal of EUROFER steel proved fracture toughness susceptibility and brittle fracture depending on the hydrogen content ranging from 2 to 4 wpThe hydrogen content of about 4 wpm decreases fracture toughness both of base and weld metals to the level of 30 KJm^{-2} or below, i.e. approx. by 90 % of original values. Hydrogen containing more than 2 wppm manifests itself significantly only in base metal. The corresponding reduce of fracture toughness in weld metal is insignificant and corresponds to the failure mechanism, involving, in case of base metal brittle fracture and in case of weld metal ductile dimple fracture only. At the 120°C testing the hydrogen effect manifests itself in base metal specimens only.

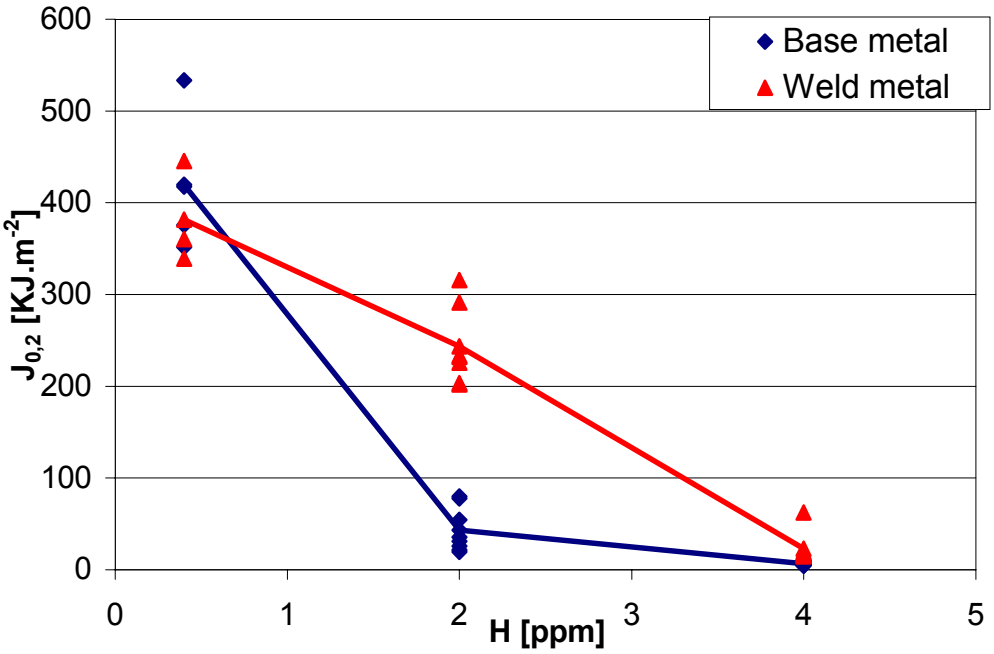

Fig.1: Fracture toughness (represented by $J_{0.2}$ integral) of EUROFER base metal and weld metal charged up to 4 wppm hydrogen and tested at 20°C decreases by approx. 90% as compared with as received state

The crack growth rate testing at RT and 250°C did not prove susceptibility to brittle fracture at hydrogen contents below approx. 2 wppm owing to release during the long-time testing. The crack growth testing did not show any hydrogen embrittlement effect on crack initiation and growth under the long-term exposure at room temperature and 250°C. Both hydrogen charged and uncharged specimens of base and weld metals have shown identical characteristics of stress-strain diagrams, which correspond to the ductile and dimple fracture mechanism.

As it is evident from the measurements performed, the evaluation of the hydrogen effect on fracture/mechanical properties of steels at higher temperatures will be difficult owing to the release and lower content of hydrogen in steel. It is evident that even if the existing methods are improved and sufficient hydrogen content reached, the experimental conditions will still differ from the operating conditions of the fusion reactor blanket. For these reasons we recommend that further work be concentrated on testing of the synergetic effect of hydrogen and irradiation damage on embrittlement in EUROFER martensitic steel.

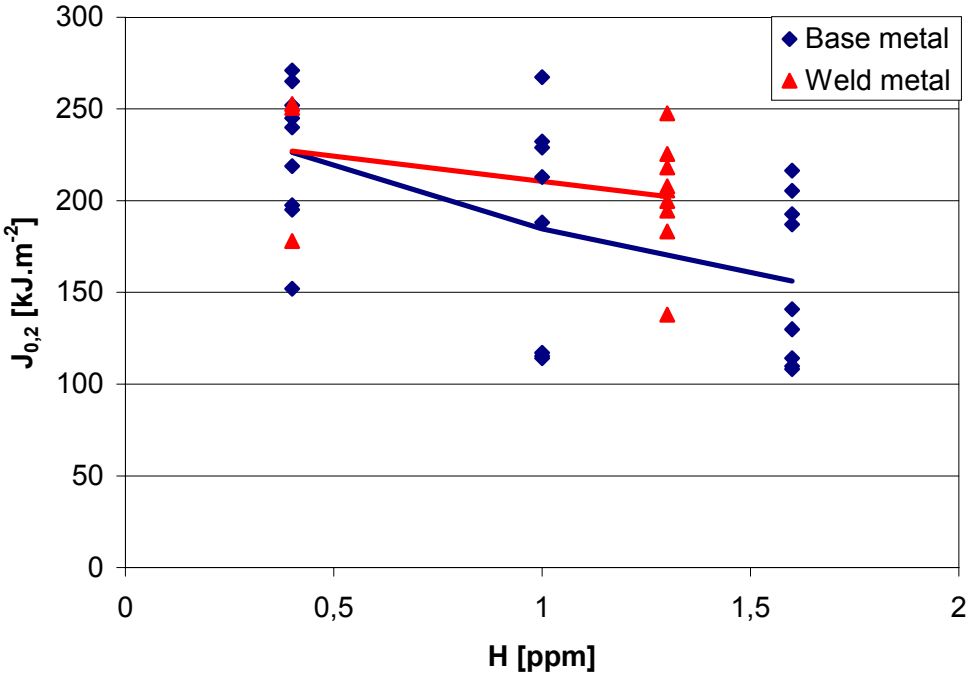

Fig.2: Fracture toughness of EUROFER base metal charged up to 1.6 wppm hydrogen and tested at 120°C decreases by cca. 44% as compared with as received state. Fracture toughness of EUROFER weld metal does not practically change.

References:

[1] K. Šplíchal, J. Berka, J. Burda, M. Žamboch: Crack growth kinetic and fracture toughness of EUROFER steel in presence of hydrogen at room and higher temperature, Report NRI 12631.M, Rez, 2006

[2] Berka J., Šplíchal K.: Efect of hydrogen on fracture mechanical properties, proceeding of Int. Conf. Chemistry of energy system circuit, Praha, 2006

[3] K. Šplíchal J. Berka: Effect of hydrogen on fracture toughness of EUROFER steel, EFDA meeting, Garching, 2005

Development and testing of components for the liquid metal loop (cold traps, high temperature flanges and circulation pump)

Principal investigator: Vladimír Masařík, NRI Řež plc
mas@ujv.cz, tel: +420-26617-2460

Task: TW5-TTBC-005 – Helium Cooled Lithium Lead: Process and Auxiliary Components

Field: Tritium Breeding and Materials, Area: Breeding blanket
Collaborative Staff: *K. Šplíchal, J. Berka, J. Dušek, P. Hájek*
Due date: 30.06.2007, in progress

This task is focused on development and testing of key components for the Pb-Li liquid metal facility of the new reference design of Helium Cooled Lithium Lead (HCLL) Test Blanket Module (TBM). Based on the previous design studies of Pb-Li auxiliary system for HCLL TBM the following components shall be developed: cold traps, high temperature flanges and circulation pump. Development of these components shall be supported by their testing in Pb-Li liquid metal conditions (260-500°C, 5-30 mm/s). The aim is to demonstrate their feasibility and operation performance regarding cold traps purification efficiency, flanges reliability and manipulations.

Manufacturing of the Liquid Metal Loop (LML) has been finished. The loop consists of circulation pump, cold trap, expansion tank with main heater, cold trap, heat exchanger, drain tank, piping and sampling devices. Loop controlling system, parameter monitoring system and data acquisition have been developed and installed. Necessary amount of Pb-Li eutectic alloy (approx. 10 kg) has been ordered and delivered by Institute of Metallic Materials.

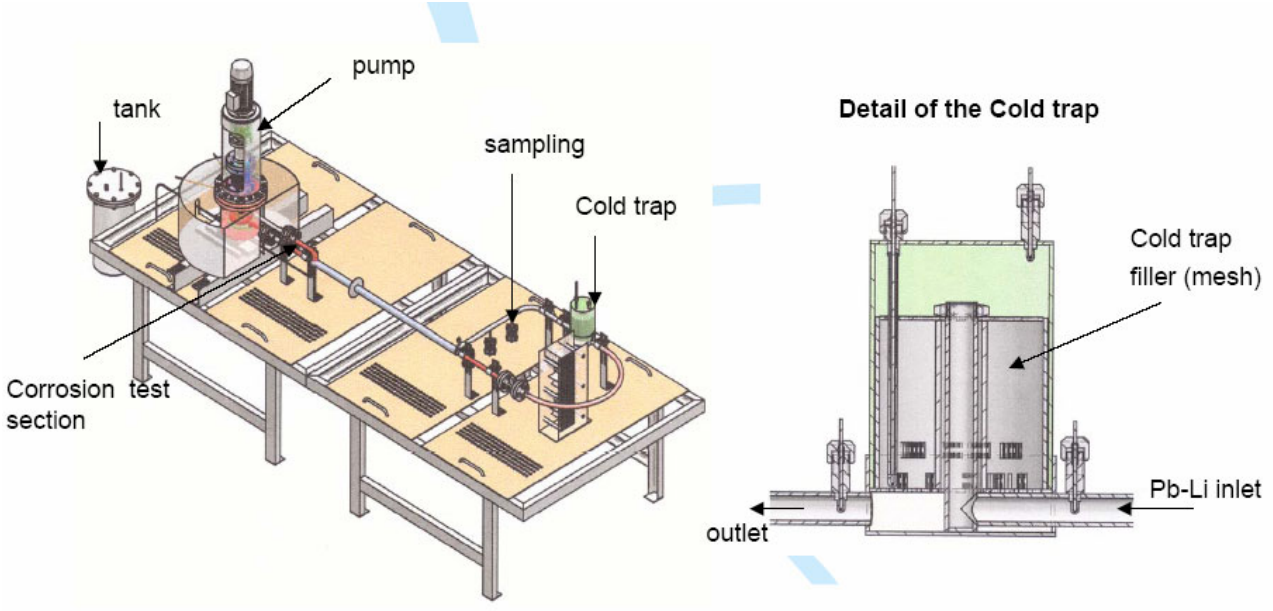

Fig. 1: Schematic layout of the Liquid Metal Loop (LML) for TBM components testing and materials compatibility / corrosion tests

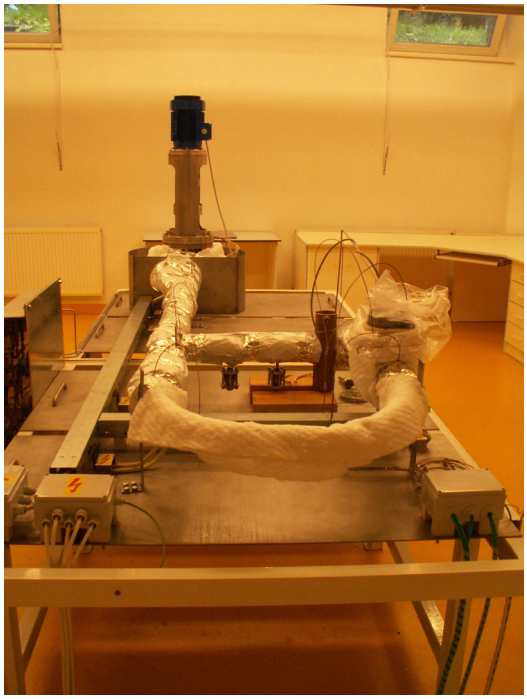

Fig. 2: A view of the Liquid Metal Loop

- To fill the Liquid Metal Loop with Pb-Li eutectic alloy
- To perform commissioning of the Pb-Li loop
- To realize tests according to the experimental testing program focused on:
  - Determination of efficiency of the cold traps
  - Feasibility and operation performance of the high temperature flanges
  - Feasibility and operation performance of the circulation pump
- To evaluate measured data and to prepare the final report.

Reference:

[1] V. Masařík et al.: Investigation study of Pb-Li eutectic behaviour at elevated temperatures (in Czech), Report ÚJV-DRS 1298, Rez, 2006

In-pile experiment on PFW Mock-ups: Performing in-pile testing of Be protected PFW mock-ups under heat flux

Principal investigator: Tomáš Klabík, NRI Rez
kla@ujv.cz, tel: +420-26617-2460

Task: TW3-TVB-INPILE - In-pile experiment on PFW Mock-ups
Field: TV- Vessel/In Vessel, Area: TVB - Blanket
Collaborative Staff: *P. Hájek, V. Masařík, J. Dušek*
Due date: originally 30.07.05, revised date 31.12.2007, task delayed

The objective of this task deliverable is to perform in-pile thermal fatigue testing of actively cooled Primary First Wall (PFW) mock-ups to check the effect of neutron irradiation on the Be/CuCrZr joints under representative PFW operation conditions. Two PFW mock-ups shall be irradiated at 0.6 dpa with parallel thermal fatigue testing at 0.5 MW/m2 for 20,000 cycles. Cooling water parameters (flow rate approx. 4 m/sec) should be selected in such a range to keep the Be/Cu-alloy joint at temperature of 150-250°C.

In the reported period the main effort has been devoted to development and testing of suitable heat flux generation system. This activity has been performed together for this task and for the task TW4-TVB-TFTEST2 (see below). Feasibility study of using a graphite and/or composite material (CFC) heating panel to evoke the required heat flux 0.5-0.8 MW/m^2 on the PFW mock-ups surfaces was performed and a dedicated test facility was designed and assembled. As a reference heating panel material graphite manufactured by SGL, Germany R8710 type has been selected. A qualification test of this graphite heating panel achieving 20,500 thermal cycles and the heat flux up to 0.5 MW/m^2 has been completed. Each thermal cycle consisted of 30 sec power ramp-up, 2 minutes power hold, 30 sec power ramp-down and 3 minutes cooling without power loading. The qualification test results have been evaluated mainly with respect of the graphite heating panel performance and generated heat flux on Be tiles surfaces. Based on the obtained results from the qualification test an adaptation of test rig design is being performed.

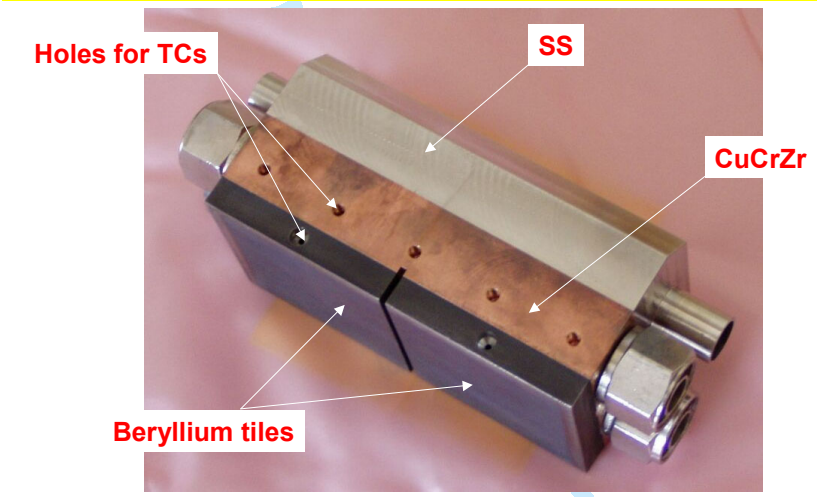

Fig.1 : Primary First Wall Mock-up specimen to be tested in-pile

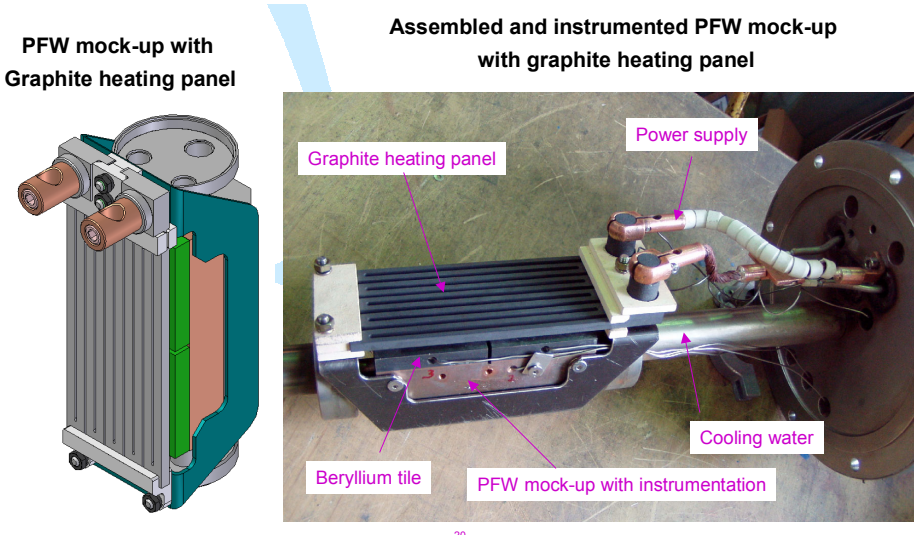

Fig.2: Prototype test assembly for in-pile thermal fatigue testing; 20,500 thermal cycles achieved by this test assembly

The following activities are expected to follow up the task:

- To adapt the test rig design according to results obtained in the qualification test
- To manufacture necessary components and assembly the test rig
- To perform commissioning of the test rig out-of- To perform commissioning of the test rig in-pile
- To realize tests according to the experimental testing program
- To evaluate measured data and prepare the final report

Reference:

[1] T. Klabík et al.: Resistivity of joints of dissimilar materials to thermal fatigue cycling (in Czech), Report ÚJV-DRS 1303, Rez, 2006

Construction of the facility for thermal fatigue tests of Beryllium coated primary first wall mock-ups

Principal investigator: Tomáš Klabík, NRI Řež
kla@ujv.cz, tel: +420-26617-2460

Task: TW4-TVB-TFTEST2 - Thermal fatigue tests of Beryllium coated Primary First Wall Mock-ups

Co-authors: P. Hájek, V. Masařík, J. Dušek
Due date: originally 30.06.2006, revised date 30.06.2007, task delayed

The objective of this task is to construct the facility ensuring thermal fatigue tests of beryllium coated primary first wall mock-ups of dimensions 250 mm x 110 mm x 70 mm to compare the fatigue performance of different beryllium/CuCrZr alloy joints. Thermal fatigue testing up to 30,000 cycles is envisaged. Each thermal cycle should last for 6 minutes. The testing shall consist of 2 test campaigns of 4 mock-ups each tested in parallel. The tests shall be performed at 0.8 MW/m^2 surface heat flux. The inlet water temperature shall be about 120 °C with a water velocity of about 5 m/s.

In the reported period the main effort has been devoted to the following activities:

- Building of a special laboratory and workplace allowing manipulation and testing of beryllium containing specimens,
- Performance of a qualification test with selected heating panel material,
- Development and testing of suitable heat flux generation system,
- Completing design and manufacturing of the test facility for thermal fatigue tests,
- Installation of the test facility in dedicated beryllium laboratory,
- Commissioning of the test facility.

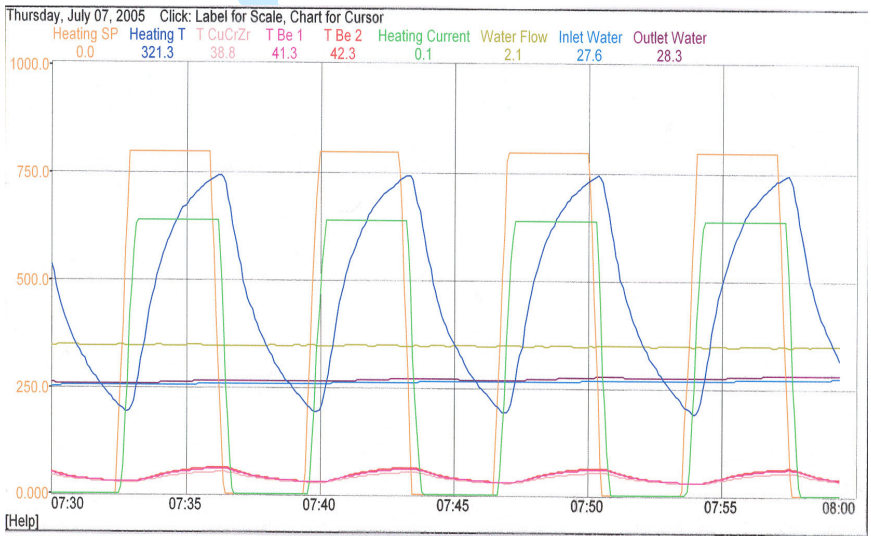

Fig.1: An example of testing results coming from the qualification test of graphite heating panel

Feasibility study of using a graphite and/or composite material (CFC) heating panel to evoke the required heat flux up to 0.8 MW/m2 on the PFW mock-ups surfaces was performed and a dedicated test facility was designed and assembled. As a reference heating panel material graphite manufactured by SGL, Germany R8710 type has been selected. A qualification test

of this graphite heating panel achieving 20,500 thermal cycles and the heat flux up to 0.5 MW/m2 has been completed. Each thermal cycle consisted of 30 sec power ramp-up, 2 minutes power hold, 30 sec power ramp-down and 3 minutes cooling without power loading. The qualification test results have been evaluated mainly with respect of the graphite heating panel performance and generated heat flux on Be tiles surfaces.

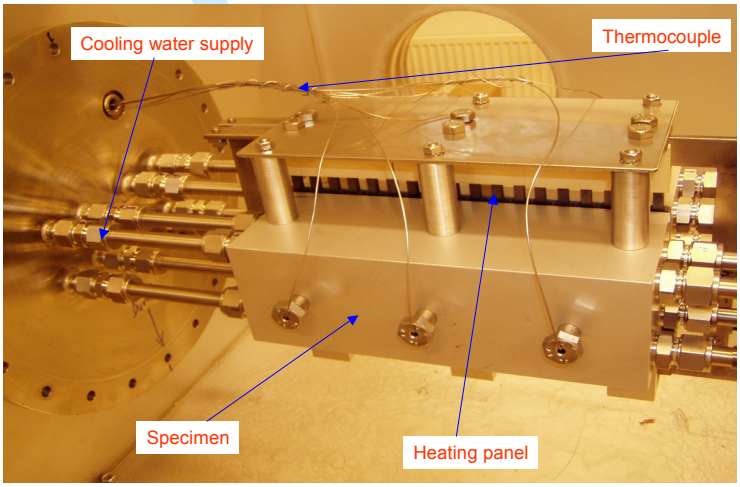

22

Fig.2 : A view of the facility for thermal fatigue testing of various PFW mock-ups

A dedicated test facility for out-of-pile tests of PFW mock-ups has been designed, manufactured and installed. Cooling water system has been designed, components procured and its installation has been completed. As well as the electrical power supply system and control system have been procured and installed. A a special laboratory for Be specimens handling and testing has been built and documentation required for an approval by the Czech Authorities has been worked out.

The following activities are expected to follow up the task:

- Completion of manufacturing of out-of-pile test facility, commissioning, adjustment
- Qualification test (up to min. 5,000 cycles) with a special Stainless steel / Aluminium dummy specimen
- Realization of thermal fatigue test of 8 specimens representing the EU version of PFW mock-up (30,000 cycles at 80 W/cm^2)
- Realization of thermal fatigue test of 6 specimens representing ITER version of PFW mock-up (30,000 cycles at 80 W/cm^2)

Development of activation foils method for the IFMIF neutron flux characterization

Principal Investigator: P. Bém, NPI AS CR, Řež
bem@ujf.cas.cz, tel: +420-26617-3506

Task: TW6-TTMI-003

Co-authors: *V. Burjan, M.Götz, M.Honusek, V.Kroha, J.Novák, E.Šimečková*
In collaboration with:
U.Fischer, S.Simakov, Association EURATOM-FZK, Karlsruhe, Germany

The application of the dosimetry foil technique has been proposed for the measurement and monitoring of the neutron spectral flux during IFMIF operation. The objective of the Task is an experimental tests of the proposed approach by activation of selected dosimetry-foil set in the IFMIF-like white neutron spectrum.

During the first period, the previously investigated dosimetry-foil samples were completed to the full set selected at FZ Karlsruhe (Task TW6-TTMI-003, Deliverable D3) and consisted of Al, Au, Nb, Y, Co, Ti, Ni, Fe, Lu, In and Bi. Sets of foil stacks were activated at two different position from D2O target and at different irradiation time in an IFMIF-like white neutron spectrum produced by the p+D_2O reaction of the NPI cyclotron-based neutron source.

The induced gamma-emitting radioactivity of the activated samples were investigated at different cooling times by the gamma- spectrometry method using HPGe detectors. Up to 29 activation reactions were employed for the neutron spectra adjustment [1]. In the unfolding procedure, a modified form of SAND-II code was used. For the unfolding iterative procedure the initial guess neutron spectrum measured by scintillation unfolding technique (at 37 MeV proton energy) was used.

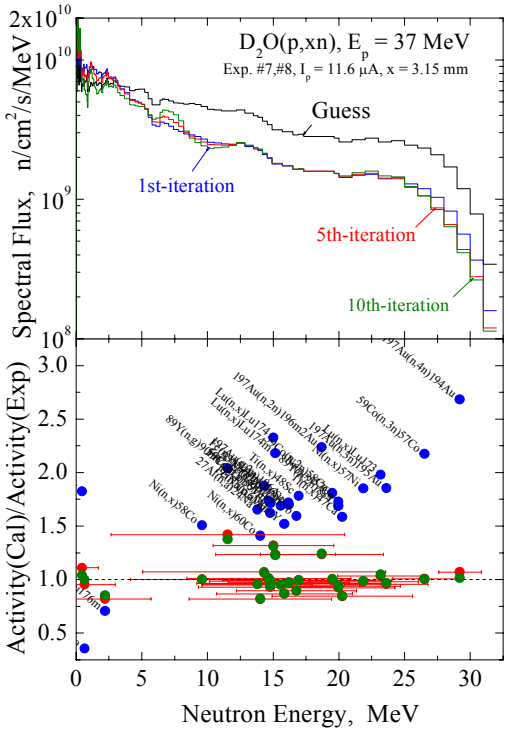

Fig. 1: Neutron flux and C/E ratios obtained from of dosimetry foils and SAND-II deconvolution code.

As a result, the spectral neutron flux of the p+D_2O neutron source could be determined at arbitrary distance from the target with an accuracy of 10-15%. Above 7 MeV neutron energy, the flux Y, amounts 5.4^{10} n/cm^2/s for the nearest distance from the target bottom and 15 μA of proton beam current.

Utilizing this neutron field, a wide program of integral test experiments on materials relevant to the fusion technology is carried out.

The concept of International Fusion Material Irradiation Facility (IFMIF) consists in high-power deuteron accelerator (40 MeV) and lithium (liquid jet) target. The neutron source reaction d(40 MeV)+Li produces a white spectrum with mean energy of 14 MeV and a energy range up to 35 MeV (weak tail up to 55 MeV). The calculations of neutronic responses in the components of IFMIF need the activation-cross-sections database, which is validated against experiments at relevant (IFMIF-like)

energy range. To simulate the IFMIF neutron spectrum for integral benchmark experiments, new neutron source was developed using the variable-energy cyclotron U-120M. and source reaction p+D_2O. To determine the spectral neutron flux across the irradiated samples, the multi-foil activation technique was utilized

In the experiment, a set of dosimetry foils Al, Ti, Fe, Co, Ni, Y, Nb, Lu and Au were irradiated by neutrons from the p-D_2O source at various distances from the target. Standard gamma-spectrometry technique was employed for determination of induced γ-ray activities of reaction products.

The reaction rates, and saturated activities were calculated from measured data. The set of foils was irradiated at different distances. Up to 29 activation reactions were employed for the neutron spectra adjustment [2]. In the unfolding procedure, a modified form of SAND-II code was used. For the unfolding iterative procedure the initial guess neutron spectrum measured by scintillation unfolding technique (at 37 MeV proton energy) was used.

The final spectrum obtained after adjustment procedure to data at 3 mm distance is shown in the Fig. 1 (upper part) where the initial guess spectrum is also displayed. In the bottom part the ratios A_{cal}/A_{exp} of calculated to measured saturated activities C/E for dosimetry reactions used in present analysis are shown. The abscissa (E) means the energy weighted with product of neutron flux and corresponding cross section, the horizontal bars are the mean square deviations. In the energy range 10 to 25 MeV, the uncertainties of adjusted spectrum amounts 3%. Above this range the uncertainty are estimated at the level of 20-30%. To achieve better knowledge of the spectrum below 10 and above 25 MeV the (n,n') reactions on ^{93}Nb, ^{103}Rh and ^{115}In and high threshold reactions ^{209}Bi(n,xn) and are used in measurements being in progress.

In the Fig. 2 (left), the reaction rates of individual reaction products are set out as a ratio of data determined at 3 and 156 mm distance and displayed along the values E. The varying of neutron spectrum with distance is clearly indicated and experimentally proven. Within quoted uncertainties of data, the variance is equally well reproduced by the 1st and 2nd order polynomial form. The ratio of spectra resulted from SAND-adjusting procedure shows some structure of this variance.

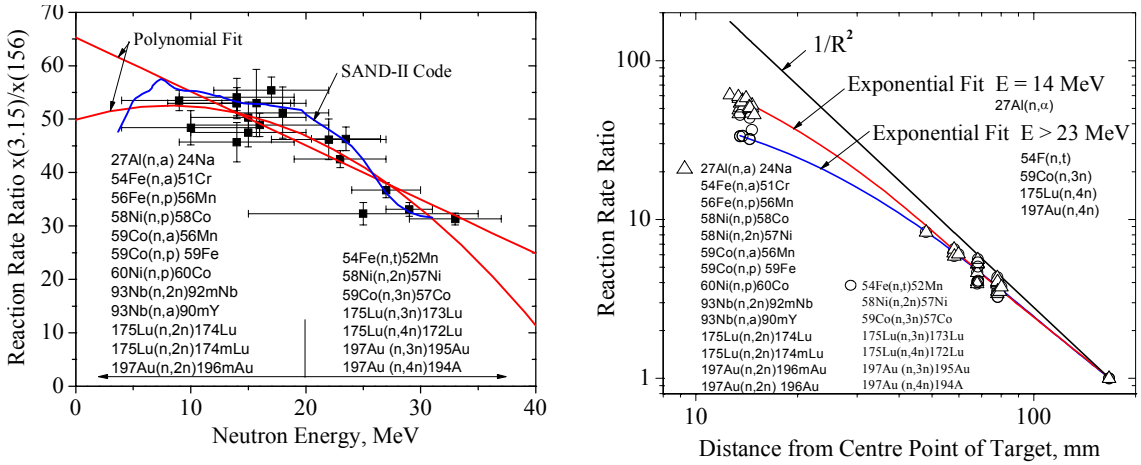

Fig. 2 (left) - reaction rates ratio obtained from the irradiation of set of dosimetry foils set by white-spectrum neutron flux of the p(37 MeV)+D_2O source at 3 and 156 mm from the source. (right) - reaction rates ratio obtained from the irradiation of the dosimetry foils at different distances. Data of individual reaction products are clustered in groups with E above and below 20 MeV (circles and triangles, respectively). For the further explanation see text.

Some selected foil combinations were irradiated also at 47, 57, and 67 mm of s-t-d distance. In the Fig. 2 (right), the rate values of reactions on foils at various distances are normalized to relevant data at longest distance. As the x-axis, the distance R from the center of effective target thickness is accepted. Such representation enables in appropriate way the comparison of measured reaction-rate ratio to the $1/R^2$ law. Data of reactions are grouped along the energy E (above and below 20 MeV).

The exponential fit was done through the data from low-threshold reaction 27Al(n,α) (upper curve) and highest-threshold reactions 54Fe(n,t), 59Co(n,3n), 175Lu(n,4n), 197Au(n,4n) (lower curve). Besides the deviation of spectral flux from the $1/R^2$ law, slightly weaker variance of the spectral shape with distance is well seen. Using data at 3 mm distance and the quantitative form of observed averaging effects, the spectral flux at arbitrary distance could be determined with an accuracy of 10-15%. Above 7 MeV neutron energy, the flux Y, amounts 5.4^{10} n/cm^2/s for the nearest distance from the target bottom and for 15 μA proton beam current. Utilizing this neutron field, a wide program of integral test experiments on materials relevant to the fusion technology is being carried out [3].

References:

[1] P. Bém, V. Burjan, U. Fischer, M. Götz, M. Honusek, V. Kroha, J. Novák, S.P.Simakov and E. Šimečková, Neutron activation experiments on chromium and tantalum in the NPI p-^{7}Li quasi-monoenergetic neutron field, Proc. on the International Conference on Nuclear Data for Science and Technology 2007, Nice, to be published

[2] S.P. Simakov, P. Bém, V. Burjan, U. Fischer, M. Götz, M. Honusek, V. Kroha, J. Novák, and E. Šimečková, Development of activation foils method for the IFMIF neutron flux characterization, Fusion Eng. and Design (to be published),

[3] R. A. Forrest, J. Kopecky, M. Pillon, K. Seidel, S. P. Simakov, P. Bém, M. Honusek and E. Šimečková: Validation of EASY-2005 using integral measurement, UKAEA FUS 526, January 2006, Monography, 553 pp

Experiments for validation of cross-sections up to 55 Mev in an IFMIF-like neutron spectrum: activation experiment on Cr

Principal Investigator: P. Bém, NPI AS CR, Řež
bem@ujf.cas.cz, tel: +420-26617-3506

Task: TW6-TTMN-002, D5
Field: Tritium Breeding and Materials, Area: Materials Development
Collaborative staff: *V. Burjan, M. Götz, M. Honusek, V. Kroha, J. Novák, E. Šimečková*
In collaboration with:
U. Fischer, S.P. Simakov, Association EURATOM – FZK, Karlsruhe, Germany

The objective of the activation experiment on Cr is to provide the experimental data base for validating the activation cross-section data in the energy range relevant for IFMIF. The experiments have used the external proton beam of the NPI variable-energy cyclotron U-120M. The samples of NiCr alloy (69.9% Cr, 29.2% Ni, defined admixture of Co, Fe, Mn, V, Ti and Sc) in foil form of 15 mm in diameter and of 0.75 mm thicknesses were activated in an IFMIF-like white neutron field produced by the p(36 MeV)+D_2O reaction at mean neutron flux density up to 10^{11} n/cm^2/s. The induced gamma-emitting radioactivity of activated samples is investigated repeatedly after different cooling time intervals by gamma-spectrometers (two calibrated High-Purity-Germanium detectors of 23 and 50% efficiency). Specific activities of observed n+Cr reaction products were determined and compared with calculation of the neutron induced activation using the EAF-2005 activation cross section database and the FISPACT inventory code [1].

As a part of experimental benchmarking of the IFMIF neutron calculations, the activation experiment on chromium has been carried out. Recently such measurement and analysis have been performed for the Eurofer-97 steel [1-3]. The objective of this sub-task was to conduct pre- and post-analyses of the validation experiments for Cr cross sections up to 55 MeV in an IFMIF – like neutron spectrum including the following steps:
(a) the Monte Carlo based pre-analysis to optimise the experimental set-up and provide a suitable modelling of the neutron source required for the analysis of the experiment,
(b) the calculation of the neutron induced activation using the EAF-2005 activation cross section database and the FISPACT inventory code, (c) comparison of the calculated activities with the activities measured in TW6-TTMN-002, D6 and production of C/E values.

In the present work, the Cr activation experiment at the NPI cyclotron-based Fast Neutron Facility has been performed with the IFMIF-like neutron spectrum produced by the source reaction p(37MeV)+D_2O. To test the consistency of experiment, the irradiation was performed at different runs and different source-to-sample distance. The induced gamma-emitting radioactivity was determined repeatedly, after different cooling time intervals, by gamma ray spectrometry using a high-purity germanium detector. The arrangement of activation experiment has been described previously [2]. In present measurement, the samples of NiCr alloy samples (69.9% Cr, 29.2% Ni and defined admixture of Co, Fe, Mn, V, Ti and Sc) in a form of foil 15 mm in diameter and of 0.75 mm thicknesses were activated at mean neutron flux density up to 10^{11} n/cm^2/s a neutron field of IFMIF-like white spectrum produced by the p(36 MeV)+D_2O reaction. Foils have been irradiated in short (11 min) and medium (89 min) runs at distances of 3.1 mm from the D_2O target bottom. In all runs, the investigated samples were sandwiched by an aluminum foils for a monitoring the neutron flux. The time profile of the neutron source strength during the irradiation (see Fig. 1) was monitored by the proton beam current on the neutron-source target, recorded by a calibrated current-to-frequency converter and scaler on PC. Up to 13 μA of proton beam current was delivered on the source target. It corresponds to the spectral flux of about 6×10^{10} cm^{-2}s^{-1}.

The activated samples were investigated by two calibrated HpGe detectors of 23 and 50% efficiency and of FWHM 1.8 keV at 1.3 MeV. Gamma spectra were measured repeatedly, after different cooling time intervals up to 95 days. Evaluation of spectra was performed utilizing the NPI code DEIMOS . By analyzing the spectra, the resulting specific activities A_{sp} in Becquerels per kilogram to the end of irradiation were obtained (the numerical data of activities at each cooling time are available on request).

In summary, the radioactive nuclides ^{51}Ti, ^{48}V, ^{52}V, ^{53}V, ^{46}Sc, ^{48}Sc, ^{48}Cr , ^{49}Cr and ^{51}Cr were identified and specific activities determined from the reactions n+^{nat}Cr investigated at short and middle irradiation times (cca 10 and 90 min, respectively). Data were provided to FZ Karlsruhe for comparison with preliminary calculation using the EAF-2005 activation cross section database and the FISPACT inventory code (TW6-TTMN 002, D 05). In addition, to investigate possible presence of weakly activated products from reactions with higher effective threshold (particularly the ^{50}Cr (n,p^{3}He)^{47}Sc reaction), the runs with long irradiation time (above 12 h) were carried out as well. Results will be analyzed separately.

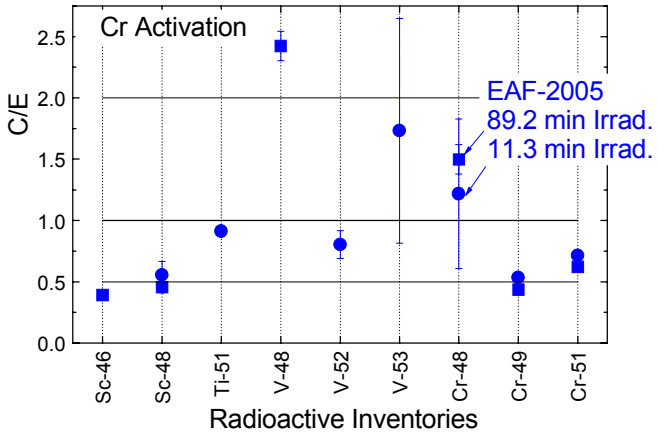

The activation calculations have been performed with FISPACT/EAF-2005. Comparison of calculated and measured activities (in terms of C/E ratios) has been performed for the 9 radio-isotopes detected in the irradiated Cr sample. An example of results see the Fig. It was found that EAF-2005 activation library satisfactorily predicts (within experimental and calculation uncertainties) the yields of ^{51}Ti, ^{52}V, ^{53}V and ^{48}Cr, but fails to reproduce the other radioactive inventories (^{46}Sc, ^{48}Sc, ^{48}V, ^{49}Cr, ^{51}Cr). Pathway analyses for the production of the specific radio-nuclides have been performed to identify the dominant reactions and the reasons of the observed discrepancies.

The results have shown that the generation of the radio-activity products in each case is dominated by one-two reactions. For these specific reactions the relevant cross sections from the EAF-2005 library were derived and compared with available measurements with mono energetic neutron sources. For example, for the reaction ^{nat}Cr(n,pa+3p)^{48}Sc (having a threshold 22 MeV) no measurements have been performed so far, whereas the present benchmark analyses gives C/E = 0.5. It is thus concluded that the particular chromium activation cross sections need to be updated in the EAF-2005 data libraries.

References:

[1] P. Bém, V. Burjan, M. Götz, M. Honusek, U. Fischer, V. Kroha, J. Novák, S.P. Simakov, E. Šimečková, Report NPI ASCR Řež , EXP(EFDA)-01/2007

[2] P. Bém, V. Burjan, M. Götz, M. Honusek, U. Fischer, V. Kroha, U. v. Möllendorff , J. Novák, S.P. Simakov, E. Šimečková, Fus. Eng. and Design, v. **75-79** (2005) p. 829

[3] S.P. Simakov et al., Development of activation foils method for the IFMIF neutron flux characterization , 24-rd Symposium on Fusion Technology (SOFT-24), Warsaw, 2006, Fus. Eng. and Design, to be published.

Assessment of PSM welding distortions and field welding

Principal Investigator: L. Junek, IAM Brno Ltd.
junekl@uam.cz, tel: +420-541-321-291 ext. 121

Task: TW6-TVV-SYSEG
Collaborative staff : *M. Slováček, V. Diviš, V. Ochodek*
Due date: 30.6.2007

The manufacturing of the vacuum vessel requires a lot of the welding operations. The weld joints are very long and contain a lot of welding passes. Each welding operations (weld joints) generate residual stresses (deformation) and distortions. The final distortion has to comply with the very strict manufacturing tolerances and requirements for final size and shape of the construction parts. Due to stated facts the several experimental mock-ups have been done and also numerically analysed. The final welding technology can be proposed based on the obtained experimental and calculated results.

In the previous project "Analysis of Welding Distortions Obtained in Manufacturing the VV Segment, Stage 2, Numerical analyses of VMO and LMVMO " [1] the VMO (validation mock up) and LMVMO (local modelling validation mock up) were numerically simulated. During the finalisation of the previous project [1] the mock-ups were not finished. In the current project "Modification of VMO and LMVMO model" the both mock-ups are recalculated with real welding condition, which were used during mock-ups manufacturing. The shrinkage and distortion measurements were performed during mock-ups manufacturing. The calculated and measured results were compared. The main object of this stage is to present the distortion prediction during the assembly process of VMO (validation mock up), LMVMO (local modelling validation mock up). The geometry of the mock-ups has been obtained from EFDA in the CAD STEP format. The mock-ups were prepared and done in Companies ANSALDO (Genova, Italy) and SIMIC (Camerana, Italy), see photos below.

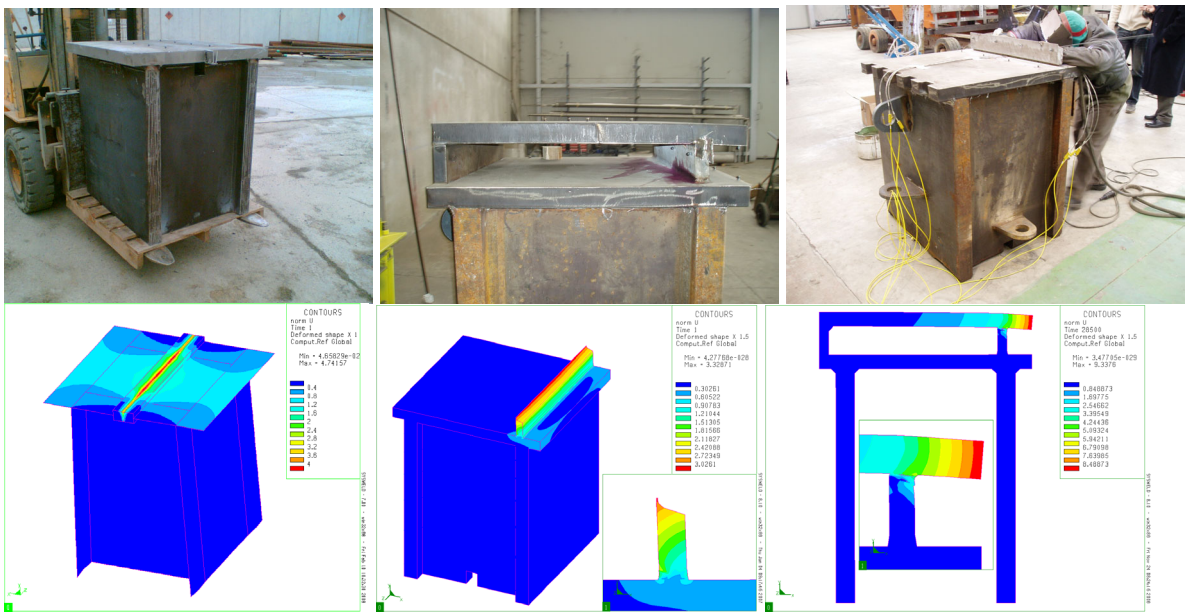

The VVPSM (Vacuum Vessels Polodial Segment model) full-scale mock-up has been prepared and done in cooperation between Companies ANSALDO (Genoa, Italy) and SIMIC (Camerana, Italy). VVPSM is the full-scale model of the PS1 and PS2 parts of the vacuum vessel. The most important area of VVPSM is connection between PS1 and PS2 parts. This

area consists of three weld joints, one on the inner shell and two on the outer shell, see figures below. These welding joints are done as last assembly step and have got the big influence on the final distortion. The numerical optimisation of the PS1 and PS2 weld joints was done and several modifications of the technology and construction stiffness were proposed.

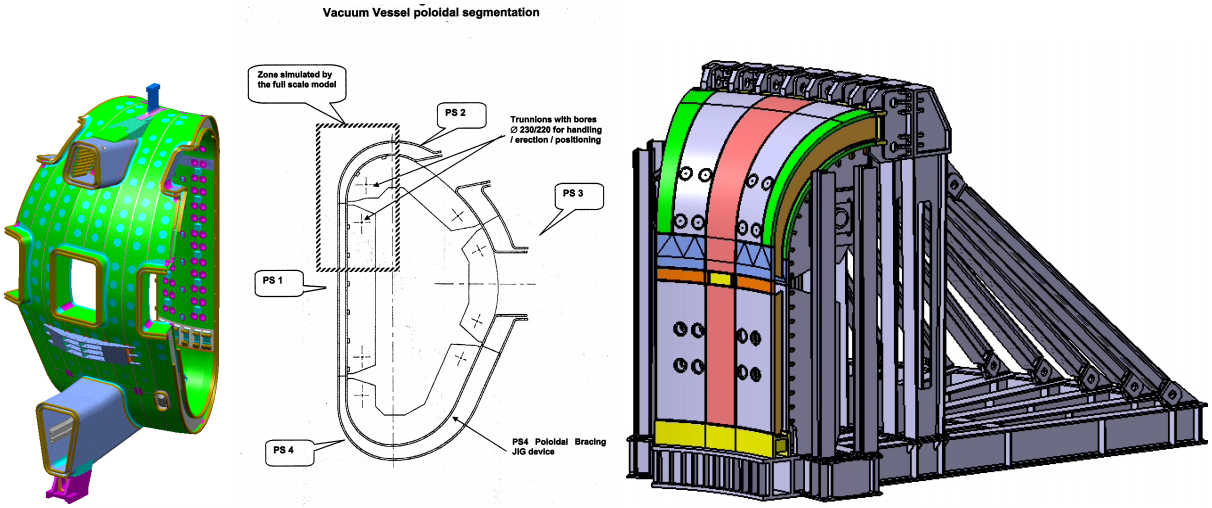

During the project the several meetings in Genoa was hold and the each calculated results were discussed with EFDA and ANSALDO representatives. During the project the several investigations were prepared and presented to EFDA and ANSALDO representatives. The optimisation stage (numerical simulation) was doing during whole 2006 year and numerical analyses were several times recalculated according to new technology information and based on internal discussion between IAM Brno, EFDA and ANSALDO companies. Presented manufacturing distortions results on final technology process were calculated.

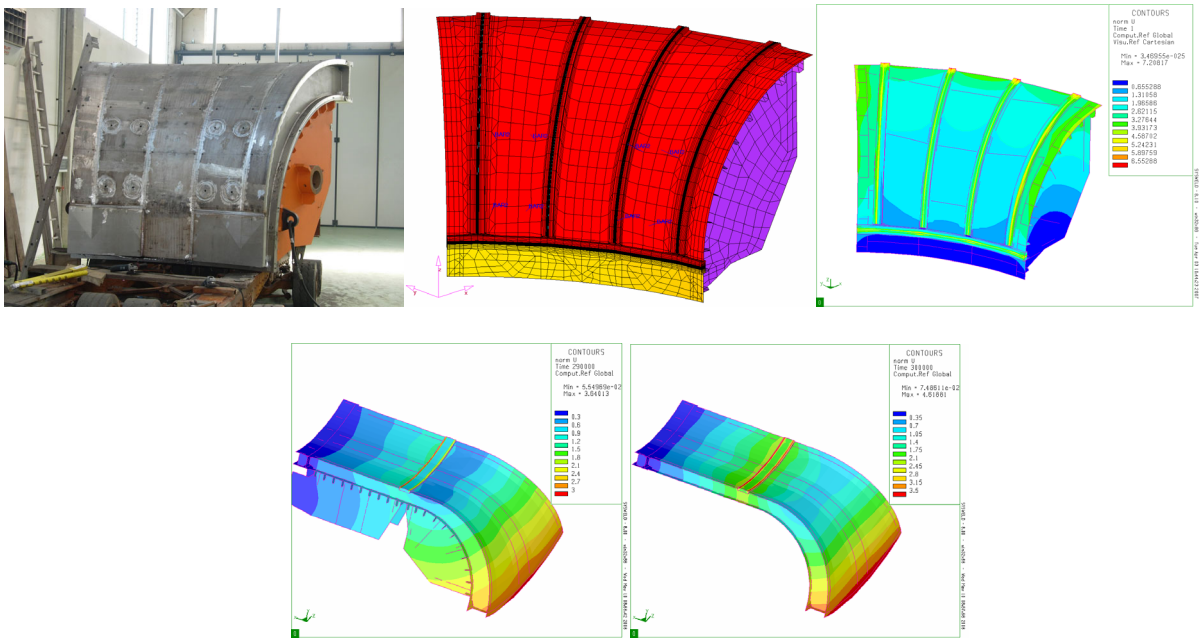

References :

[1] Diviš V., Slováček M., Ochodek V.: Analysis of Welding Distortions Obtained in Manufacturing the VV Segment, Numerical analyses of VMO and LMVMO, report IAM Brno, id. No. 3816/05, December 2005

[2] Diviš V., Slováček M., Ochodek V.: Evaluation of welding distortion of VV poloidal segment, stage 1: Validation of method, experiments, report IAM Brno, id. No. 3616/04, October 2004

[3] Slováček M., Diviš V. : Assessment of PSM Welding Distortions and Field Welding, *Task 1: Modification of VMO and LMVMO models,* research report IAM Brno, identification number: 4038/07, Brno, February 2007

[4] Marek Slováček, PhD., Vladimír Diviš : Assessment of PSM Welding Distortions and Field Welding, *Task 2: Weld joints optimisation,* research report IAM Brno, identification number: 4031/07, Brno, February 2007

2 Underlying Technology Tasks

Plasma sprayed tungsten-based components

Principal investigator: Jiri Matejicek, IPP AS CR Prague
jmatejic@ipp.cas.cz, tel.: +420-26605-3307

Task: IPP-CR_UT06_TVM_Spray
In collaboration with:
Gerald Pintsuk, Association EURATOM-FZJ, Jülich, Germany

The objective was to manufacture plasma facing compounds by plasma spraying, primarily for potential application in ITER and to optimize the spraying process, to achieve low porosity, high thermal conductivity and high thermal shock resistance. The work encompassed plasma spraying of tungsten- and copper-based materials and complex characterization of the coatings, including performance testing at fusion-relevant conditions.

A number of tungsten spraying runs with varying process parameters were conducted; the optimization was directed towards low porosity and oxide content, high thermal conductivity and adhesion. Modification of the spraying torch (in 2005), which resulted in a more stable plasma jet, necessitated a more fundamental study of particle behavior in the jet, especially with respect to powder injection. These experiments were performed with tungsten, copper and stainless steel powders. Single-material coatings were produced at selected conditions obtained in that study. Characterization included porosity, oxide content, Young's modulus, adhesion and thermal conductivity.

Demonstration panels of tungsten coatings on copper and stainless steel, 100x100 mm size, were delivered to IPP Garching as a deliverable of the EFDA Task TW5-TVM-PSW, (extended to mid-2006). Indications for optimum spraying parameters for tungsten and copper were obtained, and the effects of powder injection velocity on tungsten+copper mixing were investigated. Tungsten+copper composites of various compositions, including a linear profile graded coating (FGM) were sprayed in January 2007.

Tungsten coatings still have relatively high porosity, but very low oxide content, while copper coatings are quite dense but more oxidized. In thermal conductivity tests, the tungsten coatings showed values comparable to VPS coatings, however, no dramatic improvement over previous results was observed. Their adhesion was comparable to other plasma sprayed metallic coatings.

The coating performance was studied under heat fluxes of varying intensity and duration – by electron beam at FZ Juelich (thermal shock), by hydrogen beam at IPP Garching (prolonged exposure), and by plasma stream at BI Novosibirsk (thermal shock). The thermal shock performance was roughly comparable to VPS coatings, slightly worse during longer exposures. At the highest heat fluxes used, surface melting occurred, but not deep cracking or erosion.

Device	Loading medium	Power MW/m2	Energy MJ/m2	Duration s	P*sqrt(t) MW/m2.s0.5
CASTOR	plasma	0.7	**0.02**	0.03	0.1
JUDITH	electron beam	**500**	2	0.004	30
GLADIS	hydrogen ion beam	**7 - 11**	20 - 30	2 - 7	15 - 20
GOL-3	plasma	~60	**3**	~0.05	10 - 30
expected heat load at location		0.5 - 1	?	?	

*Tab. 1: Performance of plasma sprayed coatings under various heat load conditions. results are presented as heat loads that the coatings were able to withstand without significant damage. Only the JUDITH data represent a true "damage threshold", i.e., in this case higher loads led to significant erosion. In the case of GLADIS and GOL-3 data, only indirect observations indicate the proximity of this threshold. For CASTOR, these data show simply the highest applied load. From the energy – power pair, the number in bold is the control variable from the test, while the other is calculated. To allow for a comparison of test widely varying in power and duration, the P*sqrt(t) variable is introduced, which correlates with surface temperature increase.*

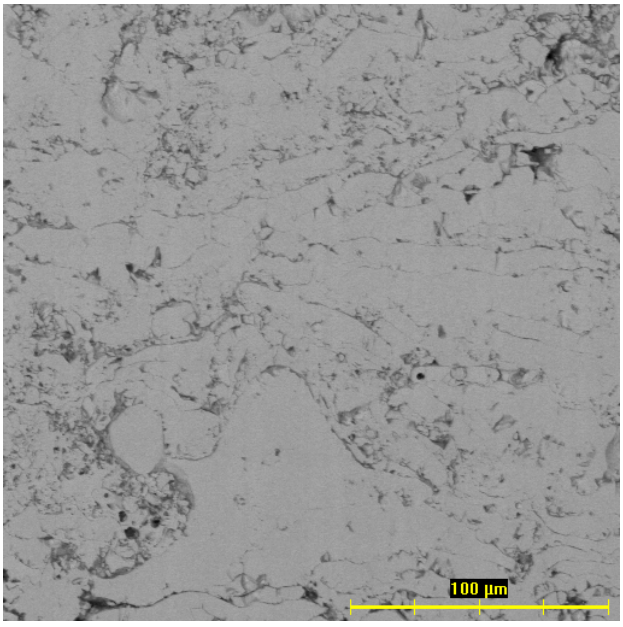

Fig. 1. Structure of the demonstration W coating, showing mostly well molten, layered particles. Image analysis on the cross sections indicated about 11% porosity.

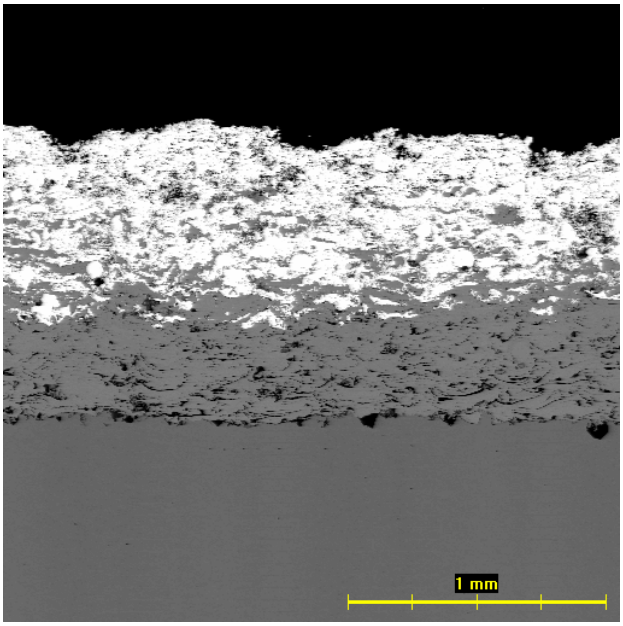

Fig. 2: Cross-section of plasma sprayed W+Cu FGM. Such coatings can be used as interlayers for mitigating stress concentration at the interface between W-based plasma facing armor and Cu-based cooling system.

References:

[1] Jiří Matějíček, Pavel Chráska and Jochen Linke: Thermal Spray Coatings for Fusion Applications—Review; Journal of Thermal Spray Technology, Vol. 16, No. 1, 2007, 64-83

[2] Jiri Matejicek: Manufacture and Characterization of Tungsten Plasma Spray Coatings for Large Area Protection, Report on EFDA Task TW5-TVM-PSW, 2006

[3] Jiri Matejicek, Vladimir Weinzettl, Edita Dufkova, Vojtech Piffl, Vratislav Perina:Plasma Sprayed Tungsten-based Coatings and their Usage in Edge Plasma Region of Tokamaks; Acta Technica CSAV, Vol. 51, No. 2, 2006, 179-191

Workplace building-up for handling and manipulations with Beryllium coated Primary First Wall mock-ups

Principal investigator: Vladimír Masařík, NRI Řež plc
mas@ujv.cz, tel: +420-26617-2460

Task: UT2006_1_NRI-PFW
Field: Vessel/In-vessel, Area: Blanket, Materials
Collaborative Staff: *T. Klabík*

The main objective of the task UT2006_1_NRI-PFW is to build-up a workplace for handling and manipulations with beryllium coated Primary First Wall (PFW) mock-ups. This workplace needs to be established to fulfil requirements for safe handling with Be to minimize health hazard of the involved personnel. This workplace will be used for preparation and realization of the thermal fatigue tests under the framework of the EFDA technology programme (EFDA tasks TW3-TVB-INPILE, TW4-TVB-TFTEST2 and TW6-TVM-TFTEST). The workplace building-up for handling and manipulations with Be coated PFW mock-ups needs to fulfil requirements of the health and safety authorities.

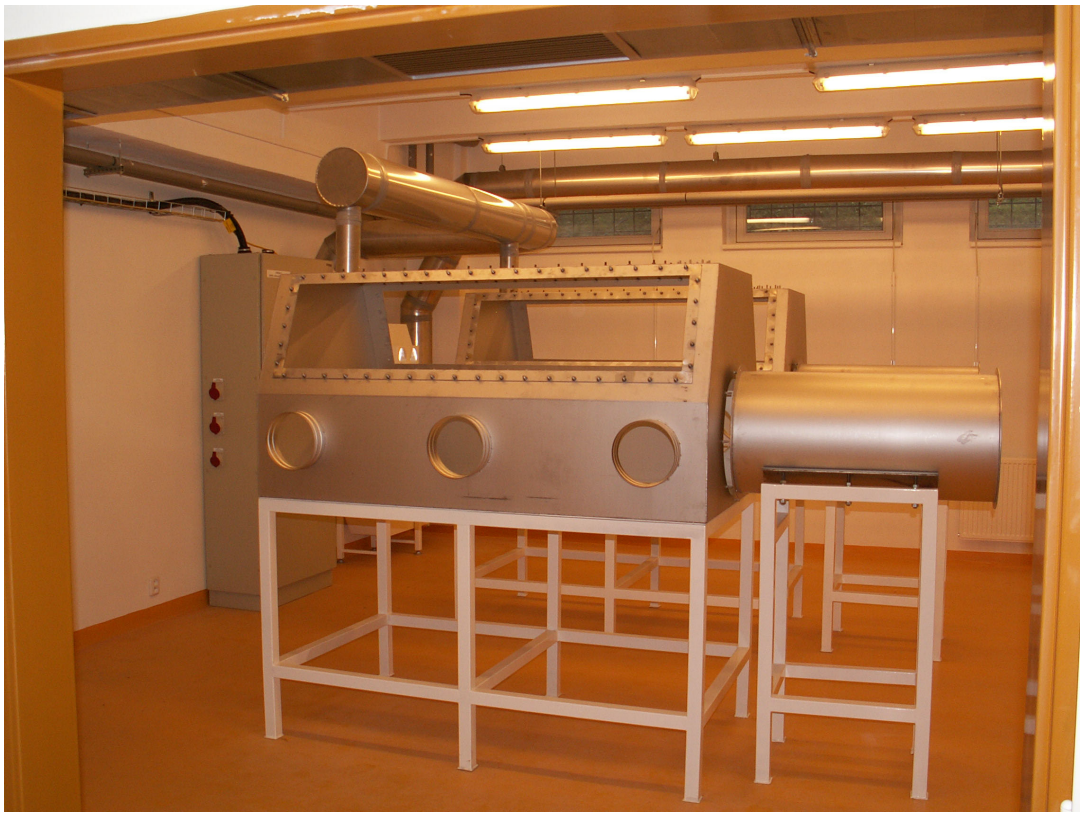

Fig. 1: A view of beryllium workplace with glove boxes for testing of Primary First Wall mock-up samples with Be armour layer

The workplace will be used for the following procedures:

- Input acceptance and checking of the PFW mock-ups with Be coating
- Necessary adaptation of the PFW mock-ups to be used for testing (e.g. drilling, grinding, polishing, blackening, etc.)
- Non-destructive ultrasonic examination of the PFW mock-ups
- Assembly of the PFW mock-ups in test rig (test facility)

- Realization of the thermal cycling test with the Be coated PFW mock-ups
- Dismantling of the PFW mock-ups from the test rig (test facility)
- Preparation and packing of the mock-ups for further transportation.

In the reporting period the following work has been performed:

1. Collection and survey of the Czech and European authorities health and safety requirements and standards for handling and manipulation with beryllium to minimize health hazard of the involved personnel.
2. A feasibility study for building-up a workplace for handling and manipulations with beryllium coated Primary First Wall (PFW) mock-ups.
3. A preliminary design study of the workplace for handling and manipulations with beryllium.
4. Dimensioning and selection of suitable technology for Be handling workplace: (i) dimensioning of independent ventilation system, (ii) selection of HEPA filters, (iii) selection of suitable measurement devices to detect Be in air and on surfaces, (iv) liquidation of Be contaminated or Be contained waste (e.g. working tools, filters, pieces from mechanical treatment etc.).

Beryllium workplace for handling and manipulations with Be coated PFW mock-up specimens, which is currently being build, needs to be commissioning and operating in accordance with the requirements of the health and safety authorities. The following aspects of the Be workplace commissioning and operation need to be addressed:

- Establishing of the registered (certified) Beryllium workplace approved by the state health and safety authorities; for this reason necessary documentation has to be prepared (e.g. elaboration of Safety Report, Limits and Conditions of the Laboratory Safe Operation, Emergency Plan, Personnel Monitoring Plan etc.)
- Application of the Quality Assurance and Quality Control system at operation of the Be workplace (e.g. elaboration of the Working Procedures, personnel training, personnel entrance/exit checking, utilization of personnel protection tools, etc.)
- Day-to day monitoring of Be contamination in the Beryllium workplace in accordance with the Monitoring Plan, i.e. monitoring of Be dust in air, surfaces contamination by Be, monitoring of Be captured by special filters in the ventilation system, etc.
- Detail evidence and checking of Be inventory including certification of Be mass and Be surface contamination
- Controlled liquidation of Be contaminated or Be contained waste (e.g. working tools, filters, pieces from mechanical treatment etc.)

Reference:

[1] Working Manual for Beryllium Workplace, NRI Internal Report (in Czech), 2006

Heat source models development for individual ITER welding technologies and its influence on the final ITER distortion

Principal Investigator: L. Junek, IAM Brno Ltd.
junekl@uam.cz, tel: +420-541-321-291 ext. 121

Task: UT06_TVV_Weld, project number 05021
Field: Vessel/In-vessel
Collaborative staff : *M. Slováček, V. Diviš, V. Ochodek*
Project was finished in 2006

The research programme was based on comparison of experimental and numerical results. ITER Vacuum Vessel welding technology consists from various welding technologies – TIG in narrow gaps, EB welding, MMAW etc. The each welding technology has got a different heat source and input welding parameters. The influence on final distortion has got a shape and size of heat affected zone (HAZ), molten zone (MZ) and mainly locked inward material expansion surrounding HAZ and MZ. The main aim of this project was to determine influence of input welding parameters for a final distortion. Set of experiments with various input parameters (welding technology, input welding parameters, size of samples) and their distortion with numerical simulation will was compared.

The object of this work has been found out the methodology of the welding numerical simulation, mainly for determination of the mathematical heat source models. The model of the thermal source is one of the most important input parameters. The computation model is loaded only with non-stationary temperature fields. Thermal load represents the thermal energy flow into the material during the welding process. The results (distortion, residual stresses) depend very much on finding the correct model of the thermal source and appropriate temperature distributions. There is paid attention to find the correct model of heat source for the each ITER welding technology. The special heat source models for the GTAW and EB welding technology have been developed for ITER welding parameters. The double ellipsoidal and conical models have been used as basis. The experimental program has been prepared as well. The measured results during the experiments have been used as input parameters (welding power, shape and size of the molten area) for numerical simulations and also for comparison calculated and measured results (temperature cycles, molten zone).

Number of welding example	c_1 [mm]	c_2 [mm]	a [mm]	b [mm]
1	1,71	1,99	1,89	1,07
2	2,9	3,59	2,79	2,31
3	2,76	2,85	2,24	1,66

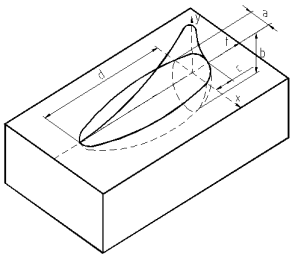

The following conclusions can be done:

1. The special experimental program has been prepared. The mock up experiments for GTAW and EB welding technologies have prepared and done. The welding parameters, temperature cycles and shape and size of the molten zones have been determined. The several welding variants with different heat inputs have been applied.

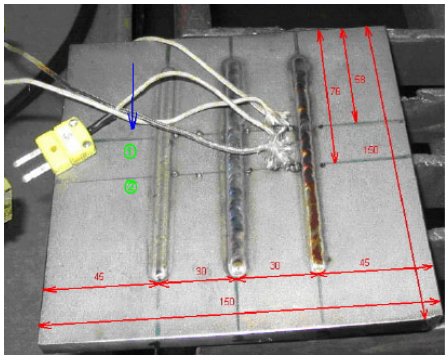

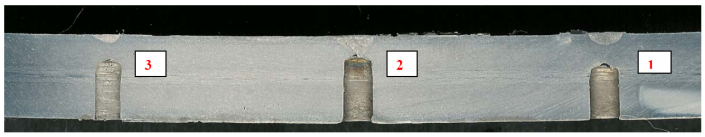

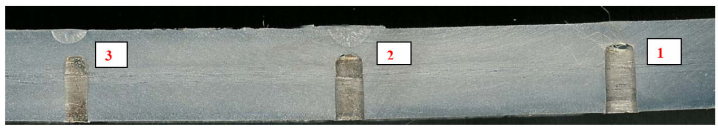

2. The appropriate heat source model for welding technology GTAW has been found. There has been found the relation between quantity of the input heat flux to material, shape and size of the molten zone and shrinkage. The double ellipsoidal modified model has been used and modified based on the comparison between calculated and measured results.

Number of sample	Voltage [kV]	Current [mA]	Focused current [A]	Source distance [mm]	Power [kW]	Weld. velocity [m/min]	Total heat [J/cm^2]
1A	55	100	2,37	167	5,5	1	3300
1B	55	50	2,37	167	2,75	0,5	3300
1C	55	150	2,37	167	8,25	1,5	3300

3. The appropriate heat source model for welding technology EB has been found. There has been found the relation between quantity of the input heat flux to material, shape and size of the molten zone and shrinkage. The conical model has not been modified. The conical model (without modification) can be used for ITER EB welding application.

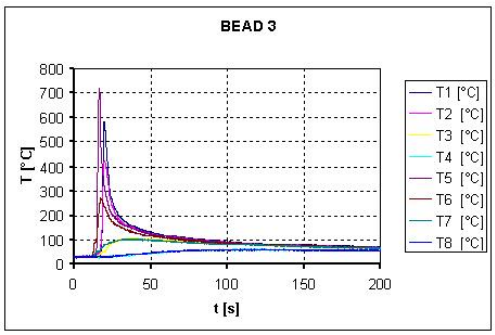

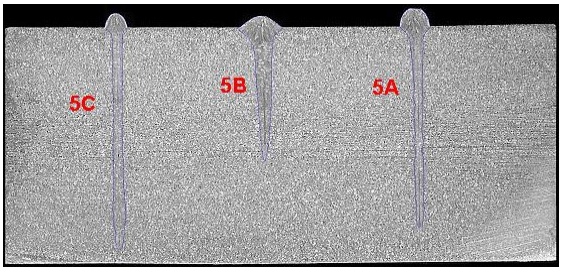

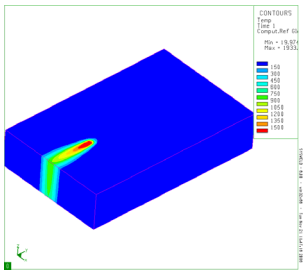

4. The local temperature distributions at welding area and surrounding (type of the heat source model and heat input) have got the big influence on the shrinkages (local distortions) and residual stresses. The precise heat source modelling is very important for obtaining precise shrinkages and residual stresses as well.

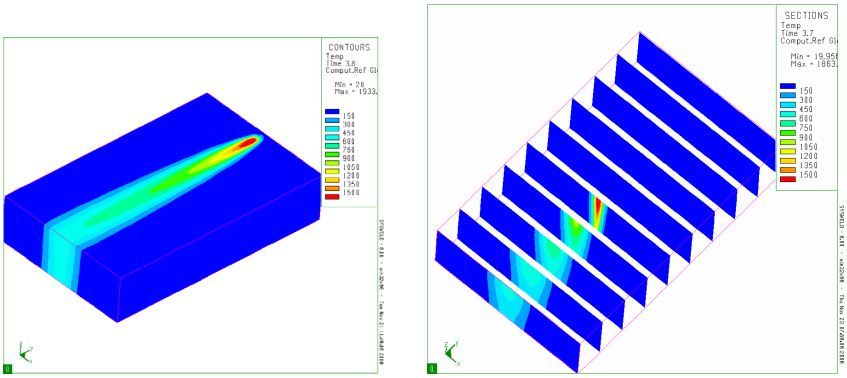

5. The very narrow and deep molten zone is typically for EB welding technology. The advantage of this method is that it is possible weld very thick plate with one weld bead. The disadvantage of this method is the very big residual stresses and deformations in narrow area and possibilities of the hot cracking. The finding correct input-welding parameters for EB welding technology are very important due to fact of the possibilities of the hot cracking. The welding numerical simulation is good tool for optimisation of the welding process.

Reference:

[1] Slováček M., Diviš V., Ochodek V. : Heat Source Models Development for Individual ITER Welding Technologies and Their Influance on the Final Distortion, report IAM Brno, Identification number : 3976/06, Brno December 2006

Surface examination of the In-vessel Components Treated by Laser Radiation

Principal Investigator: B. Kolman, IPP AS CR Prague
kolman@ipp.cas.cz, tel.: +420-26605-3077

Task: IPP-CR_UT06_TPP_LASRAD
Collaborative staff: *A.Oliveriova*
In collaboration with:
P. Gasior, J.Wolowski, Association EURATOM – IPPLM, Warsaw, Poland

Laser-induced tritium decontamination is considered to cause the material structure changes. Therefore a surface examination of the in-vessel components is necessary. Comparison of two surface states - before and after the laser treatment – is required. Non-destructive electron-optical methods, namely scanning electron microscopy (SEM), are applied in this study. For the surface topography representation, both secondary and backscattered electrons at different image magnifications can be used. In case of deep changes, surface rougness with the line profile is evaluated.

Series of experiments were conducted at IPPLM Warsaw which allowed to optimize the laser ablation method for codeposited layers removal from tokamak components using relatively low (average) power (~ 6 W) Nd-YAG nanosecond laser system. Following these experiments, analyses of the samples were realised in IPP Prague.

Glass samples 75 mm long with dust generated during the removal process were analysed by the CamScan 4 DV scanning electrom microscope (SEM) with the LINK AN 10000 X-ray analyser on glass slides with a visible “aerosol” (gray colour at one side of the sample). Before the analysis, a layer of graphite was evaporated on the samples to ensure the electrical conductivity. Although the tests started with a major delay in the last quarter of 2006, the following results can be demonstrated:

1. The aerosol is probably built from very fine particles that are under the microscope resolution. Except the aerosol, there are individual particles visible on the surface of the glass samples both by a light microscope and by SEM.
2. Typical feature of that particles is shown on images No 1 and No 2:

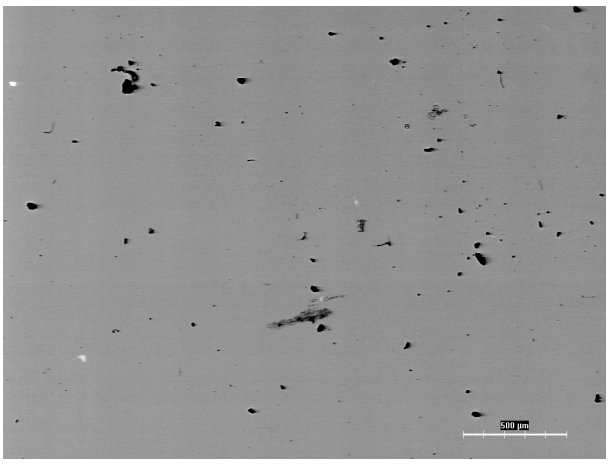

Fig. 1: Backscattered electrons image with particles on a glass sample. Magnification 40x, marker 50 µm.

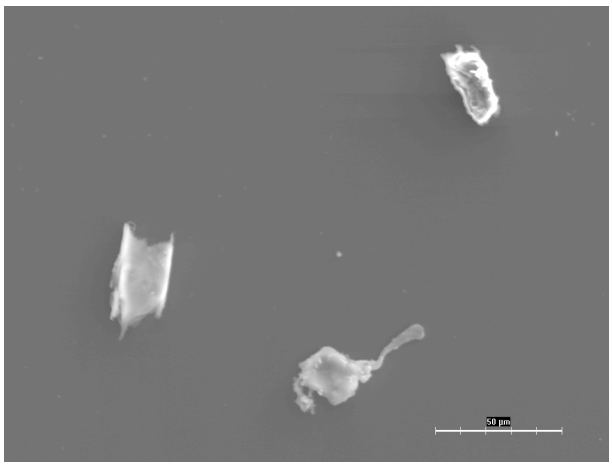

Fig. 2: Secondary electrons image with particles on a glass sample at a higher magnification (500x), marker 5 µm.

3. X-ray energy dispersive spectra from the glass bulk show presence of Si, Ca, Na, Mg, Al and K.
4. X-ray spectra from some particles are very similar; the difference is especially in a content of Na and/or Al. At some cases Cl and S and in a few cases very low content of Fe and Cu was found too.
5. Backscattered images of the particles show the darker brightness, which means the presence of elements with low atomic number.
6. According to the wavelength dispersive analysis by spectrometer Microspec, the particles contain element carbon. For comparison, the intensity of C K_α radiation from organic double-sided black tape with high content of carbon is cca 650 cps and the same item from the glass cca 20 cps; this value is assigned as a background. The positive intensities of C K_α between this maximum and minimum intensity levels (up to 480 cps) thus show different content of carbon in particles or their different dimensions.

There are some questions that need to be resolved in order to improve the results:

1. In most of the analyses, glass support may contribute to Si and other elements content.
2. Cl and S may originate from an atmosphere dust.
3. It is not clear if the analyzed particles with carbon content are really from the laser ablation or from the graphite evaporation.
4. Therefore, it is necessary to mark the area of interest on the sample or to make a photo of particles at a low magnification. We can then compare the image before and after evaporation and negate the false ones.
5. This marking is reasonable for an easier finding the particles on 75 mm long glass by the microscope at a common magnification, i.e. 200x or 500x.
6. Sample surface during transportation should be let free, not covered by another glass which may damage particles; it is possible to use any box or a new clean plastic bag.
7. Next time we may try to evaporate the samples by gold; however, this element strongly absorbs the X-rays from light elements and carbon evaluation might be difficult.

Development of methods for post-irradiation examination of Pb-17% Li alloy

Principal investigator: Karel Šplíchal, NRI Rez
spl@ujv.cz, tel: +420-26617-2456

Task: UT2006_2_NRI-PbLi
Field: Tritium Breeding and Materials, Area: Materials development
Collaborative Staff: *V. Masařík, J. Berka, J. Dušek, E. Vlasák*

The main objective of the task UT2006_2_NRI-PbLi is to develop and test suitable methods for post-irradiation examination of Pb-17%Li alloy irradiated in the framework of the EFDA task TW2-TTMS-003b-D4. An appropriate procedure will be developed and tested for dismantling the irradiation rig in the hot cells including pull out of the EUROFER test specimens from Pb-Li alloy under inert atmosphere without ingress of oxygen and surface interaction. The procedure has to prevent an escape of tritium during rig dismantling and specimens isolation. Afterwards samples of Pb-Li alloy will be taken and analysed by alpha and gamma spectroscopy to detect content (radioactivity) of the Pb-Li transmutation products (like Bi, Po, Tl, Hg). Amount of tritium in the Pb-Li alloy will be also measured and compared with theoretical calculation on tritium production during the Pb-Li rig irradiation.

In the reporting period the following work has been performed:

- Development of suitable procedure for dismantling the irradiation rig in the hot cells including pull out of the EUROFER test specimens from Pb-Li alloy under inert atmosphere without ingress of oxygen and surface interaction.
- Design and manufacturing of necessary devices, apparatus and tools to perform the planned work and post-irradiation examination in the hot cells (e.g. melting furnace, cutting machine, device for specimens cleaning in liquid sodium to remove Pb-Li residues, apparatus for tritium sampling).

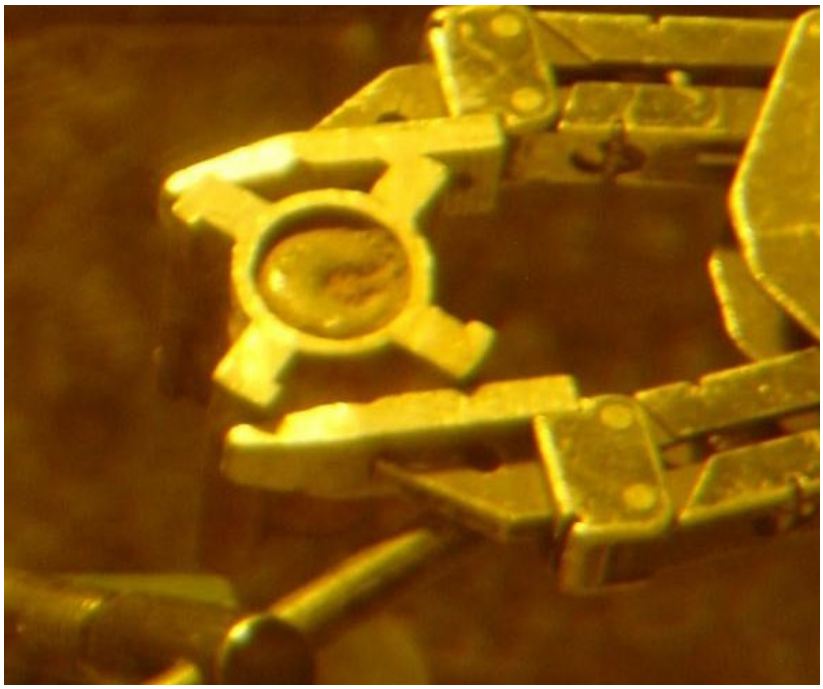

Fig. 1: A view of upper part of the Pb-Li irradiation capsule after dismantling and cutting in the hot cells

- Assembly and testing of the devices and tools in the hot cells.
- Elaboration of the Working Procedures for the work to be performed in the hot cells and during the PIE.
- Dismantling of the irradiation rig and recovery of the test specimens in the hot cells using the developed procedure, devices, apparatus and tools.
- Taking samples of Pb-Li alloy with the aim to analyse by alpha and gamma spectroscopy content (radioactivity) of the Pb-Li transmutation products like Bi, Po, Tl, Hg.
- Measurement of the amount of generated tritium in the Pb-Li alloy and comparison of the obtained results with the theoretical calculation on tritium production during the Pb-Li rig irradiation.

Plans for the next activities: Post-irradiation examination of the EUROFER corrosion and tensile specimens will be performed and samples of irradiated Pb-17Li eutectic alloy will be analysed.

Reference:

[1] Working Manual for Dismantling and PIE of Pb-Li Irradiation Rig, NRI Internal Report DRS 1104 (in Czech), 2006

Measurement of activation cross sections at neutron energies below 35 MeV - data for Chromium (constituent of the Eu-97 steel)

Principal Investigator: P. Bém, NPI AS CR, Řež
bem@ujf.cas.cz, tel: +420-26617-3506

Task: IPP-CR_UT06_TTM_IFMIF

Field: Tritium Breeding and Materials, Area: Materials Development

Collaborative staff: *V. Burjan, M. Götz, M. Honusek, V. Kroha, J. Novák, E. Šimečková*
In collaboration with:
U.Fischer, S.Simakov, Association EURATOM-FZK, Karlsruhe, Germany

Continuing the program of experimental tests of neutron activation cross section data for Eurofer constituents at IFMIF-relevant neutron energies, the activation cross sections on Chromium was measured by the activation method at 22, 27, 32, 37 MeV neutron energies using a quasi-monoenergetic neutron field based on the ^{7}Li(p,n) reaction. Samples of Chromium were irradiated in the p-Li fields generated by variable-energy proton of NPI Cyclotron-based Fast Neutron Generator. The induced gamma activity after irradiation of samples is measured at various cooling times employing the gamma spectrometry method based on the HPGe detector technique.

The analysis of resulting specific activities and reaction rates is carrying out in terms of C/E ratio (E - measured reaction rate, C - the predicted value of this observable calculated for the neutron spectrum). The neutron flux and spectra across the Cr(+Ni) samples were calculated using the modified data of the ^{7}Li(p,n) reaction measured by other authors. Activation cross-section data for selected reactions of neutrons were taken from EAF-2005 library. As an example, the value of 1.50 mb (uncertainty 5 %) of cross-section for the reaction Cr(n,x)Sc47 (normalized to the sum of stable Cr isotopes) at 35 MeV is estimated [1]. Let us report here the main results.

Fig.1: The target station of p-^{7}Li neutron source.

The overall view to the target station of neutron source is shown in fig.1. The proton beam from isochronous cyclotron strikes the Li foil at variable energies fro 11 to 38 MeV. The carbon backing serves as a beam stopper. The stacks of irradiated foils (CrNi+Au) were activated simultaneously at two distances (48 and 88 mm) from the Li foil. The CrNi alloy is used instead of pure Cr material because of the better mechanical property. The foils were of 14 and 15 mm diameter and thickness of 0.05 mm (Au) to 0.5-0.7 mm (Ta and CrNi). The time profile was monitored by the proton beam current. The typical proton beam current was about 3μA. The irradiation was carried up separately with Li+C and C target only only to investigate the contribution of neutrons from carbon stopper.

The analysis of resulting specific activities and reaction rates is carrying out in terms of C/E ratio (E - measured reaction rate, C - the predicted value of this observable calculated for the neutron spectrum). The neutron flux and spectra across the

Cr(+Ni) samples were calculated using the modified data of the ^{7}Li(p,n) reaction measured by other authors. Activation cross-section data for selected reactions of neutrons were taken from EAF-2005 library. The analysis is based on the usual C/E ratio, where C and E correspond to the calculated and experimental activity, respectively. In the calculations, the cross section data were taken from EAF-2005 [2], the neutron spectra were taken from ref. [3] with shifts described in the previous part. The data on C/E values for different incident proton energies are in the Table. Experimental uncertainties includes statistical part of errors only.

Isotope	$T_{1/2}$	reaction
Cr49	42.3 m	Cr50(n,2n)
Cr48	21.56 h	Cr50(n,3n)
V48	15.974 d	Cr50(n,t)
Sc46	83.79 d	Cr50(n,pα)
Sc47	3.3492 d	Cr50(n,p^{3}He)
		Cr52(n,dα)
Sc48	43.67 h	Cr50(n,3p)
		Cr52(n,pα)

Tab. 1: Isotopes observed from irradiations of Cr isotopes

Isotope	Ep (MeV)	C/E 48 mm	C/E 86 mm
Cr49	22.0	0.763 (4)	0.815 (3)
	27.2	0.618 (6)	0.615 (3)
	29.5	0.583 (5)	0.542 (3)
	37.5	0.608 (4)	0.633 (3)
V48	27.2	2.072 (12)	1.852 (6)
	29.5	0.875 (4)	0.763 (6)
	37.5	1.035 (3)	0.875 (3)
Sc46	27.2	0.630 (10)	0.542 (13)
	29.5	0.547 (8)	0.448 (8)
	37.5	0.452 (4)	0.375 (4)
Sc48	27.2	1.159 (6)	0.840 (6)
	29.5	0.720 (6)	0.562 (6)
	37.5	0.642 (12)	0.571 (3)
Cr48	29.5	2.118 (8)	2.319 (8)
	37.5	1.199 (4)	1.121 (3)

Tab. 2: C/E values (including exp. uncertainty in %) for the isotopes observed from irradiations of Au at proton energy Ep

Results will be compared with IFMIF activation file developed under FZ Karlsruhe /IPPE Obninsk cooperation and also with the EAF file developed in the system TALYS. The Task will be performed in close collaboration with IFMIF specialists from FZ Karlsruhe and UKAEA Culham.

References:

[1] P. Bém, V. Burjan, U. Fischer, M. Götz, M. Honusek, V. Kroha, J. Novák, S.P.Simakov, E. Šimečková, Neutron activation experiments on chromium and tantalum in the NPI p-^{7}Li quasi-monoenergetic neutron field, Proc. on the International Conference on Nuclear Data for Science and Technology 2007, Nice, to be published

[2] R.A.Forrest, J.Kopecky, M.Pillon, K.Seidel, S.P.Simakov, P.Bém, M.Honusek and E.Šimečková, UKAEA Report, UKAEA FUS 526, 2005.

[3] Y.Uwamino et al., NIM A389 (1997) 463.

Evaluation of candidate Hall sensors performance in in-vessel tokamak environment

Principal Investigator: I. Ďuran, IPP AS CR Prague
duran@ipp.cas.cz. tel.: +420-26605-2533

Task: IPP-CR_UT06_TPD_Hall
Field: Physics Integration

Magnetic diagnostic based on Hall probes is a promising concept for measurement of almost DC magnetic fields on ITER tokamak. Despite that, a very limited experience with in-vessel use of Hall probes exists within fusion community. Objective of the task is to evaluate in-vessel performance of two types of Hall probes-based systems on a small and flexible tokamak device CASTOR.

The first system (deliverable 1) is a candidate concept for ITER steady state magnetic sensors. Its performance will be tested on JET within EP2 out of vessel. Its in-vessel performance will be tested on CASTOR in terms of vacuum compatibility, noise immunity, thermal resistance, reliability. The second system (deliverable 2) is based on low-cost commercial Hall probes with on chip integrated support electronics. They form a potential low-cost alternative for monitoring of magnetic field in environmentally less demanding locations of fusion devices. Its performance on CASTOR will be evaluated from the similar points of view as the first system. Additionally, potential of these sensors to monitor plasma position on CASTOR will be evaluated.

Achievements: A new magnetometric system based on 3D Hall probe was calibrated and put in operation on CASTOR tokamak. The magnetic field vector was measured well within the plasma confinement region. Errors of the measurement caused by imperfect alignment of the probe head were analyzed and corrected. Significant remaining magnetic field up to 5 mT due to eddy currents was found to persist in the tokamak chamber for up to 300 ms after the termination of discharge. The diagnostic allows measurement of the radial profile of the safety factor on a shot to shot basis up to r/a=0.7 on CASTOR. [1]

The “low cost” A1322LUA type integrated Hall sensors produced by Allegro MicroSystems, Inc. were calibrated in frequency band DC-20 kHz and tested for the first time in tokamak environment on CASTOR. Mechanical support structure allowing precise adjustment of the individual sensors with respect to the toroidal magnetic field was designed and constructed. Particular attention has to be paid to proper electrostatic shielding of these sensors from plasma to ensure their long term survival. Based on our findings, these sensors qualify for in-vessel use on small to middle sized fusion devices where the radiation is not an issue. They offer an attractive alternative to traditional pick-up coils for applications where the good frequency response up to 10 kHz is sufficient and the temperature bellow 150ºC can be guarantied. The thermal noise level was found to be bellow 1 mT peak-to-peak. The contribution of the planar Hall effect resulting from the presence of the toroidal magnetic field was found to be bellow the resolution of the sensors. [2,3]

References:

[1] K. Kovařík, I.Ďuran, I. Bolshakova, R. Holyaka, V. Erashok: Measurement of safety factor using Hall probes on CASTOR tokamak, Czech. J. Phys. Vol. **56** (2006), Suppl. D.

[2] J. Sentkerestiová, I.Ďuran, E. Dufková, V. Weinzettl: Comparative measurements of plasma position using coils, Hall probes and bolometers on CASTOR tokamak, Czech. J. Phys. Vol. **56** (2006), Suppl. D.

[3] G. Van Oost et al.: Joint Experiments on Small Tokamaks, submitted to Nuclear Fusion.

IV Keep-in-Touch Activities on Inertial Confinement Fusion

Activities of the Prague Asterix Laser System (PALS) in the field of inertial confinement fusion have been carried out in close collaboration with Institute of Plasma Physics and Laser Micro-fusion, Warsaw, Poland, with participation of scientists from Russia, France and Australia. The experimental work was focused on investigation of various types of laser targets relevant for inertial fusion.

High-intensity laser beam interaction with multi-layer and double targets

Person in Charge: *J. Ullschmied, IPP*
Participants in the project: *Eduard Krousky, Karel Masek, Jiri Skala (PALS laboratory)*
Collaborators from other laboratories:
T. Pisarczyk (principal investigator), A. Kasperczuk, S. Borodziuk, D. Baran (Poland)
Scientific collaboration:
Association Euratom-IPPLM, Warsaw, Poland
Warsaw University of Technology, ICS, Warsaw, Poland
Institute of Physics AS CR, Prague, Czech Republic
Czech Technical University in Prague, FNSPE, Prague, Czech Republic

Energy transfer, shock wave generation, and crater creation processes at interaction of focused high-intensity laser beams with multi-layer and flyer targets were investigated at the PALS terawatt iodine laser facility in the frame of a continuing cooperative experimental project of the Czech and Polish EURATOM Associations.

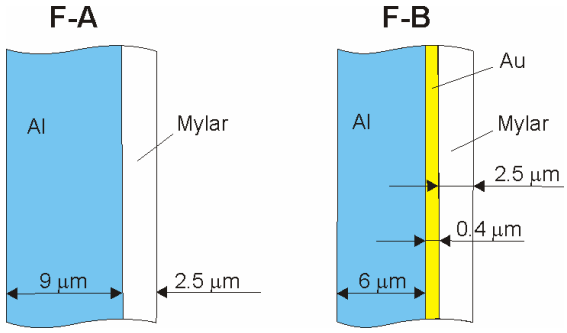

Fig. 1: The types of multi-layer foil targets used

Several series of interaction experiments with various types of laser targets have been carried out. In the first one the influence of fast electrons on the efficiency of laser energy transfer to solid planar targets was studied. The next series was aimed at investigation of shock wave generation in multi-layer foil targets of various structures. The targets exploited in the experiments were made of different materials, such as polyethylene, mylar, Al and Cu, as well as their various combinations (Fig. 1). In experiments with flyers ablative acceleration of macroparticles was studied and the efficiency of kinetic energy transfer from flyer foils to massive targets in various target configurations was determined for several types of double targets with different distances between the flyer and the massive target part.

In all the experiments the 1st and 2nd harmonic beams of the PALS laser (wavelength 1315 nm and 438 nm, pulse duration ~300 ps) of irradiation energies in between 100 J and 360 J were used. Intensity of the focused radiation on the target was varied by changing the focusing lens position and hence the focal spot radius.

The framing laser interferometry was applied as a key diagnostic tool. Density profiles of the expanding plasma plume were recorded by using an upgraded version of the three-frame laser interferometer developed at IPPLM. The interferometric measurements covered a period of up to 36 ns after the laser pulse, so that the interferograms show all the stages of the ablative plasma generation and foil acceleration, including the flyer impact on the target and crater creation. The two sequences of electron iso-densitograms shown in Fig. 2 illustrate time evolution of the ablative plasma produced by direct laser irradiation of a planar metallic target, and by impact of the flyer ablatively accelerated under the same irradiation conditions. Each subsequent equidensity lines in the diagrams are separated by the value $\Delta n_e = 2 \cdot 10^{18}$ cm^{-3}, the plasma stream boundary corresponding to the electron density $n_e = 10^{18}$ cm^{-3}. Parameters of the craters produced by both the direct laser action and the flyers were determined by means of wax replica technique and optical microscopy. The crater data were used for preliminary estimates of the flyer kinetic energy. In addition, an x-ray streak camera was used for recording temporal and spatial characteristics of the plasma x-ray emission.

The results and theoretical analysis of the experiments on the influence of fast electrons and on the shock wave generation are described in more details in Refs [1-3] and in the Annual Report 2006 of the Euratom Association IPPLM. The experiments with flyers demonstrated that by optimizing the target and irradiation parameters very high macroparticle velocities can be achieved [4]. Particularly promising are the results obtained during preliminary experiments on generation of directed plasma streams on high-Z targets [5-8], which are supposed to continue in the framework of co-operation of the IPP.CR and IPPLM Associations also in the year 2007.

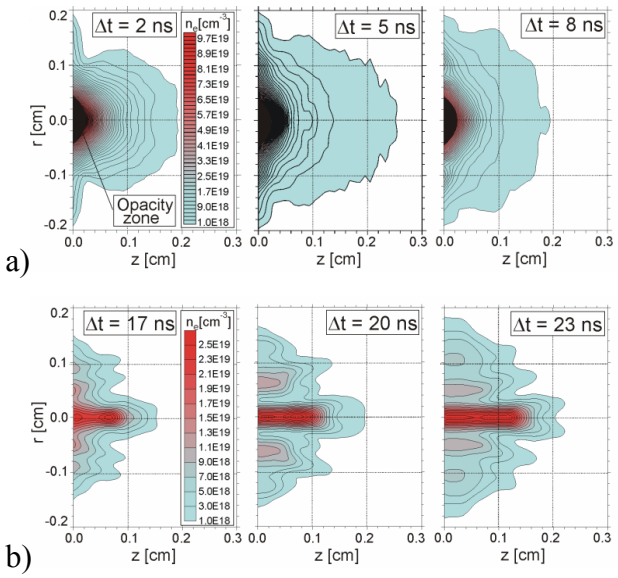

Fig. 2: Sequences of electron isodensitograms of the plasma produced by direct laser ablation of Al target (a) and by disk collision with a massive Al target (b).

References:

[1] S.Yu. Gus'kov et al., Investigation of shock wave loading and crater creation by means of single and double targets in the PALS-laser experiment, Jour. Russian Laser Res. **26** (2005), 228-244.
[2] S.Yu. Gus'kov et al., Efficiency of ablative loading of material upon the fast-electron transfer of absorbed laser energy, Quantum Electronics, 36 (2006), 429-434.
[3] A. Kasperczuk et al., Laser driven acceleration and collision of thin metal discs with massive targets: Effective energy transfer condition studies, Proc. XXIX ECLIM, Madrid 2006, 584-589.
[4] S. Borodziuk et al., Study of the conditions for the effective energy transfer in a process of acceleration and collision of the thin metal disks with the massive target, Eur. Phys. Jour D 41 (2007), 311-317.
[5] A. Kasperczuk et al., Plasma jets generation by means of interaction of defocused laser beam with metallic targets of different mass density, 33 EPS Conf. on Plasma Phys., Book of Abstracts. Roma, 2006. s. 83.
[6] P. Nicolai et al., Plasma jets produced in a single laser beam interaction with a planar target, Phys. of Plasmas, 13 (2006), Art. No. 062701.
[7] A. Kasperczuk et al., Stable dense plasma jets produced at laser power densities around 10^{14} W/cm^2, Phys. of Plasmas, 13 (2006), Art. No. 062704.
[8] A. Kasperczuk et al., The influence of target irradiation conditions on the parameters of laser-produced plasma jets, Phys. of Plasmas, 14 (2007), Art. No. 032701.

V Training, Education, Outreach and Public Information Activities

1. Training and Education

Association EURATOM-IPP.CR contributes actively to fusion education on both national and international levels. For example, in 2006 thirteen postgraduate and ten undergraduate students worked on their fusion–related theses under supervision of fusion experts from the Institute of plasma physics AS CR. Five MSc and one BSc theses with fusion relevant topics were completed in 2006 and successfully defended.

The new R&D projects combined with a sufficient amount of interested students resulted in an important qualitative change of our fusion education system. In 2006, Faculty of Nuclear Science and Physical Engineering of the Czech technical university in Prague (member of the Association) opened for the first time a brand new MSc curriculum „Physics and Technology of Thermonuclear Fusion“ (see also part V.2). This was partly supported by a grant of the Czech Ministry of Education.

Our international summer training school SUMTRAIC - focussed on development of experimental and presentation skills - has become a tradition now. The 2006 summer school was dedicated to Edge Plasma Studies on the CASTOR Tokamak. The school was attended by 13 participants from eight countries and by one Czech PhD students. See below for details.

4th Summer Training Course (SUMTRAIC) on the CASTOR tokamak

J. Stöckel, J. Brotánkova, O. Bilyk, I. Ďuran, R Dejarnac ,E. Dufková, J. Horáček, M. Hron, V. Weinzettl

In collaboration with:
M. Berta, A. Bencze, D. Dunai, G. Veres, KFKI, Association EURATOM-HAS, Budapest, Hungary

The 4th Summer Training Course (SUMTRAIC) was organized in the IPP Prague in collaboration with RMKI-KFKI, Budapest in the period of 10-19 July 2006. The topic of the summer school was: Edge Plasma Studies on the CASTOR Tokamak.

The school was attended by 13 participants from eight countries and by one Czech PhD students. The students were divided in 5 experimental groups supervised by the CASTOR staff and our Hungarian colleagues M. Berta, A. Bencze, D. Dunai, G. Veres.

1. *Magnetic measurements using SK ring* Tamás Fehér, Gergely Dobrik (Hungary) Ramona Gstrein (Austria) and Josef Havlíček (Czech)
2. *Bolometric measurements* Gergely Papp (Hungary)
3. *Rake probe measurements* Mária Kovács (Hungary), Adriano Altichieri (Italy)

4. *Tunnel probe measurements* Damian W. Rohraff (Poland), Marius Lucian Solomon (Romania), Attila Aranyi (Hungary), Dmitriy Kogut (Russia)
5. *Statistical properties of the edge microturbulence* István Pusztai (Hungary) Arvind Sharma (Norway) and Filip Janky (Slovakia)

During the experimental campaign, of about 300 tokamak discharges were performed. The edge plasma parameters were measured by several arrays of electric and magnetic probes and two arrays of bolometers. Results of experiments and of the subsequent analysis of data were presented at the closing workshop.

The next SUMTRAIC will be organized in Budapest in July 2007 by our Hungarian colleagues.

The SUMTRAIC participants in the control room of the CASTOR tokamak

Participation in the Euratom Fusion Training Scheme

I. Ďuran, J. Stöckel

In the end of 2005 the Euratom Fusion Training Scheme (EFTS) was lunched by call for participation. The main aim of EFTS is to involve and to train a few dozens of engineers within the next 5 years in several engineering areas that are key for success of the ITER project. Association IPP.CR participated on preparation of two proposals submitted within EFTS scheme.

The first one was entitled European network for Training ion cyclotron Engineers (**EnTicE**). **EnTicE** proposal was prepared by a consortium of eight institutions, namely IPP Garching Germany, UKAEA Culham United Kingdom, CEA Cadarache France, ERM-KMS Brusel Belgium, Politecnico di Torino Italy, University of Turin Italy, Spinner GmbH Germany, and IPP Prague Czech Republic. Jean-Marie Noterdaeme from IPP Garching was appointed to be the coordinator of the project. The aim of the **EnTicE** training program is to develop the engineering capabilities required to design, procure, operate and maintain the ITER Ion Cyclotron Resonance Frequency (ICRF) antenna, as well as to contribute to the fast track programme by enhancing the attractiveness and readiness of ICRF to provide a reliable heating system. For this purpose, it was proposed to train six young researchers in the ICRF area, using the five particular projects as focus and training ground. It was proposed that IPP.CR will hire one young researcher for the period of 3 years. The specific feature of

his/her training program is that he/she will spend more than three quarter of his/her time with the other **EnTicE** partners (IPP Garching, UKAEA Culham, and Spinner company), allowing for him/her an intensive contact with the leading associations and scientists and engineers in the field, and a broad exposure to a variety of aspects. Further, the IPP.CR trainee will acquire special training in areas of nuclear engineering and remote handling. Besides being a contribution to the ITER ICRF antenna project, the IPP.CR trainee will also be expected to provide direct link and to stimulate further involvement of IPP.CR in ITER ICRF project and in ITER engineering in general. The **EnTicE** proposal was accepted by EU Commission in its full proposed budget of 1.2 MEuro. The project was officially lunched on 1st November 2006 and the primary activity up to now was to prepare and to start advertisement of open positions via various channels.

The second proposal with IPP.CR involvement was entitled Engineering of Optical Diagnostics for ITER (***EODI***). This project was undertaken by seven institutions, namely: IPP Julich Germany, FOM Rijnhuizen Netherlands, UKAEA Culham United Kingdom, CEA Cadarache France, IPP Garching Germany, RISØ Denmark, and IPP Prague Czech Republic. Wolfgang Biel from IPP Julich was selected to act as the coordinator of the project. The aim of the ***EODI*** is to train eight new engineers on technological issues related to the ITER optical diagnostics particularly Charge Exchange Recombination Spectroscopy (CXRS), Infrared (IR), Thomson scattering LIDAR, X-ray, and Fast ion Collective Thomson Scattering systems. The training programmes will also including some basic elements of fusion relevant plasma physics and plasma diagnostics expertise in order to provide adequate background knowledge for a wider understanding of the design problems. The IPP.CR proposes to hire one trainee for two years. The main topic of his/her training programme will be mechanical design of ITER LIDAR and CXRS systems. The training will be executed in close collaboration with other partners within the ***EODI*** and also with the ITER diagnostic team, particularly with Chris Walker. The ***EODI*** proposal was approved by EU Commission with the total budget of 1.6 MEuro. The project was lunched on 1st September 2006 and the advertisement of the open positions was initiated.

2. Outreach and Public Information

M. Řípa, V. Weinzettl, J. Mlynář, P. Chráska, J. Stöckel, E. Dufková

The year 2006 was full of standard public information activities – including communications with media (newspapers and journals, radio broadcasts and TV shots), lectures for both high school students and wide public. However, there were some distinctive activities that deserve special attention for their success and importance.

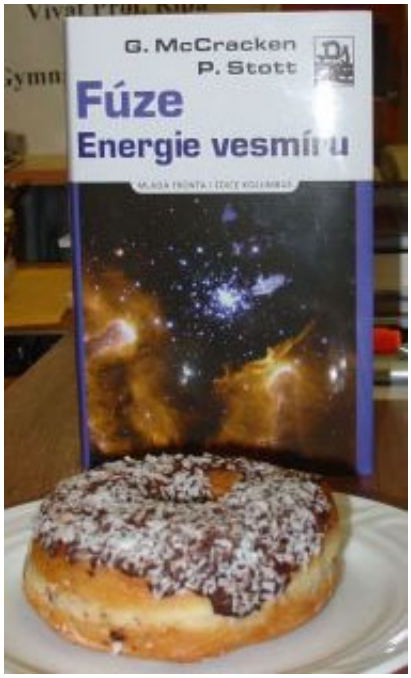

Besides the 4th Summer training course (SUMTRAIC) and the 5th Semester Course for Undergraduate Students, that are almost traditional now, a new curriculum was launched: Physics and Technology of Thermonuclear Fusion (Master's degree). The new curriculum can be studied at the Faculty of Nuclear Sciences and Physical Engineering of the Czech Technical University in Prague (member of Association EURATOM-IPP.CR) and enjoys teaching support from other Association members, in particular from the Institute of Plasma Physics. This is very timely due to the imminent transport of the tokamak Compass-D from Culham to Prague and the agreement to build the ITER tokamak in Cadarache, too. Both facilities will need young experts and our new curriculum can present an important resource.

Last November would deserve to be nicknamed the month of Czech translations. Several Public Information texts had been translated from English to Czech by our Association in past two years and, by coincidence, most of the materials were printed in Czech within one month, in November 2006.

(1) Folder *Cleaner Energy for the Future – the development of fusion energy* (EFDA CSU Garching)
(2) Poster *Fusion Energy – Cleaner Energy for the Future* (EFDA CSU Garching)
(3) Brochure *Fusion Research – An Energy Option for Europe's Future* (European Commission)

The three publications can be downloaded in Czech from the EFDA webpage, see http://www.efda.org/multimedia/. However, the major event in November was the launching ceremonial of the Czech edition of the book by Garry McCracken and Peter Scott: "*Fusion – the Energy of the Universe*", see figure. The ceremonial took place in the historical building of the Academy of Scieces of the Czech Republic and had a very positive feedback in media. The first European astronaut MEP Vladimír Remek accepted our invitation to become a godfather of the book, and the President of the Academy of Sciences of the Czech Republic, Prof Václav Pačes, had a very encouraging speech. Within four consecutive months, the first edition of the translated book was sold out. One of the translation's successes between Czech readers is surely launching ceremonial.

Public Information activities are naturally constrained by available budget and time. We believe the time is most efficiently spent while looking for personal connections to editors of the most important newspapers. At present our Association has very good professional friends in two newspapers with the largest circulation in the Czech Republic: "Mladá Fronta Dnes" and "Lidové noviny". Furthermore we foster good connection with some radio

broadcast programmes but, unfortunately, our contacts to TV are sparse. This needs to be improved for the TV plays a most important role in spreading news from science and R&D.

Some budget is required, for example, in printing some of our information materials: folders, leaflets etc. In this respect, we have established good working relations with the largest producer and distributor of electric energy in the Czech republic – the Energy company CEZ, a. s. We can participate in its educational programme and as a results we could print and distribute some of the folders, or make our PI events more visible.

Some of our projects for 2006 turned out to be more challenging. For example, within the street fair "Science on the streets" we had successful stand only in Prague, the planned stand in Pilsen was not affordable. Second, the installation of Fusion Expo had to be postponed until 2007 due to technical and contractual reasons.

Mr Vladimír Remek, Member of European Parliament

Limited budged was often substituted by enthusiasm of colleagues who regularly support our Public Information activities. This hold in particular for preparation of Fusion Expo in Prague, that started in 2006 and that included, among others, translation of the posters.

A crucial point in PI is to correctly react on time to critical opinions in media. We all know that arguments of fusion sceptics do not really change in time. That is why we have used many opportunities to explain misunderstandings and errors concerning future role of fusion in energy supply - in public lectures, interviews, PI articles etc. Very interesting feedback was provided by monitoring the media via key fusion words occurrence. Some results of search for "thermonuclear fusion" is presented in the following table:

„Fusion" media activities (newspapers, magazines, broadcasts) in all country per year

Data demonstrate sharp increase of positive media coverage in 2006

	2006/2005/2004
Total:	84/50/30
Full articles about fusion:	54/31/15
Only one occurrence of the word "fusion":	35/14/12
Brusells & Paris only	24 (7x in The most important world events 2006)
Tokamak EAST only	8
Authors from Association only	12/7/8
Negative only	5/5/?

The growth of media interest is partly due to our PI activities, and, on the other hand, it required increased involvement of our experts.

LIST OF PUBLIC INFORMATION ACTIVITIES IN 2006

Television and broadcast (video / audio)

P. Chráska, M. Hrehor (Š. Čechová): Plán lidstva, Český rozhlas 1, Radiožurnál, 06/11/24, 18:20 Radiofórum,
R. Pánek – interview for Radiožurnál
V. Weinzettl, M. Hron (L. Veverka): ITER a DEMO, Český rozhlas, internet broadcast Odpoledne s Leonardem, Nula-jednička, 06/08/07
V. Weinzettl, M. Hron (L. Veverka): Stěhování tokamaku COMPASS-D do Prahy, Český rozhlas, internet broadcast Odpoledne s Leonardem, Nula-jednička, 06/08/21
M. Řípa: Anketa (Fantazie), Český rozhlas VKV 93.1, Meteor, 06/04/29, 8:10 h
M. Řípa: Pozvánka na přednášku „ITER je cesta…“, Český rozhlas VKV 93.1, Meteor, 06/04/08, 8:10 h.
M. Řípa: Anketa (Budoucnost), Český rozhlas VKV 93.1, Meteor, 06/06/03, 8:10 h
M. Řípa, **J. Mlynář** (M. Mašková): O fúzi, Český rozhlas, internetové vysílání, Odpoledne s Leonardem – (vyprávění o fúzi), 06/06/22, from 14:00 to 15:00/from 22:00 to 23:00
M. Řípa: Minuty s … Milanem Řípou, Prezentace knížky Fúze – Energie vesmíru, UPS, six times

Papers:

E. Dufková: Compass - nový směr výzkumu fúze v Čechách, Třetí pól, 2006
J. Zajac: Akumulátory energie pro blízkou budoucnost**,** Třetí pól, 06/05, pp. 15-16
J. Mlynář: Padesát let Lawsonových kriterií, Pokroky matematiky, fyziky a astronomie, Vol. 51 (2006), No. 3, pp. 231-238
J. Mlynář: Cesta jménem ITER, Vesmír, Vol. 85 (2006), No. 6, pp. 356 - 361
M. Řípa: ITER – možnosti pro evropský průmysl, Technický týdeník, Vol. 54 (2006), No. 1, 06/01/10, p. 5
M. Řípa: Compass míří do Prahy, Technický týdeník, Vol. 54 (2006), No. 3, 06/02/07, p. 12
M. Řípa: ITER – šance pro český výzkum a průmysl, Svět vědy, Vol. 4 (2006), No. 3, p. 28-30
M. Řípa: Český fyzik: Jaderná fúze není sen, Lidové noviny, 06/03/22, issue Byznys, p. 17
M. Řípa: Český fyzik: Jaderná fúze není sen, http://www.lidovky.cz
M. Řípa: Průmyslová databáze subdodavatelů projektu ITER, CHEMagazín, Vol. 16 (2006) No.2, p. 37
M. Řípa: Databáze i pro české firmy, Technický týdeník, Vol. 54 (2006), No. 7, 06/04/04, p. 30
M. Řípa: Tajemství kolem termojaderné fúze padlo před 50 lety, MF Dnes, 06/04/29, p. B8
M. Řípa: Lze ukradnout jadernou fúzi?, Svět vědy, Vol. 4 (2006), No. 5, p. 40-43
M. Řípa: Dohoda ITER podepsána, Technický týdeník, Vol. 54 (2006), No.12, 06/06/13, p. 5
M. Řípa: Průmyslová databáze subdodavatelů, Elektroinstalatér, Vol. 12 (2006), No. 3, p. 23
M. Řípa: Řízená fúze – energie budoucnosti, Zpravodaj České energetické agentury, 2006, No. 2, p.3
M. Řípa: Global Energy Prize, Technický týdeník, Vol. 54, 06/06/27, No.13, p. 3
M. Řípa: Čína zažehne umělé slunce, Lidové noviny, Vol. 16 (2006), 06/07/22, příloha Věda, p. 9
M. Řípa: Tokamak s českou účastí, Lidové noviny, Vol. 16 (2006), 06/07/22, příloha Věda, p. 9
M. Řípa: Výzkum řízeného termojaderného slučování se dožívá 50 let, Technický týdeník, Vol. 54 (2006), No. 15, 06/08/08, p. 12
M. Řípa: Supravodivý tokamak dobyl Asii, Technický týdeník, Vol. 54, (2006), 06/09/12, No.18
M. Řípa: První plazma v tokamaku EAST, Technický týdeník, Vol. 54 (2006), 06/10/10, No.21, s. 1
M. Řípa: Čínský tokamak zapálil první plazma, Mladá Fronta Dnes, Vol. 17 (2006), No. 240, 06/10/14, příloha Věda, p. C/10
M. Řípa: Chaos dělá ve fúzi pořádek, Lidové noviny, Vol. 16 (2006), 06/10/18, sešit Byznys, s. 17

Interviews and expert reviews

J. Matyáš (**J. Matějíček**, rozhovor): Češi míří do nitra umělé hvězdy, Lidové noviny, 06/01/28, Příloha „Věda“, p. VIII
L.Veverka: (**V. Weinzettl,** rozhovor): DEMO přinese fúzi do praxe, Lidové noviny, 06/09/09

J. Sládek (**P. Chráska**, konzultace, citace):Velmoci chtějí získat energii jadernou fúzí. Hospodářské noviny, 06/11/22
Eva Bobůrková (**M. Řípa,** konzultace): Fúzní reaktor na startu, Mladá Fronta Dnes, 06/05/27, p. B8,
J. Klímová (**M. Řípa,** konzultace): České firmy mají šanci ve Francii, Mladá Fronta Dnes, 06/02/17, issue Ekonomika, p. B2
J. Matyáš (**M. Řípa**, konzultace, citace): Šance pro české vědce, Lidové noviny, 06/02/18, příloha Věda, p. VIII
M. Lázňovský (**M. Řípa**, konzultace, citace): Nejžhavější laboratoř světa, Lidové noviny, pátek, 06/03/10, sešit Byznys, p.16
Josef Tuček (**M. Řípa,** konzultace, citace): Energie budoucnosti – Vědci chtějí spoutat reakci, díky níž svítí Slunce, Hospodářské noviny, 06/0716, Injournal, pp. 10 – 11
Josef Matyáš (**M. Řípa,** konzultace): Krok k uvolnění, Lidové noviny, 06/04/24, p. 10
Autor neuveden (**M. Řípa, J. Mlynář**, konzultace, foto) The lost story of the Russian scientist Oleg Lavrentiev, EFDA Fusion Newsletter, Vol.3 (2006), 06/10/15, p. 12
Autor neuveden (**J. Mlynář**, konzultace, foto) Compass-D moves to the Czech Republic, EFDA Fusion Newsletter, Vol.3 (2006), 06/10/15, p. 12

Lectures

J. Stöckel: Fyzika plazmatu a termojaderné slučování, Západočeská universita, Plzeň, 06/03/27
J. Stöckel: Fyzika plazmatu a termojaderné slučování, Fakulta matematiky, fyziky a informatiky, Bratislava, 06/05/02
J. Stöckel: Fyzika a technika termojaderné fúze, FJFI ČVUT, Praha, 06/11/06
J. Stöckel: Fyzika plazmatu a termojaderné slučování, Jihočeská Univerzita. 06/12/06
J. Stöckel: Edge plasma diagnostics in tokamaks, Ghent University, 06/10/31
I. Ďuran: Nuclear Fusion and ITER project, Fakulta strojní ČVUT, Praha, 06/10/18
R. Pánek: Termojaderná fúze a projekt ITER, MFF UK, katedra jaderné fyziky, Praha, 06/12/**
E. Dufková: Energetika, basic school (2x), Liberec, 06/04/18
E. Dufková: Energetika, basic school (1x), Praha 4, 06/04/27
E. Dufková: Energetika, basic school (2x), Ústí nad Labem, 06/05/15
E. Dufková: Energetika, basic school (2x), Mnichovo Hradiště, 06/05/19
E. Dufková: Energetika, střední škola (2x), Brandýs nad Labem, 06/06/01
E. Dufková: Energetika, basic school (2x), Bílina, 06/07/12
E. Dufková: Energetika, basic school (2x), Stará Boleslav, 06/10/14
E. Dufková: Energetika, basic school (2x), Neratovice, 06/12/01
M. Peterka: Gymnázium Nad Alejí, (J.Brotánková, školitel): Měření turbulence v plazmatu tokamaku CASTOR, Studentská vědecká konference, Praha, AV ČR, 06/09/25 – 26
T. Feistner: Gymnázium Nad Alejí Tokamak (J. Zajac, školitel): Tokamak - reaktor řízené termojaderné syntézy – měření vyzařování plazmatu, přednáška, Studentská vědecká konference, Praha, Akademie věd ČR, 06/09/25 – 26
M. Peterka: Gymnázium Nad Alejí, (J.Brotánková, školitel): Měření turbulence v plazmatu tokamaku CASTOR", Týden vědy a techniky, Praha, Akademie věd ČR, 06/11/06
M. Řípa: ITER je cesta, Gymnasium Dr. Josefa Pekaře, Mladá Boleslav, 06/03/02
M. Řípa: ITER je cesta, Nebojte se vědy, AV ČR, Praha, 06/04/11
M. Řípa: Role O.A.Lavrentěva při výzkumu termojaderné fúze v Sovětském svazu, Disputace, Čáslav – Kutná Hora, 06/06/29
M. Řípa: ITER je cesta**,** Gymnasium J. S. Machara, Brandýs nad Labem, 06/11/23
M. Řípa: ITER je cesta, přednáška pro veřejnost v rámci série Mladý Sisyfos, Pedagogická fakulta Západočeské university Plzeň, 06/11/30, 15:00 h
M. Řípa: Jaderný reaktor bez jaderného odpadu?, SPŠ Hronov a JČMF, přednáška pro veřejnost ve SPŠ Hronov, 06/12/12
M. Řípa: ITER je cesta, přednáška pro Gymnasium Nad Kavalírkou, 06/12/19

Translations

V. Kopecký (**M. Řípa**): Věda v ulicích, posters: „ITER“ a „Podíl Česka“, Praha, 06/05/26
M. Řípa: *Termojaderná fúze? ANO!*, Folder of six pages 10 x 21 cm, ČEZ, a.s.; 2006
McCracken G., Stott P.: *Fúze – Energie vesmíru*. From English *Fusion – The Energy of the Universe*, translation **M. Řípa, J. Mlynář**. Mladá fronta, a.s., Praha 2006. 328 pages + 16 pages of colour pictures, ISBN 80-204-1453-3**.**
Rosa Antidormi: *Výzkum fúze – Volba energie pro budoucnost Evropy*, translation **M. Řípa, J. Mlynář,** from English *Fusion Research – An Energy Option for Europe's Future*, brochure 40 pages.
M. Westra, Federico Casci, Doris Lanzinger: *Čistší energie pro budoucnost*, translation **M. Řípa, J. Mlynář**, from English *Cleaner Energy for the Future*, EFDA Close Suport Unit, Garching, Folder A4 x 4.
M. Westra: *Fúzní energie – Čistší energie pro budoucnost,* translation **M. Řípa, J. Mlynář**, from English *Fusion Energy – The Cleaner Energy for the Future*, poster A0/A1, http://www.efda.org/multimedia/posters_educational.htm

Sports event:

Tour de Plasma, on bicycles from Praha to Mariánská in dresses of the IPP AS CR, 15th -17th September 2006

APPENDIX

Overview on the COMPASS-D tokamak re-installation in the Institute of Plasma Physics AS CR, Association EURATOM-IPP.CR

Contents:

1. Introduction

The thermonuclear research at the Institute of Plasma Physics of the Czech Academy of Sciences has a long tradition. The CASTOR tokamak has been taken over from the former Soviet Union in 1974, upgraded and kept in operation up to now. During this period, the IPP focused mainly on edge plasma physics, diagnostics development and wave-plasma interaction. Substantial expertise in these fields has been obtained in a broad international cooperation. However, the CASTOR tokamak is not ITER relevant being restricted by its limiter geometry and small size. In addition, problems with vacuum appear often owing to the age and consequent fragility of the tokamak vessel.

Recently, a possibility to continue and broaden tokamak research at IPP has appeared when the tokamak COMPASS-D (Fig. 1.1) was offered to IPP Prague by UKAEA. The installation of this tokamak in IPP will allow performing research on a considerably higher level and to focus on ITER-relevant physics and technology. The COMPASS-D tokamak has an ITER-like plasma shape (Fig. 1.2) and, after installation of an ion heating system, it will be able to access plasma parameters relevant in many aspects to ITER. The COMPASS-D tokamka will be an ideal device for detailed studies of edge plasma physics in the H-mode regime (e.g., pedestal, ELMs, turbulence, etc)

The COMPASS (COMPact ASSembly) device was designed as a flexible tokamak in the 1980s mainly to explore MHD physics in circular and D-shaped plasmas. Its operation began at the Culham Laboratory of the Association EURATOM/UKAEA in 1989. In 1992, COMPASS was restarted with a D-shaped vessel (COMPASS-D). It is equipped with a unique fully configurable, four quadrant set of copper saddle coils to create resonant helical fields. A hydraulic vertical preload has to be used for toroidal magnetic field above 1.2 T.

During COMPASS-D operation, extensive experiments were performed on error-field modes (pioneering the basis and design of the error field correction coils on ITER), and ECRH experiments including current drive. H-modes were found and studied extensively; a particular feature of COMPASS-D is its capability to produce clear H-mode ohmically at low field (~1T). However, with the growth of the spherical tokamak programme at the Culham Laboratory, it was decided to mothball COMPASS-D in 2001, because of the lack of manpower and hardware resources to run both the MAST and COMPASS-D programs. The potential of COMPASS-D and its scientific programme were therefore not further exploited.

The main parameters of the COMPASS-D tokamak envisaged in IPP Prague are summarized in the Table 1. Two successive steps of the COMPASS-D restart include:

1) transport and installation of the machine and its equipment with basic diagnostic systems, and start of operation;
2) installation of additional heating and diagnostics systems, which will allow execution of the scientific programme.

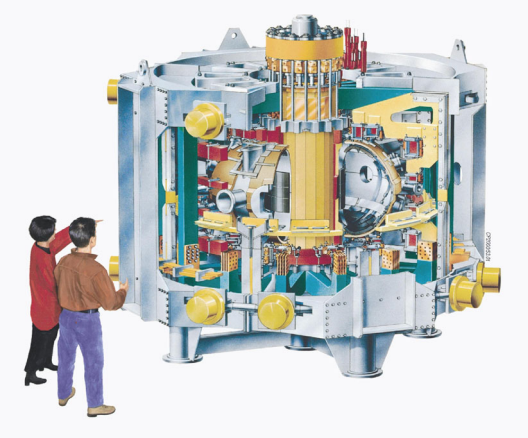

Fig. 1.1: Schematic picture of COMPASS-D tokamak.

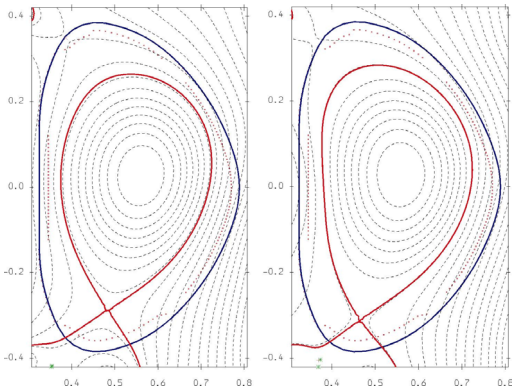

Fig. 1.2: COMPASS-D plasma cross-section.

Parameter	After Step I	After Step II
R	0.56 m	0.56 m
a	0.18 – 0.23 m	0.18 – 0.23 m
I_p (max)	200 kA	200 kA
B_T (max)	1.2 T	1.2 T
Elongation	1.8	1.8
Shape	D, SND, ellipse	D, SND, ellipse
Pulse length	1 s	1 s
P_{LH}, 1.3 GHz	-	0.4 MW
P_{NBI}	-	2 x 0.3 MW

Table 1: Main COMPASS-D parameters.

2. Computer based predictions

DESCRIPTION OF MAIN RESULTS

A number of combined ACCOME [1] and ASTRA [2] simulations were carried out in order to assess the performance of COMPASS with the planned neutral beam (NB) and lower hybrid (LH) systems.

The simulations were carried out under consideration of the following performance targets for the operation regime I = 0.2 MA, B = 1.2:

- large $\beta = 2\mu_0 \langle p \rangle / B_\phi^2$, but limited to $\beta_{\lim}[\%] \cong \frac{3I[MA]}{a[m]B_\phi} = 2.5\%$ in order to avoid ballooning and/or disruptions, etc.
- large $\beta_{poloidal}$ for large fraction of bootstrap current
  $$\beta_p = \frac{2\mu_0 \langle p \rangle}{\langle\langle B_\Theta \rangle\rangle^2} \cong \frac{4\pi^2 a^2 \langle p \rangle (1+\kappa^2)}{\mu_0 I_p^2} \cong 0.5$$
- large fraction of non-inductive driven current to assist ohmic coil dΨ/dt for longer pulse duration
- possibility of NB off-axis power deposition to support reversed shear configuration and an ITB
- high density operation, ≥ 3 - 6×10^{19} m^{-3}, for ELMy H-mode. This range falls well within the Greenwald limit [3].

The simulations proceed in a sequence of iterations between the two codes in order to reach a consistent state between power deposition profiles from ACCOME needed by ASTRA, and temperature profiles from ASTRA needed by ACCOME. We concentrated on the operating regime I_p = 0.2 MA and B_T = 1.2 T with the main results shown in Table 2.1, but we were also interested in main features of operating regime I_p = 0.35 MA and B_T = 2.1 T , shown in Table 2.2.

Auxiliary heating and current drive operation are eamined in the two basic COMPASS-D single-null magnetic equilibrium configurations: SND (low triangularity Δ ≈ 0.3 - 0.4) and SNT (high triangularity Δ ≈ 0.5 - 0.7). Tables 2.1-2.2 then give a basic idea of the differences entailed by operating in SND and SNT, respectively, with different NBI and LH configurations.

Table 2.1: B_T = 1.2 T, absorbed powers, driven currents and peak temperatures

equilibrium	P_{NB} [kW]	P_{LH} [kW]	I_{NB} [kA]	I_{LH} [kA]	T_{e0} [keV]	T_{i0} [keV]
Ohmic base case	0	0	0	0	0.81	0.25
SND	0	94	0	59.4	1.00	0.25
SND on-axis	508	0	48.0	0	1.71	3.73
SND on-axis	505	122	79.8	45.6	1.80	4.29
SND off-axis	430	87	53.6	39.1	1.04	0.62
SNT on-axis	506	0	72.6	0	1.24	2.42
SNT on-axis	507	181	83.0	53.0	1.10	2.05
SNT off-axis	416	71	50.0	33.0	1.10	0.47

Table 2.2: Comparison of B_T = 1.2 T and B_T = 2.1 T results (for information only)
B_T = 1.2 T: B = 1.2 T, I_p = 0.2 MA; B_T = 2.1 T: B = 2.1 T, I_p = 0.35 MA

equilibrium	P_{NB} [kW]	P_{LH} [kW]	I_{NB} [kA]	I_{LH} [kA]	T_{e0} [keV]	T_{i0} [keV]
SND on-axis B_T = 1.2 T	505	122	80.0	45.6	1.80	4.29
SNT on-axis B_T = 1.2 T	505	181	83.0	53.0	1.10	2.05
SND on-axis B_T = 2.1 T	519	120	83.7	101	2.10	4.60
SNT on-axis B_T = 2.1 T	514	195	82	1.39	1.88	3.66

All of the results in Tables 2.1-2.2 are obtained at peak density $n_0 = 3\times10^{19}$ m^{-3}. The density profile was prescribed in form

$$n(r) = n_0[(1-n_b)(1-\rho^2)^{1.5} + n_b], \qquad (1)$$

where n_b is the plasma edge density, ρ is a normalized equivalent radial coordinate (square root of toroidal flux), and the exponents 2 and 1.5 were selected to approximate the density profile of previous COMPASS-D auxiliary heating experiments. We immediately note that the magnetic equilibrium (SND versus SNT) has an effect on LHCD and heating. LH wave absorption is sensitive to the magnetic equilibrium because of the higher degree of poloidal asymmetry associated with SNT. More poloidal asymmetry entails larger changes in the LH slow wave refractive index $n_{//}$ during its propagation around the torus, since $n_{//}$ is not conserved [4]. The toroidal evolution of $n_{//}$ influences LH wave absorption via the electron Landau damping condition $n_{//}T_{[keV]}^{1/2} \geq 7$. Hence, in the low-temperature COMPASS-D situation it is essential that the launched value $n_{//} = 2.1$ upshift sufficiently for absorption to occur. The operating regime I_p = 0.2 MA and B_T = 1.2 T in unfavorable to LHCD in the first place because of poor LH slow wave accessibility at these conditions. This is clear from the accessibility diagram, Fig. 2.1.

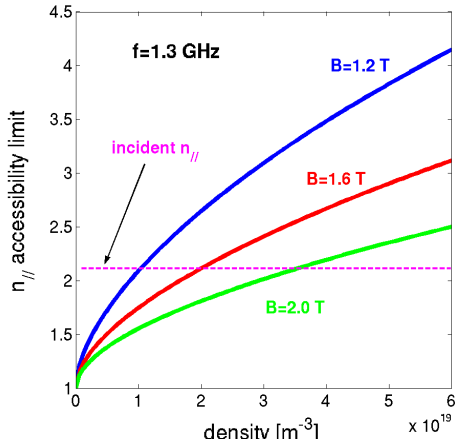

$$n_{//} \geq n_{//acc} = \frac{\omega_{pe}}{\omega_{ce}} + \sqrt{K_\perp}$$

$$K_\perp = 1 + \left(\frac{\omega_{pe}}{\omega_{ce}}\right)^2 - \frac{\overline{\omega}_{pi}^2}{\omega^2}$$

Fig. 2.1: LH slow wave accessibility (i.e. the condition for avoiding mode conversion from LH slow to fast wave) as a function of peak density and toroidal magnetic field.

In contrast, in the operating regime with B_T = 2.1 T we can expect much better LHCD operation, and this is indeed borne out by the ray-tracing diagrams of Figs. 2.2 a,b.

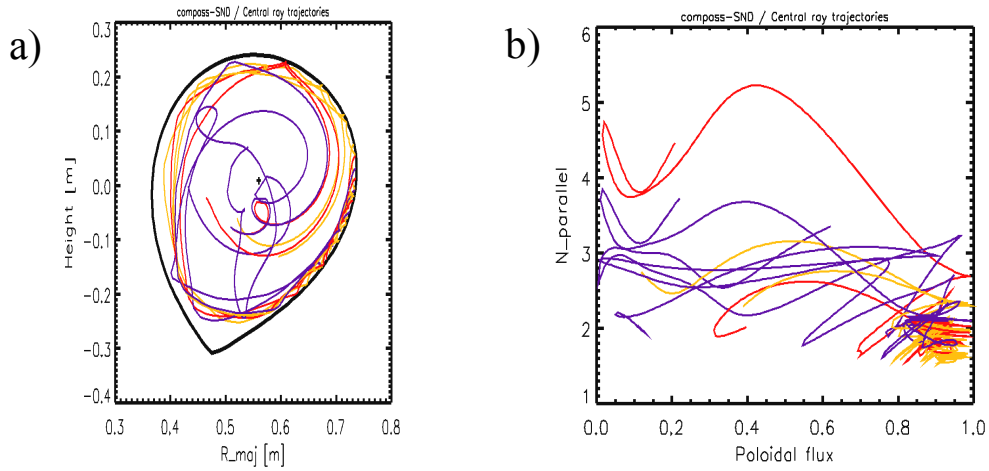

Fig. 2.2: a) Ray trajectories in poloidal plane and
b) $n_{//}$ evolution for I_p = 0.35 MA, B_T = 2 T (for information only)

SUMMARY OF RESULTS FROM ACCOME-ASTRA SIMULATIONS OF COMPASS-D

- Ion and electron heating from NBI depends sensitively on the NB power deposition profile because of very high NB power density
- T_e and T_i depend on NB co- or counter-injection
- Strong ion heating observed for on-axis co-NBI (T_{i0} » 2 keV)
- χ_i/χ_{neo} ~ 2 - 2.5 in regimes with strong central ion heating
- Weak ion heating but reversed shear observed for off-axis NBI
- LH absorption is weak because of poor slow LH wave accessibility
- LH electron heating depends sensitively on $T_e(r)$ and equilibrium
- The SNT equilibrium is more favorable to LHCD and heating than is SND because SNT has more poloidal asymmetry which leads to larger $n_{//}$ upshifts

References:

[1] K. Tani, M. Azumi, and R. S. Devoto, J. Comput. Phys. **98** (1992) 332.

[2] G. V. Pereverzev and P. N. Yushmanov, *"ASTRA – Automated System for Transport Analysis*", IPP Garching report IPP 5/98, February 2002.

[3] John Wesson, "*Tokamaks*", Third Edition, Clarendon Press – Oxford, 2004, p.377.

[4] P. T. Bonoli and E. Ott, Phys. Fluids **25** (1982) 359.

3. Scientific and Technological Programme

3.1. Introduction

The uniqueness of the contribution of COMPASS-D will originate from the fact that this is one of the most accessible and economically operating experiments that can produce H-mode plasmas. Therefore, the emphasis will be on topics which can be studied in the proper plasma regime, yet with a combination of diagnostics which is not available or not feasible in other experiments.

The scientific and technological programme should benefit mainly from the following characteristic features of the COMPASS-D tokamak:

- ITER-like geometry with a single-null-divertor (SND) magnetic configuration
- Tokamak with a clear H-mode
- Neutral beam injection heating system
- Unique set of saddle coils for the resonant magnetic perturbation
- Lower hybrid wave system

In order to reach plasma conditions relevant to ITER, the plasma performance will be improved by installation of a Neutral Beam Injection (NBI) system for an additional ion heating (see Chapters 2 and 5.1). The COMPASS-D tokamak with considerably enhanced diagnostic systems focused on the plasma edge will then be an ideal device for H-mode studies. Very useful for these studies will be the data obtained in the NBI heated ELMy H-mode. The NBI system will consist of two injectors enabling both the co- and counter-injection. These unique features will allow study of the impact of the external momentum input and NBI-driven current on plasma performance. In addition, COMPASS-D will be particularly useful in benchmarking plasma modelling codes.

Material aspects are of increasing importance in fusion research. COMPASS-D assessing the role of different can also serve as a test bed for new materials developed to sustain the hostile hot plasma environment. Samples produced by plasma spraying and other techniques will be exposed to the plasma and analysed ex-situ by sophisticated techniques available in IPP (Dept. of material engineering).

The installed Lower Hybrid Wave (LHW) system will enable to study topics related to the interaction of LH waves with the edge plasma, which are crucial for the eventual installation of the LH system on ITER. Following the recommenadation of the AHG, the LH studies will have a lower priority due to the reduced accessibility of LH wave at the lower magnetic field (Bt = 1.2 T). Nevertheless, these studies can bring new insight into the interaction of the LH slow wave with the edge tokamak plasma. Specifically, the LH wave generates fast electrons in front of the grill and consequently “hot spots” of high thermal loads at locations magnetically connected to the grill mouth have been observed in LHCD experiments on the Tore Supra and JET tokamaks. The local generation of fast electrons results in a chain of other nonlinear processes, which modify the plasma density in front of the grill and consequently also

the LH wave-plasma coupling. These processes are not fully understood yet, and they call for further exploration. The COMPASS-D tokamak equipped with appropriate diagnostics (high spatial and temporal resolution) will be an ideal device for the study of these effects in detail.

Therefore, the specific topics of the scientific programme for the COMPASS-D at the IPP.CR are:

1. Edge plasma physics
    a. H-mode studies
    b. Plasma-wall interaction
2. Wave-plasma interaction studies
    a. Parasitic lower hybrid wave absorption in front of the antenna
    b. Lower hybrid wave coupling

3.2. Edge plasma physics

3.2.1. H-mode studies

There is still considerable uncertainty to the appropriate scaling for the pedestal width, in particular whether it is entirely determined by the plasma physics (implying that the dimensionless parameters ν^*, ρ^* and β are important) or whether such processes as neutral penetration play a role. Since experiments in COMPASS-scale devices have been typically performed using ohmic or electron heating (eg COMPASS-D, TCV), or may have been affected by other factors (eg TF ripple in JFT-2M), NBI-heated experiments in COMPASS-D should constitute an extension of the present database in ν^* and ρ^* and could therefore provide additional insight into the scaling and physics processes determining of the H-mode pedestal width. This is particularly so since it is planned to have a detailed edge diagnostic capability in COMPASS-D. The difference in neutral penetration depth relative to larger, hotter tokamaks may also help to clarify the role of neutrals, if any, in determining the pedestal width.

Apart from studies of ELMs and the H-mode transition (see comments below), one such topic which combines the expertise of the IPP team and the particular possibilities of COMPASS-D can be detailed measurements of edge transport in the regime of electromagnetic drift waves, including the transition from (cold plasma) resistive ballooning to drift-Alfven wave turbulence. The experience at IPP with Langmuir probe measurements of potential fluctuations, with additional high resolution (imaging) diagnostics can lead to new insight into edge transport mechanisms and a direct comparison with turbulence modelling.

Very important edge problems for ITER are ELM physics and ELM control. The COMPASS-D tokamak used to be the smallest machine with good H-modes (depending though on good conditioning). The threshold for L-H transition was achieved and ELM-free and Type III ELMy (both OH and ECRH) discharges were attained in the COMPASS–D tokamak at Culham, UK.

For the moment it is not obvious whether the currently most desirable Type I ELM regime can be achieved in COMPASS-D even with a new neutral beam system. Based

on observations from tokamaks in the AUG through JET, to have "clean" Type I ELMs one needs at least 1.3 - 1.8*$P_{th\_L/H}$ ($P_{th\_L/H}$ = 150 kW for B_T = 1.2 T) depending on plasma shaping), which is well covered by the installed NBI power of 600 kW.

However, Type I ELMS were not observed on COMPASS-D even with 1 MW of ECRH power. This could mean that at present there is no physics basis for expecting the quoted threshold to hold at the COMPASS scale. Previous results from devices such as COMPASS-D and TCV may not be relevant to this discussion, since they are either ohmically heated or electron heated – and it is known that electron heated devices can have more difficulty accessing good Type I H-modes, since they typically have to work at lower density (to ensure access for ECRH), and it is known that the H-mode power threshold scaling turns up at low densities, possibly because of the decoupling of electrons from ions. Therefore, if COMPASS does not access good Type I H-modes with 600kW of NBI power, then this tells something fundamental about the scaling of the H-mode power threshold (namely, that (i) there is even more about the physics of the access to the H-mode that we do not understand and (ii) one needs to be careful about the use of the H-mode power threshold scaling derived from the multi-machine database, since the evidence from COMPASS would be that the physics is different at the COMPASS scale and/ or parameters). This assumes, of course, that one takes the normal precautions, including vessel conditioning, which are used on larger devices. In this respect, COMPASS could represent a valuable test of our understanding of H-mode access physics. This would be particularly valuable when combined with the very good edge and pedestal diagnostics.

Furthermore, even if Type I ELMs are not achieved, the Type-III ELMs regimes can be studied since, at high collisionality, they exhibit similar ballooning (resistive modes however) features as Type I ELMs. As an example one can mention ELM studies on MAST where many relevant results were obtained for Type III regimes. All dynamics, space structure, turbulence during ELMs, changes of the electric field and rotation during ELMs near the separatrix etc. have a lot of common features with Type I regimes. With good diagnostics, the future COMPASS-D studies in Prague could substantially contribute to ELM physics.

Since COMPASS-D will focus on this area, the planned edge and pedestal diagnostics could yield a great deal of detailed information on the phenomena associated with ELMs.

High-collisionality high-confinement regimes without ELMs as EDA, “grassy” ELMs, Type II regimes can also possibly be obtained on COMPASS-D. An operation with higher triangularity and double-null configuration will be also enabled.

The ability to make a controlled transition from a single null to a double null configuration in COMPASS will extend the database which is being developed in this area by MAST and DIII-D. Once again the combination with good edge and pedestal diagnostics would be invaluable.

For the study of edge stability or ELMs, a major requirement is the reconstruction of the plasma equilibrium including meaningful experimental constraints on the edge pressure gradient and edge current density. Therefore, the key for new contributions to this field is diagnostics that removes measurement uncertainties, which have been the limiting factor in such studies in all previous experiments. This implies high resolution measurements of the edge pressure profile, i.e. electron and ion

temperatures and densities, and attempts to measure the edge current (total or even profile) directly.

All attempts will be made to obtain the best possible radial resolution in the gradient region which in COMPASS-D is only about 1-2 centimeter wide. The key diagnostics are the following:

- **Thomson scattering system** – 1-2 mm spatial resolution in the gradient region should be achieved by a flux-surface tangential laser ray path near the plasma edge.
- **Charge exchange spectroscopy measurements** - ion temperature, density and toroidal and poloidal rotation will be measured by the Li beam technique. There exists a possibility to measure the above mentioned quantities by one of the hydrogen (or deuterium) heating beams of a suitable energy injected radially for this purpose. An effort will be put also into a flexible design of the NBI system to enable such a solution, but primarily we have in mind using both NBI systems for plasma heating and momentum injection.
- **Electric probes** – various arrays of Langmuir probes placed at different positions with high spatial and temporal resolution (2 MHz, ~ 1 mm) will be used to characterize the scrape-off layer and the pedestal region. Arrays of oriented probes (Mach and Gundestrup probes) will enable detailed measurement of flows in the edge plasma.

With the described installed diagnostics, there are several topics which will be studied:

- Detailed studies of the H-mode transition with a combination of profile and fluctuation measurements aiming to identify the relevant driving mechanisms for ExB spin-up and turbulence suppression. One possible question to address with a combination of the probe arrays and plasma rotation measurements is whether or not a turbulence-generated rotation spin-up (Reynolds stress) can account for the rotational shear observed before and at the transition.
- Modelling is advancing from the description of linear stability towards the non-linear evolution of the ELM instability. With sufficient time resolution and a suitable combination of diagnostics, the initial ELM growth from a more or less coherent precursor mode into the usually observed broad spectrum would be helpful to guide the development of ELM models.
- Plasma rotation and edge stability - two NBI systems, each 300 kW, will be flexible to produce co- and counter- injection to generate different regimes of toroidal plasma rotation. It will be also possible to arrange the injection of both systems in the same direction if required. This possibility is important to study the influence of the plasma rotation on the pedestal stability, ELMs and external (error) fields penetration. The rotation predicted for ITER is small, so these studies can be very ITER relevant. Also the access to ELM-free QH mode (and may be also low ν^* due to the particle losses in QH mode) will be tried.
- COMPASS-D is an ideal device for detailed studies of the open issues of plasma turbulence and transport. The main aim of such studies is to build up a systematic and as detailed as possible *fluctuation database* in order to improve our understanding of anomalous transport scaling, transport barrier dynamics

(shear flow generation) and turbulent electric field bifurcations (in collaboration with Association EURATOM/HAS).

The following key scientific problems will be addressed:

a) Bohm versus gyro-Bohm scaling and the transition between the two regimes
b) Transport barrier formation and dynamics including the different transport channels
c) Statistics of mesoscale intermittency in transport (e.g., avalanches, Self-Organized Criticality)
d) The dynamics of transport perturbation events such as heat pulse propagation

- Modifying the edge current profile could have a positive effect on ELMs control since the stability regimes depend strongly on the current density profile. In addition to possibly modifying the current density profile by current ramp-up (-down), some modification might be expected from applying LH power However, the edge effect of LHCD in COMPASS-D has to be first studied by simulations. On other hand, LHCD edge modification in ITER can be seen to be relevant because of the high pedestal temperatures (4-6keV) permitting more edge localized electron Landau damping and current generation by an LH system.

Resonant magnetic perturbation (RMP) technique

Existing perturbation coils are a unique capability of the COMPASS-D tokamak. Even though a lot of work on this topic has been done in UKAEA, a lot more can be done, especially in combination with the NBI system and its ability to change plasma rotation.

- **Error field studies** - the thresholds found on COMPASS-D did not fit the scaling of some of the larger devices, and this and other uncertainties may be significant for ITER. A focussed experimental programme on COMPASS-D, making use of the saddle coil set and the additional capability for momentum injection with NBI (not previously available in COMPASS-D) could contribute, together with experiments in C-Mod, DIII-D and JET, to the development of an improved understanding of error field physics and to the preparation of the techniques necessary for error field correction in ITER.
- **ELM control by external coils.** An interesting ITER relevant issue is ELM control by external magnetic perturbation. The idea was pioneered on COMPASS-D. Perturbations with the toroidal numbers n=1, n=2 can be generated. Usually low n=1 can trigger core MHD and confinement degradation. But for n > 1 one can obtain edge ergodisation in order to control edge transport and ELMs like in DIII-D experiment. The results could be used to scale and understand such control systems also for ITER.

  Similarly, the DED experiments on TEXTOR in m/n = 6/2 and 12/4 show the possibility to influence only the plasma edge. Moreover, recent results on TEXTOR show that even the 3/1 base mode may not excite the tearing mode when driven by AC current (1 kHz). Therefore, the possibility to drive the saddle coils on COMPASS–D with AC currents will be assessed. This would

provide one more degree of freedom for experiments.

This topic is ITER relevant, since ITER might have the external coils as well but only those with low mode numbers and therefore with a mode spectrum which will easily excite tearing modes. It is of course unclear now whether it would allow AC operation.

This area of plasma control is being developed and the capability of COMPASS to explore various mode structures for the applied field could make a significant contribution to the understanding of how external coils can be exploited to control ELMs.

The tools to calculate the possible field perturbations have to be exploited in parallel with experiments. There is a suite of codes developed by UKAEA, but they have to be adapted and interfaced to a field-line following code for some studies. At TEXTOR, there is also a high experience on field line mapping in order to visualize the ergodic properties imposed by the external field as well as the laminar zones.

3.2.2. Plasma-wall interaction

Samples of advanced first-wall materials (produced mainly by plasma spraying techniques in IPP.CR), will be exposed to the plasma and the mutual interaction will be studied. This involves the effects of plasma discharge on the materials (sputtering, melting, evaporation, deposition, ion implantation) as well as materials' effects on the discharge (mainly through particle release). Methods of examination of such material surfaces, both in-situ (spectroscopy of impurity radiation, miniature tunnel microscope) and ex-situ (metallography, electron microscopy, phase and compositional analyses) will be developed and applied by the IPP.CR (Department of Material Engineering). The following studies are envisaged:

- **erosion studies on plasma exposed materials**
  To get sufficient particle (or thermal fluxes), the test sample will be exposed in a position in the divertor strike zone. A specialized manipulator which will allow a relatively easy sample exchange will be developed and used.
  Alternatively the samples might be exposed on the reciprocating drive provided by UKAEA together with COMPASS-D which could be inserted rapidly inside the separatrix.

- **re-deposition of eroded material and impurity migration**
  Re-deposition of eroded wall species on plasma facing components and impurity migration in magnetic confinement experiments will be studied. In these tests, emphasis will be laid on the type of the re-deposited coatings such as structure, composition, hydrogen content etc.

  To perform these tests, a manipulator will be used to insert collector probes into the vacuum vessel.

- **removal of re-deposited layers**
  This will be done using one or more of the following options:
  - by the plasma itself (e.g. on test samples in the divertor strike zone using a manipulator)
  - by oxygen (complementary to similar experiments in TEXTOR or ASDEX-U)

- using flash lamps or laser beams (e.g. using high-power iodine laser PALS in IPP Prague to perform systematic ex-situ studies on the thermal erosion of re-deposited film generated in COMPASS-D)

- **melt layer motion in tokamaks under the influence of magnetic fields**
  Thin films (e.g. metallic films on a graphite substrate) or low melting point materials (e.g. aluminium) will be used to mimic beryllium or other first wall materials. The high Z or high-melting point material samples will be pre-heated to guarantee surface melting during the exposure to the plasma.

All the special manipulators will be supplied by IPP Prague and manufactured in the institute workshop.

3.3. Wave - plasma interaction studies

This research theme represents an evident extension of the experiments performed at COMPASS-D in the course of its UKAEA operation. The IPP.CR CASTOR team has acquired substantial experimental and theoretical expertise in this area from studies on CASTOR and collaborations on the TORE-Supra, MAST, NSTX and JET tokamaks in Lower-hybrid current drive, electron cyclotron and EBW heating and current drive.

Non-inductive generation of a tokamak plasma current using the lower hybrid slow wave is an attractive tool for control of the tokamak current density profile for the purpose of advanced operation scenarios with plasma edge or internal transport barriers for improved energy and/or particle confinement. For example, high LH power long-term operation has been successfully demonstrated on the Tore Supra tokamak and LH - supported internal transport barriers have been demonstrated on the JET tokamak.

Since the validation of LH physics is of high importance for the possible incorporation of LH systems in ITER, research contribution of COMPASS in this area should be of high interest since the COMPASS-D and JET tokamaks are the only devices with X-point divertor and LH system.

In the COMPASS-D tokamak the wave launching system with 8 wave-guides at 1.3 GHz was utilized. A number of experiments were carried out, notably plasma current and MHD activity control, and transition from the electron to the ion heating regime. The complete LH system (antenna, wave-guides, klystrons) will be taken over by IPP Prague. We plan to focus mainly on the topics connected with the antenna - edge plasma interaction such as parasitic LH wave absorption in front of the antenna and the study of LH wave coupling.

3.3.1. Parasitic lower hybrid wave absorption in front of the antenna

Main cooperation: Associations CEA and Tekes and JET

Fast electrons and ions can be produced in a several millimeter thin layer just in front of a lower hybrid (LH) wave-guide grill by the electric field of the slow LH wave in combination with random fields (fluctuations). As documented in Tore Supra, these energetic particles may cause high thermal loads (up to about 20 MW/m^2) and subsequent erosion observed on parts of the grill and other elements of the first wall.

For long and high power LH pulses envisaged for ITER, these high thermal loads could become a real problem, even if advanced launchers like Passive-Active Multijunction grill are used. We note explicitly that this problem is ITER relevant.

It is difficult to estimate in advance the mean energy of the locally generated fast particles and the intensity of the fast particles beam. The acceleration process depends on many parameters, such as the electric field intensity in front of the LH grill, the plasma density and its gradient in front of the grill, but it also depends on the details of the LH wave k-spectra, which in turn may be connected to some details of the wave-guide septa (e.g., rounding) and grill construction. It can further depend on the fluctuation level in front of the grill (random fields), and on the level of plasma sources (ionisation by the LH wave), etc. Hence, the task will be to explore the parameters of the fast particles beam, like its energy and its energy distribution, as a function of the plasma parameters and of the launched LH wave parameters. The LH wave frequency and its power density (electric field intensity) is similar to those used in the CASTOR tokamak, where the fast particle beam parameters were successfully explored, e.g., by Langmuir probes. The measurements of the fast particle beam will then form a basis for a better understanding of the nonlinear processes (hot spots, local ionisation) arising due to the local fast particle generation.

It is therefore proposed to study fast electron and ion production, and related non-linear effects just in front of the grill mouth of COMPASS-D. For the diagnostics of the fast particles, and of the random fluctuating fields, we envisage the use of electric and RF probes, magnetically connected to a region in front of the grill and mounted on the reciprocating manipulator (supplied by UKAEA). Further, a Retarding Field Analyzer (RFA) could be optionally exploited to measure the distribution function of accelerated particles, as is done in Tore Supra.

3.3.2. Lower hybrid wave coupling

Main cooperation: Associations CEA, Tekes, and Hellenic Republic and JET

The LH wave coupling represents a crucial problem for the implementation of LH system in ITER. We plan to focus on the following topics:

- **Lower hybrid wave coupling in detached plasmas -** The LH antenna on ITER would be located rather far away from the separatrix, being hidden deeply inside the SOL, therefore the coupling of the antenna with the plasma would be poor. Hence, it is necessary to develop tools to improve LH wave coupling in low density SOL plasmas. For this, gas injectors are used near the grill at JET, to increase the density in front of the grill. However, the mechanism of the underlying physics is not clear up to now and it needs further experimental exploration.

  It is therefore proposed to study the LH wave coupling in cases where the grill is rather far from the plasma, and to find ways how to improve it, e.g. by gas puffing. This system is already available in IPP Prague. The underlying physics of the gas ionization by LH waves will be studied in a broad European collaboration (Associations Tekes, CEA Cadarache). We note explicitly that this problem is ITER relevant.

  These studies will be supported by adequate numerical modelling in IPP Prague.

- **The LH coupling during the ELMy H-mode** is another important issue for possible implementation of a LH system in ITER. The transient changes of the plasma density in front of the grill cause the interruptions in LH coupling. Tools for the feedback density control in front of the grill are sought and COMPASS-D offers a unique possibility to study these mechanisms (together with JET).

  To control the plasma density in front of the grill during the ELMs, the biasing of the protecting limiters of the LH grill is envisaged to control the density profiles via ExB flows (see experiments performed on TEXTOR).

  The mechanism will be studied in details using numerical modelling before designing the experiment (in IPP Prague in collaboration with CEA).

4. Diagnostics

In this chapter, a comprehensive set of the diagnostics required to achieve goals of the scientific program is introduced. Selected diagnostics are discussed in more details. Additionally, the ex-situ plasma-wall interaction diagnostics shared with the Department of Material Engineering of IPP Prague is summarized.

4.1 Overview of diagnostics

The diagnostics necessary to meet the milestones in the scientific and technology program are summarized in Table 4.1.

	PLASMA DIAGNOSTICS	AVAILABILITY	SUPPLIER COOPERATION
STEP I	Magnetic diagnostics (*)	COMPASS-D	UKAEA+IPP.CR
	Microwave interferometer (*)	COMPASS-D	UKAEA+IPP.CR
	D_α and Z_{eff} measurement (*)	CASTOR + upgrade	IPP.CR+Budker Inst. Novosibirsk
	Fast camera for visible range (*)	not existing	HAS
	Thomson scattering	not existing	IPP.CR+FOM
	Fast bolometers	CASTOR	IPP.CR
	SXR – array of diodes	COMPASS-D	UKAEA+IPP.CR
	Neutral particle analyzer	COMPASS-D	UKAEA
	VUV and XUV spectrometers	CASTOR	IPP.CR + BI Novosibirsk
	Langmuir probes	COMPASS-D	IPP.CR+UKAEA
STEP II	Beam diagnostics	not existing	HAS
	Microwave reflectometry	not existing	IPP.CR+IST
	PWI ex-situ diagnostics	IPP.CR	IPP.CR

Table 4.1: Summary of the diagnostics to be installed on COMPASS-D and its availibility/suppliers. Blue colour represents new or considerably improved diagnostic systems not installed on COMPASS-D during its operation in UKAEA.

The distribution of individual diagnostics over the exisiting ports of the COMPASS vessel is indicated in Fig. 4.1. The beam-lines of the NBI's are schematically marked by yellow colour.

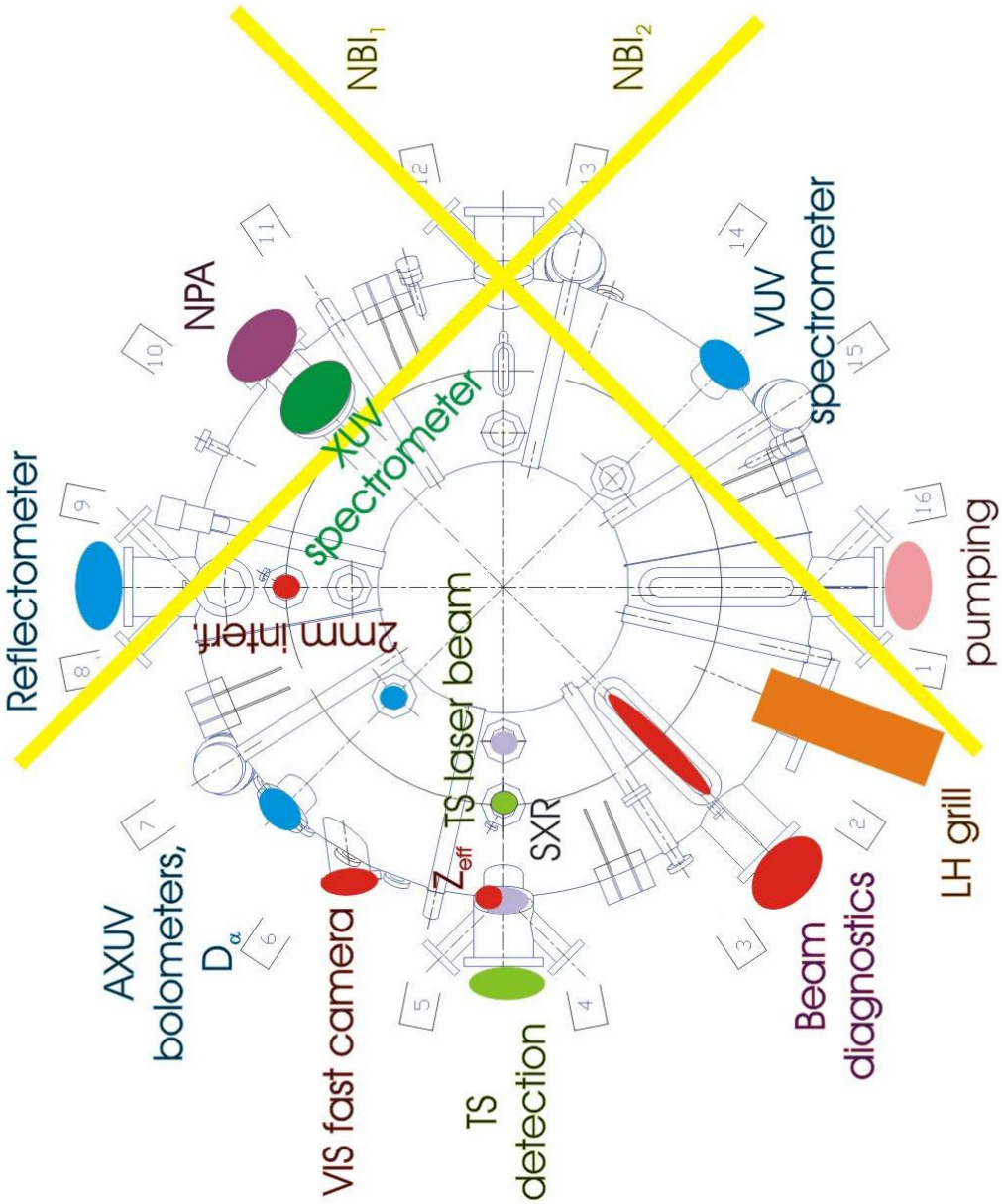

Fig. 4.1: Diagnostics overview

4.2. Description of the diagnostic systems

a) MAGNETIC DIAGNOSTICS

Magnetic diagnostic is a key diagnostic system for machine operation and protection as well as for its scientific exploitation.

The overview of the COMPASS magnetic diagnostic sub-systems including the number of sensors and the target quantity to be measured is given in Table 4.2.

Name of the coils	Number of coils	Measure
Full toroidal loops	8	loop voltage and poloidal flux (used for real time cotrol and EFIT)
Saddle loops-4x22	88	the difference in poloidal flux (used for real time cotrol and EFIT)
Saddle loops- 2x8	16	loop voltage and poloidal flux, not used routinelly (used for some neural network studies)
Remote loops	5	loop voltage and poloidal flux, not used routinelly (used for some neural network studies)
External Partial Rogowski coils	16	local magnetic field parallel to a vacuum vessel, eddy currents
Full Rogowski coils	1	plasma current
Diamagnetic Rogowski coil	1	toroidal field current
Diamagnetic loops	2	perpendicular beta
Diamag. compensation loops	2	toroidal field
Mirnov coils-3x24x3	216	local poloidal, radial and toroidal fields (hence 3 times), 24 at one cross section
High n Mirnov coils	4	n-number of MHD instabilities
Divertor Mirnov coils	16	coils imbeded in divertor plates (used for ELMs study)
Full Rogowski coils	1	plasma current
Internal Partial Rogowski coils	16	local magnetic field parallel to a vacuum vessel (used for poloidal current density distribution, real time cotrol and EFIT)
IN TOTAL	392	coils

Table 4.2: Overview of the magnetic coils and their location with respect to the vessel. Green colour indicates the sensors located out of the vessel, yellow colour corresponds to the in-vessel sensors.

In addition, the Hall sensors will be tested on COMPASS-D as a novel approach for measuring magnetic fields with respect to its potential implementation on ITER. This activity will be performed in close collaboration with Magnetic Sensor Laboratory, Lviv University, Ukraine.

The position of individual magnetic sensors with respect to the vacuum vessel is schematically indicated in Fig. 4.2.

Positioning of the Mirnov triplets and Partial Rogowski coils with respect to the COMPASS vessel is displayed in Fig. 4.3. The triplets of 24 Mirnov coil surround the whole poloidal cross-section at three toroidal positions. Every triplet is composed of three coils oriented in the radial, poloidal and toroidal direction.

A complex system of the saddle loops, covering the whole surface of the vacuum vessel is shown in Fig. 4.4 together with eight full toroidal loops.

The exact location of any magnetic sensor can be found in [1].

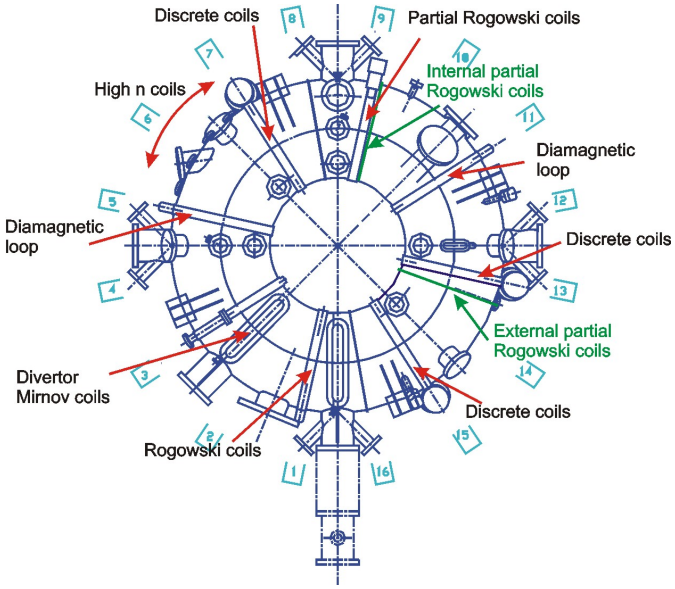

Fig. 4.2: Distribution of the magnetic sensors around the vessel

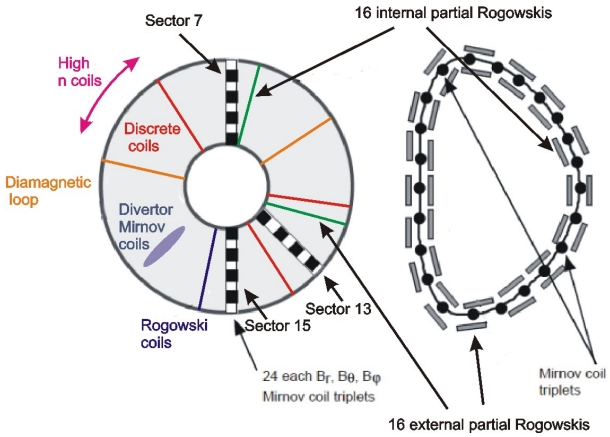

Fig. 4.3: Toroidal and poloidal distribution of the Mirnov coils and Rogowski coils [2]

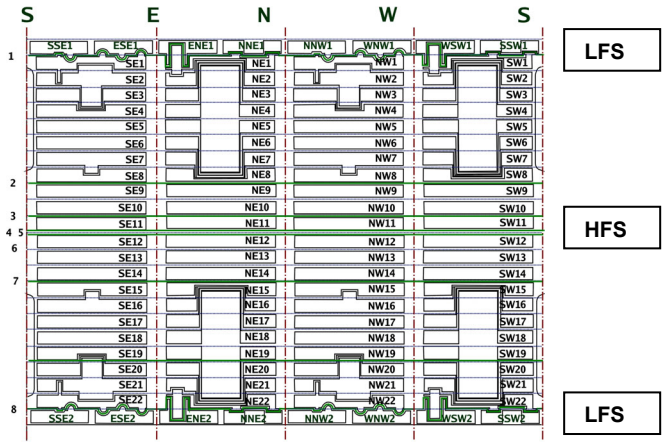

Fig. 4.4: Planar view of the full toroidal loops (8 green lines) and saddle loops (black lines). The symbol N denotes the toroidal position between sectors 8 and 9.

References:

[1] P.Knight, G.Castle, A.W.Morris, Nucl. Fusion 40 (2000) 325

[2] M. Valovic, Magnetic Diagnostics on COMPASS-D, Training course, Sept 1997

b) MICROWAVE INTERFEROMETER

Temporally resolved density measurements are based on two independent microwave interferometer systems at the wavelengths $\lambda = 2$ and 1 mm.

Single-channel interferometer at $\lambda = 2$ mm (Step 1 diagnostics)
The 2-mm interferometer was originally used on COMPASS-D to measure the line average

density over the central chord. The complete system will be transported to IPP Prague.

The system is composed of two conventional heterodyne interferometers, working at slightly different frequencies 131 and 133 GHz (two colour interferometer), which provide reliable measurement of the line-averaged density up to $1*10^{20}m^{-3}$ (almost the Greenwald limit).

c) D_α AND Z_{eff} MEASUREMENT

D_α monitors (Step 1 diagnostic)

The D_α spectral line (656.1 nm) intensity along several chords will be monitored to get information on the recycling at high and low field sides of the torus and in the divertor region. If the absolute calibration of the detection system is performed, the density of neutral atoms can be determined and the particle confinement time can be estimated. Moreover, the transition to the H-mode can be identified. A high temporal resolution, 1 μs, will be essential for ELM studies.

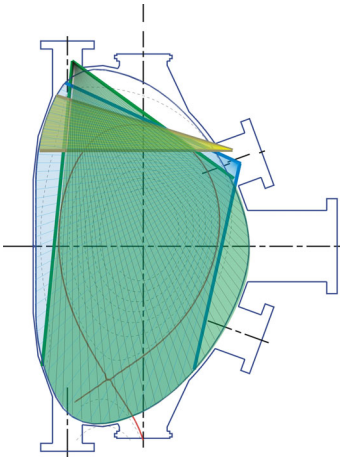

The proposed multi-chord detection system consists of 2 arrays of silicon diodes (45 elements each) covered by the interference filters (D_α spectral line, FWHM ~ 10 nm) viewing the plasma cross-section vertically and horizontally as sheen in Fig. 4.5. The spatial resolution is of about 10 mm at the midplane. The third array views the upper pedestal region with a better spatial resolution of a few millimetres. The system will be absolutely calibrated.

Fig. 4.5: Positioning of three arrays for monitoring of D_α line radiation.

Z_{eff} monitor

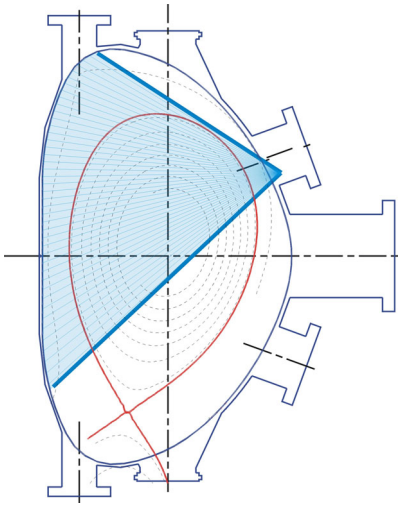

The effective ion charge Z_{eff} is a parameter containing summary information on impurity contamination of plasma.
On COMPASS, the Z_{eff} profile will be calculated from the absolute measurement of the selected line-free region by a diode array (45 elements) equipped with an interference filter (536.0 ± 1.5 nm (as on ALCATOR) or 523.5 ± 1.0 nm (as on JIPP T-IIU).

Fig. 4.6: Position of the array for Z_{eff} measurements (the toroidal section between the sectors 4 and 5).

d) FAST CAMERA FOR VISIBLE RANGE

Physics of anomalous particle/energy transport at the tokamak plasma periphery can be studied in detail using spectroscopic tools with sufficient temporal and spatial resolution. Recent experiments in many tokamaks like TFTR, ASDEX Upgrade, Alcator C-Mod, and DIII-D indicate the possibility of measuring transient phenomena (density fluctuations, ELMs, etc) in the visible range either directly or via gas puff imaging. The fast CCD or CMOS cameras, suitable for such measurements, are available (with about 1-100 kHz frame rates at a resolution of hundreds times hundreds pixels).

Fast digital video cameras for machine control, plasma overview and turbulence measurements are being developed at KFKI RMKI for the W7-X 10-camera video diagnostic system. The Association EURATOM-HAS will provide two cameras with ex-vessel optics and controlling computers with the following approximate capabilities: 1 Mpixel resolution, 500 Hz full-frame, approximately 100 kHz frame rate on a small array (about 16x16 pixels), continuous monitoring of the intensity of predefined image areas and trigger signal generation for machine protection. These could be used e.g. to protect the machine from excessive heat loads on critical areas caused by NBI.

e) THOMSON SCATTERING (Step 1 diagnostics)

The radial profiles of electron density and electron temperature are measured using a Thomson scattering diagnostics. To meet the goals of the COMPASS-D scientific program, measurements of the pedestal plasma parameters with a high spatial resolution is essential. The proposed configuration of TS is shown in Fig. 4.7.

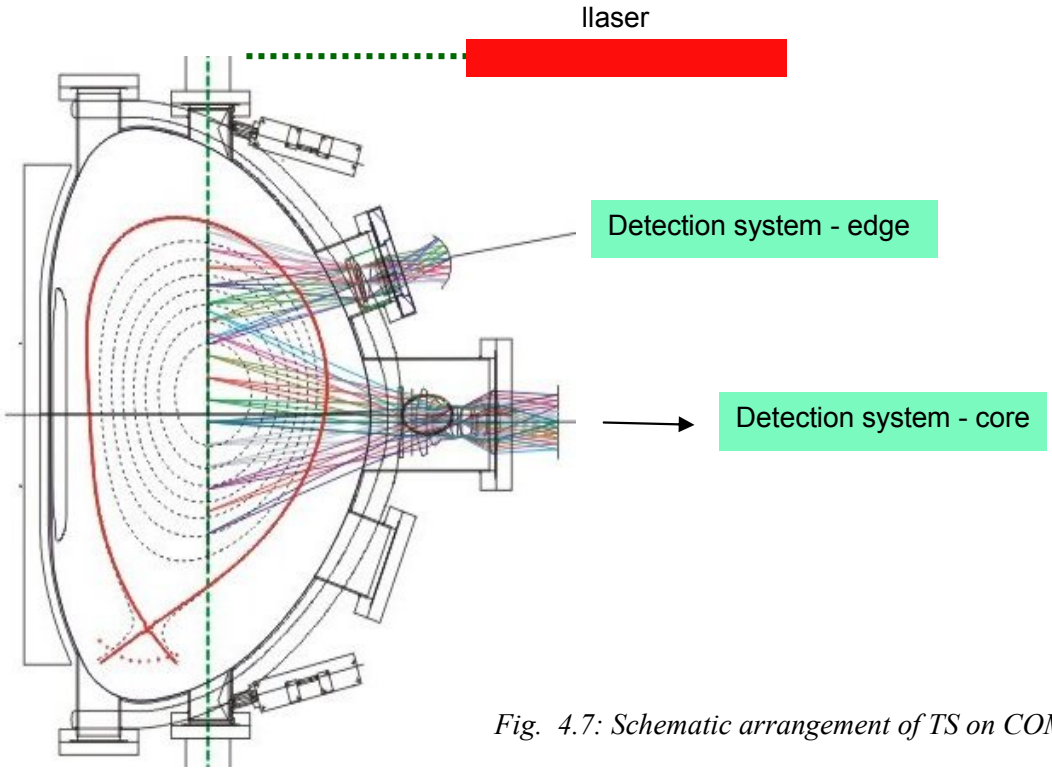

Fig. 4.7: Schematic arrangement of TS on COMPASS-D

The central vertical chord is used for injection of the laser beam and two existing ports for the top edge and central scattered light collection places are considered. Resolution of 1.5 mm (in the direction perpendicular to the B-field surfaces) is required. This configuration is selected, because it corresponds to that already used in Culham.

Edge profiles of T_e and n_e

The calculations for the edge profile measurements, based on the proposed geometry, were performed by Rolie Barth and Hennie van der Meiden, (FOM Rijnhuizen). The number of photoelectrons is summarized in the Table 4.3.

Table 4.3.

Item	symbol	Value	Dimension
chord length	L_S	180	mm
maximum full angle	α_S	0.19	rad
used full angle	α_S	0.11	rad
maximum solid angle	Ω_S	29	msr
used solid angle	Ω_S	10	msr
resolution	ΔL	3	mm
Number of points	N	60	
laser energy	E	10	J
Density		1.0×10^{19}	m^{-3}
Number photoelectrons	N_{pe}	2700	
used etendue		20	mm.rad

The lowest density with observational error of 10% is less than 5×10^{17} m^{-3}. Hence, there is enough reserve in signal which will be partly consumed by a non-ideal transparency of the optical elements, and which can be also partly used for reduction of laser energy. The specifications of the calculations are summarized in Table 4.4.

Table 4.4

Symbol	**Quantity**	**Unit**
E_{laser}	10	J
f_1	0,88	
$h\nu$	$2,86*10^{-19}$	Js
ΔL	$3,0*10^{-3}$	m
Ω	$10,0*10^{-3}$	sr
τ_{overal}	0,15	
$\eta_{intensifier}$	0,27	
σ_T	$7,94*10^{-30}$	m^{-2}
n_e	$0,95*10^{19}$	m^{-3}
f_2	0,9	
N_{pe}	$1,36*10^{2}$	
ε	8,58	%

The equipment required for the TS system on COMPASS at IPP:

Laser –Nd:YAG laser system with repetitive rate 20 Hz and with conversion to the 2nd harmonic

Fiber optics - For imaging of the laser chord onto a fiber array an input full angle at the fiber of f/3 is proposed. Therefore the height of the fiber slit is h = 60 mm, consisting of 60 fibers with 1.0 mm diameter. The corresponding width at the laser beam is about 3 mm. A possibility of installing the detection system directly to the collection window is also considered. The advantage of such an arrangement is lower losses of photons than in the optical fibres.

Camera

- UP-900DS UP-900DS-CL
- SU640SDV-1.7RT, SU640SDV-1.7RT-15Hz High Resolution InGaAs SWIR Area Camera

f) FAST BOLOMETERS

For measurement of total radiation losses and for observation of transient processes (ELMs, turbulent structures), we will use fast, low-noise silicon diodes (λ = 0.2-180 nm) with temporal resolution up to 1 μs will be used. By placing an appropriate filter in front of the detector, a narrower spectral band can be selected.

The COMPASS-D will be equipped with six 20-channel arrays located in the poloidal cross-section between sectors 6 and 7. Four arrays with the spatial resolution about 2 cm will view the whole cross-section, as shown in Fig. 4.8 and the tomographic reconstruction will be available with a high temporal resolution. For a detailed imaging of the selected part of plasma column, namely the pedestal or divertor region, two movable arrays with spatial resolution about few millimetres will be used (green viewing chords in Fig. 4.8). The data acquisition system with sampling frequency 1 MHz for all 120 channels is required. The detectors will be AXUV20-ELM arrays from International Radiation Detectors (IRD, Torrance, Canada). A fast amplifier for each channel will be manufactured at IPP according to the design of Kurchatov Institute.

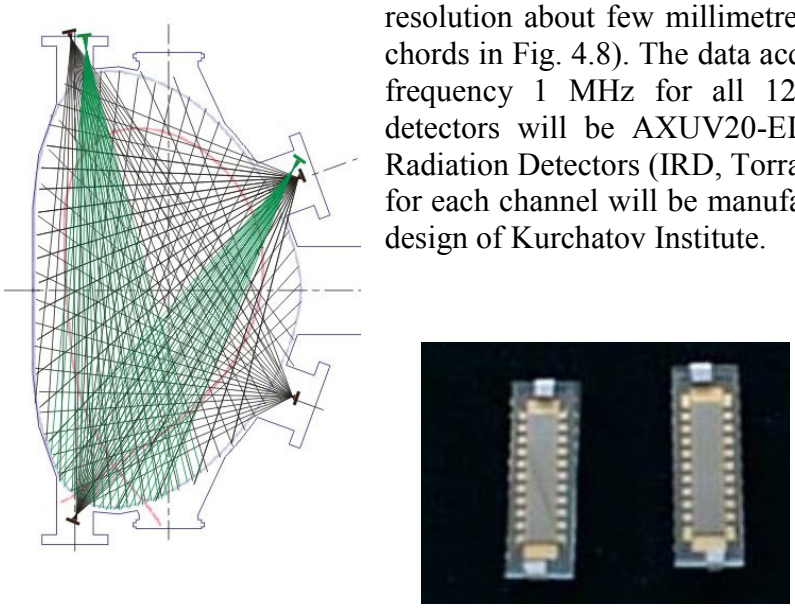

Fig. 4.8: L: Viewing chords of AXUV photodiodes. R: two AXUV20-ELM fast bolometric diodes

g) SXR ARRAYS

Monitoring of soft X-Ray radiation serves as diagnostics of MHD physics. The original SXR arrays on COMPASS-D are configured as shown in Fig. 4.9 and located in the section between the sectors 4 and 5. The system consists of the vertical and horizontal array of Silicon 16+16 diodes covered by the thin Be foils. They reach a spatial resolution of 20 x 20 mm. In addition, one new array will be focused onto a pedestal region. The set-up of this array will be similar to the D_α or AXUV arrays for the same purpose.

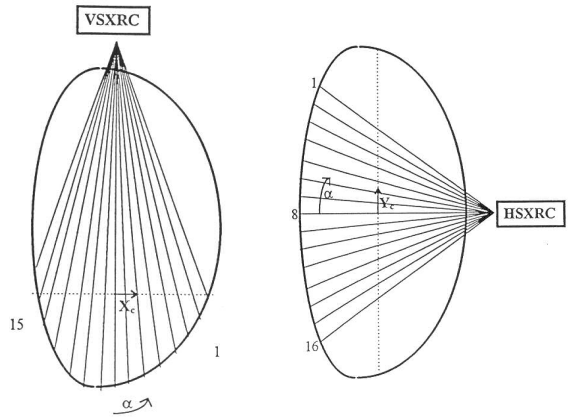

Fig. 4.9: Viewing chords of SXR arrays on COMPASS

h) XUV and VUV SPECTROSCOPY

Line radiation of impurity ions will be monitored using spectrometers in XUV (ultrasoft X-ray) and VUV (vacuum ultraviolet) wavelength ranges with a sufficient temporal and spatial resolution.

Ultra soft X-ray spectrometer

The 4-channel USX spectrometer with the resolution $\lambda/\Delta\lambda \sim 30$ will monitor spectral lines of highly ionised light impurities (B, C, N, O) in the energy range 200-800 eV. The measured radial profiles of K_α and L_α lines of He- and H-like impurities will allow estimating the impurity diffusivity by comparisons with the transport code STRAHL. Such spectrometer, equipped with a synthetic multi-layer mirror, has been designed and built at IPP.CR for the TCV tokamak, and it is available for use on COMPASS-D.

VUV Spectrometer

The VUV spectrometer of the Seya-Namioka type, equipped with a two-dimensional detection system, will provide spatially and spectrally resolved measurements of low-Z impurities in the range of 50 - 200 nm at 1 kHz frame rate. The absolutely calibrated system is proposed for measuring the impurity distribution in the divertor region of COMPASS-D. This system was developed at IPP.CR and it is routinely used on CASTOR.

The spectrometer will be absolutely calibrated using the second visible spectrometer with the same solid angle (branching ratio method). The upgrade will be done in collaboration with the Budker Institute in Novosibirsk, Russia.

i) LANGMUIR PROBES (Step I and Step II diagnostics)

COMPASS-D is equipped with an array of 39 domed graphite probes mounted in the divertor tiles, as seen in Fig. 4.10. These probes monitor the divertor plasma with the spatial resolution ~ 5 mm and the sampling rate of 1-5 MHz. The electronic equipment to measure IV characteristics is available at IPP Prague.

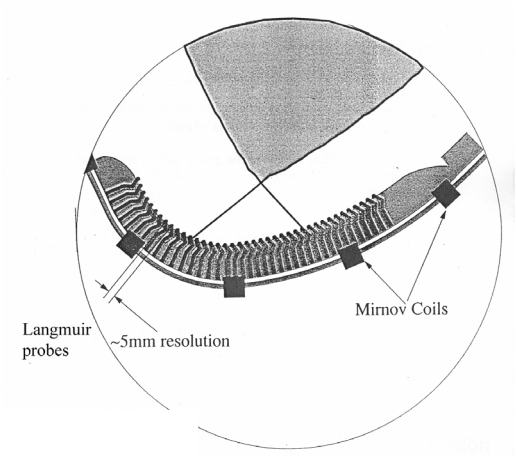

Fig. 4.10: Langmuir probes mounted in the divertor plates of COMPASS

During the Step II of the project, additional arrays of Langmuir probes will be installed at different poloidal and toroidal positions to study the SOL plasma with a reasonable spatial resolution. Furthermore, the installation of the different kinds of novel electric probes (such as the Gundestrup probe for flow measurements, the tunnel probe for fast measurement of electron and ion temperatures, the ball pen probe for direct measurement of plasma potential, etc) is envisaged. These probe system will be designed and manufactured by IPP.CR making use of a long-term expertise in this field. The close collaboration with other Associations in probe and fluctuation measurements is agreed. All these probes will be mounted on the reciprocating drive, which is provided by UKAEA.

j) BEAM DIAGNOSTICS (Step II diagnostics)

The beam diagnostics will be prepared in a close cooperation with the HAS Association. The eam emission spectroscopy by various beams (Li, Na, K) will be used for the measurement of density profiles. For accelerated beams with energies in the 10 – 70 keV range most part of the minor radius will be accessible. The temporal and spatial resolution will be in a range of 10-100 μs and ~1 cm, respectively. Such resolution would be sufficient the density profile during transient phenomena, such as ELMDs and density fluctuations. The vertical and horizontal ports between the sectors 2 and 3 are reserved for the beam diagnostics.

Two possible arrangements of the beam diagnostics are shown in Fig. 4.11:

1. The neutral beam is injected horizontaly, while the light emission is registered through a vertical port. The following quantities are measured:
   - pedestal density profile with 1cm spatial resolution (70 keV Na beam)
   - quasi 2D fluctuation measurement (SOL, edge)

   Such arrangement is routinely operational at TEXTOR by HAS.
2. Beam probe is injected vertically. The three vertical cords are available. In addition to the "standard" injection via the central chord, the HFS and LFD injention is proposed. The LFS injection will improve the spatial resolution at the plasma edge. The HFS injection will provide unique information on the density fluctuation at the gigh fied side of the torus.

   The second option for this arrangement is detection of energy spectra of secondary ions by an electrostatic analyzer, see Fig. 4.11. The aim of this experiment is the determination the electric fields in the pedestal region. This kind of diagnostions is similarly to Heavy Ion Beam Probe Calculation of trajectories of secondary ions for different magnetic configurations is underway.

					Smearing (cm)		
	Observed wavelength (nm)	Lifetime (e-8 sec)	Excitation E (eV)	Ionization E (first, eV)	35 keV	50 keV	70 keV
Li	670.9	2.7	1.8	5.4	2.6	3.1	3.7
Na	589.1	1.6	2.1	5.1	0.9	1.1	**1.2**
K	766.7	2.6	1.6	4.3	1.1	1.3	1.5

Table 4.5: Possible emitter materials for BES and their relevant properties. For pedestal physics studies, the most important parameter is the smearing, which determins the space resolution. The smearing due to the finite lifetime of excited beam atoms.

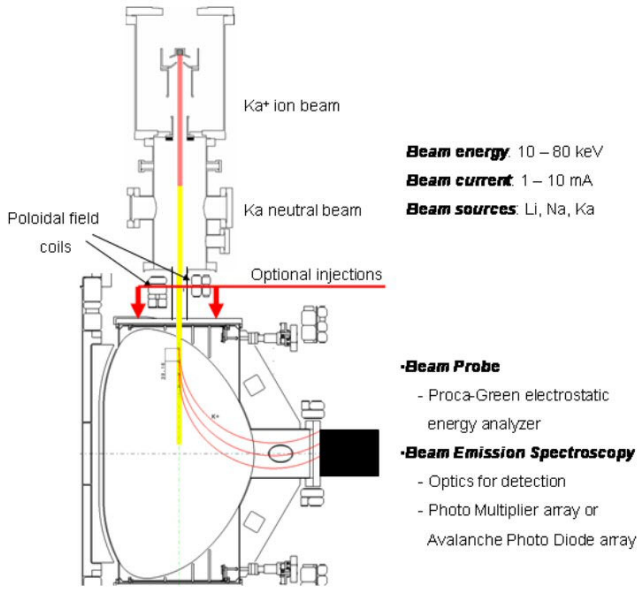

Fig. 4.11: Scheme of the beam probe with vertical injection of light atoms and two options for detection of producs of the beam-plasma interaction (photons or secondary ions).

The Association EURATOM-HAS could provide a Li or Na beam system with a maximum energy around 60-80 keV and beam current up to 10 mA, depending on beam species. The beam source would include the complete vacuum system, power supplies and control system. For the detection we could provide one camera for measuring density profiles with some ms time resolution plus an array of individual detectors (photomultipliers or avalanche photodiodes) for sub-ms profile and fluctuation measurement. The camera would be equipped with its own computer, but signals from the fast detection system would be digitized by the COMPASS-D data acquisition system at about 1 MHz sampling rate.

Collaboration with HAS is envisaged also on Beam Emission Spectroscopy on heating beams. Specification of this part of the project is underway.

k) MICROWAVE REFLECTOMETRY

This diagnostics will be designed and implemented under complete responsibility of the Association EURATOM/IST.

Two mode of operation of the reflectometer system are proposed. The burst mode technique (fast broadband sweeps), developed e.g. for ASDEX-U and JET, allows measuring density profiles during transient phenomena (ELMs, MHD activity). Alternatively, with the fixed or hopping frequency mode, the localized information on the plasma fluctuations (e.g. Doppler shift) can be investigated. The fast DAS (20 - 100 MHz) and the control unit allow reliable

measurements and automatic data processing on a shot to shot basis.

Proposed parameters of the reflectometer system for COMPASS:

- Frequency range 20 - 80 GHz in four bands
- Heterodyne receivers with the I/Q detection
- Modes of operation: fast sweeping, frequency hopes, fixed frequency

l) EX-SITU DIAGNOSTICS FOR PLASMA-WALL INTERACTION (PWI)

In addition to the plasma diagnostics listed above, there is a wide range of instruments and techniques for material characterisation available at the Department of Material Engineering of IPP Prague. These techniques will be employed for investigation of material properties in the frame of the plasma-wall interaction studies.

IPP it possesses several unique devices for plasma spraying and a large base of knowledge and experience for preparation, optimization and analysis of plasma sprayed materials. COMPASS-D can serve as a test bed for the early stage of development of new materials or technologies.

The list of facilities available at the Department of Material Engineering:

- Thermal spray facilities
- Heat treatment and thermal analysis
- Microscopy
- Compositional and phase analyses
- Mechanical testing

5. Additional heating and current drive

5.1. Neutral beam injection system (NBI)

Neutral beam injection system

COMPASS-D will be upgraded with a new Neutral Beam Injection (NBI) system for additional heating and current drive applications. The design is optimized for specific properties of COMPASS-D.

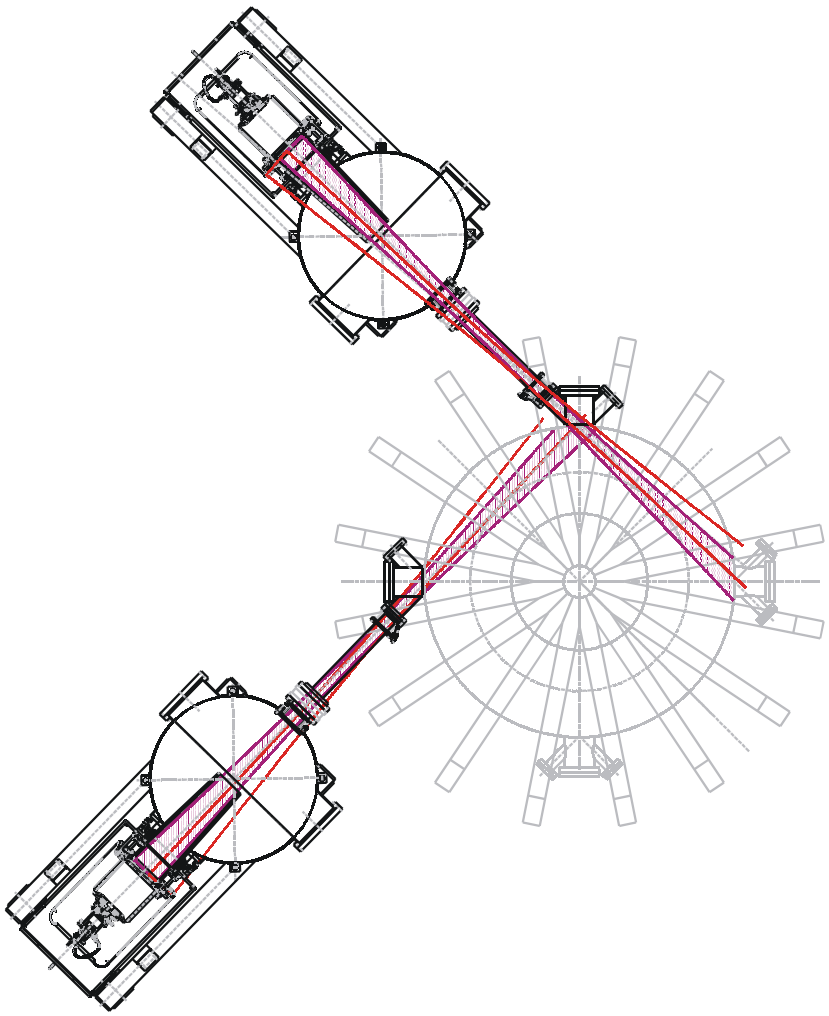

Fig. 5.1.1. Tangential unbalanceed injection.

NBI will provide a flexible heating and current drive system, which will consist of two injectors with particle energy 40 keV and 300 kW output power, delivering 600 kW of total power to the plasma. The basic configuration (Fig. 5.1.1) is optimized for plasma heating. The tangential injection is also optimal for absorption due to the longest passage through the plasma achievable on COMPASS-D. Both beams are aimed in co-direction with respect to the plasma current to minimize the orbit losses. The aiming of both injectors can be shifted outside to achieve off-axis heating and current drive. This NBI system layout has been chosen as the initial configuration.

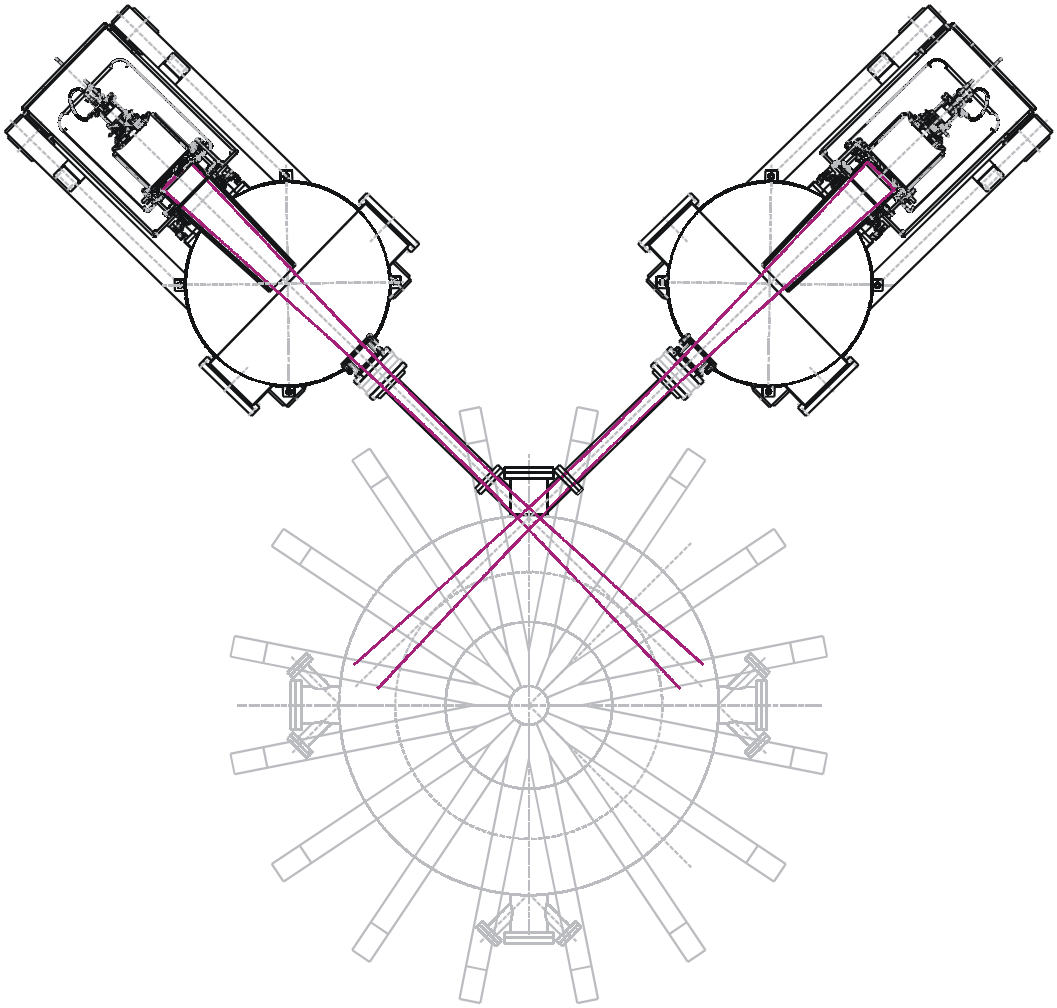

Fig. 5.1.2. Balanced injection.

For balanced injection both injectors will be located at the same port, aiming in co- and counter-current directions (Fig. 5.1.2). With proper power modulation to compensate different orbit losses for co- and counter- beams, one can obtain NBI heating scenario with minimum momentum input.

Normal injection will be also possible (Fig. 5.1.3). In this case, the port is wide enough to allow adjustment of the beam orientation over a wide range of angles. Normal injection is also more suitable for diagnostic purposes, such as charge exchange radiation spectroscopy or motional Stark effect measurements. The most extreme possible case of beam passage through the port is that of almost tangential injection (Fig. 5.1.3 right). With decreased particle energy one can obtain higher absorption in this case.

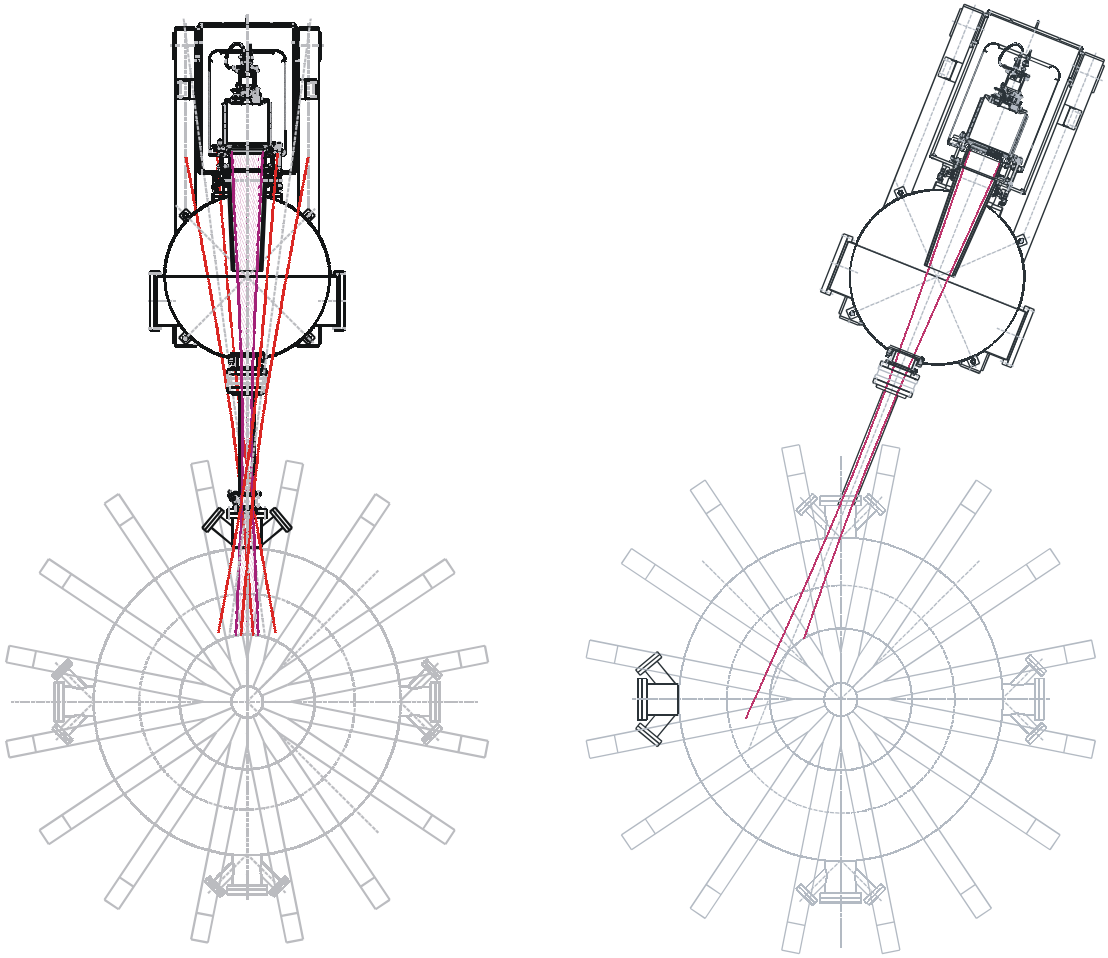

Fig 5.1.3. Schematics of the normal injection.

The injectors and their power supplies area is taken into account in the building design. The power supplies will be located far from the injectors and they are placed in the power supply hall. The injector will be designed to comply with the COMPASS-D construction, only the tangential ports will have to be modified to fit for the beam parameters. Due to the low weight of all the components, the NBI systems can be relocated manually for setting up different scenario without any special equipment like cranes or rails.

Intensive and detailed computations have been performed to simulate NBI behavior in the COMPASS-D tokamak. Codes FAFNER (IPP Garching), NBEAMS and ACCOME were adopted for these purposes. FAFNER results for tangential injection are shown in Table 1. Power deposition profiles for the SND plasma shape and B_T =1.2 T are shown in Fig. 5.1.5.

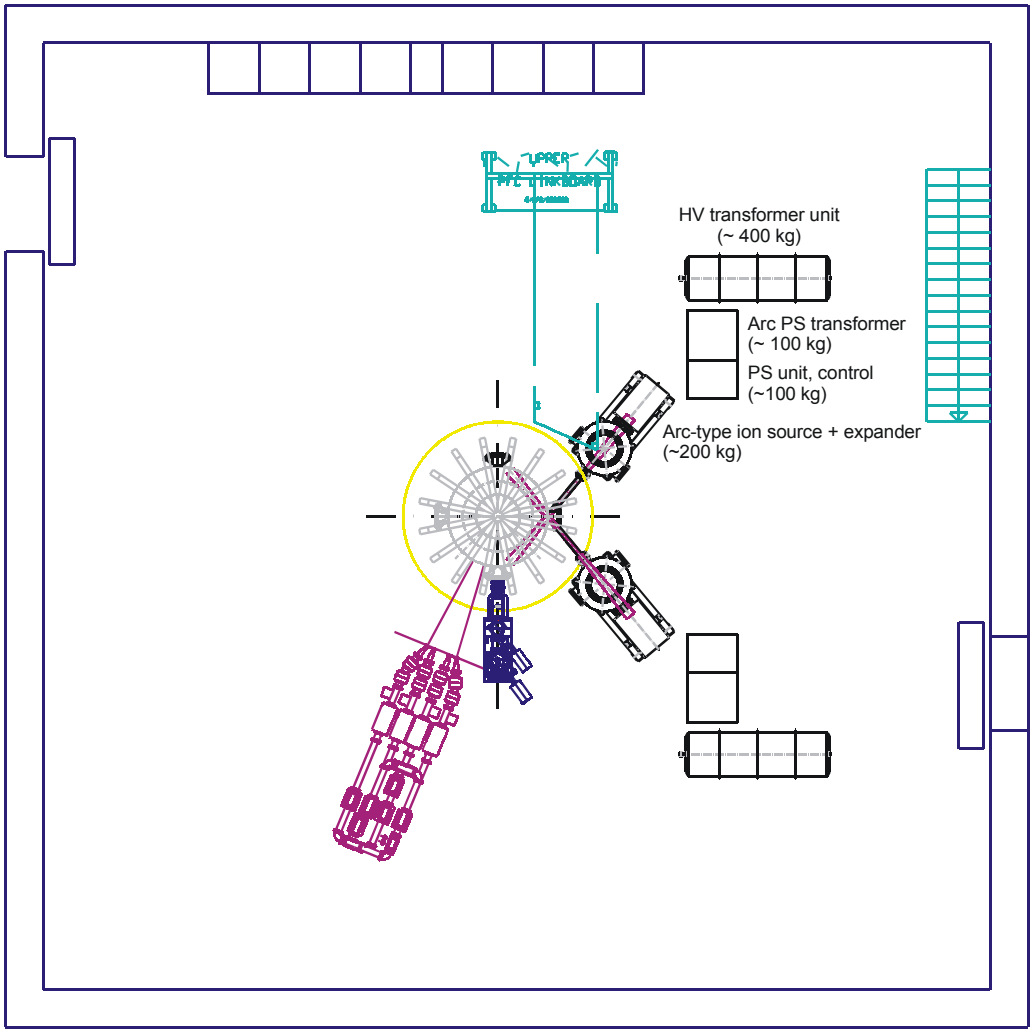

Fig 5.1.4. COMPASS-D experimental hall with LHW, vacuum pumping and NBI systems.

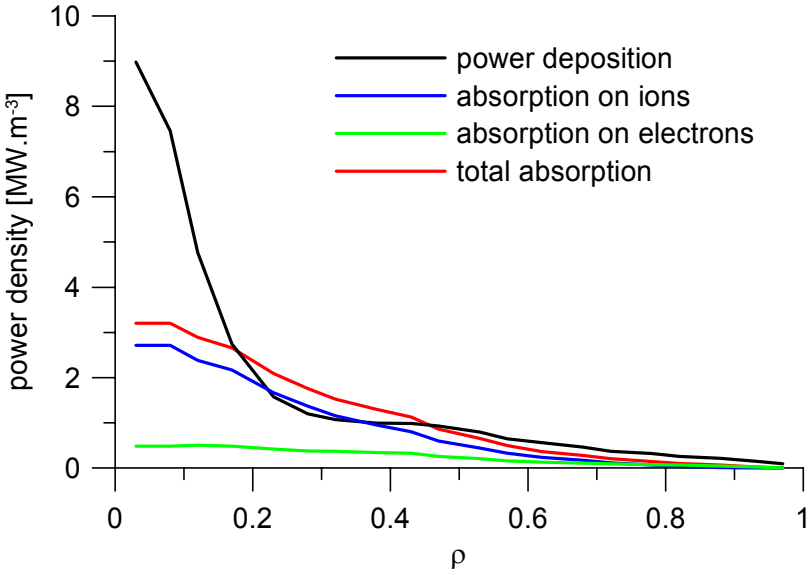

Fig. 5.1.5: Power deposition profiles for SND, 1.2 T co-injection.

	SND equilibrium, B_0=1.2 T, I_P=200 kA, <n>=4 10^{19} m^{-3}		SND equilibrium, B_0=1.2 T, I_P=200 kA, <n>=8 10^{19} m^{-3}		SND equilibrium, B_0=2 T, I_P=350 kA, <n>=3.5 10^{19} m^{-3}		Shot 29759, B_0=1.8 T, I_P=176 kA, <n>=4 10^{19} m^{-3}	
	Co	Counter	Co	Counter	Co	Counter	Co	Counter
Shine through	1 %	1 %	0 %	0 %	2 %	2 %	1 %	1 %
Orbit loss	13 %	52 %	6 %	65 %	2 %	24 %	14 %	56 %
Charge exchange loss	7 %	3 %	1 %	0 %	7 %	7 %	6 %	3 %
Power to ions	57 %	28 %	50 %	14 %	61 %	42 %	56 %	25 %
Power to electrons	22 %	16 %	43 %	21 %	28 %	25 %	23 %	15 %
Toroidal fast ion current	30 kA	19 kA	12 kA	5 kA	28 kA	22 kA	29 kA	18 kA
Current driven by NBI	20 kA	14 kA	8 kA	4 kA	18 kA	15 kA	20 kA	13 kA
Neutrons plasma-plasma	1.5 10^{11} n/s	1.5 10^{11} n/s	0.2 10^{11} n/s	0.2 10^{11} n/s	0.9 10^{11} n/s	0.9 10^{11} n/s	1.4 10^{11} n/s	1.4 10^{11} n/s
Neutrons beam-plasma	7.1 10^{12} n/s	3.4 10^{12} n/s	3.3 10^{12} n/s	0.9 10^{12} n/s	6.4 10^{12} n/s	4.2 10^{12} n/s	7.1 10^{12} n/s	2.9 10^{12} n/s

Table 5.1.1. Main results of NBI simulations by FAFNER.

The parameters of the COMPASS-D NBI system are summarized in Table 5.1.2. These parameters were carefully chosen to comply with COMPASS-D properties.

Number of injectors	2
Energy of the beam	40 keV (can be decreased)
Total ion current	2 x 12.5 A
Total power in neutrals	2 x 300 kW
Pulse length	300 ms
Beam diameter	< 5 cm
Input voltage	3 x 400 V
Total input power	~1.5 MW
Helium consumption	100 –120 l/week
Delivery	End of 2007

Table 5.1.2. NBI system parameters.

5.2 Lower-Hybrid Wave System (LH)

According to the recommendation of the AHG, the implementation of the LH system will receive lower priority during the operation at the toroidal magnetic field of 1.2 T.

Technical parameters of the system:

- Two klystrons with the frequency 1.3 GHz, maximum output power 300kW and a maximum pulse length 1.5s will be used as the RF generators. The klystrons will be transported from UKAEA together with the COMPASS-D tokamak and two HV power supplies (60kV/10A).
- The antenna is an 8-waveguide grill (without passive waveguides). The grill mouth has 138 mm in the toroidal and 165 mm in the poloidal direction (Fig. 5.1.6).
- The gold-coated mouthpiece is shaped for good matching of the plasma boundary.
- Since the LHW must traverse a low density evanescent zone, coupling is critically dependent on the scrape-off-layer (SOL) parameters and on the position of the antenna within the SOL. In order to optimize the power coupling, the antenna is therefore radially movable within limits of 27mm outside and 73mm inside the vessel wall.
- The launched spectrum (for $\Delta\phi = 60^o$), characterized by spectral peaks of the parallel refractivity index $N_{\parallel}$, can be changed manually by adjusting the phase difference $\Delta\phi$ of adjacent waveguides

$\Delta\phi$	60^o	90^o	120^o	180^o
peak $N_{\parallel}$	2.1	3.2	4.4	6.7

- The overall scheme of the LH microwave system is shown in Fig. 5.1.7.

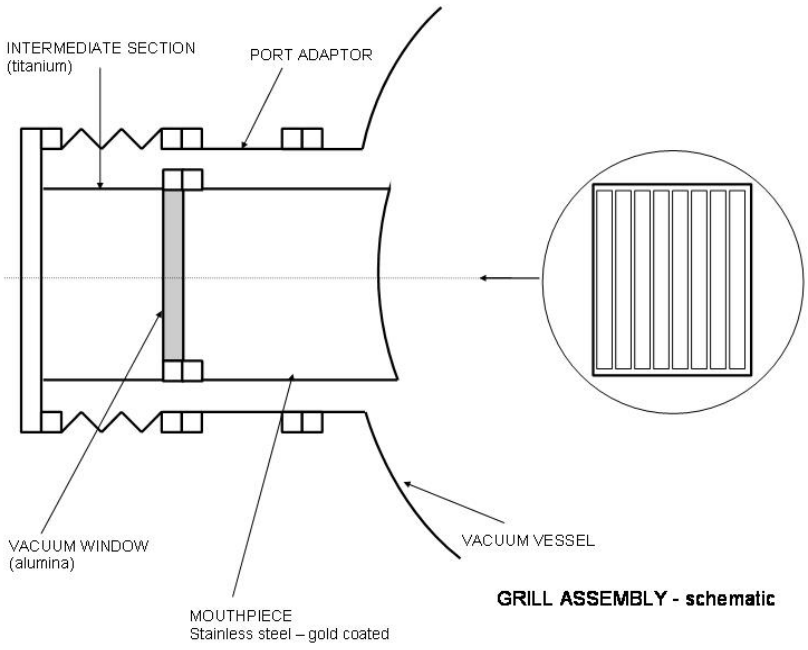

Fig 5.1.6: Schematics of the grill assembly.

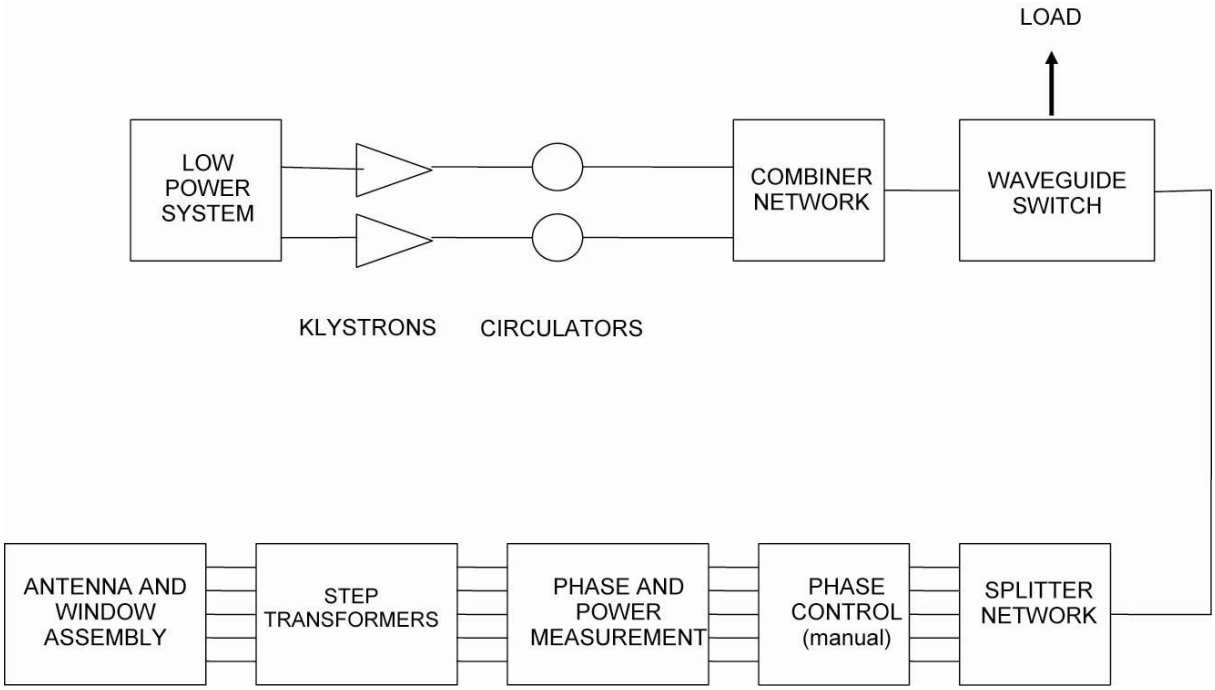

Fig. 5.1.7: Microwave system